Winter 2007

Understanding standing

Christopher Storey
Louisiana Tech University

UNDERSTANDING STANDING

by

Christopher Storey, BS MS

A Dissertation Presented in Partial Fulfillment
of the Requirements for the Degree
Doctor of Philosophy

College of Engineering and Science
Louisiana Tech University

March 2007

INFORMATION TO USERS

The quality of this reproduction is dependent upon the quality of the copy submitted. Broken or indistinct print, colored or poor quality illustrations and photographs, print bleed-through, substandard margins, and improper alignment can adversely affect reproduction.

In the unlikely event that the author did not send a complete manuscript and there are missing pages, these will be noted. Also, if unauthorized copyright material had to be removed, a note will indicate the deletion.

LOUISIANA TECH UNIVERSITY

THE GRADUATE SCHOOL

12/11/2006
Date

We hereby recommend that the dissertation prepared under our supervision by Christopher Michael Storey

entitled Understanding Standing

be accepted in partial fulfillment of the requirements for the Degree of

Doctorate of Philosophy in Biomedical Engineering

Supervisor of Dissertation Research

Head of Department

Biomedical Engineering
Department

Recommendation concurred in:

Advisory Committee

Approved:

Director of Graduate Studies

Approved:

Dean of the Graduate School

Dean of the College

GS Form 13
(5/03)

ABSTRACT

Research Objectives: Psychophysical acceleration threshold is a tool for detecting deficits in dynamic postural control. Our lab has shown differences in the acceleration threshold among young adults, elderly adults, and elderly adults with diabetes. Electromyography, Semmes-Weinstein monofilaments, and hearing tests investigate the underlying physiological mechanisms for the detriments in postural control. Due to peri-sway perturbations, the motion of a person's sway affects the signal to noise ratio for perturbed stance. Since increases in sway range accompany postural instabilities, sway entrainment will allow us to investigate changes in acceleration threshold at different points in sway. The center of pressure, observed for entrainment, only changes due to rotations about joints, specifically the ankle. The current method to model rotation about the ankle is a single orthogonal joint, and therefore inaccurate.

Methods: The SLIP-FALLS-STEPm Platform has lead to the ability to accurately measure and observe interactions in the range of postural sway. The combination of the platform with other testing modalities such as camera tracking systems, force mats, and accelerometers will allow for a comprehensive testing scheme. The new scheme can be combined with the induced sway produced by a sub-threshold sinusoidal entrainment process. The nonorthogonal modelling is programmed in Matlab®.

Results: For constant displacements, anterior accelerations thresholds via two-alternate forced choice (2AFC) showed differences in postural stability in mature,

diabetic individuals with peripheral neuropathy (DPN) and those who are neurally intact (DNI) compared to healthy mature adults (HMA), which corresponded with previous results of lateral perturbations. Both DNI and DPN had significantly higher thresholds for acceleration via 2AFC than HMA at 1 and 4 mm displacements ($p < 0.01$ and $p<0.05$) and Semmes-Weinstein monofilaments. For psychophysical amplitude threshold detection, we used our modified Single-Interval-Adjustment-Matrix to obtain amplitude thresholds for subthreshold frequency entrainment.

Conclusion: The anterior acceleration thresholds show that peripheral neuropathy is not the sole cause for postural instability with diabetes. The ability to control the motion of sway will allow us to describe acceleration threshold throughout the range of sway. With a realistic ankle model, we will be able to better simulate postural dynamics.

APPROVAL FOR SCHOLARLY DISSEMINATION

The author grants to the Prescott Memorial Library of Louisiana Tech University the right to reproduce, by appropriate methods, upon request, any or all portions of this Dissertation. It is understood that "proper request" consists of the agreement, on the part of the requesting party, that said reproduction is for his personal use and that subsequent reproduction will not occur without written approval of the author of this Dissertation. Further, any portions of the Dissertation used in books, papers, and other works must be appropriately referenced to this Dissertation.

Finally, the author of this Dissertation reserves the right to publish freely, in the literature, at any time, any or all portions of this Dissertation.

Author Christopher M. Stacy

Date 2/6/7

GS Form 14
(5/03)

DEDICATION

I would like to dedicate this work

To my Family, and Noor

who supported me throughout.

TABLE OF CONTENTS

LIST OF TABLES

LIST OF FIGURES

ACKNOWLEDGMENTS

The support for this project was provided by a State of Louisiana Board of Regents Fellowship, Merit Review grants from VA Rehabilitation R&D Service Grants #E91-355AP, #E2143PC, #E01-2097R, and a Senior Rehabilitation Research Career Scientist Award to Dr. Charles Robinson. The SLIP-FALLS-STEPm study team consisted of students at the University of Pittsburgh and Louisiana Tech University, and staff at the Shreveport, Louisiana, VA Medical Center, who helped with the collection of these data, and whose PhD dissertations and MS theses addressed different aspects of these experiments. The team members in alphabetical order are Venketesh Balasubramanian, Vikram Darbhe, Shruti Deshmuhk, Dr. Larry Faulkner, Scott Morstatt, Senthilnathan Nakappan, Kristopher K. O'Neal, Gloria Patrick, and Dr. Samantha J. Richerson. Also, I would like to thank Dr. Anne Hollister, Dr. Norman Witriol, Dr. Dale Anderson, and Dr. William Buford, Jr. for their assistance on nonorthogonal modeling. Finally, I would like to thank Dr. Charles Robinson for his guidance and mentoring.

CHAPTER 1

INTRODUCTION/LITERATURE REVIEW

1.1 Balance

The ability to stand up is often taken for granted since most people do not consciously have to control their posture. The scientific and clinical significance of postural and balance studies lie in the complexity underlying a second-nature human ability. While most people have no conscious intervention when trying to stand upright, others consciously have to maintain an upright posture. This decrease in mobility can affect personal lives and well-being. By better understanding the nature of postural control, one can devise methods of rehabilitation that will allow people greater control and stability and improve their daily lives.

Some innate mechanism must exist to keep humans standing or else everyone would fall down. Postural and balance studies have long presented many different ways to measure posture, but many are concerned with why and how people fall due to the large perturbation imparted on the subject.[1-6] Richerson has determined that humans detect perturbations as small as 0.1 mm or 60 arc-seconds of ankle movement.[7-9] Thus, small perturbations allow us to study aspects of standing rather than falling by analyzing dynamic postural control within the range of sway.[10, 11]

In studying posture, one must look at the differences in populations. Prieto et al. showed that as people age their posture becomes more unsteady.[12, 13] Many, including researchers in our lab, have shown that neuropathy secondary to diabetes, increases postural instability as compared to those of similar age.[14-16] The objective is to show that differences in postural control exist in mature diabetic individuals with and without peripheral neuropathy as compared to healthy mature adults. We have shown that people with diabetes have increased high-frequency hearing loss as compared to healthy mature adults.[17] Based on the outcomes of these analyses, I have created new tools for new tests and analyses of postural control that can be implemented to better describe our quasi-static postural control.

1.2 Posture Studies

Posture and balance are studied in static or dynamic conditions. Static conditions tend to observe differences between populations of age or pathology by observing a subject's sway during quiet standing.[18, 19] Dynamic conditions are created by imparting a sensory input or force onto the body that changes the naturally occurring sway.[2, 16] Dynamic conditions study recovery from induced falls and sway.[2, 16] Many types of movement protocols have been used to perturb the subject such as a tilt platform, translating platform (on order of cm), and force exerted on a belt about the subject's waist.[2-6, 16, 20-26] These methods, while providing insight into one's ability to prevent falls, obtain little information on how we are able to remain standing.

1.3 Studying Standing

New technology has allowed the development of a low-vibration translating platform that is accurate for displacement on the range of 10^{-5} m.[10, 11, 27, 28] When perturbations are within the range of sway, the signal-to-noise ratio becomes a factor that can lead to misses and false positives. External cues for movement must be removed—so no harness is used (only for subjects who have no tendency for falls), and the subject is blindfolded with headphones playing white noise. Studies have shown that less than 1 N of force on the body can alter postural sway by increasing stability in a subject with decreased postural control.[29-34] The decrease in sway due to light touch has been attributed to the touch providing a reference point and the completion of a kinematic chain.[34] Vision is especially important to subjects with vestibular loss. With eyes closed, those with vestibular deficits show a greatly increased instability in postural sway.[23, 35] Eyes open and eyes closed studies have also showed significant differences in age-matched elderly subjects.[12]

1.4 Diabetes

1.4.1 Peripheral Neuropathy

Diabetes is becoming an epidemic in our aging society. Those as young as 45 years old who meet certain risk factors should be tested.[36] Thomas et al. found that over 20% of the aging British population were at least glucose-intolerant, with 5% of both men and women having undiagnosed diabetes.[37] Diabetes carries with it not only decreased metabolic function but also an increased risk for other problems such as vascular and neuropathic conditions.

Allen et al. showed that diabetes was associated with an increased risk of dementia and declining cognitive performance.[38] Studies have shown that the increased occurrence of vascular disease in those with diabetes increases the cognitive deficits seen.[39, 40] Animal models suggest that hyperglycemia causes decreased synaptic plasticity in the hippocampus and concludes a direct effect of insulin on the brain.[41]

The effects of diabetes on the nervous system are not limited to the central nervous system but also can be observed on the periphery. Due to the increased risk of falls, several methods for early detection and diagnosis of peripheral neuropathy have been developed.[42-49] Due to decreased sensory information which can cause ulceration, common clinical standards for diagnosis focus on cutaneous sensory disturbances.[48] Nerve conduction studies also correlate with the presence of diabetic foot ulceration.[50] Diagnosis provides awareness to people of their disability to try decrease risk of falls and injury.[51]

The cause of the neuropathic conditions in people with diabetes is not fully understood. Hill et al. found that the perineural cell basement membrane of the sural nerve is thickened as compared to controls and those with peripheral vascular disease, which is normally found to be present in diabetic individuals with peripheral neuropathy, especially in smaller fasciculi.[52] Ishii supports that decreases in insulin-like growth factor, which is involved in axonal and nerve development, limit the ability of nerves to regenerate after damage caused by diabetes, and has been shown to be an effective treatment for neuropathy in diabetic rats.[53] Stewart et al. have shown that auto-immune and chronic inflammation cause demyelination that causes a treatable via

steroids polyneuropathy in people with diabetes.[54] Diabetes has also been shown to cause small fiber neuropathy, which can cause pain but result in normal electrophysiology exams.[55]

Genetic advancements have allowed for the research of the preceding possible causes in diabetic rat animals. The morphology of sciatic rat nerve graphs change to and from neuropathy when going to diabetic rat from control and control to diabetic rat, respectively.[56]

1.4.2 Balance

Peripheral neuropathy affects balance in several ways. Andersen et al. showed that muscle weakness in the lower leg was directly related to neuropathy, but not nephropathy or retinopathy.[57] Horak et al. found that severity of peripheral neuropathy increased the sensitivity gain in the vestibular system, which could make people with diabetes and peripheral neuropathy adapted to be more reliant on their vestibular system for postural control.[58] Simmons et al. found that those with only a cutaneous sensory deficit in the feet showed decreased postural control, while those with diabetes did not.[14] Dickstein et al. showed improvements in postural control through both light and heavy touch to the fingers in diabetic individuals with peripheral neuropathy.[30, 31] All these facets of posture and balance make it difficult to isolate a single control system.

1.4.3 Hearing

Hearing loss occurs through two normal pathways, conductive and sensorineural. Conductive hearing loss can be caused by cerumen build-up or eardrum damage. Diabetes has been associated, however, with sensorineural hearing loss. Wackym et al. suggest that the sensorineural damage seen in diabetes is caused by a thickening of the

vasculature around the endolymph causing a cytotoxic environment.[59] Duck et al. also support that the vasculature plays a role in sensorineural hearing loss since they showed diabetic individuals with hypertension had more hearing loss than normotensive diabetic indivduals.[60] Diabetic individuals have been found to have an increased risk of sudden sensorineural hearing loss, and the risked increases with age, hypertension, and hyperlipidemia.[61, 62] The progression of diabetes as measured by the serum creatinine and not hemoglobin A1c has also been shown to correlate with sensorineural hearing loss.[63] Frisna et al. shows the systemic effect of diabetes on sensorineural hearing loss by supporting vascular, cellular, and metabolic complications and alterations.[64] Several studies have found that hearing loss in those with diabetes is for high frequencies.[60, 64, 65] Although there is a higher prevalence of hearing loss in diabetic individuals, Fowler et al. state that the evidence is inconclusive on diabetes as the cause due to confounding factors such as noise exposure and hypertension.[66]

1.5 Quantitative Analysis

Specific pathologies such as cerebellar ataxia, Parkinson's disease, and vestibular loss allow the observer to compare the contributions of individual systems to posture and balance by allowing the investigator exclude those components from postural control analysis.[21, 23, 35, 67-69] To accurately measure center of mass, the current method uses three-dimensional imaging via camera systems. These systems have high data acquisition times, but new methods utilizing accelerometers and genetic algorithms show promise with the ability to estimate the center of mass with lower error rates.[70, 71] Instead of measuring the center-of-mass, the easier correlate is the center-of-pressure, which is the projection of the center of mass onto the surface on which the base of

support lies.[72] Center-of-pressure analyses have shown as a reliable method to help distinguish postural control deficiencies.[12, 13, 16, 29-31, 73-81] By quantifying postural control, we are able to statistically differentiate variations in the population and focus on what needs to be corrected in those with deficits.

1.6 Sway Metrics

Metrics have been derived from different models and estimates to account for certain descriptions of sway. The center-of-pressure time-series, both the medial-lateral (MLCoP) and anterior-posterior (APCoP) directions, are used to determine a third time-series, the resultant distance (RDCoP). Based on the three time-series, four categories of postural sway metrics are used to compare different groups. The mean velocity and RMS sway are considered the standard for postural steadiness, both of which fall into the category for time-domain-distance metrics.[12] The mean velocity is calculated by dividing the total length of the center- of-pressure (CoP) path by the total time allotted, and was shown to be higher in elderly adults.[12] The RMS sway will emphasize larges changes in the sway profile, which can indicate instability, and are also higher in elderly adults.[12] Other time-domain-distance metrics, range and mean distance, were larger for elderly adults as opposed to young adults.[12] Time-domain area metrics estimate the area covered by the CoP path using a 95% confidence circle or ellipse, which was larger in older individuals.[12] In addition, the directly calculated sway area was shown to be significantly larger in older individuals.[12] Although these metrics provide important feedback on postural stability, they lack ability to describe postural sway in the frequency domain.

To account for the frequency domain in postural sway, two methods of quantification---time-domain-hybrid and frequency-domain measures---are used. The time-domain-hybrid measures frequencies based on the time-domain-distance measures. One, the mean frequency, allows information on the frequency of the CoP if it had travelled around in a circle or crossed zero.[12] A unit-less measurement of how well a curve fills its space, fractal dimensions, can be model from the 95% confidence circle or ellipse, which the ellipse is better suited for dual force platforms for measurements of a single foot.[12] Both fractal dimensions and mean frequency differed between elderly and young adults.[12] Frequency domain metrics describe the power spectral density of sway. The three ways to describe the power spectral density is the total power, the 50% power frequency, or the centroidal frequency, which shows the frequency at which the power is concentrated. These last two metrics allow the frequency domain to be correlated with action of posture in the time domain.[12] The final frequency-domain metric, frequency dispersion was not found to be different between young and elder adults as the other three were.[12]

1.7 System Modulation

Postural control is maintained through a complex of neurological systems. Inputs for the control of posture include tactile, proprioception, kinesthesis, vestibular, and visual sensory modalities. Tactile sensors have acuity for both pressure and vibration. Therefore, low-vibration translation platforms were developed.[11] Proprioception provides orientation information of the limbs to the central nervous system; and Keshner et al. have shown that without visual input, the ankle method of balance is preferred. The knowledge of the limb and muscle movement and orientation help the central nervous

system to predict movement to maintain an upright posture.[82-87] Andersson et al. have shown that the removal of proprioceptive feedback increases sway velocity, but also those with vestibular problems do not report an increased instability.[18] The vestibular system acts to increase a reaction to a large sway but still shows correct detection of movement and similar reaction time.[23] Borel et al. showed that both vestibular and visual input combine for head orientation and posture alignment since deviation of posture and head occurred for both unilateral vestibular loss in darkness and with visual context to the hindered side and opposite side, respectively.[35] When testing thresholds in postural sway, our group has found that the amount of force generated is less than that perceivable by the vestibular system.[88] Visual cues provided motion direction feedback to the system that can be used to induce sway in a subject.

1.8 Threshold Detection

The uniqueness of our lab is our ability to study the psychophysics of balance. Its past studies have used a modified parameter estimation by sequential testing (PEST) in a two-alternate forced choice protocol.[7, 89] The study of psychophysics relates a stimulus level to the proportion of correct detections.[90] Alternate forced choice protocols have problems with bias that are not seen in yes/no tests.[91] Yes/no 1-up-1-down staircase methods can quickly come to threshold, but the statistical power is low.[90, 92] Kaernbach developed the Single-Interval-Adjustment-Matrix (SIAM) based on a probability matrix to vary stepping.[93] His focus was to improve efficiencies in the tests rather than in the stepping protocol. SIAM is based on yes/no choice for a single interval. Therefore, SIAM cuts testing time by almost 50% by removing second interval. SIAM provides lower error than alternate forced choice in fewer trials.[93] SIAM will

provide us a better method for determining threshold than alternate forced choice by reducing error and reducing the testing time. The reduced testing time provides us with the most benefit since it reduces fatigue during testing.

1.9 Induced Sway

Due to the chaotic motion of postural sway, one must have knowledge of the subject's position in postural sway for better control of the study.[94] Fransson et al. showed that sway could be induced through both vibratory stimulation of the legs and galvanic vestibular stimulation, but both caused disequilibrium in the subjects to different levels of noticeable sway.[95] De Nunzio et al. has shown that sway can be predictably controlled when eyes are opened and closed via an oscillating platform even with continuous vibratory input to leg neck and trunk muscle groups.[96] Therefore, it is concluded that the predictable nature of the oscillation is more important than the proprioceptive feedback, which was also confirmed by Nardone et al.[16]

By inducing sway, one can more accurately control the experiment when inducing changes with signals. A new area with great possibilities especially for the realm of small perturbations will allow for predictive modelling of control inputs to maintain posture via external cues. Most studies have been shown to occur with oscillating visual stimuli, which can cause an observable peak in the power spectrum that is controlled by the frequency of the oscillation.[74, 97-100] Our lab has devised a way to entrain sway via a subthreshold sinusoidally translating platform.

1.10 Posture Model

To assess quantitatively the modulation of postural control by difference sensory inputs or processing centers, mathematical models are created. The standard model for postural sway estimations is the inverted pendulum. The model usually consists of only a single joint (ankle) to simplify the model. The mathematical models provide the amount of torque required to keep the system stable by maintaining the center of mass inside the base of support.[70, 71, 101-106]

There has been a recent increase of interest in the simulation of arthropod or human limbs in robot design.[107-120] These multilinked robotic limbs use orthogonal mechanisms, usually revolute joints for their mechanisms.[121] The kinematics and kinetics of the limb segments are calculated with the Denavit–Hartenberg (DH) representation, a simplified system that uses only four of six joint parameters for motion, that has worked well for planar and orthogonal mechanisms for over fifty years by reducing matrix size and the number of matrix multiplications.[122]

Arthropod and human limbs are multilinked systems with revolute joints that are not orthogonal to each other or to the limb segments.[123-146] Such revolute joints, known as arbitrary revolute joints, produce three-dimensional spatial motion with only one degree of freedom, thus the revolute joints reduce the limb's number of degrees of freedom and control complexity. A vector (d) and two angles of offset, the twist (α) and cant (β) angles shown in Figure 1.1, define the location and orientation of arbitrary revolute joints. The resulting limb movements are in different planes at each revolute. The simplification of these linkages with the DH representation produces several problems[124] If the twist and cant angles are not 0° or 90°, the reference frames are

projected outside of the limb segments by DH representation. If the mechanisms are nearly parallel to one of the coordinate axes, DH incurs large azimuth errors.[124]

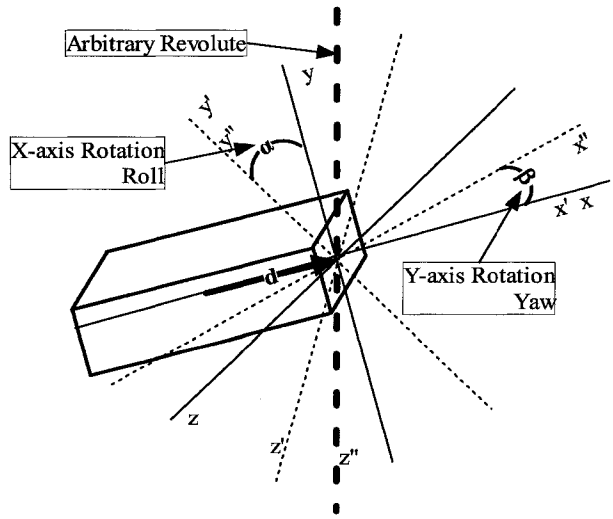

Figure 1.1. The α and β offset axes and d offset position.

We propose a representation based on computer graphics techniques for rotation about an arbitrary axis that is suitable for analysis and display of kinematic chains connected by nonorthogonal and/or orthogonal revolute joints and is optimized to reduce computational cost over traditional methods.[147-150] These three-dimensional techniques have been used successfully in human limb simulations; (Buford et al. 2005 has expanded them to the whole human body).[151-155] As with the DH system, a limb is modeled as a hierarchical kinematic chain from the ground (support) to the end effector. Each child link moves with its parent. In this system, the revolute joint to be rotated is translated to the origin; the twist (alpha) and cant (beta) angles are de-rotated, and the arbitrary axis is aligned with the global *z*-axis. The dependent points for this joint are then rotated through a specified joint actuation angle about the revolute; the twist and cant angles are re-rotated, and the revolute and dependent points are then translated back

into position. Thus, the method is more robust than either DH or multibody because it includes all six joint parameters, calculates both position and orientation of each link relative to the joints between them, and permits the origin of each revolute to lie within the joint itself. Modern computer capabilities allow this more robust method to be used easily on personal computers.

Our proposed system places the limb segment and joint reference frames within the segments or joints to facilitate the measurement, design, modeling, simulation, and control of these natural systems. Many design engineers prefer to compute and measure the motion of reference frames for each limb segment or revolute relative to the body and global reference frames with calculated values of x, y, and z displacements and yaw, pitch, and roll rotations.[156, 157] Our method facilitates this computation with outputs of x, y, and z displacements with yaw, pitch, and roll rotations if desired by the user. The parameters that determine the limb and joint orientation and motion are stated explicitly to facilitate accurate measurement in animal limbs. We simulated models of the human ankle calculated from Inman's data and crab leg base measurements from Koti's thesis.[137-139]

CHAPTER 2

METHODS AND MATERIALS

2.1 SLIP-FALLS-STEPm

2.1.1 Original SLIP-FALLS- STEPm System

A wealth of multi-dimensional data can now be collected during biomechanical studies of human motion and postural reactions to perturbation with the SLIP-FALLS-STEPm system. These include biomechanical measures like AP and ML Centers-of-Pressure, weight on platform versus weight supported by harness, horizontal ground reaction forces, head and foot accelerations in multiple dimensions, distributions of pressures under the foot, and joint and limb trajectories as measured by motion-capture marker systems. Multi-channel EMG data and psychophysical responses collected simultaneously add richness to any control model built. The SLIP-FALLS-STEPm lab has developed a low vibration translating platform to study the psychophysics of balance.[10, 11] The original setup (Figure 2.1) combined a translation force-plate with a pressure mat.

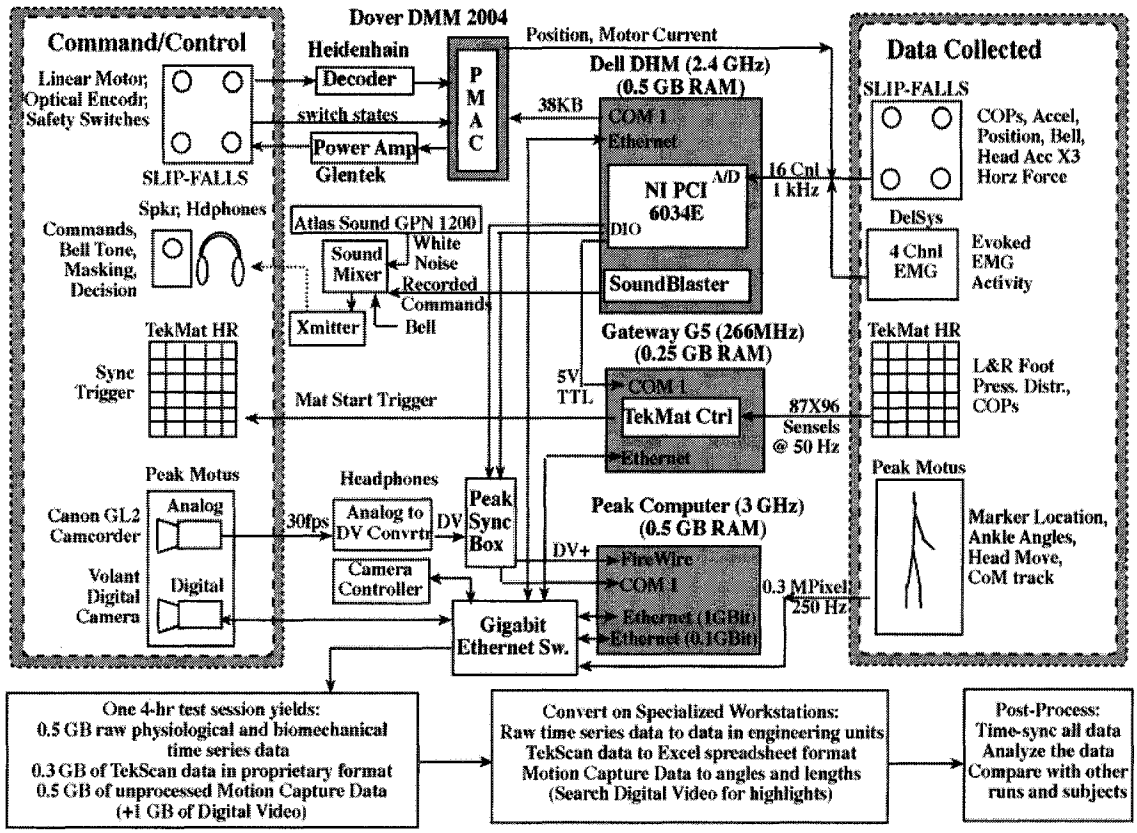

Figure 2.1. The original SLIP-FALLS-STEPm lab consists of a sliding platform (SLIP), hardware and software routines (FALLS) for collecting neurophysiological, biomechanical (Position, Acceleration, Centers-of-Pressure), EMG and psychophysical data, and equipment and software to simultaneously measure position markers, and foot pressure distributions (STEPm). The SLIP is controlled by a single board Programmable Multi-Axis Controller (PMAC®) that receives commands from the FALLS computer (Dell DHM®). This computer also relays pre-recording instructions to the subject via a SoundBlaster® card and headphones. A Tekscan HRMat® measures foot pressure distribution with an array of 87 by 96 sensels (4 per cm^2). A separate computer controls the HRMat®. Its data collection starts with an external RS232 trigger. Motion capture of the location of retro-reflective markers is achieved by a single digital camera Peak-Motus system, along with a back-up analog camcorder. The Peak-Motus® computer is triggered also by the FALLS computer with an additional sync signal generated at the start of a platform move. A single 4-hr test session generates over 2 GB of data, all of which has to be processed offline after the completion of the experiment. (Figure from ASEE St. Lawrence Section Conference Student Paper[158])

This setup provides redundancy, and has allowed the verification of the pressure mat and force plate CoP measures. The development has allowed for testing of acceleration thresholds at displacements as low as 0.1mm.[8] By combining the platform

test with other simple tests for reaction time to sound or touch, the reaction time of recognition of platform translation was higher and required a much larger perturbation than threshold to decrease reaction time.[159]

2.1.2 Platform

The platform consists of four linear air bearings on two rails, as constructed by Danaher Motion® (Westover, MA, USA). This arrangement allows near zero friction for platform movement. An optical encoder (Heidenhain® – Schaumberg, IL, USA) for position provides 20000 counts per mm. A single plate bridges the four air bearings on which reside each of the four Lebow® (Columbus, OH, USA) 200 lb. load cells. Atop the load cells lies an aluminum plate (60.96 cm x 53.34 cm) on which the subject stands. The air bearing receives the air supply from an Atlas Copco (Stockholm, Sweden) SF 4 FF® oil-free air compressor with integrated dryer. The air compressor cycles from 80 psi to 120 psi with an attached 30-gallon air storage tank. Due to the pulsatile nature of the airflow, another 3-gallon tank is placed close to the platform. A minimum of 3.8 scfm and 80 psi is required for the air bearings.

2.1.3 Controller

The platform is controlled by a Dover (Westover, MA, USA) DMM 2004® controller that uses a sinusoidally commutated Glentek® (El Segundo, CA, USA) amplifier to control platform movement via an electromagnetic linear motor (Trilogy®, Webster, TX, USA). The controller has a cutoff switch in case of loss of air pressure (below 80 psi) to the bearings to prevent damage if pressure drops. In addition, limits, and home location are programmed into the controller to kill the motor when limits are exceeded and to find the initial position.

2.1.4 Computer-Controller Integration

The controller is provided commands via a PC RS-232 serial port. Labview® 6 (National Instruments, Austin, TX, USA) was the software under which the experiment protocol was developed. Through Labview®, commands are sent via RS-232 to the Dover for control of the platform. Labview® also sends out commands to the user via a sound card that is connected to an audio mixer. The audio mixer merged the Labview® commands with bell tones and white noise, which is sent wirelessly to headphones and speakers. The bell tones provide feedback to the user that the button press registered. The white noise masks all external sounds cues to the movement. Labview® controls a National Instruments® (Austin, TX, USA) PCI 6034E multifunction data acquisition card. Data are collected for 16 channels at 1 kHz. The data are stored in plain text file comma delimited files as raw values. The data are backed-up via CD-R. All data are transferred to a USB® hard drive for offline processing in Matlab®. Data is converted via Matlab® batch programs to engineering units and are stored in Excel® spreadsheets for further analysis.

2.2 Data Collection

2.2.1 Calculations for Quiet Standing Metrics

All calculations were performed in Matlab® using self-written programs. Eq. 1 calculated the peak imparted kinetic energy (p).

$$p = \frac{m \cdot a \cdot d}{2} \tag{1}$$

Where m is the subject's mass, a is the peak acceleration threshold, and d is the platform displacement, the peak imparted kinetic energy accounts for each individual's

mass in relation to each individual's peak acceleration threshold. The peak energy occurs at the peak of velocity that is at half the displacement due to the way the controller smooths the perturbation. Due to the symmetric curve of the acceleration the average acceleration equals half the peak acceleration. Therefore, we obtain the peak velocity by multiplying half the acceleration with the displacement.

Prior to each threshold detection session, twenty seconds of quiet standing data were recorded to assess an individual's natural sway. These quiet standing periods yielded three quiet standing observation periods per individual. Sway parameters are calculated from the four load cells of the force-plate by Eqs. 2 and 3.

$$APCoP = \frac{209.55(l_3 + l_4 - l_1 - l_2)}{w} \tag{2}$$

$$MLCoP = \frac{174.625(l_3 + l_2 - l_1 - l_4)}{w} \tag{3}$$

Where 209.55 and 174.625 are the distances in millimetres between pairs of load cells in the anterior-posterior and medial-lateral directions, respectively

The anterior-posterior center of pressure (APCoP) and medial-lateral center of pressure (MLCoP) time-series profiles were derived from the load cell (l) data[11], with the convention that forward and rightward were the positive directions with w being the sum of all four load cells. The load cells were numbered counter-clockwise from the back left of the platform. All MLCoP metrics are calculated the same as APCoP as follows with the MLCoP substituting for the APCoP. The time series with the means subtracted out were filtered using a 10 Hz type 2 Chebyshev low-pass filter. From these time-series, the resultant distance (RD) is calculated to provide a time series of the vector

distance combining each APCoP and MLCoP pair (Eq. 4), where N is the total number of samples in the time-series.

$$RD(n) = \sqrt{APCoP(n)^2 + MLCoP(n)^2}; n = 1,...,N \tag{4}$$

Based on these time-series (TS), we calculated metrics suggested by Prieto et al. who had shown differences in aged and young adult groups as mentioned in the introduction.[12] They are broken up into four categories: time-domain distance, time-domain area, time-domain hybrid, and frequency domain measures. From the time-domain distance metrics, mean (MDIST) were calculated (Eq. 5) for RD, APCoP, and MLCoP[12], along with the standard deviation (Eqs. 6-7) and range (Eq. 8) of each time series. Root mean square distance (RDIST) for the AP (s_{AP}) and ML (s_{ML}) directions is the standard deviation of each respective time series.

$$MDIST = \frac{1}{N}\sum TS(n) \tag{5}$$

$$RDIST = \sqrt{\frac{1}{N}\sum TS(n)^2} \tag{6}$$

$$s_{RD} = \sqrt{RDIST^2 - MDIST^2} \tag{7}$$

$$range = \max - \min \tag{8}$$

The total excursion (TOTEX), a summation of the changes in distance per unit of time, was calculated for APCoP, MLCoP, and the vector distance (Eqs. 9-10) change of both.[12]

$$TOTEX = \sum_{n=1}^{N-1}\left[\begin{array}{l}(APCoP(n+1) - APCoP(n))^2 \\ +(MLCoP(n+1) - MLCoP(n))^2\end{array}\right]^{1/2} \tag{9}$$

$$TOTEX_{ap} = \sum_{n=1}^{N-1}\left|APCoP(n+1) - APCoP(n)\right| \tag{10}$$

The mean velocity (MVELO) is calculated from the TOTEX, $TOTEX_{ap}$, and $TOTEX_{ml}$.[12] MVELO (Eq. 11) provides the average velocity for the entire time (T) of the quiet standing period.

$$MVELO = TOTEX / T \tag{11}$$

The two time-domain area measures that are calculated are the 95% confidence circular area (AREA-CC) and 95% confidence elliptical area (AREA-CE) with 95% confidence level coming from the z and F statistic (Eqs. 12-13) for 95% confidence ($z_{.05}$ = 1.645; $F_{.05[2,\infty]}$ = 3.00) respectively.[12] The covariance (s_{APML}) is required for the AREA-CE calculation (Eqs. 13-14).

$$AREA - CC = \pi(MDIST + z_{.05} s_{RD}) \tag{12}$$

$$AREA - CE = 2\pi F_{.05[2,\infty]} \sqrt{s_{AP}^2 s_{ML}^2 - s_{APML}^2} \tag{13}$$

$$s_{APML} = \frac{1}{N} \sum APCoP(n) MLCoP(n) \tag{14}$$

The hybrid measures include sway area (Eq. 15 estimates area enclosed by COP path per unit of time), mean frequency [both rotational (Eq. 16) and in the respective APCoP (Eq. 17) and MLCoP planes], and fractal dimension (FD) (Eqs. 18-20 based on TOTEX (FD-PD), AREA-CC (FD-CC), AREA-CE (FD-CE)).[12]

$$swayarea = \frac{1}{2T} \sum_{n=1}^{N-1} \left| \begin{matrix} APCoP(n+1) MLCoP(n) \\ -APCoP(n) MLCoP(n+1) \end{matrix} \right| \tag{15}$$

$$MFREQ = \frac{MVELO}{2\pi MDIST} \tag{16}$$

$$MFREQ_{AP} = \frac{MVELO_{AP}}{4\sqrt{2} MDIST_{AP}} \tag{17}$$

Eq. 15 uses the planar diameter (d) for fractal dimension calculation, which is the difference of the range of RD. To calculate the 95% confidence interval of FD-CC and FD-CE, d is replaced with $d_{\text{FD-CC}}$ and $d_{\text{FD-CE}}$ (Eqs. 19-20).

$$FD = \frac{\log(N)}{\log\left(Nd/TOTEX\right)} \tag{18}$$

$$d_{FD-CC} = 2\left(MDIST + z_{.05}s_{RD}\right) \tag{19}$$

$$d_{FD-CE} = \sqrt{8F_{.05[2,\infty]}\sqrt{s_{AP}^2 s_{ML}^2 - s_{APML}^2}} \tag{20}$$

For the frequency domain, the total power, 50% power frequency (median power frequency), 95% power frequency (95% percentile power frequency), centroidal frequency, and frequency dispersion were calculated using discrete Fourier transform and not the sinusoidal multi-taper estimate.[12] The frequency domain metrics were calculated for all three time-series. The metrics were based on the spectral moment, μ_k (Eq. 21). Only frequencies from 0.15 to 5 Hz were analysed so i and j provide these limits while Δf is the frequency increment for the power spectrum.

$$\mu_k = \sum_{m=i}^{j} \left(m\Delta f\right)^k G(m) \tag{21}$$

Eq. 22 incorporates μ_k to calculate the total power of the spectrum (POWER). Eqs. 23 and 24 calculate the lowest frequency (index u and v respectively) of which the sum contains 50% and 95% respectively of the total power.

$$POWER = \mu_0 \tag{22}$$

$$50PFREQ = \sum_{m=i}^{u} G(m) \geq 0.50\mu_0 \tag{23}$$

$$95PFREQ = \sum_{m=i}^{v} G(m) \geq 0.95\mu_0 \tag{24}$$

The centroidal frequency (CFREQ) is the frequency in which the spectral mass is concentrated (Eq. 25), while the frequency dispersion (FREQD) is a measure of the variability of the spectrum (Eq. 26).

$$CFREQ = \sqrt{\mu_2 / \mu_0} \tag{25}$$

$$FREQD = \sqrt{1 - \mu_1^2 / \mu_0 \mu_2} \tag{26}$$

2.2.2 Subject Questionnaire

All subjects were given the RAND 36-item (with Depression Screener) health survey, a modified version of the short form 36-item (SF-36) health survey, which has shown correlations of poor health scores with individuals who had diabetes.[160-164] The RAND evaluates a person's self-reported physical and mental health in relation to his ore her quality of life. Jenkins et al. and Lyons et al. verified the validity and reliability of SF-36 health survey in an elderly population.[165, 166] Lower scores were correlated with elderly who have a fall risk.[167] Post-test scoring was performed automatically within an Excel® spreadsheet.

2.2.3 Foot Sensory Test

Semmes-Weinstein Monofilaments (SWM) were used to assess sensory thresholds on the sole of the foot by exerting a constant force based on buckling strength of the monofilament pressed to the foot. SWM is a standard measure for assessing risk of diabetic foot ulceration, and cutaneous sensory peripheral neuropathy.[43, 47, 48, 168, 169] The monofilaments are marked with a log of the force exerted in grams by the

monofilament. These threshold measurements were taken on the plantar surface at the great toe, metatarsal at the first and fourth digit, and heel. The procedure required that two out of three touches be detected for a given monofilament to be at threshold at a location. For simplicity, with eyes closed, subjects were asked to respond when they felt the probe. For the SWM test, a discrepancy in sample size exists across the test sites because we did not begin taking measurements at the heel and fourth metatarsal until after a number of subjects had been recruited.

2.2.4 Peripheral Neuropathy Test

Surface lower-limb nerve conduction tests, performed by Overton Brooks VA Medical Center Neurology Service by a technician supervised by a neurologist, determined the presence of peripheral neuropathy. Nerve conduction velocities were measured for the peroneal, tibial, and sural nerves bilaterally. In 15 subjects (4 DNI, 5 DPN, and 6 HMA), no sural nerve conduction velocity could be obtained. Inferences cannot be made from the inability to find sural nerve CVs via surface electrodes as sural nerve studies often require the use of needle electrodes.[170-173] M-wave and F-wave latency tests were performed on the peroneal and tibial nerves.

2.2.5 Analysis

Electrophysiological and subject screening results were analyzed in SPSS® via an ANOVA with Games-Howell post-hoc correction to compensate for the unequal group sizes and variances. Quiet standing metrics also used a post-hoc Games-Howell after ANOVA with repeated measures. Statistics on Mini-Mental Exam, Berg Balance Scale, RAND, acceleration thresholds, and SWM were performed in SPSS® with Kruskal-Wallis one-way ANOVA. The Kruskal-Wallis one-way ANOVA allowed us to account

for the subjects who did not reach threshold but went to the maximum allowed acceleration of the test for acceleration thresholds. The Kruskal-Wallis was performed pair-wise on groups as a post-hoc test. For SWM tests, geometric means are reported instead of the log values because of the power law nature of tactile perception.[174, 175]

2.3 Specifications for a New Lab

With a move to another university, we have had the chance to set up a second SLIP-FALLS-STEPm research lab for fundamental studies, while maintaining the original lab in a clinical setting within the VA research service. A series of specifications for the new lab, which I designed a new lab from, were presented[158] and listed below:

1. The essential elements of the user interface needed to remain the same as seen from the clinical environment.
2. The command and control aspects of the platform had to be functionally equivalent to previous implementations, and the previous code had to be reused when possible.
3. The operator should be provided a user-friendly interface with which to monitor the progress and output of all these processes in real-time during a testing sequence.
4. The number of channels of data collected by the FALLS protocol must be increased to allow for additional sensor and EMG inputs.
    a. The EMG channels were to be increased from the original four to a user-selectable between four and sixteen. The amount of support the safety harness provides to the subject should also be collected and calculated.

5. The researchers should upgrade to more sensitive sensors where needed.
6. The motion analysis system should be upgraded from a single camera, 2-D system to a multi-camera, 3-D system.
7. The FALLS data should be immediately stored in engineering units rather than in raw voltages that required post-possessing. EMG potentials should be converted on-line and stored as RMS time-series data with a further conversion to a percentage of that seen under maximal contraction if possible.

2.4 New Lab Solution

As our current setup was incapable of performing the required computations without long processing times causing testing delays, we focused on what was needed to meet these objectives. We needed a system that would remain under the Windows XP® operating system to maintain current software and equipment drivers. This requirement satisfied the first through third specifications. The remaining specifications required additional new or replacement equipment.

We developed a new multithreaded testing program in Labview® that allowed for same input methods as in previous versions. Via Labview® notifiers, processed data can be sent to the display terminal for viewing by tester. The software worked on the control and command system as previous testing protocols did. This equipment also satisfied the first three specifications for new lab setup.

To meet the fourth specification we had to upgrade our National Instruments® (NI®) multifunction data acquisition card (NI PCI 6034E®) with 16 analog inputs to a card supporting 32 analog inputs (NI PCIe 6259M®). We also freed up additional analog

input by rerouting the subject response (bell) to the digital inputs instead of counting peaks of analog input. To provide signal conditioning and signal access, we used an NI SC-2345® signal conditioner box for 16 channels and NI BNC 2090® terminal box for the other 16 channels and digital input and output. Originally, all signals were conditioned by separate external Daytronics® signal conditioning modules with numeric displays. Now, a National Instruments® SC-2345 system is used that enables us to do individual two-stage signal conditioning on each line if needed (e.g., strain gage Wheatstone bridge, followed by low pass filtering). The LabVIEW® mx driver software takes care of gain and offset calibration so that data is already in calibrated engineering units (i.e., mm), rather than in raw voltages. This automated scaling and unit conversion occurring at data collection decreases the need for post-processing and partially addresses our design criteria six.

The NI BNC 2090® has a dual functionality of allowing us access to EMG signals so they can be inputted into the Peak Motion® capture system. To acquire these signals in the Peak® system and to meet the fifth specification, the motion capture hardware had to be upgraded. Since the purchase of our previous system, Peak-Motus® was acquired by VICON®. This allowed us to upgrade to VICON's® superior cameras and hardware, while maintaining same user interface with updated Peak software. The new 16-channel Delsys Bagnoli® EMG amplifier has a 50-pin output connector that interfaces directly to a NI BNC-2090® breakout box that handles 16 analog input channels, but that also allows us access to these signals, as well as providing the DIO outputs and inputs from the data acquisition card. The EMG system had a gain of 1000 that saturated at ± 5 V. With the upgraded EMG system, we can acquire inputs from eight bilateral muscle groups on the

body via single or double differential electrodes. For the new testing setup, EMGs were acquired with the single differential electrodes for the gastrocnemius, tibialis anterior, and sternocleidomastoid muscles. To separate soleus activity from the gastrocnemius, a double differential electrode was used over the upper portion of the Achilles tendon. All EMGs were acquired bilaterally. These changes could allow EMGs to be monitored not only in the muscle groups about the ankle, but also the thigh, trunk, and neck muscles, which are now recorded.

We maintained the same hardware for our Tekscan HR Mat®. The Tekscan HR Mat® provides high-resolution foot pressure data. The pressure mat consists of 87x96 sensels (25 mm^2 each), which collect data at 50 Hz. The pressure mat confirms our own CoP calculation and has the ability to determine it in relation to regions of the foot. We are also able to determine the CoP, and its metrics, for each foot.

Using the DIO via NI BNC-2090® provided a much better method of recognizing a subject's response than analog input with peak detectors. It was setup so a subject could press one of two buttons on the Visonic® two-button wireless remote (WT-102®) to make responses based on platform movement. The WT-102® signals the WR-300 2B® receiver, which provides separate outputs for each button. Both outputs are inputted into separate digital inputs and a custom bell circuit to provide audio acknowledgement of button press to subject and tester.

The DIO on the BNC-2090® is the output for all synchronization signals. The Labview® controls the values for the three synchronizing signals: Tekscan® Start, Peak Start, and Peak Sync. Tekscan® Start signals the Tekscan I-Scan® software to begin recording when it goes high and to stop recording when it goes low. Peak® Start signals

the Peak-Motus® software to begin recording for a predetermined amount of time with a high pulse. Peak Sync signals the Peak-Motus® software, which synchronizes when the platform perturbation occurred with a high pulse.

The NI SC-2345® signal-conditioning unit provided analog data input for all non-EMG channels. Custom circuitry was developed on SC-FT-01® feedthrough- breadboard modules to provide necessary gain and null offsets to both the head and platform accelerometers. The circuitry provided a gain of 10 to the accelerometer output to provide ± 1 g range of acquirable data to the saturation of NI® data acquisition card (± 10 V). The Endevco® 7290-A was chosen as the accelerometer due to its ± 2 g range and 0.0005 g resolution. It is 10 times as sensitive as the original platform and head accelerometers. Three Endevco® 7290-A accelerometers were secured to a precisely milled steel cube to provide a single tri-axial accelerometer for the head. The accelerometers circuitry provided an output of one mV per mm/s^2. The gravitational acceleration was subtracted out for the vertical z-axis. The system maintained the original four load cells of the original force plate. We also still collect the position and motor current (shear force) from the Dover® controller.

For the final specification, the data had to be converted on the fly to engineering units without causing any testing delays. A computer was needed that could process parallel threads and not only use pre-emptive multitasking. New compact multi-processor server technologies were our focus for a new FALLS computer. We decided to purchase a Gateway® E-9515-R series server to meet the fourth specification.

Traditionally, computers multitasking in a network environment required a server-style operating system. Due to such a small consumer base, there were few hardware

drivers available, which have left a mark on those who had endeavored to use its power in the past. With the advent of Windows XP® to the general consumer, which is based off Microsoft's original server platform, the possibility of a user-friendly server platform became available. Windows XP® was chosen due to its widespread use and familiarity. Yet, Windows XP® is not supported for server systems that it can handle since companies make more money off the licensing fees of their server operating systems.

Windows XP® has both great hardware and software support, but it is difficult to purchase with a server from major computer manufacturers, because they want people to purchase one of their newly branded server operating systems, which keeps with the old tradition of having poor hardware and support for the everyday user and researcher. These server operating systems are expensive, which comes at the cost of paying per user license that allows for a true multi-user environment. Although this provides a limitation to the consumer, a multi-user environment would be a seldom-used feature in the lab environment. Since companies want the consumer to pay hundreds to thousands of dollars more for official server operating systems, they place limits on the software so it can only use a certain amount of the computer's resources.

Windows XP® has a limit of two physical processors, but thanks to new technologies in the central processing unit (CPU), the limitation has become less stifling. Our new server-class machine is composed of two Intel Xeon 2.8 GHz Dual-Core Processors® (Figure 2.2). Each core also contains hyper-threading technology that is similar to dual-core, but they share resources. The sharing of different resources is what differentiates hyper-threading and multi-core technologies from a full multiprocessor system. All cores on a multi-core processor share the same bus to peripherals and

memory but have separate registers and cache. Hyper-threading not only shares the same resources as their respective cores but also shares the respective core's registers and caches. Therefore, the software limitation imposed on us is met since we only have two physical processors. That limitation is downplayed since we have eight logical processors on which programs run.

To take advantage of extra processors, software today is multithreaded, which translates into breaking up the program into smaller operations that can run independently and asynchronously. New multithreaded programs are able to push the processing envelope by distributing the workload across all the logical CPUs. For our SLIP-FALLS-STEPm platform, we use Labview® to run our experiment, record data, process data, and synch with other research systems. Labview® provides a nice graphical programming interface so novice programmers can use it. It also allows for the flexibility in advanced programming for creating threaded applications, with communication streams between each, and for communicating with third party software.

The majority of our data analysis is performed in the Matlab® package. With Labview® 8.0, you have an easy way to script object code for communication and processing in Matlab®. Given that we integrated and threaded our data acquisition and analysis, we have virtually eliminated offline processing time. In addition, Matlab® can take advantage of Intel's Extended Memory 64-bit Technology® (EM64T). The EM64T® permits us to run Matlab® 64-bit on our server, which also requires a 64-bit operating system (Windows XP 64-bit®). With 64-bit software, the EM64T® allows one to address over 4GB of memory, which will dramatically decrease the processing time by removing

hard drive reads and writes due to virtual memory usage. In addition, the EM64T® provides 64 bits of precision for accurate calculations.

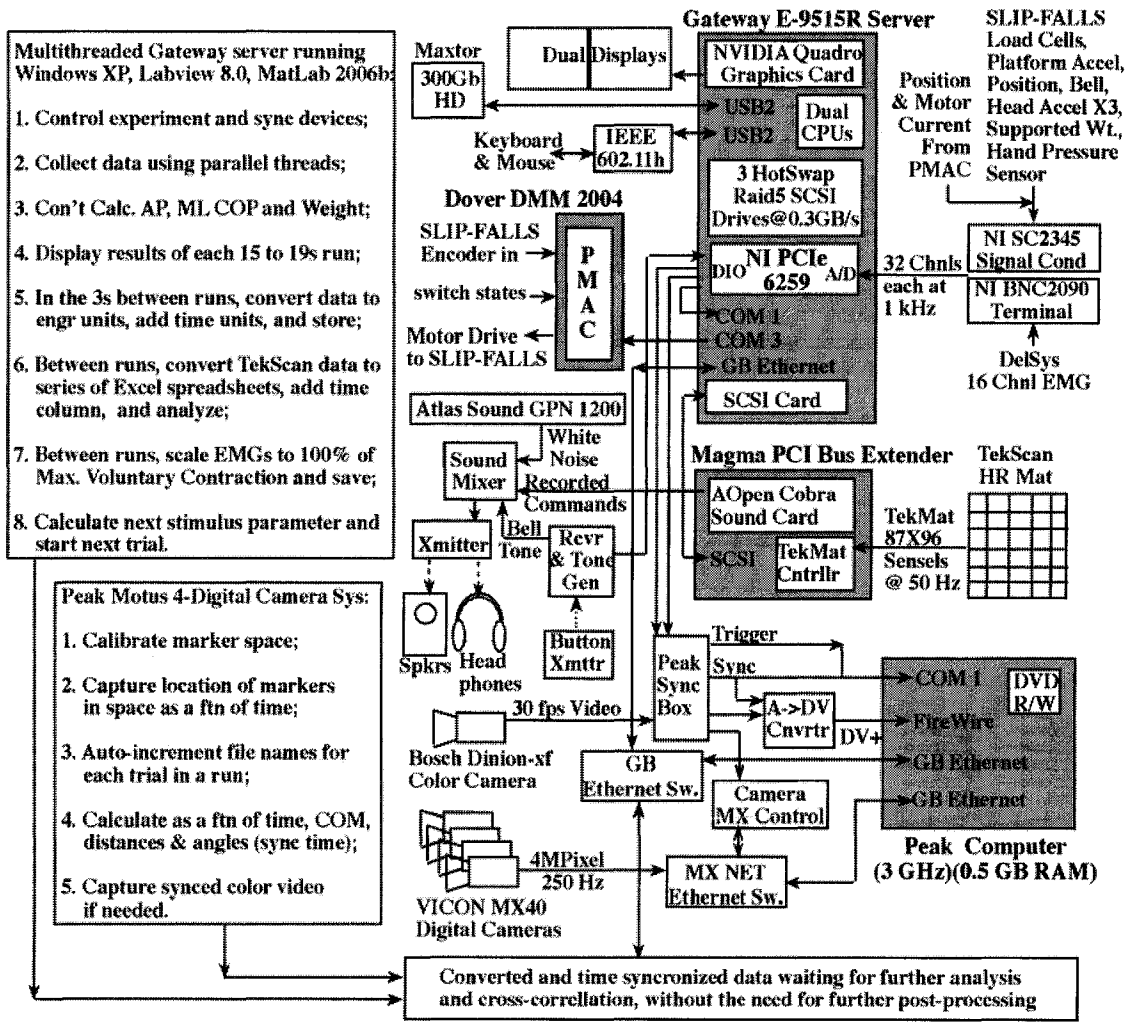

Figure 2.2. New equipment set up. A dual core, multi-processor Gateway® server running Windows XP®, Labview® 8.0 and Matlab® 2006b is the new FALLS computer. The Magma® PCI bus extender attached to it via a SCSI connection allows the use of vender cards with the older PCI bus structure. The graphics card in the computer supports up to four simultaneous monitors. Three hot-swappable 200GB drives are configured as a RAID 5 set, to provide for data collection redundancy. The A/D card is expanded to 32 channels, with 16 now coming via cable from a 16-channel Delsys® EMG amplifier. The Tekscan HR Mat® controller PCI card no longer resides in a separate machine, so that data can now be better time-synchronized. The motion capture system is upgraded to a four-camera system, each at four MPixel at 250 Hz, along with faster CPU. If desired, an analog video record of the test can be acquired. The output of the new system is such that no post-processing is required before correlative analyses can be carried out. [Figure from ASEE St. Lawrence Section Conference Student Paper[158]]

The new server provided the processing abilities to run Tekscan I-Scan® and our experimental protocol in Labview® simultaneously. Some older cards (audio and Tekscan® PCI cards) are set up for the old 5V protocol that was removed in the latest revision (3.0) to the PCI/PCX standard. We installed a rack-mounted PCI bus extension system by Magma®, which allowed up to four 5V PCI devices to share a single 3.0 PCI slot in the server and be backward-compatible. The bus extension worked well with the audio card (used for subject commands) and Tekscan® card (used for foot-pressure data acquisition) allowing us to incorporate both in our server configuration.

The small physical size of our server (form factor 2U of a rack enclosure) cuts down the volume of the equipment need for the testing system, which is aided by having low-profile PCI ports. We used low-profile PCI slots for a serial port (RS232) expansion card and SCSI 320 Mb/sec hot swappable RAID 5. The extra serial ports allowed us to control multiple pieces experimental hardware (Dover DMM 2004® and Tekscan HR Mat®), simultaneously. Using RAID 5 for disk storage gives great data protection with only minimal loss of space as opposed to mirroring the hard drives. By striping the data across the hard drives with a parity bit (RAID 5), it enables the user to rebuild a hard drive's data completely for high data security if one crashes. In addition, the speed of the hard-drive is increased by a factor greater than three, which cuts down on drive access time during file storage after processing.

Server hardware was not designed for any flashy graphics cards, and there is no set high-speed graphic bus to use. However, the server has the new PCIe standard that many high-powered video cards currently use today. For our test monitoring, we chose the workstation class video card by NVIDIA® because it gives us the ability to monitor

all test parameters simultaneously given its ability to run up to four digital monitors. Also on the PCIe bus, we have our National Instruments® data acquisition card.

The Vicon-Peak® system is a three-dimensional marker based camera system. The digital input and output (DIO) ports of the National Instruments® DIO allow for triggering and synchronizing the video capture data to test events. Synchronizing is needed since there is a delay before the cameras began recording. Synchronizing also allows the three-dimensional motion capture data to be aligned with the other data acquired by the server.

2.5Ankle Model

2.5.1 Software

Analysis routines were written in Matlab® to have access of the matrix mathematics functions. The program was object-oriented to allow for ease and robustness of expansion.[176] The software provided text (Excel® Spreadsheet), jpg (picture), and avi (video) output representing motion.

2.5.2 System representation

The simplest system has two segments and a single revolute joint. The reference frame for the first link is placed at the origin of a Cartesian coordinate system. The displacement vector ($\mathbf{d}_1$), the x, y, and z coordinates, represent the distance from the first segment's reference frame to the center of the first revolute. The limb local coordinates may be placed anywhere, including a location along the revolute axis. The α_1 and β_1 angles are the twist and cant angles of offset from the preceding segment's reference frame that are needed to align the revolute axis of motion with the z-axis of the preceding limb. In relation to the second limb, the α_2, β_2, and $\mathbf{d}_2$ are the variables defined that are

needed to rotate the axis of rotation to align with z-axis of the next segment and to find the distance from the joint center to the following segment's center. Setting subsequent displacement vectors to zero simulates saddle (2-orthogonal revolute joints) and ball and socket joints (3-othogonal revolute joints).

CHAPTER 3

DIABETIC POSTURAL CONTROL

Our objective was to show that detriments to postural control exist prior to the development of peripheral neuropathy in Type-2 diabetes with no fall history. This study tested diabetic mature adults with peripheral neuropathy (DPN: n=17, nerve conduction velocity < 40 m/s) and without peripheral neuropathy (DNI: n=11) and healthy mature adults (HMA: n=34), all aged 50 to 74 years. No nerve conduction or latency differences existed between HMA and DNI. All underwent static and quasi-static postural assessments, with the latter assessed by short anterior platform perturbations.

3.1 Hypotheses

3.1.1 Acceleration Threshold Hypotheses

- Diabetic mature adults with peripheral neuropathy would have higher acceleration thresholds than those who are neurally intact and healthy mature adults.

3.1.2 Quiet Standing Metrics Hypotheses

- Diabetic mature adults with peripheral neuropathy would have higher mean distance of sway than those who are neurally intact and healthy mature adults

- Diabetic mature adults with peripheral neuropathy would have higher root mean square distance of sway than those who are neurally intact and healthy mature adults.
- Diabetic mature adults with peripheral neuropathy would have higher range of sway than those who are neurally intact and healthy mature adults.
- Diabetic mature adults with peripheral neuropathy would have higher area of sway than those who are neurally intact and healthy mature adults.
- Diabetic mature adults with peripheral neuropathy would have larger 95% confidence circle and ellipse of sway than those who are neurally intact and healthy mature adults.
- Diabetic mature adults with peripheral neuropathy would have higher fractal dimensions of sway than those who are neurally intact and healthy mature adults.
- Diabetic mature adults with peripheral neuropathy would have different frequency components of sway than those who are neurally intact and healthy mature adults.

3.1.3 Physiological Measure
Hypotheses

- Diabetic mature adults with peripheral neuropathy would have lower nerve conduction velocities than those who are neurally intact and healthy mature adults.
- Diabetic mature adults with peripheral neuropathy would have higher Semmes-Weinstein monofilament thresholds than those who are neurally intact and healthy mature adults.

3.1.4 Self-reported Health Measures
Hypotheses

- Diabetic mature adults with peripheral neuropathy would have poorer self-reported health scores than those who are neurally intact and healthy mature adults.

3.2 Subjects

Our subjects were well-controlled diabetic mature adults with peripheral neuropathy (DPN: 4 female and 13 male) and without peripheral neuropathy (DNI: 4 female and 7 male) and healthy mature adults (HMA: 14 female and 20 male). To enable a precise comparison, only subjects who completed our entire electrophysiological and acceleration threshold test protocol were used for this analysis. Their primary care physician had previously diagnosed each DPN or DNI with Type-2 diabetes. Subject recruiting took place via flyer advertising at the Overton Brooks VA hospital in Shreveport, Louisiana, and in the local area. Individuals from 50 to 75 years of age, inclusive, were labeled as mature adults. Our test protocol was approved by the IRBs of the Shreveport VAMC and Louisiana Tech University.

3.3 Screening

A medical history questionnaire was given to each potential subject. Individuals were not tested further if they had a medical history of cardiovascular and/or respiratory disease, neurological problems such as cerebrovascular disease, stroke, head or spine injury, vestibular ailments and dizziness, memory and concentration deficits, muscle activity deficits, or non-healing skin ulcers. Orthopaedic problems such as lower back pain or spasms, arthritis or joint disease, and deformations of joints or bones led to

exclusion of individuals from the study. Those with past or current drug or alcohol dependence were also excluded.

All consented subjects were screened with the Berg Balance Scale and Sharpened Romberg Test to assure that they were able to operate independently from assistance, and their vision was tested (Snellen Eye Chart). In addition, the subjects were tested with the Mini-Mental State Exam to insure that they were mentally competent to follow instructions during the experiment. Patellar and Achilles' reflexes were tested to confirm that they were present and normal. The DPN and DNI groups had hemoglobin A1c values below 9%., with no group differences seen in values or in number of subjects with values >7.0 (4 DPN, 2 DNI).

A temporary classification of Healthy Mature Adult (HMA) was made for all consenting subjects who reported no history of diabetes or neurological impairment. Perturbation testing on all of our subjects commenced before, during, or after the nerve conduction tests were carried out, as the scheduling of the nerve conduction velocity tests by the Neurology Service were on a fill-in basis between clinical tests. Once the nerve conduction velocity results were in, a final classification into an HMA group could be made. Of the 46 individuals without a history of diabetes that went through our protocol, 34 were classed as HMA and are studied here. The remaining twelve were positive for peripheral neuropathy during the nerve conduction velocity testing. These individuals were excluded from this analysis since we did not know the cause or the extent of the neuropathy, as Nardone et al. showed that different types of peripheral neuropathy affect postural stability to different degrees, and we could not rule out diabetes, given the epidemic prevalence of undiagnosed diabetes in mature adults.[16, 36, 37]

3.4 Procedures

The preceding tests provide physiological backgrounds on individuals for our posture test protocol. The 2-Alternate Forced Choice acceleration thresholds to forward perturbations of constant displacement were carried out on the SLIP-FALLS-STEPm platform while subjects were blindfolded.[11] The acceleration was varied based on a modified version of the parameter estimation by sequential testing (mPEST) method.[92, 177] During the first ten trials, two consecutive correct responses (1-up-2-down method) were required to decrease acceleration, whereas only three (1-up-3-down method) were needed afterwards, which increased the statistical power behind the threshold.[177] The 1-up-2-down and 1-up-3-down methods provided 70.7% and 79.4% correct responses, respectively, to attain a reliable psychophysical threshold.[90]

Threshold was said to be reached when increments became less than 2% of the original increment value unless the subject completed all 30 trials where we required 79% correct at a specific acceleration to be taken as threshold.[90] Air bearings insure that the ultra-low vibration, frictionless platform provides no movement cues and allows for the test of movements within the range of sway. The subjected is presented via wireless headphones pre-recorded commands with white masking noise of "Ready," "One," "Two," and "Decide." During the four second decision period, the subject must decide in which period he or she perceived the perturbation to have occurred, by a single (Interval 1) or double (interval 2) bell press. The subject needed to accrue a correct detection percentage of 79% for an acceleration to be considered threshold. The platform moves in a 100% smoothed s-curve, which allows for symmetrical acceleration and deceleration of which the peaks are used as the measurement for threshold.[8, 11]

3.5 Results

We hypothesized the peripheral neuropathy secondary to Type-2 diabetes would cause a decreased ability to detect subtle platform perturbations. We found instead that the ability to detect platform perturbations is diminished in well-controlled diabetic mature adults with peripheral neuropathy (DPN) and without peripheral neuropathy (DNI), both as compared to healthy mature adults (HMA), suggesting that the presence of diabetes itself was a major factor in an increased detection threshold.

3.5.1 Subjects

There was no significant difference in age, height (h), or body mass index (BMI) (Eq. 27) between DNIs, DPNs, and HMAs.

$$BMI = \frac{m}{h^2} \tag{27}$$

While mass (m) was not significantly different between HMA and DNI or DNI and DPN, it was significantly different ($p < 0.05$) between HMA (83.2 kg) and DPN (98.3 kg), as shown in Table 3.1.

Table 3.1. Subject Information.

	HMA (n=34)			DNI (n=11)			DPN (n=17)		
	Mean	95% CI		Mean	95% CI		Mean	95% CI	
Age (yrs)	57.4	±	2.16	59.1	±	5.31	60.9	±	2.72
Height (m)	1.68	±	0.03	1.69	±	0.06	1.74	±	0.05
Mass (kg)	83.2*	±	5.6	97.8	±	17.12	98.3	±	9.28
Body Mass Index (kg/m^2)	29.5	±	1.71	33.7	±	4.22	32.7	±	3.18

* HMA vs. DPN $p<0.05$.

3.5.2 Peak Acceleration Thresholds

A difference exists in DNI and DPN acceleration threshold values for all move displacements (Figure 3.1). Both DNI and DPN had significantly higher thresholds than HMA at 1 mm ($p<0.01$) and 4 mm ($p<0.01$ and $p<0.05$, respectively) displacements (Table 3.2). A strong trend was also noted for significantly increased threshold of DNI over HMA ($p=0.054$).

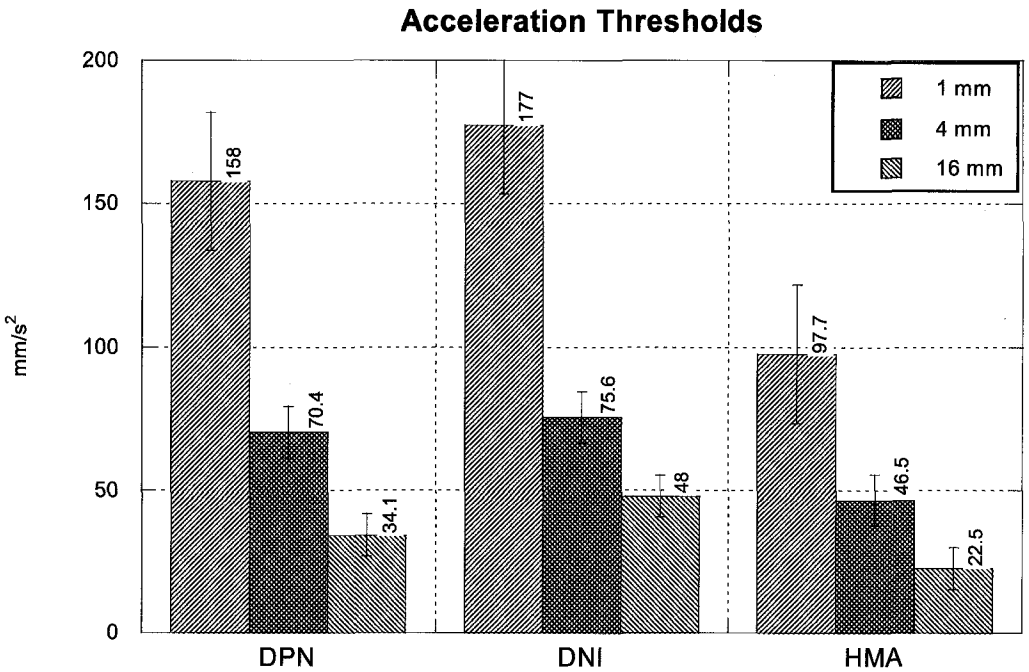

Figure 3.1. The left-slanting lines refer a 1mm move. The cross-hatched lines refer to a 4 mm move. The right-slanting lines refer to a 16 mm move. Error bars provide the standard error. DPN and DNI show pronounced decreased acuity in detecting small anterior perturbations as compared to HMA at 1 and 4 mm movements. Values are the arithmetic means.

Table 3.2. Detection Thresholds.

	HMA (n=34)		DNI (n=11)		DPN (n=17)	
	gMean	aMean	gMean	aMean	gMean	aMean
Acceleration	mm/s^2					
1 mm	78.4[*†]	97.7	158.2	177.4	143.4	157.9
4 mm	34.1[†‡]	46.5	59.4	75.6	54.8	70.4
16 mm	16.4[§]	22.5	32.0	48.0	23.4	34.1
Peak Kinetic Energy	mJ					
1 mm	3.20[*¶]	4.14	7.48	8.58	6.94	7.85
4 mm	1.39[‡¶]	2.05	2.81	3.85	2.65	3.51
16 mm	0.67[¶‖]	0.95	1.51	2.44	1.13	1.71

[*] HMA vs. DPN $p<0.01$ [†] HMA vs. DNI $p<0.01$ [‡] HMA vs. DPN $p<0.05$
[¶] HMA vs. DNI $p<0.05$ [‖] HMA vs. DPN $p=0.058$ [§] HMA vs. DNI $p=0.054$. The gMean is the geometric mean of the SWM due to their log nature. The arithmetic means, aMean, are including solely for comparison.

Using the calculated peak energy imparted on the subject, we gain significantly higher peak energies ($p<0.05$) for DNI over HMA for all displacements. While significantly higher imparted peak energies were seen in DPN over HMA for 1 mm ($p<0.01$) and 4 mm ($p<0.05$) displacements, only a strong trend was noted for the 16 mm displacement. Due to safety constraints of our system, we set a maximal peak acceleration value at 200 mm/s^2 for 1 mm moves and 100 mm/s^2 for 4 mm and 16 mm moves. A number of subjects reached these values (rail condition). Analysis of the negative power-law relationship [7, 15, 174, 175, 178] between acceleration and displacement values provided reason to raise the maximum peak acceleration test values

to 256, 181, and 128 mm/s^2 (or 2^8, $2^{7.5}$,and 2^7 mm/s^2) respectively for 1 mm, 4 mm, and 16 mm perturbations. HMA subjects reaching the rail (11%, 3%, and 0%) were fewer than both DPN (41%, 18%, and 6%) and DNI (63%, 36%, and 18%) at 1 mm, 4 mm and 16 mm displacement respectively as seen in Table 3.3.

Table 3.3. Rail Conditions.

	1mm	4mm	16mm
HMA	4 (11%)	3 (9%)	0 (0%)
	2 @ 200 mm/s^2	1 @ 100 mm/s^2	0
	2 @ 256 mm/s^2	2 @ 181 mm/s^2	0
DNI	7 (63%)	4 (36%)	2 (18%)
	2 @ 200 mm/s^2	4 @ 100 mm/s^2	2 @ 100 mm/s^2
	2 @ 200 mm/s^2		
DPN	7 (41%)	3 (18%)	1 (6%)
	2 @ 200 mm/s^2	3 @ 100 mm/s^2	1 @ 100 mm/s^2
	2 @ 200 mm/s^2		

3.5.3 Quiet Standing Metrics

In the anterior-posterior time-series, significant ($p < 0.05$) differences were seen in range, standard deviation, and RMS distance for HMA versus DPN (Table 3.4). The total power for anterior-posterior was significantly increased ($p < 0.01$) for the DPN versus HMA. Trends in HMA versus DPN groups were seen with increased mean resultant distance, mean anterior-posterior distance, RMS distance, anterior-posterior total excursion, and anterior-posterior mean velocity. No differences were seen between DNI

and either DPN or HMA groups. In addition, no differences were seen between any group for fractal dimensions, sway area, and frequency components except total power.

Table 3.4. Quiet Standing Metrics.

	HMA (n=34)			DNI (n=11)			DPN (n=17)		
	Mean	95% CI		Mean	95% CI		Mean	95% CI	
Stddev RD	2.5	±	0.6	3.2	±	3.1	3.1	±	1.0
Stddev AP	4.0*	±	0.7	4.7	±	2.6	5.0	±	1.4
Stddev ML	2.7	±	0.9	3.6	±	5.2	3.5	±	1.6
Range-RD	13.1	±	3.4	16.4	±	17.2	15.5	±	5.7
Range-AP	19.2*	±	3.5	23.4	±	13.4	24.6	±	7.6
Range-ML	14.7	±	5.6	17.7	±	25.5	17.1	±	8.2
Mean Dist RD	4.2†	±	0.9	5.3	±	4.5	5.3	±	1.8
Mean Distance-AP	3.2†	±	0.6	3.8	±	2.1	3.9	±	1.1
Mean Distance-ML	2.1	±	0.6	2.8	±	3.7	2.7	±	1.3
RMS Distance-RD	4.9†	±	1.1	6.2	±	5.5	6.2	±	2.0
RMS Distance-AP	4.0*	±	0.7	4.7	±	2.6	5.0	±	1.4
RMS Distance-ML	2.7	±	0.9	3.6	±	5.2	3.5	±	1.6
Total Excursion-RD	230.2	±	64.0	288.0	±	189.1	295.6	±	121.1
Total Excursion-AP	178.3†	±	47.0	221.7	±	100.4	235.0	±	97.7
Total Excursion-ML	111.1	±	40.3	134.7	±	149.9	132.1	±	60.4
Mean Velocity-RD	11.5	±	3.2	14.4	±	9.5	14.8	±	6.1
Mean Velocity-AP	8.9†	±	2.4	11.1	±	5.0	11.7	±	4.9
Mean Velocity-ML	5.6	±	2.0	6.7	±	7.5	6.6	±	3.0
Mean Frequency-RD	0.5	±	0.1	0.5	±	0.1	0.5	±	0.1
Mean Frequency-AP	0.5	±	0.1	0.6	±	0.1	0.5	±	0.2
Mean Frequency-ML	0.5	±	0.1	0.5	±	0.2	0.5	±	0.1
95% Conf. Area Circle	269.5	±	138.0	571.1	±	1370.9	395.8	±	259.2
Sway Area	17.8	±	9.5	34.6	±	81.3	26.3	±	18.3
95% Conf. Area Ellipse	225.3	±	117.4	437.2	±	1036.8	339.8	±	240.9
Fractal Dimension Circle	1.4	±	0.0	1.4	±	0.1	1.4	±	0.1
Fractal Dimension Ellipse	1.4	±	0.0	1.4	±	0.0	1.4	±	0.1
Total Power-RD	42400	±	26235	94362	±	234490	60375	±	36617
Total Power-AP	67467‡	±	26878	122807	±	184208	121177	±	59236
Total Power-ML	50774	±	58018	183355	±	696399	60522	±	61366
Median Frequency-RD	0.3	±	0.1	0.4	±	0.1	0.4	±	0.2
Median Frequency-AP	0.2	±	0.1	0.3	±	0.1	0.3	±	0.1
Median Frequency-ML	0.2	±	0.1	0.2	±	0.1	0.2	±	0.1
95% peak frequency-RD	1.6	±	0.4	1.8	±	0.4	1.7	±	0.5
95% peak frequency-AP	1.4	±	0.4	1.4	±	0.4	1.3	±	0.3
95% peak frequency-ML	1.2	±	0.3	1.3	±	0.4	1.3	±	0.4
Centroid Frequency-RD	1.0	±	0.1	1.1	±	0.2	1.1	±	0.2
Centroid Frequency-AP	0.9	±	0.1	0.9	±	0.2	0.9	±	0.1
Centroid Frequency-ML	0.9	±	0.1	0.9	±	0.2	0.9	±	0.2
Frequency Disp-RD	0.6	±	0.04	0.6	±	0.08	0.6	±	0.05
Frequency Disp-AP	0.6	±	0.04	0.6	±	0.07	0.6	±	0.05
Frequency Disp-ML	0.7	±	0.04	0.7	±	0.08	0.7	±	0.04

* HMA vs. DPN $p<0.05$, † HMA vs. DPN $p<0.1$, ‡ HMA vs. DPN $p<0.01$ All metrics based on mm. Frequency metrics are in Hz. Mean Velocity is in mm/s. Area metrics are in mm^2.

3.5.4 Health Surveys

The mean scores on all health survey results (except for the RAND emotional well-being) score were better for HMA than for DNI and DPN, but not all mean differences were significant (Table 3.5). Although the scores on the Berg Balance Scale were within an acceptable range for DNI and DPN (they showed no risk of falls and could operate independently), these latter scores were still significantly lower than those of HMA. The only significant group difference gained from the RAND survey was in general health. Both DPN and DNI showed significant decreased feelings of general health ($p<0.05$ and $p<0.01$, respectively). Strong trends were observed in RAND measures of pain and physical health [pain in HMA vs. DPN ($p=0.06$) and in HMA vs. DNI ($p=0.051$); physical health in HMA vs. DPN ($p=0.06$)]. No significance was seen between diabetic subjects with or without lower limb peripheral neuropathy.

Table 3.5. Health Surveys.

	HMA			DNI			DPN		
	n	Mean	Rank	n	Mean	Rank	n	Mean	Rank
Mini-Mental Exam	34	29.6	34.91	11	29.0	26.32	17	29.3	28.03
BERG	34	56.0*†	34.00	11	55.5	23.18	16	55.7	30.00
RAND	Modified SF-36 with depression screener								
Physical Function	32	84.0	32.72	11	78.5	26.86	16	75.9	26.72
Physical Health	32	85.2‡	33.56	11	73.8	27.09	16	67.6	24.88
Emotional Health	32	84.4	31.48	11	78.4	28.55	16	78.0	28.03
Emotional Well-Being	32	76.4	30.69	11	77.6	27.82	16	75.9	30.13
Energy/ Fatigue	32	67.3	32.42	11	63.3	30.00	16	56.6	25.16
Social Function	32	87.1	33.25	11	82.2	26.77	16	80.2	25.72
Pain	32	83.4‡¶	34.77	11	69.8	23.23	16	70.6	25.13
General Health	32	76.9*†	36.47	11	58.5	20.91	16	63.0	23.31

* HMA vs. DPN $p<0.05$ † HMA vs. DNI $p<0.01$ ‡ HMA vs. DPN $p=0.06$ ¶ HMA vs. DNI $p=0.051$

3.5.5 Foot Sensitivity

SWM testing displayed several significant differences in the geometric mean among the groups (Table 3.6). Bilateral significant differences provide a more significant measure of tactile sensory acuity. The first and fourth metatarsals had significantly different bilateral thresholds between HMA and DPN. The significance at the first metatarsal is higher ($p<0.01$) than at the fourth metatarsal ($p<0.05$). SWM of HMA had geometric means of thresholds less than 0.77 g for both first and fourth metatarsal

bilaterally, while DPN had thresholds greater than 1.49 g. None of the geometric means is above the threshold for developing diabetic ulcers (>10.0 g) for HMA, DNI, or DPN; however, two DNI and five DPN subjects did have thresholds at risk for developing ulcers, while no HMA did. Thresholds of the fourth metatarsal differed bilaterally, significant and trend, respectively, for the left ($p<0.05$) and right ($p=0.062$) feet, between HMA and DNI. DPN had a significantly higher ($p<0.05$) SWM threshold at the left heel versus HMA, but none was seen in the right heel. DNI had a significant bilateral decrease in thresholds versus HMA at the heel. There was not a significant difference seen at the 0.05 level for any measures between DNI and DPN. No differences were seen in the right great toe and only for DPN versus HMA for the left great toe.

Table 3.6. Semmes-Weinstein Monofilament Test.

	HMA			DNI			DPN		
	n	gMean	aMean	n	gMean	aMean	n	gMean	aMean
Left Great Toe	34	0.45*	0.99	11	0.59	0.81	17	1.72	3.18
Left 1st MT	34	0.44†	0.79	11	0.74‡	2.11	17	2.10	7.74
Left 4th MT	20	0.59*¶	0.96	8	2.15	4.02	11	1.64	3.24
Left Heel	21	1.91*‖	3.34	8	9.94	41.11	12	8.41	21.55
Right Great Toe	34	0.44	0.78	11	0.78	1.02	17	1.32	2.59
Right 1st MT	34	0.51†	0.76	11	0.70	1.16	17	1.49	3.91
Right 4th MT	20	0.77*§	1.15	8	1.20	2.02	11	2.75	11.20
Right Heel	21	2.30¶	3.08	8	6.33	7.75	12	5.45	14.74

* HMA vs. DPN $p<0.05$ † HMA vs. DPN $p<0.01$ ‡ DNI vs. DPN $p=0.07$
¶ HMA vs. DNI $p<0.05$ ‖ HMA vs. DNI $p<0.01$ § HMA vs. DNI $p=0.062$. The gMean is the geometric mean of the thresholds due to their power law perceptual relationship between displacement and acceleration threshold. All units are in grams. The arithmetic means, aMean, are including solely for comparison. MT is Metatarsal.

3.5.6 Lower Limb Electrophysiology

Both DNI and HMA have higher ($p<0.01$) nerve conduction velocities than DPN bilaterally for the peroneal, tibial, and sural nerves (Table 3.7). No difference was observed in nerve conduction velocities between HMA and DNI. No bilateral difference was observed for the M-wave latency test. The weaker significance in the tibial M-wave latency test can be attributed to the increased variance as seen in Table 3.7 by the 95% confidence interval, which for both DPN and DNI was greater than double the 95% confidence interval of HMA. Between HMA and DPN, bilateral significance ($p<0.01$ for all except left peroneal $p<0.05$) was seen for both peroneal and tibial nerves in the

F-wave latency test. Significant lower ($p<0.05$) latencies were seen in DPN versus DNI for all F-wave latencies except that of the left peroneal.

Table 3.7. Electrophysiology Results.

	HMA				DNI				DPN			
	n	Mean	95% CI		n	Mean	95% CI		N	Mean	95% CI	
Conduction Velocity (m/s)												
L. Peroneal	34	46.9*	±	1.31	11	45.4†	±	1.86	17	40.5	±	1.89
L. Tibial	34	45.8*	±	1.30	11	46.4†	±	1.88	17	39.6	±	1.92
L. Sural	28	45.1*	±	1.30	7	44.7†	±	3.36	12	39.3	±	2.72
R. Peroneal	34	46.9*	±	1.28	11	46.1†	±	2.18	17	40.3	±	2.03
R. Tibial	34	45.6*	±	1.71	11	45.9†	±	2.41	16	40.5	±	2.37
R. Sural	28	44.9*	±	1.39	7	46.0†	±	2.62	12	38.9	±	2.26
Conduction Latency (ms) for M-wave and F-wave tests												
M. L. Peron.	34	4.5	±	0.37	11	4.5	±	0.44	16	5.1	±	0.48
M. L. Tibial	33	4.3‡	±	0.41	11	4.7	±	1.21	16	5.8	±	1.09
M. R. Peron.	33	4.7*	±	0.34	11	4.6†	±	0.27	15	5.8	±	0.51
M. R. Tibial	33	4.5	±	0.52	11	5.4	±	1.12	15	5.5	±	1.09
F. L. Peron.	33	50.1‡	±	1.78	11	51.9	±	3.00	16	56.9	±	4.22
F. L. Tibial	33	51.9*	±	1.86	11	55.3¶	±	2.65	16	60.9	±	3.14
F. R. Peron.	33	49.8*	±	2.62	11	51.0¶	±	3.10	15	57.2	±	4.03
F. R. Tibial	31	53.1*	±	1.56	11	53.5¶	±	3.87	15	60.8	±	4.10

* HMA vs. DPN $p<0.01$ † DNI vs. DPN $p<0.01$ ‡ HMA vs. DPN $p<0.05$
¶ DNI vs. DPN $p<0.05$.

3.6 Summary

The DMAs with and without peripheral neuropathy show increased threshold for the detection of movement, which is believed increase their risk of falls since they would be less likely to detect an initiation of a fall, and disproved our acceleration threshold hypothesis. However, only DPN displayed significantly different quiet standing metrics compared to HMA, which leads to nerve conduction as a possible cause of the instability. Quiet standing metrics hypotheses one through three were found to be true for APCoP distance metrics. The fourth and fifth quiet standing metric hypotheses for sway area and 95% confidence interval of ellipse and circle were proven false. The sixth quiet standing hypothesis on frequency was found to only be true for APCoP power. For physiological measures, DPN's nerve conduction velocities were significantly different from both DNI and HMA, which supported the first physiological hypothesis. The lack of difference for Semmes-Weinstein monofilament thresholds between DPN and DNI give rise those cutaneous sensory deficits either precede peripheral neuropathy or has a separate cause, which proves the second physiological hypothesis wrong. The self-reported health measure hypothesis was wrong because both DPN and DNI reported poorer general health than HMA.

CHAPTER 4

HEARING LOSS AND TYPE-2 DIABETES

4.1 Hypotheses

- Diabetic mature adults would have a higher level of hearing loss than age-matched controls.

4.2 Subjects

Our subjects were a subset of our previous population. They were diabetic mature adults (DMA: 6 female and 18 male) with peripheral neuropathy (PN) and without peripheral neuropathy (NI) and healthy mature adults (HMA: 13 female and 14 male). To enable a precise comparison, only subjects who completed our entire electrophysiological, audiological, and acceleration threshold test protocol were used for this analysis. Their primary care physician had previously diagnosed each DMA with Type-2 diabetes. Subject recruiting took place via flyer advertising at the Overton Brooks VA hospital in Shreveport, Louisiana, and in the local area. Individuals from 50 to 75 years of age, inclusive, were labeled as mature adults. Our test protocol was approved by the IRBs of the Shreveport VAMC and Louisiana Tech University.

4.3 Screening

A medical history questionnaire was given to each potential subject. Individuals were not tested further if they had a medical history of cardiovascular and/or respiratory disease, neurological problems such as cerebrovascular disease, stroke, head or spine injury, vestibular ailments and dizziness, memory and concentration deficits, muscle activity deficits, or non-healing skin ulcers. Orthopaedic problems such as lower back pain or spasms, arthritis or joint disease, and deformations of joints or bones led to exclusion of individuals from the study. Those with past or current drug or alcohol dependence were also excluded.

All consented subjects were screened with the Berg Balance Scale and Sharpened Romberg Test to assure that they were able to operate independently from assistance, and vision was tested (Snellen Eye Chart). In addition, the subjects were tested with the Mini-Mental State Exam to insure that they were mentally competent to follow instructions during the experiment. Patellar and Achilles' reflexes were tested to confirm that they were present and normal. DMA had hemoglobin A1c values below 9%. (Six DMA had values >7.0).

4.4 Procedures

The preceding tests provide physiological backgrounds on individuals for our posture test protocol. The 2-Alternate Forced Choice acceleration thresholds to forward perturbations of constant displacement were carried out on the SLIP-FALLS-STEPm platform while blindfolded.[11] The acceleration was varied based on a modified version of the parameter estimation by sequential testing (mPEST) method.[92, 177] During the first 10 trials, two consecutive correct responses (1-up-2-down method) were required to

decrease acceleration, whereas only three (1-up-3-down method) were needed afterwards which increased the statistical power behind the threshold.[177] The 1-up-2-down and 1-up-3-down methods provided 70.7% and 79.4% correct responses, respectively, to attain.[90] Threshold was said to be reached when increment became less that 2% of the original increment value unless the subject completed all 30 trials where we required 79% correct at a specific acceleration to be taken as threshold.[90] Air bearings insure that the ultra-low vibration, frictionless platform provides no movement cues and allows for the test of movements within the range of sway. The subjected is presented via wireless headphones pre-recorded commands with white masking noise of "Ready," "One," "Two," and "Decide." During the four second decision period, the subject must decide in which period he or she perceived the perturbation to have occurred, by a single (Interval 1) or double (interval 2) bell press. The subject needed to accrue a correct detection percentage of 79% for an acceleration to be considered threshold. The platform moves in a 100% smoothed s-curve, which allows for symmetrical acceleration and deceleration of which the peaks are used as the measurement for threshold.[8, 11]

Air-conduction hearing exams were conducted at 1, 2, 4, and 8 kHz and measured in decibels of hearing loss (dBHL). Audiology exams were given by certified audiologists at Overton Brooks VA Medical Center using large cushion headphones to reduce crossover and ambient noise. All subjects who had confounding factors for hearing loss such as cerumen build up and close proximity to gun or cannon blast were excluded from analysis.

4.5 Results

4.5.1 Acceleration Thresholds

As was the case also for our previous analysis, DMA with PN did not differ from those who were NI in acceleration thresholds (Figure 4.1). DMA displayed a significantly decreased ability to detect forward perturbations at 1 and 4 mm than HMA ($p < 0.003$ and $p < 0.002$).

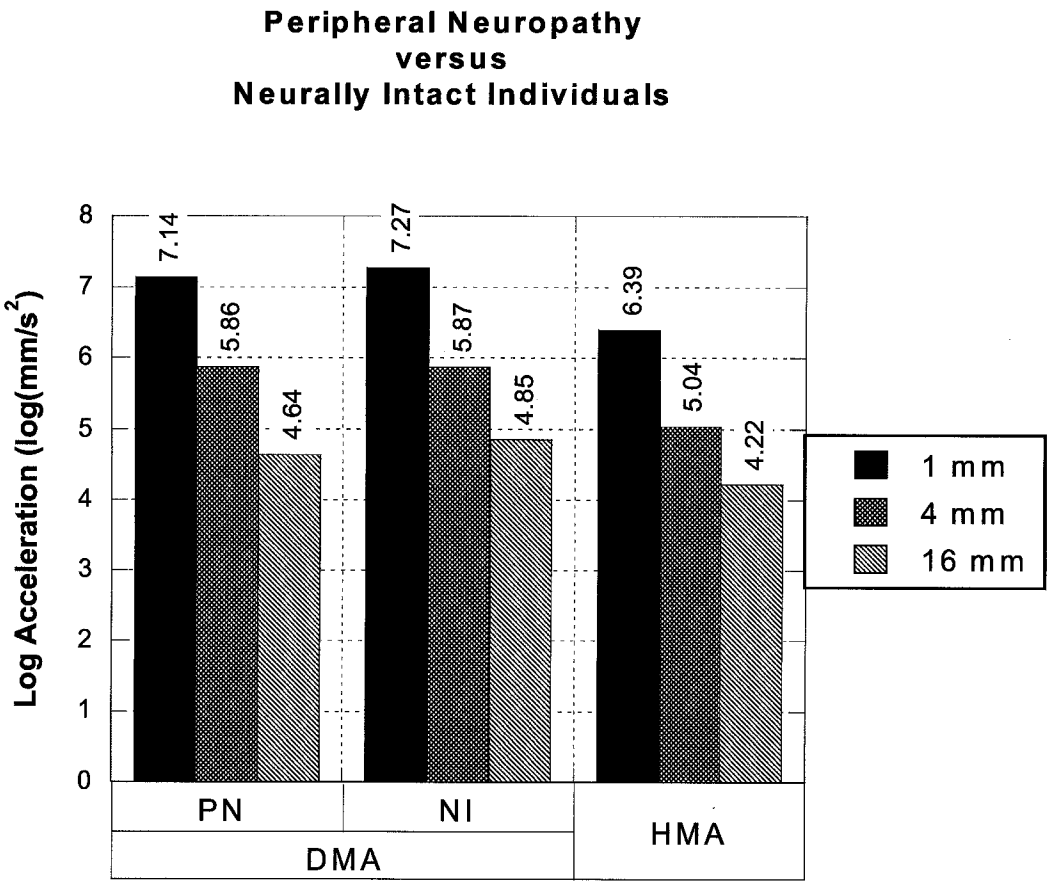

Figure 4.1. Acceleration thresholds for those with hearing tests.

4.5.2 Hearing Loss

4.5.2.1 DMA versus HMA

DMA showed significantly more hearing loss than HMA at 4 and 8 kHz bilaterally ($p < 0.027$ and $p < 0.007$ respectively). No significant difference was found at 1 kHz and 2 kHz (Figure 4.2).

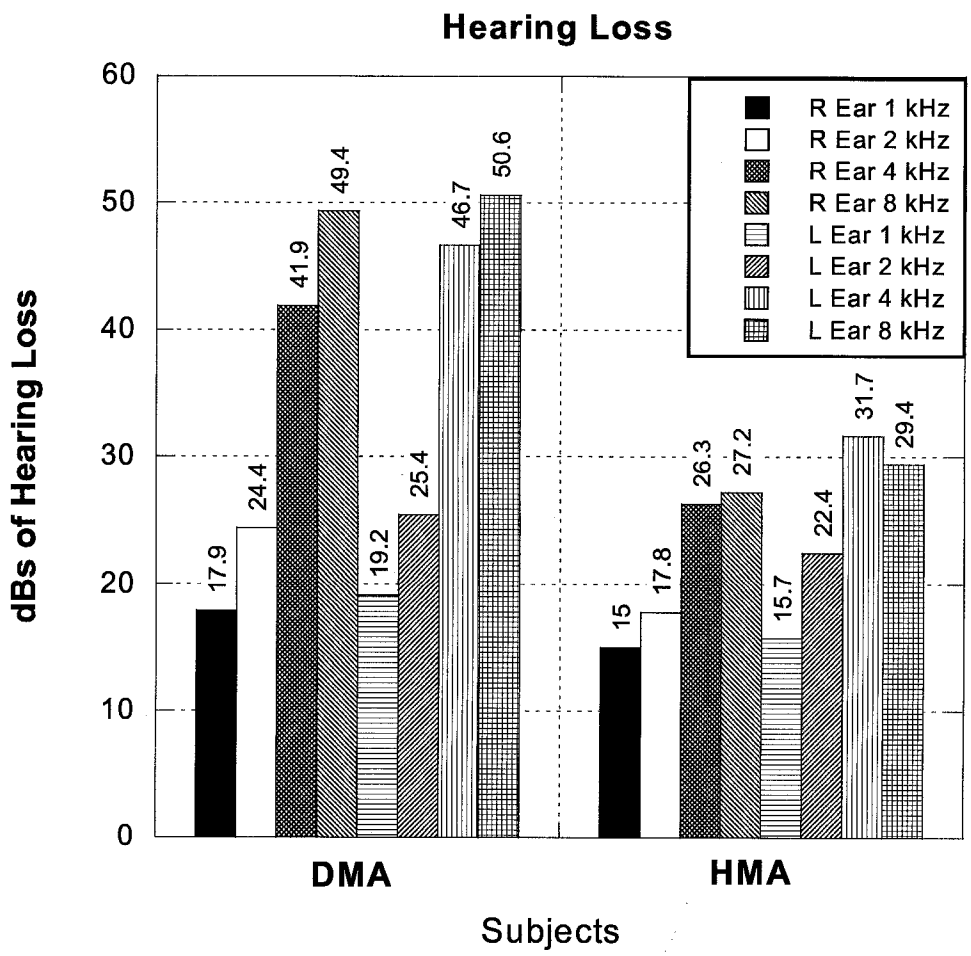

Figure 4.2. Hearing loss DMA vs. HMA.

Hearing Loss in DMA at 4 and 8 kHz is greater than HMA for both PN and NI, but 4 kHz Hearing Loss is less in NI than in PN (Figure 4.3).

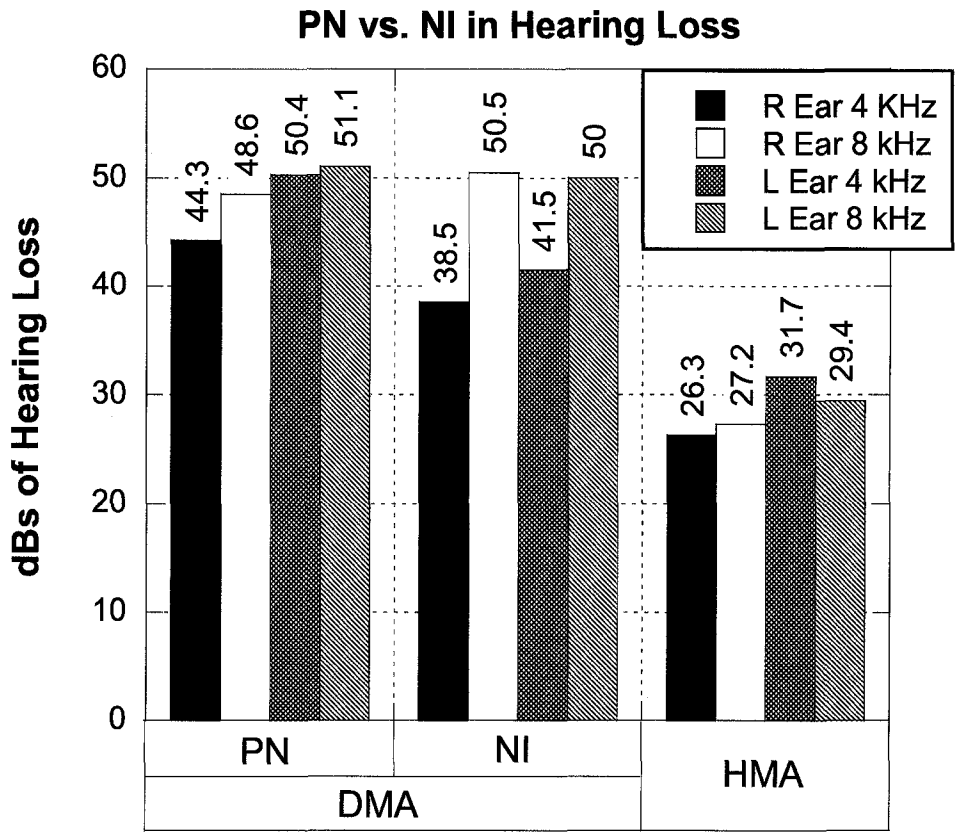

Figure 4.3. Hearing loss PN vs. NI vs. HMA.

4.5.2.2 Sex Related Differences

Male DMA have significantly more hearing loss than other groups at 4 and 8 kHz except on the left ear at 4 kHz versus male HMA (Figure 4.4). No difference is seen between women DMA and HMA, but this lack may be attributed to their low sample size.

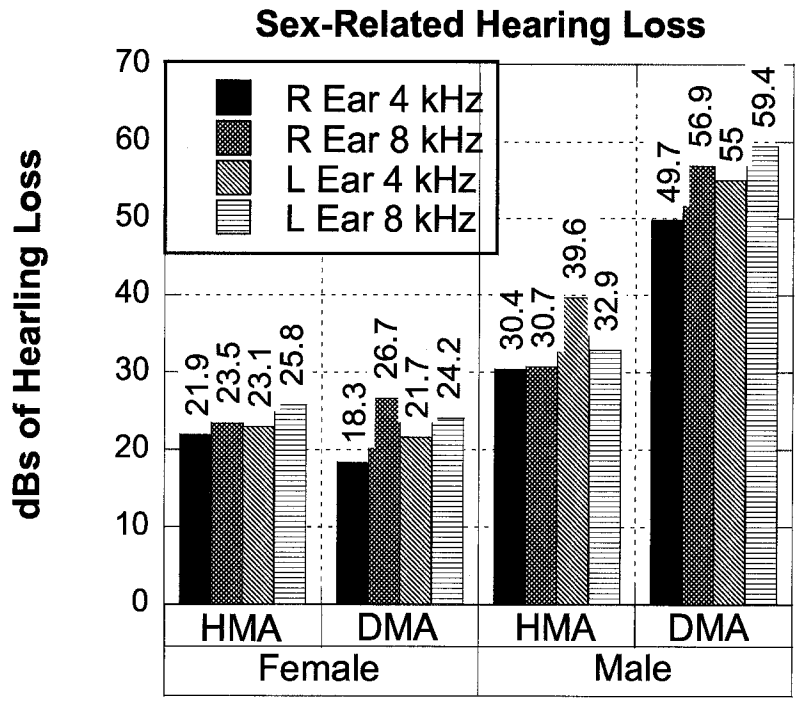

Figure 4.4. Hearing loss sex-related differences.

4.6 Summary

These findings provide evidence that detriments to the nervous system are wide-spread in diabetes and are not localized as in the case of lower-limb peripheral neuropathy. Our data show increased hearing loss in DMA, specifically in males. Based on our evidence, diabetes affects the hearing system, but we cannot conclusively state which part (cranial nerve VIII, hair cells, or sound transduction) is affected. The sensorineural hearing loss leads to the conclusion that similar damage could occur to the vestibular system that can affect balance.

CHAPTER 5

MODIFIED SINGLE-INTERVAL ADJUSTMENT MATRIX

5.1 Hypotheses

- The modified single-interval adjustment matrix (mSIAM) method will reject false positives in thresholds better than the two-alternate forced choice (2AFC) with modified parameter estimation by sequential testing (mPEST) by reaching threshold randomly fewer times within the 30 trial limit.
- The mSIAM method will settle on threshold in fewer trials than 2AFC with mPEST.

5.2 Advantage over 2AFC with mPEST

Our previous acceleration threshold test required a stimulus perturbation that took a maximum of six seconds to complete its motion. Therefore, we could afford to use two-alternate forced choice protocol, which gave us a total trial time of 19 seconds. For our new entrainment study, we needed to determine amplitude thresholds at different frequencies while allowing enough time for the sway to be locked in during a sinusoidal perturbation. We can compare previous studies of the linear relationship of acceleration, a, and displacement with the amplitude, A, and frequency, ω (rad/s) and f (Hz) of the sinusoidal platform movement (Eq. 28).

$$a = A\omega^2 = A(2\pi f)^2 \tag{28}$$

5.3 Integration with mPEST

Although SIAM had a staircase method integrated into it, the increment is set to constant, which does not allow us to increase the resolution as we get closer to the threshold. The mPEST increased or decreased the resolution of the search depending on the distance the algorithm predicted it was away from the actual threshold. In the previous experiments with 2AFC with mPEST, they used a 1-up/2-down or 1-up/3-methodology. With every reversal (change from up to down or vice versa), the increment was halved. Consecutive ups and downs were doubled.

To integrate mPEST, some difficulties had to be overcome. The mSIAM method is a single interval yes/no method, which means sometimes there will be no stimulus presentation as opposed to the forced choice of the 2AFC method. In addition, there is an increment after every trial, except correct rejections. Since the system must always change, a simple 1-up-2-down system could be used.

The p=0.50 SIAM (Table 5.1) was chosen since it is the best estimate for threshold.[93] Table 5.1 has values in parenthesis that are multipliers of the increment to determine the amplitude of the next stimulus.

Table 5.1. SIAM Matrix for Study.

	Movement	No Movement
Detect	Hit (-1)	False Alarm (2)
No Detect	Miss (1)	Correct Rejection (0)

The correct rejection and false alarm multipliers handled the no stimulus trials. Therefore, if there were a correct rejection then the stimulus amplitude would not change, but if there were a false alarm, the subject would be penalized for guessing by increasing the stimulus by twice the increment.

Since a true 1-up-2-down method could not be used, we used a semi-1-up-2-down method. Thus, every consecutive miss or false alarm caused the increment to double (1-up). The increment value would be halved for every reversal. Reversals were defined as every miss or false alarm followed by a hit, and two consecutive hits followed by a hit or miss (2-down). To allow the method to reach the threshold more quickly, the increment is doubled every time a hit is preceded by two consecutive hits. Another problem arises due to the amplitude change after every trial. A situation can occur when a subject enters a hit-miss-hit-miss occurrence where the amplitude is alternating above and below the threshold. To counteract, the fourth consecutive hit-miss alternating occurrence causes the threshold to be halved, which increases the resolution for defining threshold nearer to the actual threshold. In addition, we could have negative perturbations or perturbations of zero. Therefore, we had to implement a schema to set the increment and the amplitude to half of the amplitude of the previous trial. Although this implementation alleviated our problem, it does allow threshold criteria to be met prematurely. Thus, the halving of the increment value could cause it to shrink to 2% or 5% of its initial value, causing the signal that threshold had been found in simulations. This signal should not happen in our sinusoidal threshold tests with human subjects since the subject could not have a threshold of 20 μm or 50 μm (our initial increment is 1 mm).

5.4 Monte Carlo Simulations

Monte Carlo simulations were run on both the previously used mPEST method and our new mSIAM method. Simulations were run for 10,000 subjects and 1000 trials per subject. Two methods for simulation were used. The first method assumed a uniform distribution of button presses and platform perturbations. The second method used a simulated human response. Both methods were run until the 2% and 5% criteria were met or until it finished the 1000 trials.

5.4.1 Random Choice

The random choice method simulated a subject pressing the button at random to signal he or she felt a move. This methodology determines the power of an algorithm by showing the ability to reject false positives, since correct guesses could lead to a premature threshold value.

The random choice simulations showed more power for mSIAM with less randomly reached threshold within 30 trials as opposed to the mPEST method (Table 5.2). Thirty trials were chosen since we use a maximum of 30 trials for our threshold testing. For the 2% and 5% rules in mSIAM, less than 2% reached threshold randomly, which is lower than both the 2% and 5% rules of mPEST. Therefore, we can conclude that the mSIAM provides better rejection of false positives than mPEST.

Table 5.2. Percentages of Subjects Reaching Threshold by Random Choice.

	2%		5%	
Trials	mPEST	mSIAM	mPEST	mSIAM
5	1.53%	0.00%	1.70%	0.00%
10	2.09%	0.11%	2.78%	0.04%
15	2.30%	0.28%	3.16%	0.52%
20	2.40%	0.53%	3.37%	1.11%
25	2.53%	0.69%	3.56%	1.68%
30	2.64%	0.90%	3.62%	1.95%

5.4.2 Simulated Human Response

The simulated human response (SHR) method simulated a subject pressing the button with probability depending on the stimuli's relationship to the subject's threshold. This methodology determines the ability of an algorithm to converge to a threshold. SHR worked by providing miss and false alarm trial a second chance to get a hit. The probability (Eq. 29) was compared to a randomly generated number. If a random number was lower than the probability, the subject's answer would be changed to a hit.

$$probability = \frac{amplitude \cdot 3}{threshold} \tag{29}$$

The SHR simulations showed higher convergence to a threshold with mPEST within 30 trials as apposed to the mSIAM method (Table 5.3). Thirty trials were chosen since we use a maximum of 30 trials for our threshold testing. All simulated subjects converged to a threshold within the 1000 trials. The mPEST method had higher convergence percentages within each rule, but the 5% rule percentage at 30 trials for

mSIAM (58.08%) was higher than that of the 2% rule of mPEST (48.01%). Therefore, we decided to use the 5% rule for mSIAM since it gave us a higher convergence over the 2% rule, and mSIAM had a higher false positive rejection.

Table 5.3. Percentages of Subjects Reaching Threshold by SHR.

	2%		5%	
Trials	mPEST	mSIAM	mPEST	mSIAM
5	6.96	0.11	13.56	1.14
10	17.96	2.76	35.20	12.03
15	26.64	9.51	47.05	26.02
20	34.96	17.99	58.47	38.67
25	42.15	27.00	67.36	49.61
30	48.01	35.59	74.45	58.08

5.5 Summary

The mSIAM method provided us an improved method to estimate threshold. It cut down on overall testing time, which reduces subject fatigue. The methodology improved our threshold estimation by better rejecting false positives, since we had fewer thresholds reached via random button pushing, and allowed for a faster convergence to the threshold.

CHAPTER 6

SUBTHRESHOLD SINUSOIDAL ENTRAINMENT

6.1 Subjects

This study consisted of eight new subjects who were 21 to 29 years of age. All subjects were required to wear a harness per IRB approval at Clarkson University. Subjects were recruited via advertising at Clarkson University in Potsdam, NY, and the surrounding area. Only subjects who completed all trials were included for this analysis.

6.2 Screening

A medical history questionnaire was given to each potential subject. Individuals were not tested further if they had a medical history of cardiovascular and/or respiratory disease; neurological problems such as cerebrovascular disease, stroke, head or spine injury; vestibular ailments and dizziness; memory and concentration deficits; muscle activity deficits; or non-healing skin ulcers. Orthopaedic problems such as lower back pain or spasms, arthritis or joint disease, and deformations of joints or bones led to exclusion of individuals from the study. Those with past or current drug or alcohol dependence were also excluded.

All consenting subjects were screened with the Berg Balance Scale and Sharpened Romberg Test to assure that they were able to operate independently from

assistance, and correctable vision was required. In addition, the subjects were tested with the Mini-Mental State Exam to insure that they were mentally competent to follow instructions during the experiment. Patellar and Achilles' reflexes were tested to confirm that they were present and normal.

6.3 Test Protocol

All subjects were tested via an experimental protocol that first finds a subject's threshold to a sinusoidal perturbation and then entrains sway subthreshold. First, 60 seconds of quiet standing were recorded. The data from the 60 second quiet standing period was used to calculate the top two peak power frequencies (natural frequencies) of anterior-posterior center-of-pressure (APCoP) sway. The top two had to be within 30 dB of the maximum peak. If not, than 0.4 Hz was used as the second natural frequency, which was arbitrarily chosen. This procedure was performed to insure that the secondary peak was due to a frequency power outside the power of the noise level. The upper level limit was 1 Hz due to the high acceleration values at low amplitudes at larger frequencies. The lower level was limited to 0.15 Hz because we obtain so few cycles that the data is unreliable.

Each subject is tested to determine threshold of amplitude of sinusoidal motion at four different frequencies. The first two, 0.5 Hz and 0.75 Hz, (constant frequencies) were chosen since preliminary data suggested these frequencies, a low (0.5 Hz) and a high (0.75 Hz), were around the ideal sway frequencies; but this information could not be found to be conclusive since we only had 20 seconds of quiet standing in previous studies, and therefore the data could not be reliable enough to publish. The order of the constant frequencies was randomly chosen to factor out learning. Next, the amplitude

threshold is found for each of the natural frequencies. This test is performed to determine whether if entrainment does not occur at the constant frequencies then would it at the natural frequencies. The two natural frequencies are also randomly ordered. Each threshold set of trials is preceded by 10 seconds of quiet standing to provide a baseline average to subtract from the threshold trials. The amplitude for each frequency was varied using the mSIAM algorithm for threshold detection (Figure 6.1).

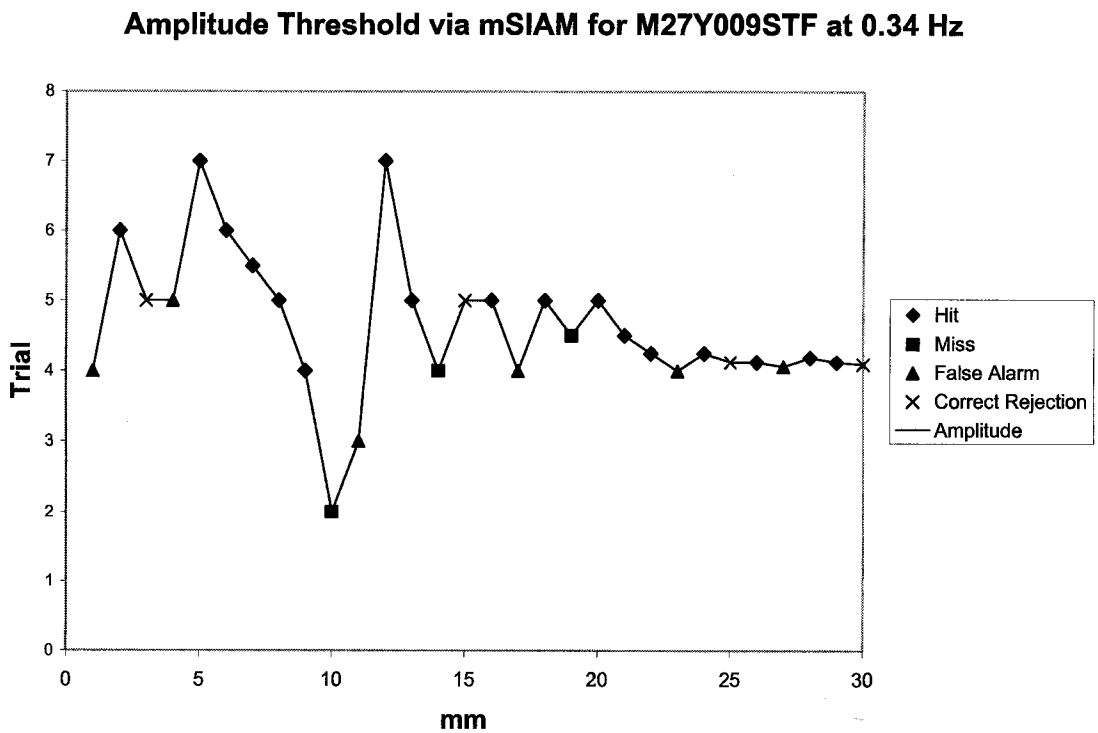

Figure 6.1. Iterating amplitude towards threshold via mSIAM for subject M27009STF.

At the start of each trial, a baseline sinusoid was begun. Its purpose was to avoid any abrupt jerks at the beginning of the stimulus interval to follow. This amplitude was chosen to be well below threshold. The acceleration was set at 5 mm/s^2 and the amplitude was calculated from Eq. 28 (e.g., at 0.5 Hz, the sinusoidal amplitude A≈0.5

mm). The baseline sinusoid was followed four seconds later by the full amplitude sinusoidal perturbation for those trials in which a move was to occur (Figure 6.2).

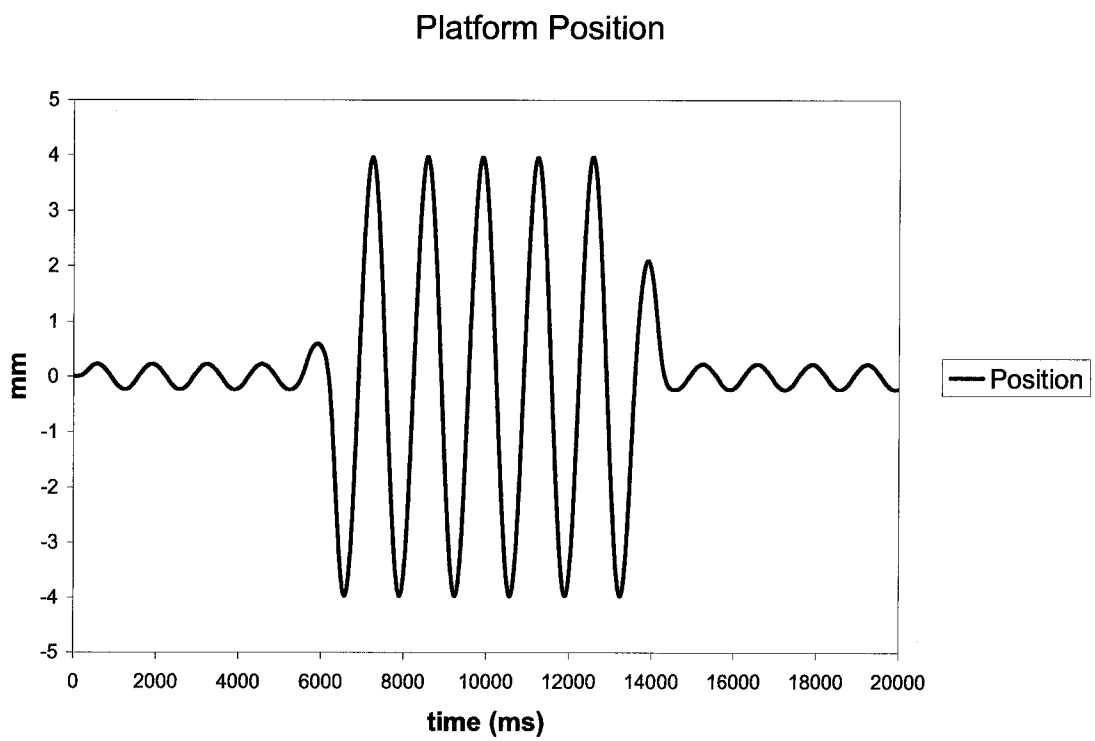

Figure 6.2. Position of platform during a sinusoidal perturbation for a "stimulus" trial. A "non-stimulus" trial would contain only the baseline sinusoid.

The ratio of perturbation to non-perturbation trials was set at 2:1. Trials were randomly sorted. The threshold detection algorithm went for a maximum of 30 trials if subject did not meet the 5% stopping criteria. If a subject went through all 30 trials, then the threshold was estimated by using the lowest amplitude that had 79% hits.

After all four amplitude thresholds were obtained, the subject proceeded to the entrainment protocol. The subject received five seconds of quiet standing followed by 120 seconds of sinusoidal motion at 80% of the threshold for each frequency. Power

spectral density was performed applying a fast Fourier transform to the APCoP lock-in data to evaluate a subject's sway entrainment.

6.4 Verification

Because APCoP was calculated from the load cells, confirmation was needed to show that the resulting APCoP was due to a subject's sway and not the shear force of the plate from the inertia of the weights. Sixty-five kilograms of steel plates (bar bell weights) were placed on a 10 cm rod affixed to the center of the platform, and the APCoP was calculated. The resultant APCoP deviated no more than 0.5 mm, which was substantially smaller than the subject's APCoP sway (6 to 8 mm).

In addition, to show that the peak frequency spectrum detection function worked and that the platform was moving at the correct frequency, the system was set up to calculate the peak frequency of the platform position instead of the APCoP. The spectral density showed that the tabulation was correct but also verified the frequency precision of the platform sine wave (Figure 6.3).

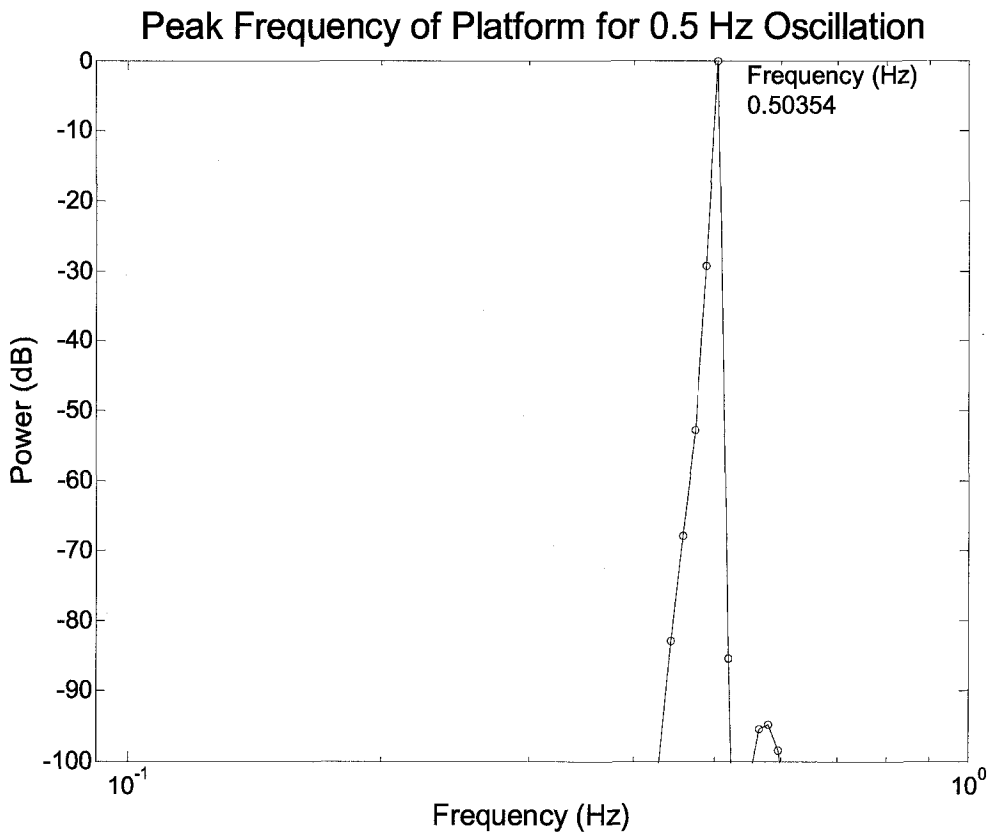

Figure 6.3. Power spectral density of platform position move signal.

6.5 Analysis and Results

6.5.1 Natural Frequencies

By determining the amplitude threshold for separate frequencies, we were able to explore the relationship of frequency and amplitude threshold. Table 6.1 provides the details of our subjects and the determined natural sway frequencies. The thresholds for the different natural frequencies will assist in better defining the curve for the relationship between frequency and amplitude.

Table 6.1. Subject Information and Natural Frequencies.

Subject Information				Natural Frequencies	
SUBJECT ID	AGE	RACE	GENDER	Nat_Freq_1	Nat_Freq_2
F24Y001STF	24	INDIAN	F	0.37	0.40
M24Y002STF	24	INDIAN	M	1.13	0.92
M24Y003STF	24	ASIAN	M	0.31	0.60
F26Y004STF	26	ASIAN	F	0.40	0.43
M20Y006STF	20	CAUCASIAN	M	0.79	0.92
M20Y007STF	20	CAUCASIAN	M	0.98	0.92
M29Y008STF	29	ASIAN	M	0.89	0.40
M27Y009STF	27	INDIAN	M	0.34	0.98
M24Y011STF	24	INDIAN	M	0.67	0.43

A power-law relationship may exist between the amplitude threshold and perturbation frequency (Figure 6.4). With increased sample size, we will have more duplicated natural frequencies between subjects, which will better define the curve of the power-law relationship between perturbation amplitude and frequency.

Since our lab previously had found a negative power-law relationship between peak acceleration detection threshold and a linear perturbation distance with the 2AFC tests, we also plotted acceleration at thresholds versus amplitude thresholds (Figure 6.4)

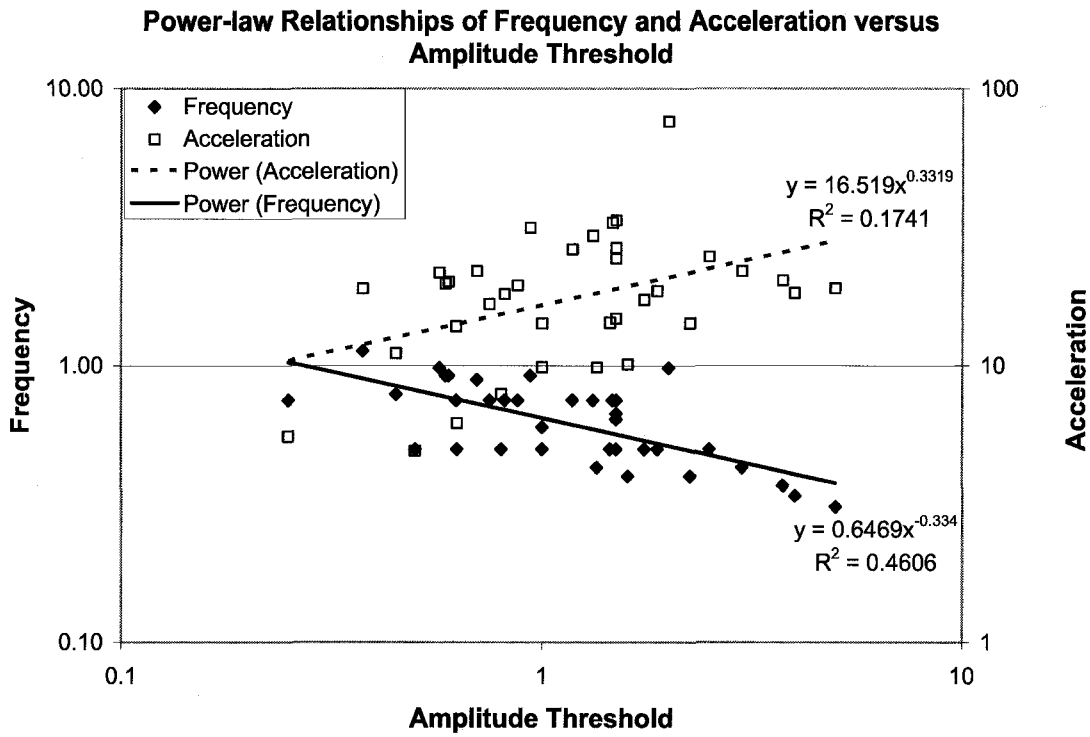

Figure 6.4. Power-law Relationship of Frequency and Amplitude.

6.5.2 Frequency Lock in

To analyze the frequency lock-in, we allowed a 5% error. Therefore, a subject was considered frequency locked if the difference between the predicted and observed sway frequency was within 5% of the predicted frequency (Eq. 30).

$$\frac{\left| f_{Observed} - f_{predicted} \right|}{f_{predicted}} \leq 0.05 \tag{30}$$

Where $f_{observed}$ is the peak frequency of the entrainment test, and $f_{predicted}$ is the frequency of the platform sinusoid for entrainment.

Figure 6.5 shows the entrainment of anterior-posterior center of pressure for asingle subject. The next highest peak is about 55 dB below the lock-in peak. This peak shows a good signal to noise ratio for the subject's lock-in frequency.

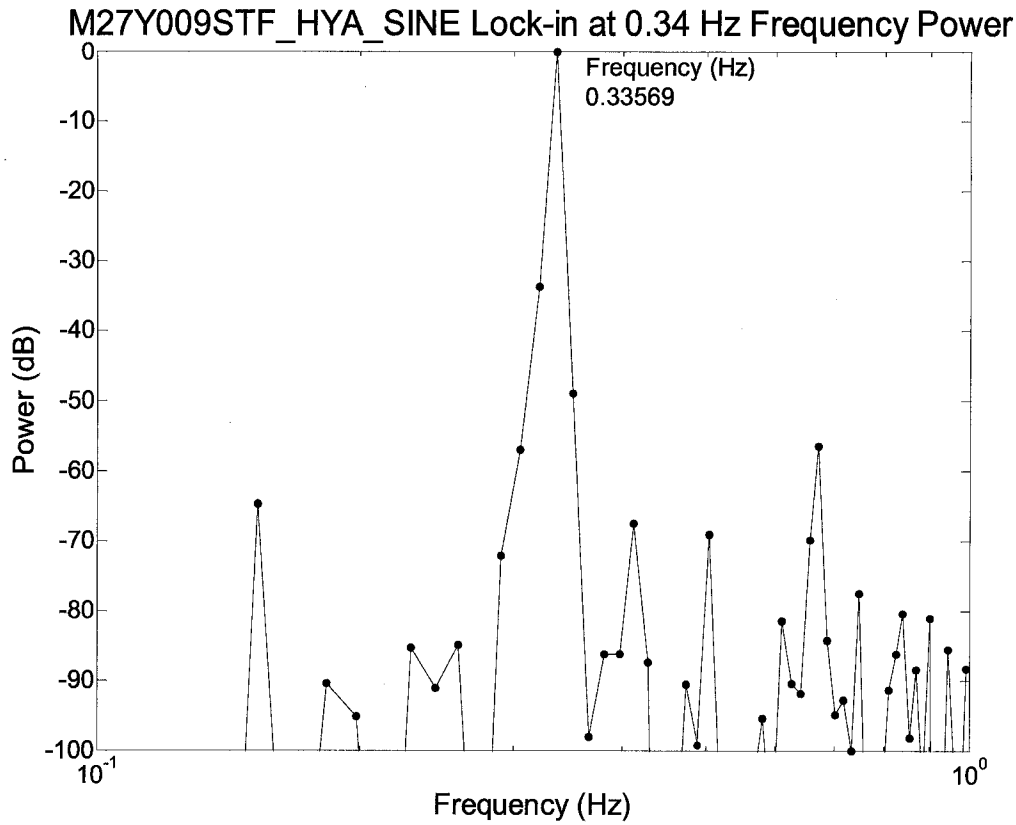

Figure 6.5. Lock-in Power Spectral Density of APCoP.

The 5% error rule accommodated the problem so that we could mathematically determine frequency lock. The peak frequencies of the entrainment section (Table 6.2) were found to be entrained for 89% of the subjects at each frequency group. One subject (M24Y002STF) did not show frequency lock at 0.5 Hz, 0.75 Hz, or his first natural frequency (1.13 Hz). The lack of lock for the first natural frequency may be due to its high frequency. The only other subject (M20Y006STF) not to achieve frequency lock was also at a high natural frequency (0.92). The entrainment trial was within 1.5 dB of power from qualifying as entrained.

Table 6.2. Peak Entrainment Frequencies.

	Peak Entrainment Frequencies			
SUBJECT ID	0.5 Hz	0.75 Hz	Nat_Freq_1	Nat_Freq_2
F24Y001STF	0.50354	0.74768	0.36621	0.39673
M24Y002STF	0.36621*	0.41199*	0.47302*	0.91553
M24Y003STF	0.50354	0.74768	0.30518	0.59509
F26Y004STF	0.50354	0.74768	0.39673	0.42725
M20Y006STF	0.50354	0.74768	0.79346	0.53406*
M20Y007STF	0.50354	0.74768	0.97656	0.91553
M29Y008STF	0.50354	0.74768	0.88501	0.39673
M27Y009STF	0.50354	0.74768	0.33569	0.97656
M24Y011STF	0.50354	0.74768	0.67139	0.42725

* Did not achieve frequency lock.

6.5.3 Physiological Measures

To investigate the system controlling the lock-in of frequency, power spectra were performed on the physiological time-series measures. The first physiological measures are those from the three-axis head accelerometer, which can describe the input to the vestibular system. In addition, EMGs allowed us to look at the motor output. The soleus, gastrocnemius, and tibialis anterior EMGs provided information for muscles actuating the ankle joint. The sternocleidomastoid muscle is believed to provide information on vestibular out due to its efferents from the auditory-vestibular nerve.[179] Lock-in was observed in a maximum of 50% for physiological measures (Table 6.3).

Table 6.3. Physiological Entrainment Percentages.

Measurement	0.5 Hz		0.75 Hz		Nat. Freq. 1		Nat. Freq. 2	
	Peak 1	Peak 2	Peak 1	Peak 2	Peak 1	Peak 2	Peak 1	Peak 2
Head Accel X	0.00	0.00	0.25	0.00	0.13	0.13	0.00	0.00
Head Accel Y	0.13	0.00	0.25	0.13	0.50	0.00	0.00	0.25
Head Accel Z	0.00	0.25	0.25	0.13	0.25	0.13	0.00	0.13
EMGs								
RTA	0.13	0.00	0.13	0.25	0.00	0.13	0.00	0.13
LTA	0.00	0.13	0.00	0.00	0.00	0.25	0.13	0.00
RGS	0.25	0.13	0.25	0.00	0.38	0.00	0.25	0.00
LGS	0.25	0.13	0.25	0.00	0.25	0.13	0.13	0.00
RSCM	0.00	0.00	0.25	0.00	0.00	0.00	0.00	0.25
LSCM	0.00	0.00	0.00	0.00	0.00	0.00	0.00	0.00
Rsoleus	0.33	0.17	0.17	0.00	0.33	0.17	0.17	0.00
Lsoleus	0.33	0.00	0.17	0.17	0.33	0.17	0.33	0.00

Although the physiological entrainments were considerably lower than the APCOP entrainment, higher peak entrainments were observed at subjects' highest peak natural frequency.

6.6 Summary

More subjects will allow us to better define the relationship between frequency and amplitude threshold. With increased sample size, it might be possible to characterize subjects who cannot entrain or frequencies with decreased entrainment efficiencies.

CHAPTER 7

ANKLE MODEL

In parallel with a new method to study postural control, this dissertation also now presents a new method to characterize movement about the joints of the body, as a precursor to later using this new technique to model postural and balance control.

Arthropod and human limbs are multilinked systems in which the revolute joints are not orthogonal to the limb segments or to each other. The Denavit-Hartenberg (DH) representation is the traditional model used for orthogonal systems such as industrial robots. When applied to systems with non-orthogonal linkages, the DH representation projects the reference frames outside of the limb segments and presents other computational difficulties. A new method to represent kinematics of multilinked lower-pair mechanisms is proposed. Three-dimensional computer graphics techniques act on arrays of points describing bodies that move about arbitrary revolute joints. This computational model has been adapted to represent multilinked systems such as animal limbs to calculate both position (X, Y, Z) and orientation (yaw, pitch, and roll) of individual limb segments and joints for measurement comparisons. The linkage parameters are explicitly stated. This method allows a simplified representation for the kinematics of human and animal limbs by maintaining reference frames within the limb segments. It reduces errors such as the arc sine errors associated with Euler calculations

and the azimuth errors seen with the DH representation. A common computational system is provided for simulation, design, measurement and animation.

7.1 Mathematics

7.1.1 Definitions

A vertices matrix ($[V_n]$, (Eq. 31)) is defined by the joint number to be rotated, n; therefore, all limbs distal to it (limbs $[n+1{:}d]$) are operated on or accessed in the matrix. The subscript d is equal to the number of the most distal limb. Each limb requires 12 columns of the matrix (expandable for more vertices). The first eight columns are the limb vertices. The ninth column is the limb center, and the 10th, 11th, and 12th columns are the local x, y, and z-unit vectors of the local coordinate system relative to global Cartesian coordinate system. The 13th column contains the position of the distal revolute joint of each respective limb, (jp).

$$\begin{bmatrix} x_{1,1} & x_{1,2} & \cdots & x_{n+1,1} & \cdots & x_{d,13} \\ y_{1,1} & y_{1,2} & \cdots & y_{n+1,1} & \cdots & y_{d,13} \\ z_{1,1} & z_{1,2} & \cdots & z_{n+1,1} & \cdots & z_{d,13} \\ 1 & 1 & 1 & 1 & 1 & 1 \end{bmatrix} \tag{31}$$

A translation matrix ($[T_{n,r}]$, (Eq. 32)) is defined by n (same as above) and r, such that the offset as "from proximal" (fp) or "to distal" (td) is defined in reference to the joint in relation to the limb.

$$\begin{bmatrix} 1 & 0 & 0 & \Delta x \\ 0 & 1 & 0 & \Delta y \\ 0 & 0 & 1 & \Delta z \\ 0 & 0 & 0 & 1 \end{bmatrix} \tag{32}$$

Rotation matrices ($[R_{n,a,r}]$) are defined by n, a, and r, where a is the axis of rotation. Eqs. 33-35 show the rotation matrices for rotating about the x, y, and z-axes,

respectively. Roll (α) is defined by the rotation about the x-axis. Yaw (β) provides the rotation about the y-axis. Pitch (θ) describes the rotation about the z-axis.

$$\begin{bmatrix} 1 & 0 & 0 & 0 \\ 0 & \cos(\alpha) & -\sin(\alpha) & 0 \\ 0 & \sin(\alpha) & \cos(\alpha) & 0 \\ 0 & 0 & 0 & 1 \end{bmatrix} \tag{33}$$

$$\begin{bmatrix} \cos(\beta) & 0 & \sin(\beta) & 0 \\ 0 & 1 & 0 & 0 \\ -\sin(\beta) & 0 & \cos(\beta) & 0 \\ 0 & 0 & 0 & 1 \end{bmatrix} \tag{34}$$

$$\begin{bmatrix} \cos(\theta) & -\sin(\theta) & 0 & 0 \\ \sin(\theta) & \cos(\theta) & 0 & 0 \\ 0 & 0 & 1 & 0 \\ 0 & 0 & 0 & 1 \end{bmatrix} \tag{35}$$

A joint rotation matrix [[Rev] (Eq. 36)] defines the amount of rotation about the arbitrary axis of the revolute joint. The α and β angles of offset are calculated from the z-axis to allow for the rotation of the joint to be about the z-axis as in Eq. 35. A single rotation matrix ([RM (row, column)]) is used to define the orientation of a limb in space through a single rotation once the yaw, pitch, and roll have been tabulated.

$$\begin{bmatrix} c(\beta)c(\theta) & s(\theta) & -c(\theta)s(\beta) & 0 \\ -c(\alpha)s(\theta)c(\beta)+s(\alpha)s(\beta) & c(\alpha)c(\theta) & c(\alpha)s(\beta)s(\theta)+s(\alpha)c(\beta) & 0 \\ c(\beta)s(\theta)s(\alpha)+s(\beta)c(\alpha) & -c(\theta)s(\alpha) & -s(\alpha)s(\beta)s(\theta)+c(\theta)c(\beta) & 0 \\ 0 & 0 & 0 & 1 \end{bmatrix} \tag{36}$$

In Eq. 36, c refers to cosine and s to sine.

7.1.2 System Description

A relative object-oriented design utilizing limb, joint, and system objects facilitates the setup of the model using global positions and angles. The global origin and axis are designated at the local origin of the most proximal limb segment. The limb is modeled as a cuboid defined by length, width, and height for simplicity, but any shape

with any number of vertices can be used. The local reference frame for each limb segment is located arbitrarily at the segment's geometric center. The joint is defined in relation to the proximal and distal limbs. Due to the sequential operation in traversing the limb, the program progresses arbitrarily proximal to distal. The displacement offset for each joint is the x_{fp}, y_{fp}, and z_{fp} offset from the geometric center of the proximal limb. These define its position in space in relation to proximal limb. Next, the α_{fp} (x-axis), β_{fp} (y-axis), and θ_{fp} (z-axis) are defined as the offset orientations from the local axis of the proximal limb. Then a similar set of offset orientations (α_{td}, β_{td}, and θ_{td}) are defined to allow the rotation of the revolute joint to align it with the z-axis of the distal limb. Finally, the offset is defined from the center of the revolute joint to the geometric center of the distal limb, x_{td}, y_{td}, and z_{td}. No range limitation is enabled to allow axis positions or orientations that are considered out of the range of natural joint motion as in fractures or dislocations.

7.1.3 Kinematics of the Multi-Linked System

A multi-linked system assembled to the specifications of an initial state and followed by a series of rotations is shown in Figure 7.1.

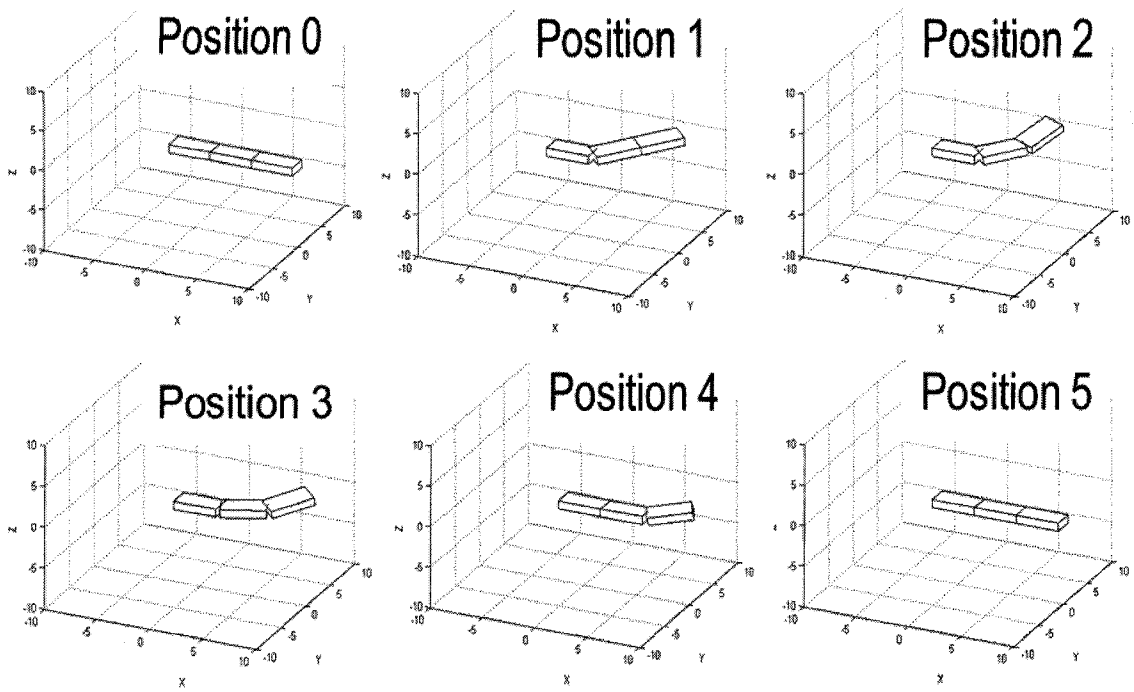

Figure 7.1. Displays positions of a two joint system going through a series of closed loop rotations defined in Table 7.1, which verifies the algorithm with the identity matrix.

The local coordinate systems are set at the origin for all limbs. Therefore, the limbs are moved to their positions and orientations in space via the matrix multiplications shown in the pseudocode below:

1. $[V_1] = [T_{1,fp}]\ [R_{1,x,fp}]\ [R_{1,y,fp}]\ [R_{1,z,fp}]\ [R_{1,z,td}]\ [R_{1,y,td}]\ [R_{1,x,td}]\ [T_{1,td}]\ [V_1]$
2. $[V_2] = [T_{2,fp}]\ [R_{2,x,fp}]\ [R_{2,y,fp}]\ [R_{2,z,fp}]\ [R_{2,z,td}]\ [R_{2,y,td}]\ [R_{2,x,td}]\ [T_{2,td}]\ [V_2]$
3. . . . . .
4. . . . . .
5. . . . . .
6. $[V_n] = [T_{n,fp}]\ [R_{n,x,fp}]\ [R_{n,y,fp}]\ [R_{n,z,fp}]\ [R_{n,z,td}]\ [R_{n,y,td}]\ [R_{n,x,td}]\ [T_{n,td}]\ [V_n]$.

To rotate the distal limbs around a respective joint (n), the joint axis is translated to the global origin, and the axis of rotation is aligned with the *z*-axis. The convention for

local z-axis rotations has been designated as the rotation for each arbitrary joint. All other axes are held constant at the initial specification.

Once the system is built, it can be optimized from the pure computer graphics framework. By using the position (jp) of the revolute joint stored in the vertex matrix, we can use one translation to bring the joint to the origin. This optimization creates a reduction in translational matrix multiplications by a factor of 2(n-1) if n is the number of the joint to be rotated. In addition, the optimization provides less overhead as the number of vertices to be operated is reduced by c·n where c is the number of vertices per limb and n is the number of the joint to be rotated. The optimization is detailed in the pseudocode below:

1. $[V_n] = [T_{n,jp}]^{-1} [V_n]$
2. $[V_n] = [R_{1,y,fp}]^{-1} [R_{1,x,fp}]^{-1} [V_n]$

a. If the joint is the joint of rotation, jump to step nine.

3. $[V_n] = [R_{1,x,td}]^{-1} [R_{1,y,td}]^{-1} [R_{1,z,td}]^{-1} [R_{1,z,fp}]^{-1} [V_n]$
4. $[V_n] = [R_{2,y,fp}]^{-1} [R_{2,x,fp}]^{-1} [V_n]$

a. If the joint is the joint of rotation, jump to step nine.

5. $[V_n] = [R_{2,x,td}]^{-1} [R_{2,y,td}]^{-1} [R_{2,z,td}]^{-1} [R_{2,z,fp}]^{-1} [V_n]$
6. . . . . .
7. . . . . .
8. . . . . .
9. $[V_n] = [R_{n,x,fp}] [R_{n,y,fp}] [Rev] [V_n]$.

After joint is rotated, the system is returned to its proper global coordinates as follows:

1. $[V_n] = [R_{n,x,fp}]\ [R_{n,y,fp}]\ [R_{n,z,fp}]\ [R_{n,z,td}]\ [R_{n,y,td}]\ [R_{n,x,td}]\ [V_n]$

2. . . . . .

3. . . . . .

4. . . . . .

5. $[V_n] = [R_{2,x,fp}]\ [R_{2,y,fp}]\ [R_{2,z,fp}]\ [R_{2,z,td}]\ [R_{2,y,td}]\ [R_{2,x,td}]\ [V_n]$

6. $[V_n] = [R_{1,x,fp}]\ [R_{1,y,fp}]\ [R_{1,z,fp}]\ [R_{1,z,td}]\ [R_{1,y,td}]\ [R_{1,x,td}]\ [V_n]$

7. $[V_n] = [T_{n,jp}]\ [V_n]$

7.1.4 Yaw, Pitch, and Roll of Limbs

The rotation about an arbitrary revolute joint in a multilinked system allows joint motion to include displacements in all three dimensions and rotations about all three coordinate axes. In mechanisms with orthogonal revolute joints, three revolute joints would be required to achieve the same rotations. Changes in link yaw, pitch, and roll Euler angles occur from rotation about a single revolute joint. Therefore, the new yaw, pitch, and roll are calculated after proximal joints are rotated. To avoid errors in back calculation of the orientation via position coordinates in real data, the yaw, pitch, and roll are calculated via the rotation sequence through multiplication of only the rotation matrices. The sequence necessary for rotation using Euler angles required that the orientations be calculated in the order roll, pitch, and yaw as in (Eq. 36). The calculation of yaw, pitch, and roll is tabulated both ways so that each method could verify the other. The method of back calculation is accomplished by first translating the limb back to the global origin of the coordinates system by using the limb center as the offset for the translation matrix in (Eq. 37).

$$\begin{bmatrix} 1 & 0 & 0 & x_{\alpha,9} \\ 0 & 1 & 0 & y_{\alpha,9} \\ 0 & 0 & 1 & z_{\alpha,9} \\ 1 & 1 & 1 & 1 \end{bmatrix} \tag{37}$$

Roll (α) is calculated by projecting the local *y*-axis unit vector (*x_uy*, *y_uy*, *z_uy*) onto the *yz*-plane (Eq. 38) and calculating the angle of rotation (*α*) between *u'* and the global *y*-axis (Eq. 39).

$$u' = [0, y\_uy, z\_uy] \tag{38}$$

$$\alpha = -\frac{\cos^{-1}(u' \cdot [0,1,0])}{|u'|} \times \frac{z\_uy}{|z\_uy|} \tag{39}$$

The arc cosine function only returns values between zero and *π* radians so it is multiplied by a factor that is -1 or 1 depending on *z_uy* in respect to the *xy*-plane. A similar respective factor is multiplied to determine angle direction for yaw and pitch. The computer animation standard rotations used designate positive angles as counter-clockwise rotations [147]. For *α*, a positive angle requires a clockwise rotation to align *u'* with the global *y*-axis. Therefore, the calculated *α* is inverted. The remaining calculations of pitch (*θ*) and yaw (*β*) follow the standard convention of positive angles for counter-clockwise rotations. Using *α*, an *x*-axis rotation matrix is used to rotate the limb so that the local y-axis vector lies in the *xy*-plane.

Since *u"* already lies within the *xy*-plane but was calculated with the absolute value of *u'* (Eq. 40), the pitch (*θ*) must be calculated from the angle of rotation between *u"* and the global *y*-axis (Eq. 41).

$$u'' = [x\_uy, 0, |u'|] \tag{40}$$

$$\theta = \frac{\cos^{-1}(u'' \cdot [0,1,0])}{|u''|} \times \frac{x\_uy}{|x\_uy|} \tag{41}$$

Yaw (β) requires the use of a separate local axis since the local y-axis unit vector is aligned with the global y-axis. The local x-axis unit vector (x_ux, y_ux, z_ux) is projected onto the xz-plane (Eq. 42) so that the angle between the x-axis vector (x_ux) and the global x-axis is calculated as the yaw of the limb (Eq. 43).

$$u''' = [x\_ux, 0, z\_ux] \tag{42}$$

$$\beta = \frac{\cos^{-1}(u''' \cdot [1,0,0])}{|u'''|} \times \frac{z\_ux}{|z\_ux|} \tag{43}$$

Utilizing the calculated yaw, pitch, and roll, one is able to move and orient the limb without resorting to sequential steps as in Eq. 44.

$$[\mathrm{V_n}] = [T][R_\alpha][R_\theta][R_\beta][V_n] \tag{44}$$

The inability to make small, precise measurements for the position of limbs introduces the possibility for the researcher to make large errors when back calculating the yaw, pitch, and roll for a limb, especially at the asymptotes. So in addition to back calculating the yaw, pitch, and roll from the limb's position relative to global axis, the researcher calculates the yaw, pitch, and roll solely with the inputted rotation matrices. The rotation matrices are ordered as they would be for the multiplication to build a limb as previously shown in pseudocode above, but no translations are used. The rotation matrix of Eq. 31 is then obtained. By using an ordered sequence of rotation matrix multiplications, the researcher uses the pseudocode to back-calculate yaw, pitch, and roll from the values in the rotation matrix as follows:

1. $[RM_1] = [R_{1,x,fp}]\ [R_{1,y,fp}]\ [R_{1,z,fp}]\ [R_{1,z,td}]\ [R_{1,y,td}]\ [R_{1,x,td}]$
2. $[RM_2] = [R_{2,x,fp}]\ [R_{2,y,fp}]\ [R_{2,z,fp}]\ [R_{2,z,td}]\ [R_{2,y,td}]\ [R_{2,x,td}]$
3. . . . . .

4. . . . . .

5. . . . . .

6. $[RM_n] = [R_{n,x,fp}]\,[R_{n,y,fp}]\,[R_{n,z,fp}]\,[R_{n,z,td}]\,[R_{n,y,td}]\,[R_{n,x,td}]$

Pitch (Eq. 45) is calculated first, since Eq. 36 has one unknown. Because the arc-sine function's range is $[-\pi/2, \pi/2]$, roll is rotated first; this rotation guarantees that the pitch will always be less than $\pi/2$ via the order to calculate Euler's yaw, pitch, and role.

$$\theta = \sin^{-1}\left(RM(1,2)\right) \tag{45}$$

Roll (Eq. 41) as in Eq. 34 is negated to provide the correct rotation direction. The z component of the y and x unit vectors is the same for roll and yaw in Eqs. 43 and 47.

$$\alpha = -\cos^{-1}\left(\frac{RM(2,2)}{\cos(\theta)}\right)\left(\frac{z\_uy}{|z\_uy|}\right) \tag{46}$$

$$\beta = \cos^{-1}\left(\frac{RM(1,1)}{\cos(\theta)}\right)\left(\frac{z\_ux}{|z\_ux|}\right) \tag{47}$$

This method allows one to track the yaw, pitch, and roll of the limbs without the need for position data (except to track the sign for yaw and roll).

7.2 Identity Verification

To verify our methods we rotated to an end position and then back to an initial home position with different rotations on the way back to the home position. Our final vertices matrix equaled the initial one thus verifying our method, since a closed loop rotation is the identity matrix. Table 7.1 shows the sequence of rotations and initial offsets that are illustrated in Figure 7.1. Figure 7.1 shows a simple system of only two arbitrary revolute joints; however, it is given as an example as it is simple to expand to a matrix of vertices representing detailed objects. The yaw, pitch, and roll are calculated

both through rotations and by back-calculation from the end position of each limb for both joints with rotations from -180° to 180° in 1° increments. The angles were found to be equal.

Table 7.1. Offsets and Rotations of a Simple System with Nonorthogonal Revolute hinges.

Joint	α_{fp}	β_{fp}	θ_{fp}	α_{td}	β_{td}	θ_{td}
1	5°	10°	0°	-5°	-10°	0°
2	15°	20°	0°	-15°	-20°	0°
Position		Rotated Joint			Degrees	
0		None				
1		1			45°	
2		2			30°	
3		1			-25°	
4		1			-20°	
5		2			-30°	

7.3 Orthogonal Verification

To compare our methodology to real physical data, a mechanical linkage system (restricted to orthogonal axes) using joints with adjustable twist, cant, and joint angles has been devised and fabricated. Measurements were made with respect to the right-hand Cartesian coordinate system using a grid on drafting paper and a ruler for the vertical *z*-axis. The drafting paper was taped to a flat tabletop, and one end of the multi-linked system was secured to the tabletop (Figure 7.2).

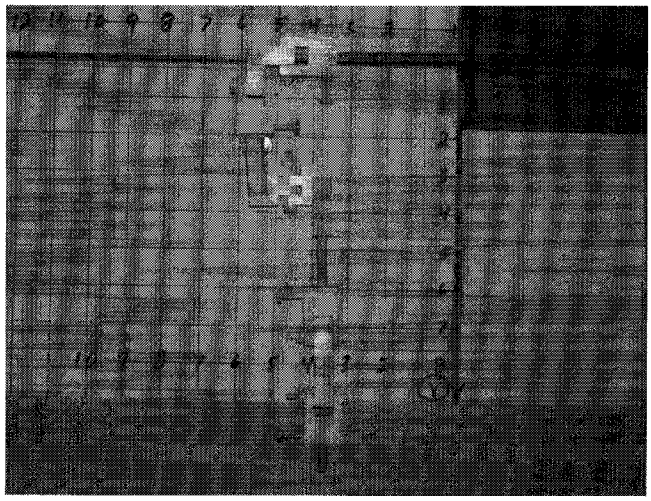

Figure 7.2. Verification measurement setup.

The system was offset since it was above the tabletop. Adding 2.313 to the x values and 1.375 to the z values adjusted the calculations. An offset was used since the our method takes the global zero to be at the center of the most proximal limb, while the test apparatus begins at the end of the most proximal limb, whose center is located at 1.375 inches on the positive *z*-axis. After measurements and adjustments were finalized, the data were converted to centimeters. The differences were calculated between the confirmation values and the modified calculated values. Error was calculated as the Root Mean Square (RMS) of the difference between the measured and calculated coordinates. Table 7.2 shows a maximum 6 mm error, which is within the experimental error of the measurement method used.

Table 7.2. Root Mean Square Difference of Calculation and Measurements (cm).

RMS	0	1	2	3	4
Segment #1	0.34	0.51	0.60	0.33	0.07
Joint #1	0.18	0.17	0.36	0.36	0.17
Segment #2	0.30	0.25	0.41	0.41	0.25
Joint #2	0.20	0.58	0.58	0.58	0.48
Segment #3	0.17	0.36	0.36	0.36	0.36

7.4 Nonorthogonal Verification

Measurements were also performed on snow crab legs (*Chionoecetes opilio*) to verify rotations for nonorthogonal biological revolute crab joints as seen in Table 7.3.[139] Two different crab legs were used, and measurements were performed on each crab leg in two different positions. The measurements were made using methods of the orthogonal section above (Figure 7.3). One of the positions of the crab legs is shown in Figure 7.4; the results are given in Table 7.3.

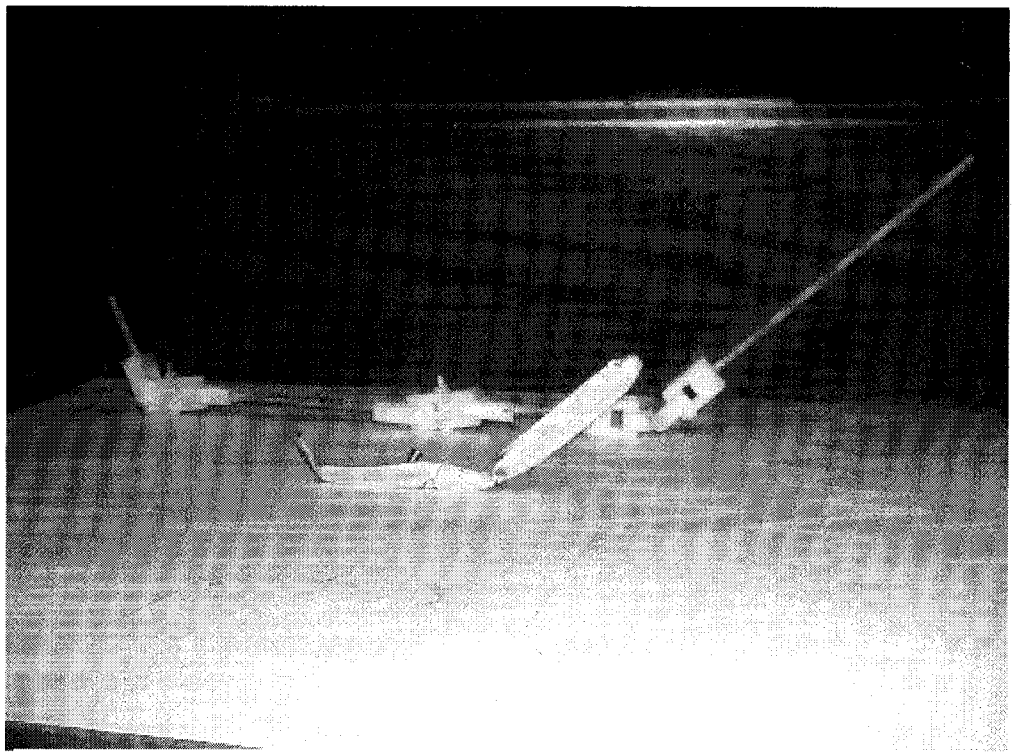

Figure 7.3. Crab leg measurement setup.

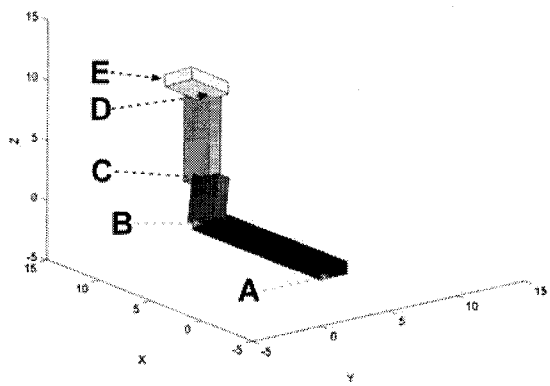

Figure 7.4. Position one of crab leg three.

Table 7.3. Rotations and offsets of crab limb joints.

Crab 1	Joint	α_{fp}	β_{fp}	θ_{fp}	α_{td}	β_{td}	θ_{td}
Pos 2	1	-5°	90°	90°	5°	-90°	0°
	2	-35°	90°	0°	35°	-90°	0°
	3	-5°	90°	-90°	5°	-90°	0°
Crab 3	Joint	α_{fp}	β_{fp}	θ_{fp}	α_{td}	β_{td}	θ_{td}
Pos 1	1	-5°	90°	90°	5°	-90°	0°
	2	-40°	90°	0°	35°	-90°	0°
	3	-3°	90°	-90°	5°	-90°	0°

The methods used to make the measurements were similar to those of the orthogonal axes measurements. The level of accuracy in the measurements was determined by comparing the vector lengths of the limbs compared to the measured length of the limb (accuracy within 0.3 cm required, which allows for ±1.5 mm error for each axis coordinate). Measurements meeting this requirement attained comparable results (Table 7.4) with our simulation shown in Figure 7.4. Since the measurements were carried out similar to the orthogonal linkage measurements with measurements taken in centimeters instead of inches, the errors were the same. All the nonorthogonal measurements that met the required accuracy had RMS error less than six mm.

Table 7.4. RMS of differences in crab limb position (cm).

RMS	B	C	D	E
Crab 1 Pos 2	0.0	0.2	0.6	0.6
Crab 3 Pos 1	0.0	0.2	0.2	0.4

7.5 Ankle Simulation

A model of the human ankle was developed based on three segments with two arbitrary revolute joints (Table 7.5). The segments are the calcaneus, talus, and mortise (comprised of the tibia, fibula and ligaments). The talocrural joint (upper ankle joint) and the subtalar joint (lower ankle joint) are arbitrary revolute joints.[137, 138, 145] Isman and Inman measured the locations of the axes in the bones relative to each other (Table 7.5).[137, 138] A computer animation of the ankle joints was made as seen in Figure 7.5.

Table 7.5. Offset of the human ankle joint.

Joint	α_{fp}	β_{fp}	θ_{fp}	α_{td}	β_{td}	θ_{td}
talocrural	-20°	-16°	0°	20°	16°	0°
subtalar	-41°	-67°	0°	41°	67°	0°

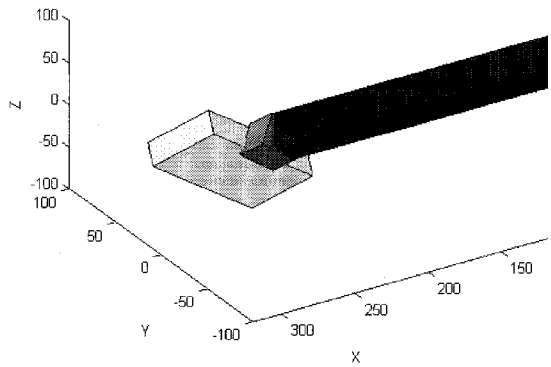

Figure 7.5. The ankle model in the second position of our simulation to show both a slight plantarflexion and supination.

7.6 Summary

Animal limb mechanisms are three-dimensional kinematic chains with nonorthogonal revolute joints. We proposed a more complete method (intermediate calculations are in Tables Q.1-Q.11) for the representation and analysis of the movements of these and other three dimensional linkages. Our SEA (Storey et al.) representation is similar to that used in computer animation and provides a common and clear language for designers, modelers, animators and biologists.

CHAPTER 8

DISCUSSION

8.1 Diabetic Postural Control

The comprehensive study allowed us to look at alterations in both static and dynamic posture caused by Type-2 diabetes in mature adults. Lower limb peripheral neuropathy, prevalent among those with Type-2 diabetes, has been assumed the cause of the increased likelihood of falls and instability.[51, 180] Our study was able to compare perception acceleration thresholds of perturbations and static postural metrics in people who have diabetes with and without lower limb peripheral neuropathy. We found that both DPN and DNI have significantly increased acceleration threshold as compared to HMA while only DPN and significantly different static postural metrics as compared to HMA. The only factor we could not control for was mass, with DPN having significantly higher mass than HMA. Although no direct link between mass and postural instability has been seen, BMI and neuropathy has been correlated, especially in diabetic individuals.[181, 182] Although links were observed, our subjects were not controlled for physical fitness or body fat percentage.

The acceleration threshold tests showed a distinct decrease in the ability to sense forward platform movement in both DPN and DNI as compared to HMA. Our electrophysiology examinations could not account for the decrease, since HMA and DNI

did not significantly differ in nerve conduction velocities; yet DNI had significantly increased detection thresholds at both 1 mm and 4 mm displacements. The SWM examination did not reveal any significant differences between DPN and DNI but did show a bilateral significant difference in the heel and a significant difference with a trend on the left and right fourth metatarsal, respectively, between DNI and HMA. The high SWM thresholds provide a cause for decreased sensitivity of DNI to motion, since the DNI have higher mean thresholds than the DPN; and the geometric mean of the SWM threshold at both heels was higher in the DNI than the DPN, but was not significant. More DPN (5) than DNI (2) had SWM greater than 10.0g, but none had any history of ulceration or vascular problems. DPN subjects had significantly higher SWM threshold at the big toe, first and fourth metatarsal, and heel than HMA on the left foot, while only at the first and fourth metatarsal on the right foot. We did not collect any data on subject handedness or footedness so we cannot correlate that with any certain side deficits.

To prevent ulceration, people must shift their body weight away from pressured tissue.[183] Therefore, if subjects have foot-preference for stance the chronic increase in pressure in the preferred foot could cause damage to nerves and vasculature, which could be exacerbated by diabetes. Our quiet standing period was 20 seconds in length, which is shorter than the time required to force the subject to shift his or her weight several times to alleviate pressure in the feet.[184] The decreased sensation at the heel could provide a reason why both DNI and DPN scored significantly lower than HMA on the Berg Scale. The DPN and DNI self-reported in the RAND poorer general health and had trends with more pain and poorer physical health, which could be attributed to the increased SWM thresholds of both DPN and DNI groups.

Simmons et al. studied diabetic individuals both with and without cutaneous sensory deficit versus controls.[14, 168] Our data confirms their findings that DPN who had significantly different SWM thresholds from HMA, also had significantly larger anterior-posterior sway lengths than our control (HMA) for quiet standing analysis.[14] This difference could be associated with motor nerve neuropathy, which is deficient in its ability to activate muscle efficiently to balance a person, or with sensory nerve neuropathy since the control systems inputs are delayed. The evidence of the involvement of spindle fibers provides reason, since longer sway deviations would be expected with length-sensitive sensory loss. Our data also show that our DNI subjects who also had significantly different SWM thresholds from HMA did not significantly differ from HMA for any quiet standing posture metric. The only significant difference between DPN and HMA was found on the great toe of the left foot. Tanaka et al. has shown that increased pressure on the great toe is shown with increased age, which leads to its increased role in posture, balance, and gait. Although the big toe seems to have an increasing role in balance with increasing age, it does not appear to be significantly affected by diabetes. The other higher pressure centers of the foot (metatarsal and heel) provide more evidence that pressure damage may be the result of cutaneous sensory loss with diabetes.

Lafond et al. also studied quiet standing in diabetic individuals with sensory neuropathy versus healthy elderly. Their data and ours confirmed the increased anterior-posterior sway, but our data did not indicate different medial-lateral sway between groups that was seen in their groups.[77] Richerson et al. has shown an age-related decline in medial to lateral direction.[9] Since subjects of Lafond et al. were on average 10 years

older than ours, age could be the reason for the difference seen. Nardone et al. studied both dynamic and static postural stability in subjects with polyneuropathy diagnosed by nerve conduction testing. They proposed that the increase in sway could be attributed to the loss of group II spindle fibers instead of group Ia motor fibers.[16] Improper functioning of spindle fibers has decreased efficacy of muscle stretch receptors, which could lead to postural instability.[22, 185, 186] Our HMA and DPN subjects had similar nerve conduction velocities as Nardone, et al.; and our DPN group corresponds with Nardone et al. by the increased sway over HMA, especially in anterior-posterior plane.[16] Simoneau et al. found that sensory neuropathy found by SWM threshold was more sensitive to quiet standing postural instability, where our data provides that the decreased nerve conduction velocities of the DPN group cause their significant postural instability.[187] The metric that Simoneau et al. used to quantify stability was total excursion, for which we found a trend only in the anterior-posterior direction.[187] No studies to date have compared diabetic individuals grouped by peripheral neuropathy depending on nerve conduction velocities, SWM thresholds, or both. That information is needed to control for the different types of neuropathy seen.

8.2 Hearing Loss and Diabetes

Studies have shown deficits in the visual-vestibular interactions and suggests degeneration of the sensorineural components of the vestibular system due to microangiopathy and cellular changes from hyperglycemia.[64, 188, 189] Our study is in agreement with Duck et al. with the finding of increased hearing loss at 4 kHz and 8 kHz, but their study found substantially more hearing loss in those who were hypertensive. However, because the hypertensive data were not available to us, we cannot conclude

that hypertension also had effects on our subjects' balance.[60] Contrary to our study, Weng et al. found no difference in high frequency audiology in men and women.[61] Vaughan et al. provide support to our findings in that only their high frequency hearing loss was significantly higher in diabetic veterans (27 of their 692 subjects were women).[65] Frisina, et al. observed only low frequency hearing loss. The impossible task of controlling for previous noise exposure especially in veteran populations makes it difficult to confirm findings.

8.3 Modified SIAM

The mSIAM method allowed us to improve our threshold estimation over our mPEST method by reducing our threshold detection algorithm from two intervals to one interval. By integrating PEST into SIAM, we were able to then achieve efficiency of the 2AFC with our mPEST threshold detection scheme. This choice changes the psychophysics that we examine from a two-period differentiation protocol to detection of a perturbation from background noise. We therefore set a constant peak acceleration for the background noise for all trials. This condition also helped to alleviate large acceleration peaks observed at the onset of a sine wave from stationary platform. The mSIAM with 5% rule provides us with better rejection of false positives and higher convergence to threshold than the 2% rule of mPEST, which was the current rule for acceleration threshold tests. This method will allow us to now find amplitude thresholds for different frequencies, with presentation of multiple cycles of less than 1 Hz.

8.4 Sinusoidal Entrainment

Our sinusoidal entrainment method will allow us to improve how we study dynamic peri-sway postural control. Our methods have achieved higher levels of entrainment than those using visual stimulation.[190] De Nunzio et al. used 60 mm translations, and they were able to show the importance of proprioception for entrainment by removing the sensation with vibratory stimulation.[96] Therefore, proprioception may be more important for control of quiet stance than visual stimulation. The frequencies used by De Nunzio et al. were low (0.1 Hz and 0.25 Hz), and they only recorded 60 seconds of quiet standing data.[96] We recorded two minutes and looked at 0.5 Hz, 0.75 Hz and the two peak natural frequencies. Their low entrainments could also be due to the low frequencies they investigated. Although we cannot account for the entrainment via an analysis of EMGs and head accelerometers, the new three-dimensional (3d) motion capture system will allow us to focus on the subject's strategy (ankle or hip) during entrainment to allow us to focus EMG studies to the appropriate muscle group involved in entrainment. They also conclude that their moves may be too large, and that anticipatory reaction to regular oscillation via higher brain functions cannot be ruled out as cause for entrainment.[96] Corna et al. (60 mm peak-to-peak) show that the body under oscillations is not a rigid inverted pendulum and that the different segments respond differently.[191] This study shows the need for nonorthogonal biomimetic modeling of posture for an oscillating subject under entrainment. This study also confirms our findings that the head did not entrain readily as the APCoP did. The head was stabilized separately from the body, although it cannot be determined if it was via vestibular mean or higher predictive processing due to the predictability of the regularly

oscillating platform. The head stabilization mechanism under entrainment could be investigated in those with vestibular loss.

8.5 Ankle Model

The DH representation has been used to measure the movements of animal joints with a six revolute orthogonal mechanisms[192, 193] and represents the mechanics of arthropod limbs with their arbitrary revolute joints.[129, 140] Albright et al. described the difficulties encountered using DH for linkages with arbitrary axes and suggested a more flexible method, which used directional cosines.[124] Buford et al. used computer graphics techniques and arbitrary revolute joints for computer simulation of human hand joints' motions.[151, 154, 155]

Our proposed model is a more complete method for multilinked systems than the DH representation or the Albright method, but it also requires more computational power for motion simulation. These computations, whose complexity presented difficulties in past years, are now feasible because of the increases in desktop computing capabilities. Programming in Matlab®, a common software program, allows for flexibility in a variety of settings. Outputs for motion of limb segments can be in yaw, pitch, roll, x, y, and z values; a representation commonly used by engineers. The method is three-dimensional and has the same computational approach used in computer graphics and CAD software, thereby providing a common language to modeler, designers, engineers, and biologists. The technique involves translating and rotating the limb joint mechanism to align with a reference coordinate axis, rotating the joint revolute, and then de-rotating the mechanism and de-translating it back to its correct position. There is no order dependence for joint rotations. This approach reduces the azimuth errors and keeps the

limb or joint reference frames within the limb segments. The parameters describing each limb segment and revolute are clearly defined, simplifying the limb's mechanical description and kinematic modeling. The errors between the measured data and our technique are within the experimental errors of our measurement process. Thus, it is reasonable to assume that our methods of calculating the positions of the limbs are correct for orthogonal and non-orthogonal rotations. The identity matrix that is attained from the closed loop rotation also validates the methodology.

The method can also be used to compute limb dynamics and control. Giurintano et al. used sophisticated non-linear optimization to resolve static thumb joint forces using a five arbitrary revolute manipulator.[152] The solutions of static and dynamic forces in a non-orthogonal system are much more difficult than in the more common orthogonal robot designs.[121] A design advantage of our method is that the resultant forces are three-dimensional and can project out of the plane of the limb segments. Solutions for the dynamics of non-orthogonal systems are also more complicated than for orthogonal systems.

In addition to centripetal forces, Coriolis forces—a fictitious force deduced from inertia—become real factors for each moving linkage and may project out of the plane of the limb segments or the limb itself. These forces can be additive and are of great use to the evolved efficiency of the moving crab or human. They are probably an important factor in the evolutionary design of limbs and their joints. Robotic designs exploiting such forces could improve robot efficacy including more rapid motion, improved efficiency of motion, increased dynamic torque, and increased (or decreased) impact forces.

A better representation of the forward kinematics of animal limbs should assist in the understanding of limb motion, in designing limbs and joints, and in finding better solutions for inverse kinematics. Lupichuk developed a method for finding the position and orientation of an arbitrary revolute from three-dimensional data (x, y, z, yaw, pitch, and roll) with application to the elbow.[142] The method was accurate and precise, but it was limited to joints with only one degree of freedom, a relatively long limb segment, and an arc of motion of at least 60 degrees. Moore et al. used configuration space analysis of human wrist three-dimensional data to determine the number of degrees of freedom in the joint and to determine the paths of motion within the space, which showed only one degree of freedom.[143] Our model uses single degree of freedom joints and is not limited by linkage size or rotation.

This method will allow for improved postural modeling with entrainment since ankle or hip strategy can be investigated with three-dimensional imaging. This method will allow us to simulate and model how the bones of the ankle rotate to provide to the overall APCoP entrainment. Currently this method is limited to simulating only position and orientation. The amount of work required to provide inverse kinematics and kinetics is substantial. Currently this model could be used to calibrate an orthosis that measures the ankle joints rotations.

8.6 Conclusion

Diabetes as an epidemic will continue to affect our aging society. Clinicians can now be made aware that detriments to postural sway exist in the absence of peripheral neuropathy since our dynamic postural analysis methods show differences that are not detected by the current static methods in the absence of peripheral neuropathy as

determined by nerve conduction studies. Furthermore, the sensorineural hearing loss observed in our diabetic subjects provided evidence that similar deficits exists within the vestibular system. With our new sinusoidal entrainment method, our lab will be able to characterize sway depending on subjects sway status to provide us with a better understanding perturbation threshold by investigating the dependence on postural motion of acceleration thresholds. With future studies investigating ankle and hip strategies for entrainment, model will by able to mimic the nonorthogonal properties of joints through our nonorthogonal multilinked system. While the observed increase in acceleration thresholds of diabetic individuals shows the power of this method in detecting changes in the postural system, the proposed entrainment method will allow us to better control for a subject's sway for acceleration threshold detection.

8.7 Future Work

Further studies focusing on diabetic individuals with cutaneous sensory neuropathy, individuals with lower limb neuropathy, and those with both will help better define the cause for instability in diabetic individuals. In addition, further studies on individuals with peripheral neuropathy but who are confirmed to not have diabetes or be glucose-intolerant will better define peripheral neuropathy's and Type-2 diabetes' contributions to postural instability. The asymmetric profiles of some of the SWM thresholds provide evidence to investigate handedness, footedness, and foot preference for quiet stance. In addition, recruiting equal numbers of male and female subjects would be paramount in differentiating sex-related differences especially in hearing loss. With future studies between groups, we can look at differences in amplitude and frequency thresholds to perturbations between diabetic individuals, elderly adults, and young adults.

The sinusoidal entrainment will also allow us to study perturbation thresholds during different points in the sway between groups. Future research will improve our measurement of joint motion and the analysis and design of joint and limb kinematic mechanisms.

APPENDIX A

IRB INFORMED CONSENT VA

VA Department of Veterans Affairs

VA RESEARCH CONSENT FORM

PROTOCOL # H00-022

Subject Name: _____ **Date:** _____

Title of Study: Threshold Detection of Postural Control in Diabetic Neuropathy and Aging

Principal Investigator: C. J. Robinson, DSc, PE; A. M. Hollister, MD **VAMC:** Shreveport

We are asking you to volunteer to take part in a research study at the Shreveport Veterans Affairs Medical Center (VAMC) and Louisiana State University Medical Center (LSUMC). It is important that you read and understand the information on this form.

DEFINITION OF CONSENT FORM

This Consent Form gives detailed information about the research study which you will be able to discuss with your doctor. It is not meant to frighten or alarm you; it is an effort to make you better informed in order for you to make a decision as to whether or not you wish to participate. This process is known as "informed consent."

PURPOSE OF STUDY AND SELECTION OF SUBJECTS

Slips and falls, and even the fear of falling, can represent a major medical and functional barrier to living independently. A fall is normally prevented by the detection of abnormal motion and by strategies used to correct or compensate for imbalances. Therefore, to react to a potential slip or fall, one must be able to detect motion changes that may lead to slips or falls.

You are invited to participate in a research study related to standing balance and postural control. Researchers at the Overton Brooks VAMC and Louisiana State University Medical Center hope to learn how much the senses of the limbs (touch sense, joint angle sense, muscle tension sense) contribute to stability. Such knowledge may well lead to better evaluation and training methods in order to prevent slips and falls. You were selected as a possible participant in this study because you are an average healthy adult and your senses are intact. Your responses will be used as verification of results previously attained. You should be between 18 years or older to participate in this study. Before proceeding further, we need your permission to ask you if you have had certain illnesses or neurological problems which might confound our study results, and hence, make you not a candidate for this particular research study. Your answers will remain confidential.

May we ask you some questions about your medical history, and verify them from the information in your medical chart (if available within the VA)?

Yes or No: _____ Initials: _____

SUBJECT'S IDENTIFICATION (I.D. plate of give name - last, first, middle)

Subject's Initials: _____

VA FORM
[illegible] 10-1086

VA Department of Veterans Affairs

VA RESEARCH CONSENT FORM
PROTOCOL # H00-022 (Continuation Page 2)

Subject Name: _____ **Date:** _____

Title of Study: Threshold Detection of Postural Control in Diabetic Neuropathy and Aging

Principal Investigator: C. J. Robinson, DSc, PE; A. M. Hollister, MD **VAMC:** Shreveport

QUESTIONS

Persons with severe cardiac or cardiopulmonary involvement, chronic lower back spasms or pain, central neurological deficits, history of non-healing skin ulcers or peripheral vascular occlusive disease, current drug or alcohol dependence, or orthopaedic deformities (such as kyphosis, arthritic changes or amputation) must be excluded from this study. Those with a history of repeated falls, previous joint injury, or a bone or articular cartilage disease must also be excluded. (Any information obtained during this study and identified with you as a subject will remain confidential and will be disclosed only with your permission.)

You do not have now, or have ever had, any of the problems just listed. Yes or No: _____ Initials: ____

If you answered "Yes," thank you for your time and effort in volunteering to participate, but we cannot use you in this particular study. Please fill out the personal information on the last page before you go. If you answered "No," then you are a likely candidate for our study, which we will now explain to you.

PROCEDURES

If you are an older adult or a person with changes in the nerves in your limbs, you may have had a change in how you sense changes in the standing environment. If you are in good health, have no physical or neurological problems, you will serve in a group that we call "control." We will compare these two groups to better understand how the nervous system assists in maintaining postural stability and dynamic balance.

If you decide to participate in this research study you will be asked to answer a brief medical history questionnaire. This may be done over the phone or in the laboratory. All subjects will be evaluated for sensory and motor function, lower limb strength and joint range-of-motion, and any possible lower limb asymmetries.

The main test will have you standing with bare feet on a platform that will be stationary for approximately 30 seconds then moving forward during randomized time intervals. You will be informed when a possible move may occur and you will be asked to state whether the device is moving. In these tests the platform will move your whole body. You will be wearing a blindfold that will restrict your vision and headphone to reduce outside noise, so that you may only receive motion inputs from your sensory system or balance system. For all tests you will be wearing surface muscle activity sensors on your legs. If you go through all tests, we estimate that their completion will take less than four hours. We may stop testing if you become dizzy, or nauseous. You can stop the test at any time that you wish, without reprisal.

Subject's Initials _____

VA FORM
JAN 1990 10-1086

VA Department of Veterans Affairs

VA RESEARCH CONSENT FORM
PROTOCOL # H00-022 (Continuation Page 3)

Subject Name: _____ **Date:** _____

Title of Study: Threshold Detection of Postural Control in Diabetic Neuropathy and Aging

Principal Investigator: C. J. Robinson, DSc, PE; A. M. Hollister, MD **VAMC:** Shreveport

DISCOMFORTS AND RISKS

All motions of the platform will be near your natural sway change of position. Because of this, you may not always be able to feel the device move. Also because the movements will be so slight, there is very little chance of your falling. During the times when the platform is moving and while your eyes are closed or blindfolded, and you are wearing the headphones to block out external noises, you may feel a slight loss of balance, dizziness or nausea. You will be spotted by an investigator standing behind you who will correct your position before a potential fall event can occur.

For all tests, all joint motions will be small and fairly slow. However there is a possibility that your ankle or knee joints could be injured in these tests, especially if the joints are already weakened. For this reason if you have a previous joint injury or have been diagnosed with a bone or articular cartilage disease, we ask you tell us now and not participate in this study.

Since we use properly isolated electrical amplifiers, there should be no risk of shock from our measurement of muscle activity. The muscle activity sensors will be held to your skin with a small piece of double sided tape. The gel that helps conduct your muscle activity the sensors may have a salt base. You may experience some redness from the tape or conduction gel. This is common and the redness should disappear within a few hours.

BENEFITS

You may not personally be helped by taking part in this study, but your participation may lead to knowledge that will help others. We will review your own results with you before you leave, and significant overall findings developed as a result of this study will be provided to you at the conclusion of the study.

RESEARCH RESULTS

Information and research results will be used to further the field of posture and balance control and to benefit the evaluation and therapy processes related to posture and balance. Therefore the research results will possibly be used for scholarly papers, presentations, and future grant applications.
Any information obtained during this study and identified with you as a subject will remain confidential and will be disclosed only with your permission.If results of this study are reported in medical journals or at meetings, you will not be identified by name, by recognizable photograph, or by any other means without your specific consent. Your medical records will be maintained according to this medical center's requirements. By signing this form you are giving permission for us to make records available to the Shreveport VAMC and LSU Medical Center's Institutional Board for Human Research to which information will be released, all of whom must maintain confidentiality.

Subject's Initials _____

VA FORM
10-1062

VA Department of Veterans Affairs

VA RESEARCH CONSENT FORM

PROTOCOL # H00-022 (Continuation Page 4)

Subject Name: _____ **Date:** _____

Title of Study: Threshold Detection of Postural Control in Diabetic Neuropathy and Aging

Principal Investigator: C. J. Robinson, DSc, PE, A. M. Hollister, MD **VAMC:** Shreveport

OTHER TREATMENT AVAILABLE

Participation in this project will not effect your usual clinical treatment here at the VA. You are aware that you are under no obligation to participate in this study and you may withdraw at any time without prejudice to your medical care or loss of benefits to which you are entitled. Should you choose not to participate, you will still receive the usual medical care and treatment to which you are entitled. You may withdraw participation from the project at any time without prejudice

SPECIAL INFORMATION

You will be paid $25.00 by check for each session in which you participate. A session may last up to 4 hours. Payment will be through the Overton Brooks VAMC in Shreveport, LA.

1. You are not required to take part in this study — your participation is entirely voluntary.
2. You can refuse to participate now or you can withdraw from the study at any time after giving your consent.
3. Your decision whether or not to participate in this study will not involve any penalty or loss of rights nor will it prejudice your future relation with the VAMC or LSUMC.
4. There will be no costs to you for any of the treatment or testing done as part of this research study
5. In case of adverse (bad) effects or physical injury resulting from this study, eligible veterans are entitled to medical care and treatment. Compensation may or may not be payable in the event of physical injury arising from this study under applicable federal law. Further information about compensation and medical treatment may be obtained from the medical administration service at this.
6. VA medical center. Non-eligible veterans are entitled only to medical emergency care and treatment on a humanitarian basis.
7. If you have questions about your rights as a research participant, you may contact the Chairman of the Institutional Review Board at (318)-675-5409 or the Chief of Staff, Overton Brooks VA Medical Center at (318)-424-6089.
8. If you are a patient of the VAMC, a copy of this consent form will be placed in your medical record.

Subject's Initials _____

VA FORM
JAN 1990 10-1086

VA Department of Veterans Affairs

VA RESEARCH CONSENT FORM

PROTOCOL # H00-022 (Continuation Page 5)

Subject Name: _____ **Date:** _____

Title of Study: Threshold Detection of Postural Control in Diabetic Neuropathy and Aging

Principal Investigator: C. J. Robinson, DSc, PE; A. M. Hollister, MD **VAMC:** Shreveport

AFFIRMATION FROM SUBJECT

RESEARCH SUBJECTS' RIGHTS: I have read or have had read to me all of the above. Dr. Charles Robinson or his associate has explained the study to me and answered all of my questions. I have been told of the risks or discomforts and possible benefits of the study. I have been told of other choices of treatment available to me.

I understand that I do not have to take part in this study, and my refusal to participate will involve no penalty or loss of rights to which I am entitled. I may withdraw from this study at any time without penalty or loss of VA or other benefits to which I am entitled.

In case there are medical problems or questions, I have been told I can call Dr. Charles Robinson at (318)-424-6080 or Dr. Anne Hollister (675-6181) during the day and Dr. Robinson at (318)-513-9122 after hours. If any medical problems occur in connection with this study the VA will provide emergency care.

I understand my rights as a research subject, and I voluntarily consent to participate in this study. I understand what the study is about and how and why it is being done.

I will receive a signed copy of this consent form.

"I have been given the opportunity to ask questions and have them explained to me."

_____ _____

Subject's Signature Date

_____ _____

Signature of Witness Witness (print)

_____

Signature of Investigator

Institutional Review Board Approval Start Date 3/27/02 - End Date 03/26/03

Subject's Initials _____

VA FORM

APPENDIX B

IRB INFORMED CONSENT

CLARKSON UNIVERSITY

INFORMED CONSENT FORM

PROJECT TITLE: Phase-Locked Postural Perturbation Psychophysical Models

PRINCIPAL INVESTIGATOR: Dr Charles Robinson IRB Approval: 6/19/2006 #06-24

Objectives.

We are asking you to volunteer to take part in a research study at Clarkson University related to standing balance and postural control. Researchers at Clarkson University hope to learn how much the senses of the limbs (touch sense, joint angle sense, and muscle tension sense) contribute to the stability of your posture. With such knowledge, we might later reduce the risk of falling or slipping.

Methods.

You are a possible participant in this study because your senses are reasonably intact and you are not afflicted with, severe cardiac or cardiopulmonary involvement, chronic lower back spasms or pain, central neurological deficits, history or presence of foot ulcers or peripheral vascular occlusive disease, current drug or alcohol dependence, or orthopedic deformities, injury or disease (such as kyphosis, arthritic changes, broken or replaced joints, or amputation). Having adult-onset diabetes does not bar your participation.

This research is centered upon subtly guiding your natural sway pattern and determining where in your sway pattern that you can best sense a mild shift in your balance. When you balance, you use your senses of foot pressure and/or of muscle effort (as signaled by your leg nerves); your vision; or the balance sense organ in the head (called the vestibular system), or any combination. It is important to our study to be able to separate out these effects, so we do the tests outlined below.

We will give you some initial screening tests to determine whether you meet the study criteria for proceeding further. We will test how well you can pay attention to detail, since our movement tests are subtle. We will also measure via a standard written test what your feelings are about the quality of your health status. We will ask you certain questions about your health, and past and present illnesses and injuries. Based on your responses, we may need to not continue with you beyond that point, as we have found certain factors that exclude from the study.

We will measure how well and how fast you sense small touches to the bottom of your foot or toes; how well and how fast you sense tones of various pitches; and how far your big toes, ankles, knees and hips move (called your range-of-motion) and the strength and stiffness of the muscles of these joints. We will measure your height, weight and the length of various parts of your body. We will specifically ask you for permission to measure your hip circumference and your waist circumference, and you may refuse for us to do that without suffering any reprisals. We will do two standard balance tests to see how well you balance on both legs, on one leg, with one foot behind the other with your eyes open, and with your eyes closed; and other balance measures, like your ability to stand form a sitting position. You will do these tests standing on a tile floor or rising from a chair. All of these tests will take about 40 minutes, and may be given in-between other tests.

All humans sway. It is a natural, every second, occurrence. What we do is to add a small forward sliding movement (a fraction of an inch to 1.5 inches) to the plate on which you are standing. An initial test will have you standing with bare feet on a platform that will be stationary for about 20 seconds before it is moved. You will be told when a possible move may occur and you will be asked to decide and signal at what time the device was moving.

We may gently rock the platform forward and backward to see how it influences your sway, and at what level you can detect such sliding.

In these tests the platform will move your whole body. You will be wearing a blindfold that will restrict your vision and headphones to reduce outside noise, so that you may only receive motion inputs from your touch sensory system or balance system. You will be wearing adhesive surface muscle activity sensors on your legs. You will be tested on a special mat that sits on top of the platform. This mat measures the pressure under each part of your foot.

As part of our testing, we want to find out how the various parts of the body react to the platform movement. To do this, we may attach small reflective marker dots to selected places on your skin (generally between 10 and 20 spots). Typical locations for placing these markers are on your ankles, shin, knee, hip shoulder, and head, among others. We then determine the location of the markers using special cameras. Only the location of the markers is collected. You cannot be identified. In some cases, we will ask a participant to allow us to videotape the testing, and will ask these individuals to sign an additional "Permission to Videotape" document. You have the right to request that we do not use the markers or videotape you. In no way will such a refusal impact the rest of the testing.

In most cases, you as a test participant will be placed in a harness. Its purpose is not to support you, but only to catch you in the unlikely event that you start to fall. In fact, the harness is designed so as not to provide you with any clues as to what the platform is doing. With some of you, we will see if this is true by comparing your responses to our tests with and without the harness.

What to expect.

Your first visit will involve initial screening and clinical measures related to postural stability. A questionnaire will assess known problems of neurological, orthopedic and neuromuscular origin. You will be evaluated for sensory and motor function, lower limb strength and how far your joints rotate. Balance tests will be performed, including, but are not limited to, the heel-to-toe test and one-foot-balancing. These tests will be performed by an experienced technician or the Principal Investigator.

You will be asked to stand still upon a platform within a steel superstructure, blindfolded, barefooted and wearing headphones that emit a masking white noise for up to 15 minutes at a time. If you choose to allow us via a separate document to videotape you, markers will be placed with adhesive to several important joints on your limbs and torso to capture your movement. On the video, your image will not be recognizable because the headphones and blindfold you wear will obscure your identity.

Electrodes will be placed on your shins and calves to detect your muscle impulses as you sway upon the platform. These electrodes are isolated and do not pose any risk of shock. They will be affixed to your skin with double-sided adhesive tape.

Before the trials begin, the platform will calibrate itself to your particular standing sway pattern and will, when testing begins, gently rock you back and forth. This motion will be imperceptible to you, but if you become dizzy at any time, please let us know and we will stop the trials immediately. Prompts, given via audio instructions through the headphones will guide you through a series of trials, during which you will be asked to determine whether or not you detected a movement in the platform. In between trials you will be supplied with a heated blanket for your feet and a chair to rest on. We will wait until you are rested and ready to continue before we proceed.

Your initial screening and initial testing on the platform will take up to 4 hours. You may be asked to participate in one or two more 4-hour test sessions.

There will be no cost to you for any of the testing done as part of this research study. You can end the research session at any time if you feel uncomfortable for any reason.

Risks.

If you go through all of these platform tests, we estimate that the completion of this part will take less than four hours. We may stop testing if you become dizzy or nauseous. You can stop the test at any time that you wish,..

All motions of the platform will be near your natural sway change of position. Because of this, you may not always be able to feel the device move. Also because the movements will be so slight, there is very little chance of your falling.

During the times when the platform is moving and while your eyes are closed or blindfolded, and you are wearing the headphones to block out external noises, you may feel a slight loss of balance, dizziness or nausea. Let us know immediately if that is the case.

In most cases, you will be in a harness during testing to prevent you from falling. If you are not harnessed during a test, a member of the laboratory staff will be standing behind or beside you at all times when you are blindfolded. He or she is located there to correct your position before a potential fall event can occur.

Additionally, for this research, participants will be moved to and fro by the platform in an effort to guide their natural sway patterns. The movement will be designed with a goal for them not to be able to sense this movement, and therefore the effect on most participants will be slight. However, such rocking may produce a higher risk of you experiencing dizziness. Again, let us know if that occurs to you.

The risks to you from our special cameras are very small as the markers are illuminated with light that is beyond the capacity of the eye to see (called infrared light).

Since we use properly isolated electrical amplifiers, there should be no risk of shock from our measurement of muscle activity. Both the muscle activity sensors and the video markers will be held to your skin with small pieces of double-sided tape. You may experience some redness from the tape. This is common and the redness should disappear within a few hours.

Benefits.

Taking part in this study may not personally help you, but your participation may lead to knowledge that will help others. We will review your own results with you before you leave, and significant overall findings developed as a result of this study will be provided to you at the conclusion of the study.

Obligations.

Participation is voluntary. Refusal to participate or deciding to discontinue participation at any time will involve no penalty or loss of benefits to which you are otherwise entitled.

Confidentiality.

Information and research results will be used to further the field of posture and balance control and to benefit the evaluation and therapy processes related to posture and balance. Therefore the research results will possibly be used for scholarly papers, presentations, and future grant applications. Any information obtained during this study and identified with you as a subject will remain confidential and cannot be disclosed without your written permission. If results of this study are reported in medical journals or at meetings, you will not be identified by name, by recognizable photograph, or by any other means without your specific consent. In all testing, you will be identified only by a special unique identifying code and not your name. The form linking your name to that code is kept in a locked file cabinet. By signing this form you are giving permission for us to make your name, ID code, and test results available to Clarkson University's Institutional Review Board for Human Research, if they wish such information, again under conditions of confidentiality.

Subjects' Rights.

If you have any questions concerning your rights as a subject or if you wish to report any injuries or mistreatment, please contact Dr. Leslie Russek, Chair of the Human Subjects Institutional Review Board, Clarkson University, 204 Clarkson Hall, Box 5880, Potsdam, NY 13699 (315) 268-5880, lnrussek@clarkson.edu.

Informed Consent.

Please sign here to indicate you received and understood a verbal and written explanation of the procedures and objectives of this study, and had all questions answered to your satisfaction. I certify that I am 18 years of age or older.

Signed _____ Date _____

Signed _____ Date _____
Witness

Signed _____ Date _____
Principal Investigator or approved delegate

APPENDIX C

INITIAL QUESTIONNAIRE

Protocols for "Sinusoidal Entrainment study of Postural Control"

Initial Contact Questionnaire
Front Page

Name: _____ Date of Contact (mm/dd/yy) _____

How did subject learn of study? Paper Announcement Internet Word of Mouth

Subject informed of: Age Criteria: _____ Exclusion Criteria: _____

Scope of Research: _____ Reason / Benefit of Research: _____

Time Required: _____ Financial Compensation: _____

Is subject interested in participating in study? Yes No

Has Subject been found to be Vestibularly Normal? Yes No Unknown

Is subject able to get to the Clarkson lab? Yes No

Subject Contact via: Phone #: _____ E-Mail: _____

Address: _____

Subject Availability / Scheduled Testing Date (mm/dd/yy) _____ Time(hh:mm) _____

(mm/dd/yy) _____ Time(hh:mm) _____

How has subject been given directions to lab? Phone Internet Mail Personally

Subject's Date of Birth (mm/yy): _____ Subject's Gender: Male Female

Subject's Race: Caucasian Black Hispanic Native American Middle Eastern Indian Asian

Other: _____

Subject Code: _____ _____ _____ _____ _____ _____ _____ _____ _____ _____

Gender Age Age Contact # # # IC1 IC2 IC3

The above information, and provided medical history is true to the best of my knowledge.

Investigator signature: _____ Date(mm/dd/yy): _____

Investigator Initials: _____

Initial Screen Questionnaire
Medical History

Date: _____

Subject Code: ____ ____ ____ ____ ____ ____ ____ ____ ____ ____
Gender Age Age Contact # # # IC1 IC2 IC3

Subject weight as measured by the weighing scale: _____

Does the subject have any history of (Check if Yes):

Cardiac Problems: Tachy/Bradycardia: _____ Cardiac Arrhythmias: _____

Heart / Lung Disease: _____ Shortness of Breath: _____

Other: _____

Neurologic Problems: Stroke/TIA: _____ Head Injury: _____

Peripheral Nerve Injury: _____ Spinal Injury: _____

Advanced Diabetes: _____ Vision Loss: _____

Hearing Loss / Ear Infections: _____ Loss of Balance: _____

Memory/Concentration Deficits: _____ Sensory Loss: _____

Muscle Tone Abnormalities: _____ Coordination Deficits: _____

Other: _____

Orthopaedic Problems: Arthritis / Joint Disease: _____ Osteoporosis: _____

Lower Back Pain/Spasms: _____ Spinal Stenosis: _____

Fractures: _____ - Specify: _____

Other: _____

Alcohol Use / week: None < 3 Drinks 3-14 Drinks >14 Drinks

Record Caffinated Items within last 12 hours: _____

Medication / Drug Use: Pain Medication: _____ Depressants: _____ Anti-Depressants: _____

Psychoactive: _____ Other: _____

Investigator Initials: _____

Protocols for "Sinusoidal Entrainment study of Postural Control"

Initial Sensory-Motor Screen

Date: _____

Subject Code: ____ ____ ____ ____ ____ ____ ____ ____ ____ ____
Gender Age Age Contact # # # IC1 IC2 IC3

Reflex Testing (+ = normal, - = abnormal, 0= absent):

Patellar Reflex: Right: _____ Left: _____

Achilles' Reflex: Right: _____ Left: _____

Vision Testing (+ = normal, - = abnormal, 0= absent):

Read Newsprint: _____ Read _____ point font @ 20 feet: _____

Uses Eyeglasses / Contacts: _____

Visual Fields: Right: _____ Left: _____ Up: _____ Down: _____

Sharpened Romberg Test Findings (+ = normal, - = abnormal, 0= absent):

Balance: _____ Recovery from Loss of Balance: _____

Time to Loss of Balance (seconds): _____

Precession Test: (Subject hops on one foot should remain facing forward)

Right Foot: _____

Left Foot: _____

Tactile / Somato-Sensory Tests with Stoelting Monofilaments to Foot Sole (mm diameter):

Right:		Left:	
Base MetaTarsal 4:	_____	Base MetaTarsal 4:	_____
Base Big Toe:	_____	Base Big Toe:	_____
Base MetaTarsal 1: (Big Toe)	_____	Base MetaTarsal 1: (Big Toe)	_____
Base Heel:	_____	Base Heel:	_____

Investigator Initials: _____

Initial Therapeutic Screen

Date: _____

Subject Code: _____ _____ _____ _____ _____ _____ _____ _____ _____ _____
Gender Age Age Contact # # # IC1 IC2 IC3

Posture and Balance (+ = normal, - = abnormal, 0= absent):

Sit to Stand: _____ Standing eyes Closed: _____ Ambulation: _____

Joint Stiffness / Tone (+ = normal, - = abnormal, 0= absent):

Shoulder: _____ Elbow: _____ Hip: _____ Knee: _____ Ankle: _____

Limb / Body Segment Length (mm):

Length of Foot:	Right: _____	Left: _____
Floor to Lateral Malleolus:	Right: _____	Left: _____
Floor to Lateral Epicondyle of the Femur:	Right: _____	Left: _____
Floor to Greater Trochanter:	Right: _____	Left: _____
Floor to Lateral Aspect of Humeral Head	Right: _____	Left: _____
Floor to Top of Head (Total Height):	Dorsal Aspect: _____	
Lat. Aspect Humeral Head to Lat. Epicondyle of the Humerus:	Right: _____	Left: _____
Lat. Aspect Humeral Head to Tip Digit III:	Right: _____	Left: _____

Investigator Initials: _____

Protocols for "Sinusoidal Entrainment study of Postural Control"

Time Sheet for Testing

Date: _____

Subject Code: _____ _____ _____ _____ _____ _____ _____ _____ _____ _____
Gender Age Age Contact # # # IC1 IC2 IC3

Subject arrival: _____

End introduction of subject to platform and people: _____

Start Informed consent: _____

End Informed consent: _____

Start Medical questionnaire (Page 2 plus Romberg and hop test): _____

End Medical questionnaire: _____

Start hooking up electrodes: _____

End hooking up electrodes: _____

Start EMG_COP calibrate routine: _____

End EMG_COP calibrate routine: _____

Start ____Hz Sinusoidal practice: _____

End ____Hz Sinusoidal practice: _____

Start ____Hz Sinusoidal recorded: _____

End ____Hz Sinusoidal recorded: _____

Start ____Hz Sinusoidal recorded: _____

End ____Hz Sinusoidal recorded: _____

Start sensory and other evaluation (page 3): _____

End sensory and other evaluation: _____

Start ____Hz Sinusoidal recorded: _____

End ____Hz Sinusoidal recorded: _____

Start ____Hz Sinusoidal recorded: _____

End ____Hz Sinusoidal recorded: _____

Start ____Hz Sinusoidal Lock-in recorded: _____

End ____Hz Sinusoidal Lock-inrecorded: _____

Start Anthropometric measures (page 4): _____

End Anthropometric measures: _____

Start Mini-mental evaluation test: _____

End Mini-mental evaluation test: _____

Start debrief: _____

End signing off: _____

List Order of Lock-in:

_____

_____

_____

_____

Investigator Initials: _____

APPENDIX D

START-UP PROTOCOL 2-AFC

Start-Up Protocol
Prior to Subject Arrival

On Entry to the Lab:

1. Check the following ON switches:

Lab Lights:_____Daytronic Signal Conditioners: _____Gould Signal Conditioners: _____

SLIP Computer: _____ Delsys EMG Box: _____Headphone Transmitter: _____ Mixer: _____

Speakers: _____ Doorbell:_____

2. Check Air Compressor:

Open Compressor and 2nd Tank Water Valves: _____ Close Compressor and 2nd Tank Water Valves: _____

Turn on Compressor, Check for Leaks and Dry air Conditioners: _____

3. Check the following CONNECTIONS:

SLIP computer Serial A to A/B Box (Switch to SLIP): _____

SLIP computer AT-MIO to Connector Box (Analog and Digital): _____

SLIP computer Sound-Blaster to Mixer: _____ SLIP computer to Laser Printer: _____

Power to Accelerometer: _____ Accelerometer **X** to Gould #3: _____

Accelerometer **Y** to Gould #6: ____

Accelerometer **Z** to Gould #5: _____ Gould #3 Monitor Out to Connector Block: _____

Gould #5 Monitor Out to Connector Block: ___Gould #6 Monitor Out to Connector Block: ____

AB, CD EMG Sensors and ground to Belt Box: __Belt Box to EMG Box Channels 1, 2, 3, 4: ___

Radio Shack Doorbell Alarm to Connector Block: __Radio Shack Doorbell Alarm to Mixer: ____

White Noise Generator (Radio) to Mixer: _____ Mixer to Headphone Transmitter: _____

4. Have on Hand the following fresh BATTERIES:

Radio Shack Doorbell Receiver (3-AA): _____ Radio Shack Doorbell Transmitter (1-9volt): _____

5. Find the following "loose" ITEMS and place on Platform:

Radio Shack Doorbell Transmitter: _____ Blindfold: _____

Prepare Electrodes with One side of the adhesion pads: _____

Form Completed by: _____Date/Time: _____

Start-Up Protocol
Prior to Subject Arrival

Test Equipment by:

1. Turn on Air to Platform and turn on DMM-2100:
Air pressure @ platform >70psi: _____ DMM-2100 w/o reset light: _____Platform floats: _____

2. Open Continuous Acquire Buffered Chart.VI (Examples\Analogin\) Read Channels:
Channels 0:3, CoP: _____ Each channel lesser voltage as weight over each vertical force sensor increases.

Channels 4 and 5, Position of Platform: _____ Voltage increases as platform moves toward bookshelf. Acceleration: _____ Voltage is initially positive with towards the door movement.

Channels: 8:11, EMG: _____ Open EMGtest.VI, check each channel against Biceps.

Channels: 12,13,14,15, Head Accel: _____ Voltage = +/- 5V with gravity., Doorbell switch: _____ "rings" and gives approximately 4 volts spike.

3. Turn on Headset and Open Get_Sound.VI
Headphones / Mixer: _____

In headphones able to hear continuous "white noise", overlaid by wave file (*.wav), and/or doorbell: _____

4. Turn off: EMG box, Headphones, and Doorbell receiver.

5. Open "5 RANDOMS.VI" to determine the order of testing

__1__1 mm Forward Smooth: _____
__1__2 mm Forward Smooth: _____
__1__4 mm Forward Smooth: _____
__1__8 mm Forward Smooth: _____
__1__16 mm Forward Smooth: _____

6. Run VDA Initialize and Home.VI

7. Open the Following VI's.

***5Jog.VI*, *FC Learning7f.VI, *EMG_CoP Calibrate.VI*, *Reaction VDA5.VI* Forced Choice VDA 7f.VI, and *Latencies VDA7f.vi**

Form Completed by: _____Date/Time: _____

Testing Protocol
When Subject Arrives

Subject Code: _____ _____ _____ _____ _____ Date: _____
Gender Age Age Alpha Alpha

1. Introduce Investigator: _____

2. Show Platform and run "5 jog.VI" which shows length of jogs and approximate speed (25mm/s2): _____

"This is the test platform that you will be standing on. It will be making very small moves (run VI) and you will have to determine when the move occurred." But before you step on the platform I need you to read and sign the informed consent document and take some clinical measurements."

3. Give subjects IRB approved consent form. Subjects must initial and sign form as appropriate: _____

4. Determine and record Subject "ID" and have them fill out Medical History form if not already completed: _____

5. Give the mini-mental evaluation form from Linda Ferguson (OT).

6. Based on the schedule take the subject over for Nerve conduction study at Dept. of Neurology (for elderly subjects only) or perform the perturbation study in RNL.

7. Have subject remove shoes and socks, and Perform Clinical assessment according to form/ protocol: _____

8. Perform Therapeutic/Anthropometrical measures: _____

9. Turn on Doorbell receiver, have them test transmitter, explain forced choice protocol: _____
"With this doorbell transmitter, you will be able to tell me when you feel the platform move."
"For (this) (the first test), you will be asked to step on the platform, place the headphones over your ears, and cover your eyes with the blindfold. From your headphones you will be hearing a constant 'masking white noise', and four verbal cues: 'Ready', 'One', 'Two', and 'Decide'. Each will be two seconds apart. If you think that the platform moved between the words 'One' and 'Two', press the button once; if between the words 'Two' and 'Decide', press the button twice. All decisions should be made as quickly as possible, but no later than two seconds after the word 'Decide'. Go ahead and try the button with your left hand to make sure you are comfortable with it. It may take several pushes to get the second doorbell chime."

10. Place EMG sensors on bilateral Tib. Anterior and Solius muscles, *A*=R. TA, *B*=R S., *C*=L. TA, *D*=L. S.: _____

"I will be collecting EMG data to determine how your muscles react to the slight movements the platform will be making, to help me determine if this is part of what helps YOU to decide if the platform has moved. After I'm done placing these sensors, I'll ask you to do some movements to help me calibrate them."

Testing Protocol
When Subject Arrives

Subject Code: _____ _____ _____ _____ _____ Date: _____
Gender Age Age Alpha Alpha

11. Run "EMG_CoP Calibrate.VI" and cue subject to movements: _____
Wait for platform calibration, "Step up onto the platform and stand with even weight on both your feet." Record 20 seconds static eyes open. "Now stand on your toes." Record toes. "Now on your heels." Record heels. "OK, relax on both feet again" Record static. "You can now step off the platform, watch that you don't tangle the EMG lines."

12. Run FC Learning.VI for 10 trials at appropriate displacement (guaranteed detect) under FC protocol. _____
First 4 trials with eyes open for subject psychological safety, last 6 trials under eyes closed condition for learning under testing conditions. This VI can be repeated up to 3 times for learning purposes.
"I'd like you to try to feel the platform move a few times. After you decide when the platform moved, you will hear a response 'one' or 'two' stating when the platform actually moved. Do the first 4 trials with your eyes open, then close your eyes."

13. Explain forced choice protocol again and run "Forced Choice VDA.VI" for 1 condition: Note: First 20 seconds of test ask subject to stand still. _____

14. Allow subject 5-minute rests while checking summary file(s) for lowest detected acceleration, for the forced choice tests, write these thresholds below:

_____1 mm Forward Smooth: _____
_____2 mm Forward Smooth: _____
_____4 mm Forward Smooth: _____
_____8 mm Forward Smooth: _____
_____16 mm Forward Smooth: _____

15. Explain "Latency" test protocols: _____
"For these last sets of tests, I've chosen an acceleration level that you have previously detected. So while you're standing on the platform with the headphones and blindfold on, I want you to press the detect button as soon as you feel the platform move. However, to make sure you're not pressing the button at random, I'm going to have a few trials when after the word "Ready", there will be no movement."

17. Repeat steps 12-15 for other two displacements, then have subject rest 10-15 minutes.

18. Explain all portions of "Reaction time" tests, then repeat prior to testing each portion. Open "Reaction.VI" and run as stated, then allow 5-10 minute rest.
"To test your overall reaction time, I'm going to run 3 sets of tests. For the first test, I'm going to have you step on the platform, wear the headphones and blindfold. After the word "Ready", the platform will move within three seconds. I('ll) want you to press the door bell button as soon as you feel the platform move."

Run platform portion of test.

Testing Protocol
When Subject Arrives

Subject Code: _____ _____ _____ _____ _____ Date: _____
Gender Age Age Alpha Alpha

18 continued:
Have subject sit in chair. "For the second reaction time test, I ('ll) want you press the door bell button as soon as you feel me touch you on your big toe with this force sensor." (Five trials)

Run toe-touch with press detect reaction portion of test.

"Finally, for the third reaction time test, I'll want you to press the force sensor as fast as you can, after you hear the doorbell." (Five trials)

Run sound with press detect reaction portion of test.

19. De-brief subjects: _____

20. Reschedule subjects for additional test time if needed: _____

Day/Date: _____
Time: _____

Alternate Day/Date: _____
Time: _____

21. Have Subject fill out payment slip to be kept as a receipt: _____

To: Overton Brooks VA Medical Center
510 East Stoner Avenue, Shreveport, LA 71101.
Phone: (318) 424-6080, Fax: (318) 429-5733.
Attn.: Ms. Linda Ritmo - Executive Director.

Re: Subject Reimbursement Date: _____

Please reimburse (subject) _____, (Soc. Sec. #) _____

For the amount of: _____dollars, for participation in the research protocol titled "Postural Control in Diabetes, Peripheral Neuropathy, and Aging", Charles J. Robinson, principal investigator. Rehabilitative Neuroscience Lab, Overton Brooks VA Medical Center, LA. (318) 424-6080.

The mailing address is as follows: (street, number and apartment): _____

(City, State and Zip): _____

(Subject Signature): _____ (Investigator Signature): _____

Date: _____

Within the next three weeks you should be receiving a check from the Overton Brooks VAMC. If you do not receive a check, please notify Charles J. Robinson or Samantha Richerson, at: (318) 424-6080, or E-mail at: sricherson@ieee.org. Please leave your name and method(s) by which you can be contacted.

To: Overton Brooks VA Medical Center
510 East Stoner Avenue, Shreveport, LA 71101.
Phone: (318) 424-6080, Fax: (318) 429-5733.
Attn.: Ms. Linda Ritmo - Executive Director.

Re: Subject Reimbursement Date: _____

Please reimburse (subject) _____, (Soc. Sec. #) _____

For the amount of: _____dollars, for participation in the research protocol titled Postural Control in Diabetes, Peripheral Neuropathy, and Aging", Charles J. Robinson, principal investigator. Rehabilitative Neuroscience Lab, Overton Brooks VA Medical Center, LA. (318) 424-6080.

The mailing address is as follows: (street, number and apartment): _____

(City, State and Zip): _____

(Subject Signature): _____ (Investigator Signature): _____

Date: _____

Within the next three weeks you should be receiving a check from the Overton Brooks VAMC. If you do not receive a check, please notify Charles J. Robinson or Samantha Richerson, at: (318) 424-6080, or E-mail at: sricherson@ieee.org. Please leave your name and method(s) by which you can be contacted.

APPENDIX E

START-UP PROTOCOL SINUSOIDAL ENTRAINMENT

Start-Up Protocol
Prior to Subject Arrival

On Entry to the Lab:

1. Check the following ON switches:
   a. _____ Lab Lights
   b. _____ MX NET
   c. _____ Peak Sync Box
   d. _____ SLIP Computer & Monitor
   e. _____ Delsys EMG Box
   f. _____ Headphone Transmitter (Unplug Charging cord, turn on power switch, adjust volume)
   g. _____ Radioshack SSM-1850 Mixer
   h. _____ Wireless Room Speakers (2)
   i. _____ Peak Computer & Monitor
   j. _____ Magma PCI Bus Extension

2. Check Air Compressor:
   a. _____ Turn On Compressor In Outdoor Equipment Room, Check For Leaks
   b. _____ Open Lab Supply Air Valve Supply Pressure to cycle between 80 – 115 psi
   c. _____ Open Platform Air Valve Platform Pressure >70 psi, Air Flow > 2 scfm

3. Have on Hand the following fresh BATTERIES:
   a. _____ Visonic Two button Transmitter (1-9volt)

4. Find the following "loose" ITEMS and place on Platform:
   a. _____ Visonic Two button Transmitter
   b. _____ Blindfold
   c. _____ Prepare Electrodes with One side of the adhesion pads (4)
   d. _____ Prepare Ground (Reference) Electrode

Test Equipment by:

1. Turn on Dover PMAC DMM-2004:
   a. _____ Supply Pressure to cycle between 80 – 115 psi
   b. _____ Platform Pressure >70 psi, Air Flow > 2 scfm
   c. _____ Manually Verify Platform is Floating
   d. _____ Energize DMM-2004
   e. _____ Press Reset if Red Reset indicator illuminated
2. Run Cont Acq&Graph Voltage
   a. Check each signal to ensure proper response
   b. Also recheck EMGs after connected to subject

Subject Code: _____ _____ _____ _____ _____ _____ _____ _____ _____ _____
Gender Age Age Contact # # # IC1 IC2 IC3

Date: _____ Page 1 Investigator Initials: _____
rev. 10/29/2006 sgm

Protocols for "Sinusoidal Entrainment Study of Postural Control"

	Signal	Response
____	Load Cell 1	Signal should decrease with load
____	Load Cell 2	Signal should decrease with load
____	Load Cell 3	Signal should decrease with load
____	Load Cell 4	Signal should decrease with load
____	Hand Sensor (Mini Load Cell)	
____	Position	Movement away from wall should increase signal
____	Shear Force (Motor Current)	Force towards wall on platform should decrease signal
____	Platform Accelerometer	Signal should Increase acceleration towards the wall. (Be careful no to dislodge wood.)
____	Head X-axis Accelerometer	Should increase with movement in X direction.
____	Head Y-axis Accelerometer	Should increase with movement in Y direction.
____	Head Z-axis Accelerometer	Should increase with movement in Z direction.
____	EMG Right TA	Rub Electrodes with thumb to observe signal response
____	EMG Left TA	Rub Electrodes with thumb to observe signal response
____	EMG Right GS	Rub Electrodes with thumb to observe signal response
____	EMG Left GS	Rub Electrodes with thumb to observe signal response
____	EMG Right SCM	Rub Electrodes with thumb to observe signal response
____	EMG Left SCM	Rub Electrodes with thumb to observe signal response
____	EMG Right Soleus	Rub Electrodes with thumb to observe signal response
____	EMG Left Soleus	Rub Electrodes with thumb to observe signal response

3. ___ Open "**Get_Sound2.vi**"
   a. _____ In headphones, able to hear continuous "white noise", overlaid by wave file (*.wav), and/or doorbell (adjust mixer channel levels 1, 2 &3 as necessary)
4. ___ Disable Screen savers
5. ___ Run Tekscan Software (I-scan)
   a. If you don't run before Labview might not work
6. ____ Run RealVNC
   a. ___ Login to Peak Computer
   b. ___ Disable screensavers
   c. ___ Start Peak Software
   d. ___ Click options
      i. ___ set subject name and trial
      ii. ___ set subject folder
      iii. ___ set time to 17 secs
   e. ___ Calibrate Vicon-peak
      i. open new trial
      ii. import template
      iii. Remove back right reflector from tekscan
      iv. Place calibration triangle and properly align
      v. Click Calibration capture and clear data
      vi. Record 90 secs of calibration data
   f. ___ Click Tools select protocol then import 2AFC
      i. ___ Click next 130 times
   g. Click Tools goto Batch Protocol
      i. Select clear trials

Subject Code: ____ ____ ____ ____ ____ ____ ____ ____ ____ ____
Gender Age Age Contact # # # IC1 IC2 IC3

Date: _____ Page 2 Investigator Initials: _____

Protocols for "Sinusoidal Entrainment Study of Postural Control"

ii. Select All 130 trials
iii. Select Detection_2AFC
iv. Select Execute

h. Remove Calibration Triangle
i. Replace back right reflector
j. Place all static reflectors

7. ____ Open "**5Jog2.vi**"
8. ____ Open "**Detect_Sine_v2.vi**"
   a. Enter information
   b. Run
   c. After Creation of Tekscan Folder
   d. ___ Goto Options
      i. Select acquisition parameters
      ii. ___ Enable triggering
         1. Click triggering and insure both set to external
         2. Click OK set Frames to Record to 3250
         3. Set period to 0.04
         4. Frequency should be 25 Hz (frm/sec)
         5. Ensure external port/sync is COM1
   e.
   f. ___ Goto Options in I-scan
      i. Select acquisition parameters
      ii. ___ Enable ASR
         1. Click ASR
         2. Click Browse
            a. Goto e:\data\[subject]\[subject]_[trial]\Tekscan\
            b. Name should be formatted as following
            c. [Subject]_[trial]_[Group]_.fsx
            d. If you do not have the "_" (underscore) on the end program will crash
            e. Set number of Movies to 150
            f. Set starting Movie number to 1
   g. Goto Tools in I-scan
      i. Select Calibrate
         1. Do this before Harness and EMGs
         2. Enter Subjects mass into box
         3. Have subject step onto platform
         4. Click start to calibrate.
         5. Save to same folder as above with same name convention
   h. Click the Record Button on I-scan
   i. Allow calibration
   j. Perform EMG COP Calibrate
   k. Perform 60 Sec quiet Standing
      i. For Threshold trial
      ii. Perform SIAM
   l. For Sine Lockin trial
      i. Change time to 125secs

Subject Code: ____ ____ ____ ____ ____ ____ ____ ____ ____ ____
Gender Age Age Contact # # # IC1 IC2 IC3

Date: _____ Page 3 Investigator Initials: _____
rev. 10/25/2006 sgm

Testing Protocol
When Subject Arrives

1. _____ Introduce Investigator.
2. _____ Show Platform and run "**5 jog2.vi**" which shows length of jogs and approximate speed (25mm/s2).

"This is the test platform that you will be standing on. It will be making very small moves (run VI) and you will have to determine when the move occurred." But before you step on the platform I need you to read and sign the informed consent document and take some clinical measurements."

3. _____ Give subjects IRB approved consent form. Subjects must initial and sign form as appropriate.
4. _____ Determine and record Subject "ID" and have them fill out Medical History.
5. _____ Administer the mini-mental evaluation exam, BERG, and RAND.
6. _____ Have subject remove shoes and socks, and Perform Clinical assessment according to form/ protocol.
7. _____ Perform Tekscan Calibration
8. _____ Turn on Doorbell receiver have them test transmitter, explain forced choice protocol:.

"With this doorbell transmitter, you will be able to indicate if you felt the platform move."

"For this test, you will be asked to step on the platform, place the headphones over your ears, and cover your eyes with the blindfold."

"From your headphones you will be hearing a constant 'masking white noise', and two verbal cues: 'Ready' and 'Decide'. Each will be ten seconds apart".

"If you think that the platform moved between the words 'Ready' and 'Decide', press the button once, but do not press the button if you did not feel the platform move"

"All decisions should be made no later than two seconds after the word 'Decide'. Go ahead and try the button to make sure you are comfortable with it. "

9. _____Have subject put on Harness if required
10. _____ Place EMG sensors bilaterally on the: Tib. Anterior, Gastrocnemius, Soleus, and sternocleidomastoid muscles:
    a. Wipe both the EMG Electrodes and the skin with Alcohol Wipes before application
    b. EMG Box should be placed on back Harness straps if used, or center of back clipped onto shorts
    c. TA EMGs should wrap around body, and then tucked inside the harness and ran down to the front of the legs
    d. GS and SCM are run down and up directly from the box.
    e. All extra length should be twist tied at the box behind the subject

Subject Code: _____ _____ _____ _____ _____ _____ _____ _____ _____ _____
Gender Age Age Contact # # # IC1 IC2 IC3

Date: _____ Page 4 Investigator Initials: _____
rev. 10/29/2006 ajm

Protocols for "Sinusoidal Entrainment Study of Postural Control"

"I will be collecting EMG data to determine how your muscles react to the slight movements the platform will be making, to help me determine if this is part of what helps YOU to decide if the platform has moved. After I'm done placing these sensors, I'll ask you to do some movements to help me calibrate them."

Wait for platform calibration, Then perform onscreen commands from for EMG COP Calibration. Hook up Harness.

"You can now step off the platform, watch that you don't tangle the EMG lines."

11. _____ Explain Learning SIAM test protocol.

"I'd like you to try to feel the platform move a few times. You will hear a "Ready" and "Decide." After, decide press the button if you felt the platform move, but do not press the button if you do not feel the platform move. Please keep hands at your sides during the trial. Also, Please do not pick your feet up and move them during test but you can re adjust your weight on them for comfort."

First 4 trials with eyes open for subject psychological familiarization, last 6 trials under eyes closed condition for learning under testing conditions.

**(Must get 7 correct before continuing) This VI can be repeated up to 3 times for learning purposes.*
**** CHECK EMGs BEFORE EACH TEST****

12. _____ Explain SIAM protocol again and continue with test for 1 condition:

Note: First 60 seconds of test ask subject to stand still. Then 10 secs for each trial

13. _____ Allow subject 5-minute rests while checking summary file(s) for lowest detected acceleration, for the forced choice tests, write these thresholds below:

Movement	Amplitude Threshold	Order
0.75 Hz	_____ mm	_____
0.5 Hz	_____ mm	_____
_____ Hz	_____ mm	_____
_____ Hz	_____ mm	_____

14. _____ De-brief subject.

15. _____ Reschedule subjects for additional test time if needed.

Day/Date: _____ Alternate Day/Date: _____

Time: _____ Time: _____

16. _____ Enable Computers Screensavers (Peak and SLIP computer
17. _____ Close Labview
18. _____ Close Peak Software and RealVNC
19. _____ Burn DATA to DVD
a. One to Polly And One to be kept in Lab

Subject Code: _____ _____ _____ _____ _____ _____ _____ _____ _____ _____
Gender Age Age Contact # # # IC1 IC2 IC3

Date: _____ Page 5 Investigator Initials: _____

APPENDIX F

VA RECRUITING FLYER

Subjects Needed

Investigators:

Charles Robinson, DSc, PE, Anne Hollister, MD, and Samantha Richerson, B.S.

Overton Brooks VA Medical Center, Shreveport, LA and
Louisiana Tech University, Ruston, LA.

ADULTS AGED 50–80, WITH OR WITHOUT DIABETES, ARE BEING RECRUITED FOR A STUDY IN HUMAN MOVEMENT DETECTION

We are looking for individuals who are healthy or who have diabetes. All subjects must not have a history of acute heart or lung problems, back spasms, pain or other spinal problems, central neurological deficits, stroke or head trauma, or other problems that might preclude a person from standing blindfolded for 10 to 15 minute increments over a two–hour period. A neurological screening will be performed, and a psychological test also administered. Individual research results will be retained by the researchers and are not made part of the subject's clinical record.

Maximum time commitment: 4 hours (Usually 3–4 hours.)

Location: Overton Brooks VAMC, Shreveport,LA.

Compensation: $25 each session (up to 4 hours)

If you are interested in participating, or for further information,
Contact: Samantha Richerson
Or Charles Robinson, DSc., PE
Phone: (318) 424–6080 or Email: sricherson@ieee.org

APPENDIX G

CLARKSON RECRUITING FLYER

Clarkson
UNIVERSITY

CENTER FOR REHABILITATION ENGINEERING, SCIENCE & TECHNOLOGY INVITES INDIVIDUALS FROM AGES 18 TO 75 YEARS OLD, TO PARTICIPATE IN A STUDY OF HUMAN BALANCE

This study will generally require a minimum of 4 hours to complete. Participants may be asked to complete 1 to 3 sets of these 4-hour protocols, generally on different days.

A minimum amount of physical effort will be required for this study, as participants will be standing in place and answering questions. We are unable at this time to offer any compensation to participants.

FOR DETAILED INFORMATION PLEASE CONTACT POLLY TIERNAN
315.268.6528 MONDAY THRU FRIDAY 8-4:30

We must exclude you from this study if you have a current or past history of severe heart, circulation or breathing prob-lems; chronic lower back spasms or pain; deformities of the spine, bones or joints (such as abnormal spinal curvature, arthritic changes); brain strokes, spinal cord injury or other damage to the nervous system; history or presence of foot ulcers; current drug or alcohol dependence; or repeated falls; or if you are taking prescription medication that causes or prevents dizziness.

Clarkson IRB Approval # 06-24

APPENDIX H

MINI-MENTAL STATE EXAM

Mini-Mental State Examination (MMSE)

Subject: _____ Date: _____

Activity	Score
ORIENTATION – one point for each answer *Ask:* "What is the: (year)(season)(date)(day)(month)?" *Ask:* "Where are we: (state)(county)(town)(hospital)(floor)?"	_____
REGISTRATION – score 1,2,3 points according to how many are repeated *Name three objects:* Give the patient one second to say each. *Ask the patient to:* repeat all three after you have said them. Repeat them until the patient learns all three.	_____
ATTENTION AND CALCULATION – one point for each correct subtraction *Ask the patient to:* begin from 100 and count backwards by 7. Stop after 5 answers. (93, 86, 79, 72, 65)	_____
RECALL – one point for each correct answer *Ask the patient to:* name the three objects from above.	_____
LANGUAGE *Ask the patient to:* identify and name a pencil and a watch. (2 points) *Ask the patient to:* repeat the phrase "No ifs, ands, or buts." (1 point) *Ask the patient to:* "Take a paper in your right hand, fold it in half, and put it on the floor " (1 point for each task completed properly) (Use 2nd Page) *Ask the patient to:* read and obey the following: "Close your eyes." (1 point) *Ask the patient to:* write a sentence. (1 point) *Ask the patient to:* copy a complex diagram of two interlocking pentagons. (1 point)	_____
TOTAL: Out of 30	_____

CLOSE YOUR EYES

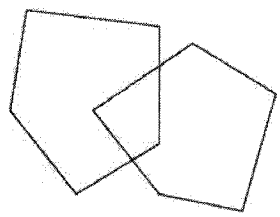

APPENDIX I

BERG SCALE

BERG BALANCE SCALE

Patient Name: _____
Rater Name: _____
Date: _____

Balance Item	Score (0-4)
1. Sitting unsupported	_____
2. Change of position: sitting to standing	_____
3. Change of position" standing to sitting	_____
4. Transfers	_____
5. Standing unsupported	_____
6. Standing with eyes closed	_____
7. Standing with feet together	_____
8. Tandem standing	_____
9. Standing on one leg	_____
10. Turning trunk (feet fixed)	_____
11. Retrieving objects from floor	_____
12. Turning 360 degrees	_____
13. Stool stepping	_____
14. Reaching forward while standing	_____

TOTAL (0–56): _____

Interpretation

0–20, wheelchair bound
21–40, walking with assistance
41–56, independent

References

Berg K, Wood-Dauphinee S, Williams JI, Maki, B: Measuring balance in the elderly: Validation of an instrument. **Can. J. Pub. Health, July/August supplement 2:S7-11, 1992.**

Berg K, Wood-Dauphinee S, Williams JI, Gayton D: Measuring balance in the elderly: Preliminary development of an instrument.
Physiotherapy Canada, 41:304-311, 1989.

Provided by the Internet Stroke Center — www.strokecenter.org

APPENDIX J

RAND WITH DEPRESSION

SCREENER TEST

Medical Outcomes Study: 36-Item Short Form Survey Instrument

RAND 36-Item Health Survey 1.0 Questionnaire Items

Subject: _____

Date: _____

1. In general, would you say your health is:	
Excellent	1
Very good	2
Good	3
Fair	4
Poor	5

2. **Compared to one year ago**, how would your rate your health in general **now**?	
Much better now than one year ago	1
Somewhat better now than one year ago	2
About the same	3
Somewhat worse now than one year ago	4
Much worse now than one year ago	5

The following items are about activities you might do during a typical day. Does **your health now limit** you in these activities? If so, how much?

(Circle One Number on Each Line)

	Yes, Limited a Lot	Yes, Limited a Little	No, Not limited at All
3. **Vigorous activities**, such as running, lifting heavy objects, participating in strenuous sports	[1]	[2]	[3]
4. **Moderate activities**, such as moving a table, pushing a vacuum cleaner, bowling, or playing golf	[1]	[2]	[3]
5. Lifting or carrying groceries	[1]	[2]	[3]
6. Climbing **several** flights of stairs	[1]	[2]	[3]
7. Climbing **one** flight of stairs	[1]	[2]	[3]
8. Bending, kneeling, or stooping	[1]	[2]	[3]
9. Walking **more than a mile**	[1]	[2]	[3]
10. Walking **several blocks**	[1]	[2]	[3]
11. Walking **one block**	[1]	[2]	[3]
12. Bathing or dressing yourself	[1]	[2]	[3]

During the **past 4 weeks**, have you had any of the following problems with your work or other regular daily activities **as a result of your physical health**?

(Circle One Number on Each Line)

	Yes	No
13. Cut down the amount of time you spent on work or other activities	1	2
14. **Accomplished less** than you would like	1	2
15. Were limited in the **kind** of work or other activities	1	2
16. Had **difficulty** performing the work or other activities (for example, it took extra effort)	1	2

During the **past 4 weeks,** have you had any of the following problems with your work or other regular daily activities **as a result of any emotional problems** (such as feeling depressed or anxious)?

(Circle One Number on Each Line)

	Yes	No
17. Cut down the **amount of time** you spent on work or other activities	1	2
18. **Accomplished less** than you would like	1	2
19. Didn't do work or other activities as **carefully** as usual	1	2

20. During the **past 4 weeks,** to what extent has your physical health or emotional problems interfered with your normal social activities with family, friends, neighbors, or groups?

(Circle One Number)

Not at all 1

Slightly 2

Moderately 3

Quite a bit 4

Extremely 5

21. How much **bodily** pain have you had during the **past 4 weeks**?

(Circle One Number)

None 1

Very mild 2

Mild 3

Moderate 4

Severe 5

Very severe 6

22. During the **past 4 weeks,** how much did **pain** interfere with your normal work (including both work outside the home and housework)?

(Circle One Number)

Not at all 1

A little bit 2

Moderately 3

Quite a bit 4

Extremely 5

These questions are about how you feel and how things have been with you **during the past 4 weeks**. For each question, please give the one answer that comes closest to the way you have been feeling.

How much of the time during the **past 4 weeks** . . .

(Circle One Number on Each Line)

	All of the Time	Most of the Time	A Good Bit of the Time	Some of the Time	A Little of the Time	None of the Time
23. Did you feel full of pep?	1	2	3	4	5	6
24. Have you been a very nervous person?	1	2	3	4	5	6
25. Have you felt so down in the dumps that nothing could cheer you up?	1	2	3	4	5	6
26. Have you felt calm and peaceful?	1	2	3	4	5	6
27. Did you have a lot of energy?	1	2	3	4	5	6
28. Have you felt downhearted and blue?	1	2	3	4	5	6
29. Did you feel worn out?	1	2	3	4	5	6
30. Have you been a happy person?	1	2	3	4	5	6
31. Did you feel tired?	1	2	3	4	5	6

32. During the **past 4 weeks,** how much of the time has your **physical health or emotional problems** interfered with your social activities (like visiting with friends, relatives, etc.)?

(Circle One Number)

All of the time 1

Most of the time 2

Some of the time 3

A little of the time 4

None of the time 5

How TRUE or FALSE is each of the following statements for you.

(Circle One Number on Each Line)

	Definitely True	Mostly True	Don't Know	Mostly False	Definitely False
33. I seem to get sick a little easier than other people	1	2	3	4	5
34. I am as healthy as anybody I know	1	2	3	4	5
35. I expect my health to get worse	1	2	3	4	5
36. My health is excellent	1	2	3	4	5

Patient Questionnaire

Almost everyone has experienced times of feeling sad or depressed, like when suffering from a severe illness, when a person close to you has died, or if there are problems at work or in the family. The following questions are about such times.

1. Have you ever had 2 years or more in your life when you felt depressed or sad most days, even if you felt OK sometimes? (Circle one)

Yes **No** (Skip to Question 2)

a. Did any period like that ever last 2 years without an interruption of 2 full months when you felt OK?

Yes **No** (Skip to Question 2)

b. Did any of those long periods of feeling sad or depressed continue into the last 12 months?

Yes **No**

2. In the last 12 months, have you had 2 weeks or longer when ... (Circle one answer on each line)

a. nearly every day you felt sad, empty or depressed for most of the day?

Yes **No**

b. you lost interest in most things like work, hobbies, and other things you usually enjoyed?

Yes **No**

3. In the last month did you have a period of 1 week or more when ... (Circle one answer on each line)

a. nearly every day you felt sad, empty or depressed for most of the day?

Yes **No**

b. you lost interest in most things like work, hobbies, and other things you usually enjoyed?

Yes **No**

OFFICE USE ONLY

Check if ☐

1 AND 1a and 1b are yes
OR
2a OR 2b is yes

AND

3a or 3b is yes

23

APPENDIX K

RAND WITH DEPRESSION

SCREENER SCORER

Subject: _____ Date: _____

RAND	Test Score	Conversion
1		Bad Answer
2		Bad Answer
3		Bad Answer
4		Bad Answer
5		Bad Answer
6		Bad Answer
7		Bad Answer
8		Bad Answer
9		Bad Answer
10		Bad Answer
11		Bad Answer
12		Bad Answer
13		Bad Answer
14		Bad Answer
15		Bad Answer
16		Bad Answer
17		Bad Answer
18		Bad Answer
19		Bad Answer
20		Bad Answer
21		Bad Answer
22		Bad Answer
23		Bad Answer
24		Bad Answer
25		Bad Answer
26		Bad Answer
27		Bad Answer
28		Bad Answer
29		Bad Answer
30		Bad Answer
31		Bad Answer
32		Bad Answer
33		Bad Answer
34		Bad Answer
35		Bad Answer
36		Bad Answer

Depression Screener	
Question	Answer(Yes/No)
1	
1a	
1b	
2a	
2b	
3a	
3b	

Scale	Grade
Physical Functioning	#DIV/0!
Limited due to Physical health	#DIV/0!
Limited due to Emotional health	#DIV/0!
Energy/Fatigue	#DIV/0!
Emotional Well-being	#DIV/0!
Social Functioning	#DIV/0!
Pain	#DIV/0!
General Health	#DIV/0!

Depression	Present
Dysthymia	No
Major Depression	No
Symptoms Present	No

APPENDIX L

BATCH MATLAB® CODE

```
%   Main Script main_script.m
clc
clear all
clear classes

%****Define Home Directory Where batch files are located****
%****   Format should be [DRIVE]:\FILE_PATH\          ****
%****       include trailing slash                    ****
addpath '[DRIVE]:\FILE_PATH\'
HOME_DIR= '[DRIVE]:\FILE_PATH\';
%*************************************************************

if strcmp(HOME_DIR,'[DRIVE]:\FILE_PATH\')
   error(['HOME_DIR must be set']);
end

% ProcessID gives each run a unique folder store run specifc Data into
% Format is 'yyyymmdd##' Four Digit Year, Month, Day, Number of the Run for
% that day

%****MUST SET************
ProcessID = 'yyyymmdd##';
%************************

if strcmp(ProcessID,'yyyymmdd##')
   error(['ProcessID must be set']);
end

%   Check to insure that same Process ID is not Repeated
PROCESS_FOLDER=[HOME_DIR,'Process_',ProcessID,'\'];
[status,message,messageid] = mkdir(PROCESS_FOLDER);
if ~strcmp(message,'')
   error(['Process_',ProcessID,' ',message]);
end

%**** Location of Subjects text File*****
SUBJECTS_FILE = [HOME_DIR,'subjects.txt'];

%***** MUST CHANGE FOR NUMBER OF SUBJECTS TO RUN***
NUMBER_OF_SUBJECTS = 99; %99; in current list;
%*************************************************

%   Read in from file subjects.txt
[subjs,diab] =textread(SUBJECTS_FILE,'%s %c',NUMBER_OF_SUBJECTS);

if length(subjs)~=NUMBER_OF_SUBJECTS
```

```
   error(['NUMBER_OF_SUBJECTS too high']);
end

%  Save Copy of subjects.txt with Results for Process
copyfile(SUBJECTS_FILE,[PROCESS_FOLDER,'subjects.txt']);

%****Define Main Directory Where files are located****
%****  Format should be [DRIVE]:\FILE_PATH\     ****
%****      include trailing slash              ****
MAIN_DIR= '[DRIVE]:\FILE_PATH\';
%*****************************************************

if strcmp(MAIN_DIR,'[DRIVE]:\FILE_PATH\')
   error(['MAIN_DIR must be set']);
end

%  Put all File name in Lowercase
subjs = lower(subjs);

%  Intialize Counters
e=1;
g=1;

%  Initialize Waitbar to Show Process Status
wbar=waitbar(0,'Processing QS Data...');
for i=1:length(subjs)

   %  Update Waitbar
   waitbar(i/NUMBER_OF_SUBJECTS,wbar,['Processing QS Data.....
',char(subjs(i)),' : ',num2str(i),'/',num2str(NUMBER_OF_SUBJECTS)])
   set(wbar,'WindowStyle','modal')

   %  Initialize goodarr for times
   goodarr(g,1)=subjs(i);
   goodarr(g,2)={'0'};
   goodarr(g,3)={'0'};
   goodarr(g,4)={'0'};
   goodarr(g,5)={'0'};
   goodarr(g,6)={'0'};
   goodarr(g,7)={'0'};
   goodarr(g,8)={'0'};
   goodarr(g,9)={'0'};

   %  Beginning of Data Processing
   %     Checks to insure sunject run data folder exist before
   %     attempting to run.
```

```
%       Upon completion, it writes status spreadsheets on the data
%       processed and processing time
%       Will Process trials that start with [blank],r,b,c,d,e,f
%       Makes Periodic Saves in case of Crash

A = exist([MAIN_DIR,char(subjs(i)),'\',char(subjs(i)),'\'],'dir');

if (A~=0)
   tic
   main_tr(char(subjs(i)),diab(i),MAIN_DIR,'');
   t=toc;
   disp(['Trial A for ',char(subjs(i)),' finished in ',num2str(t),' secs.'])
   goodarr(g,2)=num2cell(t);

end

R = exist([MAIN_DIR,char(subjs(i)),'\',char(subjs(i)),'r\'],'dir');

if (R~=0)

   tic
   main_tr(char(subjs(i)),diab(i),[MAIN_DIR],'r');
   t=toc;
   disp(['Trial R for ',char(subjs(i)),' finished in ',num2str(t),' secs.'])
   goodarr(g,3)=num2cell(t);

end

B = exist([MAIN_DIR,char(subjs(i)),'\',char(subjs(i)),'b\'],'dir');

if (B~=0)

   tic
   main_tr(char(subjs(i)),diab(i),[MAIN_DIR],'b');
   t=toc;
   disp(['Trial B for ',char(subjs(i)),' finished in ',num2str(t),' secs.'])
   goodarr(g,4)=num2cell(t);

end

C = exist([MAIN_DIR,char(subjs(i)),'\',char(subjs(i)),'c\'],'dir');

if (C~=0)

   tic
   main_tr(char(subjs(i)),diab(i),[MAIN_DIR],'c');
```

```
    t=toc;
    disp(['Trial C for ',char(subjs(i)),' finished in ',num2str(t),' secs.'])
    goodarr(g,5)=num2cell(t);

end

D = exist([MAIN_DIR,char(subjs(i)),'\',char(subjs(i)),'d\'],'dir');

if (D~=0)

    tic
    main_tr(char(subjs(i)),diab(i),[MAIN_DIR],'d');
    t=toc;
    disp(['Trial D for ',char(subjs(i)),' finished in ',num2str(t),' secs.'])
    goodarr(g,6)=num2cell(t);

end

E = exist([MAIN_DIR,char(subjs(i)),'\',char(subjs(i)),'e\'],'dir');

if (E~=0)

    tic
    main_tr(char(subjs(i)),diab(i),[MAIN_DIR],'e');
    t=toc;
    disp(['Trial E for ',char(subjs(i)),' finished in ',num2str(t),' secs.'])
    goodarr(g,7)=num2cell(t);

end

F = exist([MAIN_DIR,char(subjs(i)),'\',char(subjs(i)),'f\'],'dir');

if (F~=0)

    tic
    main_tr(char(subjs(i)),diab(i),[MAIN_DIR],'f');
    t=toc;
    disp(['Trial F for ',char(subjs(i)),' finished in ',num2str(t),' secs.'])
    goodarr(g,8)=num2cell(t);

end


errarr(e,1)=subjs(i);
errarr(e,2)=num2cell(i);
errarr(e,3)=num2cell(A);
```

```
    errarr(e,4)=num2cell(R);
    errarr(e,5)=num2cell(B);
    errarr(e,6)=num2cell(C);
    errarr(e,7)=num2cell(D);
    errarr(e,8)=num2cell(E);
    errarr(e,9)=num2cell(F);
    e=e+1;
    g=g+1;

    cd(PROCESS_FOLDER);
    save(['periodic_save_',num2str(i)]);
end

close(wbar);

cd(PROCESS_FOLDER);
err_head={'Subject' 'Run Number' 'A' 'R' 'B' 'C' 'D' 'E' 'F'};
xlswrite('SUBJECT_ERR.xls',err_head,'Sheet1','A1:I1');
xlswrite('SUBJECT_ERR.xls',errarr,'Sheet1',['A2:I',num2str(e)]);

good_head={'Subject' '  A' '  R' '  B' '  C' '  D' '  E' '  F'};
xlswrite('SUBJECT_GOOD.xls',good_head,'Sheet1','A1:H1');
xlswrite('SUBJECT_GOOD.xls',goodarr,'Sheet1',['A2:H',num2str(g)]);
cd(HOME_DIR);
clear all
clear classes

function main_tr(subject,rawid,MAIN_DIR,trial)
%Defines Where files to be processed are located
%  Files To be processed must be copied to this folder
%  All zip Files must be unzipped
%  This file has been customized for acceleration trials



global Loc_ToBeProcessed Loc_Processed
global SAMPLING_RATE DAT_DATA_SIZE SMOOTH_FILTER

SAMPLING_RATE = 0.001;
DAT_DATA_SIZE = 30000;
Loc_ToBeProcessed = [MAIN_DIR,subject,'\',subject,trial,'\'];

% Load Filter From File
load SMOOTH_FILTER

%****Define where postprocessed files will be stored****
```

```
%****   Format should be [DRIVE]:\FILE_PATH\       ****
%****      include trailing slash                  ****
Loc_Processed = '[DRIVE]:\FILE_PATH\';
%*****************************************************

if strcmp(Loc_Processed,'[DRIVE]:\FILE_PATH\')
   error(['Loc_Processed must be set']);
end

%****Define File name for xls spreadsheet for***********
%****   process of subject. DO NOT PUT .xls        ****
SUBJECT_PROCESS_SUMMARY = 'FILE_NAME';
%*****************************************************

if strcmp(SUBJECT_PROCESS_SUMMARY,'FILE_NAME')
   error(['SUBJECT_PROCESS_SUMMARY must be set']);
else
   ERR_CHK =
exist([MAIN_DIR,subject,'\',SUBJECT_PROCESS_SUMMARY,'.xls'],'file')
   if ERR_CHK~=0
      error(['Sorry the File: ', SUBJECT_PROCESS_SUMMARY,'.xls already
exist.  Please Change SUBJECT_PROCESS_SUMMARY.']);
   end
end

%****Define where postprocessed files will be stored************
%****   Below describes how to choose which files you want  ****
%****      to process, which are followed by the ending of ****
%****      those files.                                    ****
%****   Enter 1 for Processing Trial Run Files      "##"    ****
%****   Enter 2 for Processing Quiet Standing Files "_sta"  ****
%****   Enter 3 for Processing Summary Files        "_sum"  ****
%****   Enter 11 for Processing QS Metrics Files    "_QS"   ****
%****   Enter 12 for Processing EMG Calibration Data "emcp" ****
%****   Enter 13 for Processing EMG Norm Data    "_EMG_COP" ****
FILE_TYPE_SW = 0;
%*************************************************************

switch FILE_TYPE_SW
   case 0
      error(['FILE_TYPE must be set']);
   case 1
      FILE_TYPE='01.xls';
   case 2
      FILE_TYPE='_sta.xls';
   case 3
```

```
      FILE_TYPE='_sum.xls';
%*************************************************************
%****                                                    ****
%****   By Seperating these it provides room for expansion  ****
%****      for types of files where there are more than    ****
%****      one for a specific test run.                    ****
%****                                                    ****
%*************************************************************
   case 11
      FILE_TYPE='_QS.xls';
   case 12
      FILE_TYPE='emcp.xls';
   case 13
      FILE_TYPE='norm_EMG_COP.mat';
   otherwise
      error('Incorrect Setting for FILE_TYPE');
end

% Intialize ERR_CHK
ERR_CHK=zeros(1,5)

cd(Loc_Processed);

CHCK = exist([MAIN_DIR,subject,'\',subject,trial,'\'],'dir');

if (CHCK~=0)

   if FILE_TYPE_SW > 10

      ERR_CHK(1) =
exist([MAIN_DIR,subject,'\',subject,trial,'\',subject,trial,FILE_TYPE],'file');

      if (ERR_CHK(1)~=0)

         %****MUST INSERT YOUR DATA PROCESSING FUNCTION HERE****

         %*****************************************************

      else
         disp(['Error: ',ERR_FILENAME,' File not found for ',subject,trial])
      end

   else

      if (trial=='r')
         % 1 mm Calc
```

```
        ERR_CHK(1) =
exist([MAIN_DIR,subject,'\',subject,trial,'\',subject,trial,rawid,'1as0rf',FILE_TYPE],'
file');

        if (ERR_CHK(1)~=0)

           %****MUST INSERT YOUR DATA PROCESSING FUNCTION
HERE****

           %*****************************************************

        else
           disp(['Error: 1 mm ',ERR_FILENAME,' File not found for ',subject,trial])
        end

        %  2mm

        ERR_CHK(2) =
exist([MAIN_DIR,subject,'\',subject,trial,'\',subject,trial,rawid,'1as1rf',FILE_TYPE],'
file');

        if (ERR_CHK(2)~=0)

           %****MUST INSERT YOUR DATA PROCESSING FUNCTION
HERE****

           %*****************************************************

        else
           disp(['Error: 2 mm ',ERR_FILENAME,' File not found for ',subject,trial])
        end


        %   4mm

        ERR_CHK(3) =
exist([MAIN_DIR,subject,'\',subject,trial,'\',subject,trial,rawid,'1as2rf',FILE_TYPE],'
file');

        if (ERR_CHK(3)~=0)

           %****MUST INSERT YOUR DATA PROCESSING FUNCTION
HERE****

           %*****************************************************
```

```
        else
           disp(['Error: 4 mm ',ERR_FILENAME,' File not found for ',subject,trial])
        end

        %   8mm

        ERR_CHK(4) =
exist([MAIN_DIR,subject,'\',subject,trial,'\',subject,trial,rawid,'1as3rf',FILE_TYPE],'
file');

        if (ERR_CHK(4)~=0)

           %****MUST INSERT YOUR DATA PROCESSING FUNCTION
HERE****

           %*****************************************************

        else
           disp(['Error: 8 mm ',ERR_FILENAME,' File not found for ',subject,trial])
        end


     else

        % 1 mm Calc

        ERR_CHK(1) =
exist([MAIN_DIR,subject,'\',subject,trial,'\',subject,trial,rawid,'1as0ff',FILE_TYPE],'
file');

        if (ERR_CHK(1)~=0)

           %****MUST INSERT YOUR DATA PROCESSING FUNCTION
HERE****

           %*****************************************************

        else
           disp(['Error: 1 mm ',ERR_FILENAME,' File not found for ',subject,trial])
        end

        %  4mm
```

```
        ERR_CHK(3) =
exist([MAIN_DIR,subject,'\',subject,trial,'\',subject,trial,rawid,'1as2ff',FILE_TYPE],'
file');

        if (ERR_CHK(3)~=0)

           %****MUST INSERT YOUR DATA PROCESSING FUNCTION
HERE****

           %*****************************************************

        else
           disp(['Error: 4 mm ',ERR_FILENAME,' File not found for ',subject,trial])
        end

        %   16mm

        ERR_CHK(5) =
exist([MAIN_DIR,subject,'\',subject,trial,'\',subject,trial,rawid,'1as4ff',FILE_TYPE],'
file');

        if (ERR_CHK(5)~=0)

           %****MUST INSERT YOUR DATA PROCESSING FUNCTION
HERE****

           %*****************************************************

        else
           disp(['Error: 16 mm ',ERR_FILENAME,' File not found for ',subject,trial])
        end

     end

   end

   switch trial
      case ''
         trial_num=1;
      case 'r'
         trial_num=2;
      case 'b'
         trial_num=3;
      case 'c'
         trial_num=4;
      case 'd'
```

```
        trial_num=5;
      case 'e'
        trial_num=6;
      case 'f'
        trial_num=7;
    end

 cd([MAIN_DIR,subject,'\']);
 err_head={'Subject' 'Trial' '1 mm' '2 mm' '4 mm' '8 mm' '16 mm'};
 xlswrite([SUBJECT_PROCESS_SUMMARY,'.xls'],err_head,'Sheet1','A1:G1');
 xlswrite([SUBJECT_PROCESS_SUMMARY,'.xls'],{subject
trial},'Sheet1',['A',num2str(trial_num+1),':B',num2str(trial_num+1)]);

xlswrite([SUBJECT_PROCESS_SUMMARY,'.xls'],ERR_CHK,'Sheet1',['C',num2s
tr(trial_num+1),':G',num2str(trial_num+1)]);

else
   disp 'sorry folder existed no work done'
end
```

APPENDIX M

ENGINEERING UNIT CONVERSION

BATCH MATLAB® CODE

```
function datchanger(subject,rawid,pert,trial)
%Processes EMG COP Calibrate

global Loc_ToBeProcessed Loc_Processed Accel_CF Shear_CF Load_Cell_CF
global DAT_DATA_SIZE SMOOTH_FILTER SAMPLING_RATE
norm_EMG_COP


   filenameplate = [Loc_ToBeProcessed,subject,trial,rawid,'.dat'];
 FILEPLATEID = fopen(filenameplate,'rt');
if (FILEPLATEID ~= -1)
  clear cop msmoothdata temp convdata dat
   fclose(FILEPLATEID);
   %  Initializations
   cop(1:DAT_DATA_SIZE,1:16) =0;
   msmoothdata(1:DAT_DATA_SIZE,1:16)=0;
   minitavg =0;
   temp =0;
   convdata(1:DAT_DATA_SIZE,1:16) =0;
   dat =0;
   %  Data Extraction from raw plate data

   cop =dlmread(filenameplate,'\t',[0 0 29999 15]);

      %  Zero Baseline
   for i = 5:16
      minitavg(i) = initavg(cop,i);
      msmoothdata(1:DAT_DATA_SIZE,i)=cop(1:DAT_DATA_SIZE,i)-minitavg(i);
   end

   %  Conversions

   convdata(:,1:4) = cop(:,1:4) .* Load_Cell_CF;                    %  Load Cells
   convdata(:,5) = msmoothdata(:,5) .* pert.*1.25;  %  Position
   convdata(:,6) = msmoothdata(:,6) * Accel_CF;                          %
Acceleration
   convdata(:,7) = msmoothdata(:,7) * Shear_CF;                          %
Shear
   convdata(:,8) = msmoothdata(:,8);                                  %  Touch
   convdata(:,9:12) = abs(msmoothdata(:,9:12));                          %
EMGs
   convdata(:,13:15) = msmoothdata(:,13:15) * Accel_CF;                     %
Head Accel X,Y,Z
   convdata(:,16) = msmoothdata(:,16) /
max(msmoothdata(1:DAT_DATA_SIZE,16));     %  Bell
```

```
% Smoothing done after conversions to prevent roughening of data

smdat=filtfilt(SMOOTH_FILTER.tf.num,SMOOTH_FILTER.tf.den,convdata);


% Make Output Array
  % Add milliseconds to first column
dat(1:DAT_DATA_SIZE,1) = (1:DAT_DATA_SIZE)';

  % Add Position

  dat(1:DAT_DATA_SIZE,2) = smdat(1:DAT_DATA_SIZE,5);

   % Add differentiated velocity

  temp(2:DAT_DATA_SIZE,7) = (smdat(2:DAT_DATA_SIZE,5)-
smdat(1:DAT_DATA_SIZE-1,5))./SAMPLING_RATE;

% Smooth velocity
  minitavg(7) = initavg(temp,7);
  temp(2:DAT_DATA_SIZE,7) = temp(2:DAT_DATA_SIZE,7)-minitavg(7);
  dat(2:DAT_DATA_SIZE,3) =
filtfilt(SMOOTH_FILTER.tf.num,SMOOTH_FILTER.tf.den,temp(2:DAT_DATA_SI
ZE,7));


   % Add differentiated Acceleration

 temp(3:DAT_DATA_SIZE,8) = (dat(3:DAT_DATA_SIZE,3)-
dat(2:DAT_DATA_SIZE-1,3))./SAMPLING_RATE;

  % Smooth Acceleration
  minitavg(8) = initavg(temp,8);
 temp(3:DAT_DATA_SIZE,8) = temp(3:DAT_DATA_SIZE,8)-minitavg(8);
  dat(3:DAT_DATA_SIZE,4) =
filtfilt(SMOOTH_FILTER.tf.num,SMOOTH_FILTER.tf.den,temp(3:DAT_DATA_SI
ZE,8));


   % Add Acceleration
dat(1:DAT_DATA_SIZE,5) = smdat(1:DAT_DATA_SIZE,6);
  % Add Differentiated Jerk
```

```
   temp(2:DAT_DATA_SIZE,5) = (dat(2:DAT_DATA_SIZE,5)-
dat(1:DAT_DATA_SIZE-1,5))./SAMPLING_RATE;
      % Smooth Differentiated Jerk
   minitavg(5) = initavg(temp,5);
   temp(2:DAT_DATA_SIZE,5) = temp(2:DAT_DATA_SIZE,5)-minitavg(5);
   dat(2:DAT_DATA_SIZE,6) =
filtfilt(SMOOTH_FILTER.tf.num,SMOOTH_FILTER.tf.den,temp(2:DAT_DATA_SI
ZE,5));


      %  Shear
   dat(1:DAT_DATA_SIZE,7) = smdat(1:DAT_DATA_SIZE,7);

      %  Touch
   dat(1:DAT_DATA_SIZE,8) = smdat(1:DAT_DATA_SIZE,8);
      %  Add APCOP
      %  Add APCOP Velocity
      %  Add MLCOP
      %  Add MLCOP Velocity

   filenamecal = [Loc_ToBeProcessed,subject,trial,rawid];
   fpcal = calmod(filenamecal);

   [temp(:,13),temp(:,15)] =
apmlcop(smdat(:,1),smdat(:,2),smdat(:,3),smdat(:,4),fpcal);


   for i=13:2:15
      minitavg(i) = initavg(temp,i);
      temp(1:DAT_DATA_SIZE,i) = temp(1:DAT_DATA_SIZE,i)-minitavg(i);
      dat(1:DAT_DATA_SIZE,i-4) =
filtfilt(SMOOTH_FILTER.tf.num,SMOOTH_FILTER.tf.den,temp(1:DAT_DATA_SI
ZE,i));
   end

   temp(2:DAT_DATA_SIZE,14) = (dat(2:DAT_DATA_SIZE,9)-
dat(1:DAT_DATA_SIZE-1,9))./SAMPLING_RATE;
   temp(2:DAT_DATA_SIZE,16) = (dat(2:DAT_DATA_SIZE,11)-
dat(1:DAT_DATA_SIZE-1,11))./SAMPLING_RATE;


   for i= 14:2:16
      minitavg(i) = initavg(temp,i);
      temp(2:DAT_DATA_SIZE,i) = temp(2:DAT_DATA_SIZE,i)-minitavg(i);
```

```
    dat(2:DAT_DATA_SIZE,i-4) =
filtfilt(SMOOTH_FILTER.tf.num,SMOOTH_FILTER.tf.den,temp(2:DAT_DATA_SI
ZE,i));
  end

    %  ADD RMS EMG RTA
    %  ADD RMS EMG RGS
    %  ADD RMS EMG LTA
    %  ADD RMS EMG LGS

  dat(:,13:16)=smdat(:,9:12);

    %  Head Accel X
    %  Head Accel Y
    %  Head Accel Z
  for i = 21:23
    dat(1:DAT_DATA_SIZE,i-4) = smdat(1:DAT_DATA_SIZE,i-8);
  end

     %  Bell
  dat(1:DAT_DATA_SIZE,20) = smdat(1:DAT_DATA_SIZE,16);

  %  Create Normalization Array

  for i=13:16
    norm_EMG_COP(1,i-12) = mean(dat(2000:5000,i));
    norm_EMG_COP(2,i-12) = mean(dat(11000:14000,i));
    norm_EMG_COP(3,i-12) = mean(dat(16000:19000,i));
    norm_EMG_COP(4,i-12) = mean(dat(25000:28000,i));
  end
  for i=9:2:11
    norm_EMG_COP(1,i-4-(i-9)./2) = mean(dat(2000:5000,i));
    norm_EMG_COP(2,i-4-(i-9)./2) = mean(dat(11000:14000,i));
    norm_EMG_COP(3,i-4-(i-9)./2) = mean(dat(16000:19000,i));
    norm_EMG_COP(4,i-4-(i-9)./2) = mean(dat(25000:28000,i));
  end


  % Add Headings
  %     1  2        3              4     5     6
  A = {'Time' 'Position' 'Diff velocity' 'Diff Accel' 'Accel' 'Diff jerk'...
          'Shear' 'Touch' 'APCOP' 'APCOP Vel' 'MLCOP' 'MLCOP Vel' 'RTA'
'RGS' 'LTA' 'LGS' 'Head Accel X' 'Head Accel Y' 'Head Accel Z' 'Bell'};
    %     7     8     9     10       11     12       13     14  15     16  17
18          19          20
```

```
   %  Writes File
   cd([Loc_Processed,subject,'\',subject,trial,'\']);
%     save([subject,r,rawid]);
     xlswrite([subject,trial,rawid],A,'Sheet1','A1:T1');
     xlswrite([subject,trial,rawid],dat,'Sheet1','A2:T30001');
else
   cd([Loc_Processed,subject,'\',subject,trial,'\']);
   save('error_dat','filenameplate');
end
clear dat smdat convdata msmoothdata temp cop A minitavg subject trial rawid

function  filechanger(subject,rawid,pert,trial)
%Processes Threshold trials

global Loc_ToBeProcessed Loc_Processed Accel_CF Shear_CF
global SMOOTH_FILTER SAMPLING_RATE norm_EMG_COP

testnum = 1;


%************************************
%************************************

%      Special Case


switch pert
   case 1
      rawid_move=0;
   case 2
      rawid_move=1;
   case 4
      rawid_move=2;
   case 8
      rawid_move=3;
   case 16
      rawid_move=4;
end

if (strcmp(subject,'m72z137'))
   if (strcmp(trial,''))
      wrawid=['n1as',num2str(rawid_move),'ff'];
      rawid=['c1as',num2str(rawid_move),'ff'];
   else
      wrawid=rawid;
   end
```

```
else
   wrawid=rawid;
end

%          End

%   Must Change wrawid back to rawid to remove

%****************************************

filenamesum = [Loc_ToBeProcessed,subject,trial,rawid,'.sum'];
file_sum_id = fopen(filenamesum,'rt');
if file_sum_id==-1
   filenamesum = [Loc_ToBeProcessed,upper(subject),trial,rawid,'.sum'];
   file_sum_id = fopen(filenamesum,'rt');
   if file_sum_id ==-1
      error(['No such Sum File: ',filenamesum]);
   end
end
fsumh=cell(2,1);
fsumh(1,1)=cellstr(fgetl(file_sum_id));
fsumh(2,1)=cellstr(fgetl(file_sum_id));

fgetl(file_sum_id);

fsuml={'File #' 'Step Crit.?' 'Detect?' 'Accel.' 'Vel.' '%S-Curve' 'Displ.' 'Shear Max.'
'I-Time'...
   'Filename' 'Date and Time' 'Detection and Jog' 'Movement Period'};

fclose(file_sum_id);
fsumd=cell(30,13);
fsumc=cell(1,1);

avg_h ={'Trial' 'APCOP' 'APCOPV' 'MLCOP' 'MLCOPV' 'Position' 'Acceleration' ...
   'Shear' 'Touch' 'RTA' 'RGS' 'LTA' 'LGS' 'Head Accel X' 'Head Accel Y' ...
   'Head Accel Z' 'Bell' 'Diff velocity' 'Diff Accel' 'Diff jerk'};

sta_avg(1:19)=0;
sta_avg=stachanger(subject,rawid,pert,trial);
xlswrite([subject,trial,wrawid,'_sum'],avg_h,'AVG','A1');
xlswrite([subject,trial,wrawid,'_sum'],{'QS'},'AVG','A2');
xlswrite([subject,trial,wrawid,'_sum'],sta_avg,'AVG','B2');


h = waitbar(0,['Subject: ',subject,trial,' Processing move ',num2str(pert),'mm Move
Data...']);
```

```
if (testnum <10)
   filenameplate = [Loc_ToBeProcessed,subject,trial,rawid,'
',num2str(testnum),'.raw'];
else
   filenameplate =
[Loc_ToBeProcessed,subject,trial,rawid,num2str(testnum),'.raw'];
end
FILEPLATEID = fopen(filenameplate,'rt');
while (FILEPLATEID ~= -1)
   clear cop msmoothdata temp convdata dat

   fsumd(testnum,10)=cellstr(fgetl(FILEPLATEID));
   fgetl(FILEPLATEID);
   fsumd(testnum,11)=cellstr(fgetl(FILEPLATEID));
   fsumd(testnum,12)=cellstr(fgetl(FILEPLATEID));
   fsumd(testnum,13)=cellstr(fgetl(FILEPLATEID));
   fclose(FILEPLATEID);

   waitbar (testnum/30,h);

   % Intialization
   minitavg(1:19)=0;
   %  Data Extraction from raw plate data

   cop =dlmread(filenameplate,'\t',7,0);

   [RAW_DATA_SIZE,COLs]=size(cop);

   %  Zero Baseline
   for i = 5:COLs
      minitavg(i) = initavg(cop,i);
      msmoothdata(1:RAW_DATA_SIZE,i)=cop(1:RAW_DATA_SIZE,i)-
minitavg(i);
   end

   %  Conversions

   convdata(:,1:4) = cop(:,1:4);                    %  Load Cells

   convdata(:,5) = msmoothdata(:,5) .* pert.*1.25;   %  Position
   convdata(:,6) = msmoothdata(:,6) .* Accel_CF;                    %
Acceleration
   convdata(:,7) = msmoothdata(:,7) .* Shear_CF;                    %
Shear
   convdata(:,8) = msmoothdata(:,8);                          %  Touch
```

```
   convdata(:,9:12) = abs(msmoothdata(:,9:12));                    %
EMGs
   convdata(:,13:15) = msmoothdata(:,13:15) .* Accel_CF;                %
Head Accel X,Y,Z
   convdata(:,16) = msmoothdata(:,16) ./
max(msmoothdata(1:RAW_DATA_SIZE,16));     %  Bell


   %  Smoothing done after conversions to prevent roughening of data

   smdat=filtfilt(SMOOTH_FILTER.tf.num,SMOOTH_FILTER.tf.den,convdata);


   %  Make Output Array
   %  Add milliseconds to first column

   dat(1:RAW_DATA_SIZE,1) = (1:RAW_DATA_SIZE)';


   %  Add Position

   dat(1:RAW_DATA_SIZE,2) = smdat(1:RAW_DATA_SIZE,5);

   %  Add differentiated velocity

   temp(2:RAW_DATA_SIZE,7) = (smdat(2:RAW_DATA_SIZE,5)-
smdat(1:RAW_DATA_SIZE-1,5))./SAMPLING_RATE;

   %  Smooth velocity
   minitavg(17) = initavg(temp,7);
   temp(2:RAW_DATA_SIZE,7) = temp(2:RAW_DATA_SIZE,7)-minitavg(7);
   dat(2:RAW_DATA_SIZE,3) =
filtfilt(SMOOTH_FILTER.tf.num,SMOOTH_FILTER.tf.den,temp(2:RAW_DATA_SI
ZE,7));


   %  Add differentiated Acceleration

   temp(3:RAW_DATA_SIZE,8) = (dat(3:RAW_DATA_SIZE,3)-
dat(2:RAW_DATA_SIZE-1,3))./SAMPLING_RATE;

   % Smooth Acceleration
   minitavg(18) = initavg(temp,8);
   temp(3:RAW_DATA_SIZE,8) = temp(3:RAW_DATA_SIZE,8)-minitavg(8);
```

```
   dat(3:RAW_DATA_SIZE,4) =
filtfilt(SMOOTH_FILTER.tf.num,SMOOTH_FILTER.tf.den,temp(3:RAW_DATA_SI
ZE,8));

   %  Add Acceleration
   dat(1:RAW_DATA_SIZE,5) = smdat(1:RAW_DATA_SIZE,6);

   temp(2:RAW_DATA_SIZE,5) = (dat(2:RAW_DATA_SIZE,5)-
dat(1:RAW_DATA_SIZE-1,5))./SAMPLING_RATE;
   % Smooth Acceleration
   minitavg(19) = initavg(temp,5);
   temp(2:RAW_DATA_SIZE,5) = temp(2:RAW_DATA_SIZE,5)-minitavg(5);
   dat(2:RAW_DATA_SIZE,6) =
filtfilt(SMOOTH_FILTER.tf.num,SMOOTH_FILTER.tf.den,temp(2:RAW_DATA_SI
ZE,5));


   %  Shear
   dat(1:RAW_DATA_SIZE,7) = smdat(1:RAW_DATA_SIZE,7);

   %  Touch
   dat(1:RAW_DATA_SIZE,8) = smdat(1:RAW_DATA_SIZE,8);
   %  Add APCOP
   %  Add APCOP Velocity
   %  Add MLCOP
   %  Add MLCOP Velocity

   filenamecal = [Loc_ToBeProcessed,subject,trial,rawid,'1'];
   fpcal = calmod(filenamecal);


   [temp(:,13),temp(:,15),dat(:,20)] =
apmlcop(smdat(:,1),smdat(:,2),smdat(:,3),smdat(:,4),fpcal);


   for i=13:2:15
      minitavg(i-12) = initavg(temp,i);
      temp(1:RAW_DATA_SIZE,i) = temp(1:RAW_DATA_SIZE,i)-sta_avg(i-12);
      dat(1:RAW_DATA_SIZE,i-4) =
filtfilt(SMOOTH_FILTER.tf.num,SMOOTH_FILTER.tf.den,temp(1:RAW_DATA_SI
ZE,i));
   end

   temp(2:RAW_DATA_SIZE,14) = (dat(2:RAW_DATA_SIZE,9)-
dat(1:RAW_DATA_SIZE-1,9))./SAMPLING_RATE;
```

```
   temp(2:RAW_DATA_SIZE,16) = (dat(2:RAW_DATA_SIZE,11)-
dat(1:RAW_DATA_SIZE-1,11))./SAMPLING_RATE;


   for i= 14:2:16
      minitavg(i-12) = initavg(temp,i);
      temp(2:RAW_DATA_SIZE,i) = temp(2:RAW_DATA_SIZE,i)-sta_avg(i-12);
      dat(2:RAW_DATA_SIZE,i-4) =
filtfilt(SMOOTH_FILTER.tf.num,SMOOTH_FILTER.tf.den,temp(2:RAW_DATA_SI
ZE,i));
   end

   %  ADD RMS EMG RTA
   %  ADD RMS EMG RGS
   %  ADD RMS EMG LTA
   %  ADD RMS EMG LGS

   dat(:,13)=smdat(:,9)./norm_EMG_COP(3,1);
   dat(:,14)=smdat(:,10)./norm_EMG_COP(2,3);
   dat(:,15)=smdat(:,11)./norm_EMG_COP(3,3);
   dat(:,16)=smdat(:,12)./norm_EMG_COP(2,4);


   %  Head Accel X
   %  Head Accel Y
   %  Head Accel Z
   for i = 21:23
      dat(1:RAW_DATA_SIZE,i-4) = smdat(1:RAW_DATA_SIZE,i-8);
   end

   %  Bell
   dat(1:RAW_DATA_SIZE,21) = smdat(1:RAW_DATA_SIZE,16);

   % Add Headings
   %     1  2        3              4     5     6
   A = {'Time' 'Position' 'Diff velocity' 'Diff Accel' 'Accel' 'Diff jerk'...
      'Shear' 'Touch' 'APCOP' 'APCOP Vel' 'MLCOP' 'MLCOP Vel' 'RTA' 'RGS'
'LTA' 'LGS' 'Head Accel X' 'Head Accel Y' 'Head Accel Z' 'Mass' 'Bell'};
   %     7     8     9     10        11     12        13     14  15     16  17
18          19          20     21

   %  Writes File

   cd([Loc_Processed,subject,'\',subject,trial,'\']);
   if (testnum<10)
      %     save([subject,r,rawid,'0',num2str(testnum)]);
```

```
      xlswrite([subject,trial,wrawid,'0',num2str(testnum)],A,'Sheet1','A1:T1');

xlswrite([subject,trial,wrawid,'0',num2str(testnum)],dat,'Sheet1',['A2:T',num2str(R
AW_DATA_SIZE+1)]);
   else
      %    save([subject,r,rawid,num2str(testnum)]);
      xlswrite([subject,trial,wrawid,num2str(testnum)],A,'Sheet1','A1:T1');

xlswrite([subject,trial,wrawid,num2str(testnum)],dat,'Sheet1',['A2:T',num2str(RAW
_DATA_SIZE+1)]);
   end
   xlswrite([subject,trial,wrawid,'_sum'],testnum,'AVG',['A',num2str(testnum+2)]);
   xlswrite([subject,trial,wrawid,'_sum'],minitavg,'AVG',['B',num2str(testnum+2)]);

   testnum = testnum + 1;
   if (testnum <10)
      filenameplate = [Loc_ToBeProcessed,subject,trial,rawid,'
',num2str(testnum),'.raw'];
   else
      filenameplate =
strcat(Loc_ToBeProcessed,subject,trial,rawid,num2str(testnum),'.raw');
   end
   FILEPLATEID = fopen(filenameplate,'rt');

end
% fclose(FileIDsum);
close(h);
cd([Loc_Processed,subject,'\',subject,trial,'\']);
save([subject,trial,wrawid,' ',num2str(testnum)],'filenameplate');
if testnum<5
   save(['error_trial_subject',trial],'filenameplate');
end

fsumd(1:testnum-1,1:9)=num2cell(dlmread(filenamesum,'\t',[4 0 testnum+2 8]));

file_sum_id = fopen(filenamesum,'rt');
for(i=1:testnum+4)
   fsumct=fgetl(file_sum_id);
end

if (fsumct~=-1)
   fsumc=cellstr(fsumct);
   xlswrite([subject,trial,wrawid,'_sum'],fsumc,'Sheet1','A35');
end
xlswrite([subject,trial,wrawid,'_sum'],fsumh,'Sheet1','A1:A2');
xlswrite([subject,trial,wrawid,'_sum'],fsuml,'Sheet1','A4:M4');
```

```
[r_fsumd,c_fsumd]=size(fsumd);
xlswrite([subject,trial,wrawid,'_sum'],fsumd,'Sheet1',['A5:M',num2str(r_fsumd+4)])
;


%  Clear workspace
clear dat smdat temp convdata msmoothdata cop minitavg subject rawid pert trial
testnum fsumd fsumct fsumc fsumh fsuml A

function minitavg = stachanger(subject,rawid,pert,trial)
%Processes Quiet Standing

global Loc_ToBeProcessed Loc_Processed Accel_CF Shear_CF Load_Cell_CF
global SMOOTH_FILTER SAMPLING_RATE norm_EMG_COP

%************************************
%************************************

%      Special Case

  switch pert
     case 1
        rawid_move=0;
     case 2
        rawid_move=1;
     case 4
        rawid_move=2;
     case 8
        rawid_move=3;
     case 16
        rawid_move=4;
  end

if (strcmp(subject,'m72z137'))
   if (trial=='')
      wrawid=['n1as',num2str(rawid_move),'ff'];
   else
      wrawid=rawid;
   end
else
   wrawid=rawid;
end


%          End
```

```
%   Must Change wrawid back to rawid to remove

%****************************************

   filenameplate = [Loc_ToBeProcessed,subject,trial,rawid,'.sta'];
 FILEPLATEID = fopen(filenameplate,'rt');
if (FILEPLATEID ~= -1)
  clear cop msmoothdata temp convdata dat
   fclose(FILEPLATEID);


   %  Data Extraction from raw plate data

   cop =dlmread(filenameplate,'\t',2,0);
   [STA_DATA_SIZE,q]=size(cop);

   minitavg(1:q+3)=0;
      %  Zero Baseline
   for i = 5:16
      minitavg(i) = initavg(cop,i);
      msmoothdata(1:STA_DATA_SIZE,i)=cop(1:STA_DATA_SIZE,i)-minitavg(i);
   end

   %  Conversions

   convdata(:,1:4) = cop(:,1:4) .* Load_Cell_CF;                    %  Load Cells
   convdata(:,5) = msmoothdata(:,5) .* pert.*1.25;  %  Position
   convdata(:,6) = msmoothdata(:,6) * Accel_CF;                          %
Acceleration
   convdata(:,7) = msmoothdata(:,7) * Shear_CF;                          %
Shear
   convdata(:,8) = msmoothdata(:,8);                                  %  Touch
   convdata(:,9:12) = abs(msmoothdata(:,9:12));                          %
EMGs
   convdata(:,13:15) = msmoothdata(:,13:15) * Accel_CF;                     %
Head Accel X,Y,Z
   convdata(:,16) = msmoothdata(:,16) /
max(msmoothdata(1:STA_DATA_SIZE,16));     %  Bell


   %  Smoothing done after conversions to prevent roughening of data

   smdat=filtfilt(SMOOTH_FILTER.tf.num,SMOOTH_FILTER.tf.den,convdata);


   %  Make Output Array
```

```
    % Add milliseconds to first column
  dat(1:STA_DATA_SIZE,1) = (1:STA_DATA_SIZE)';

    % Add Position

    dat(1:STA_DATA_SIZE,2) = smdat(1:STA_DATA_SIZE,5);

    % Add differentiated velocity

    temp(2:STA_DATA_SIZE,7) = (smdat(2:STA_DATA_SIZE,5)-
smdat(1:STA_DATA_SIZE-1,5))./SAMPLING_RATE;

  % Smooth velocity
    minitavg(17) = initavg(temp,7);
    temp(2:STA_DATA_SIZE,7) = temp(2:STA_DATA_SIZE,7)-minitavg(17);
    dat(2:STA_DATA_SIZE,3) =
filtfilt(SMOOTH_FILTER.tf.num,SMOOTH_FILTER.tf.den,temp(2:STA_DATA_SI
ZE,7));


    % Add differentiated Acceleration

  temp(3:STA_DATA_SIZE,8) = (dat(3:STA_DATA_SIZE,3)-
dat(2:STA_DATA_SIZE-1,3))./SAMPLING_RATE;

    % Smooth Acceleration
    minitavg(18) = initavg(temp,8);
    temp(3:STA_DATA_SIZE,8) = temp(3:STA_DATA_SIZE,8)-minitavg(18);
    dat(3:STA_DATA_SIZE,4) =
filtfilt(SMOOTH_FILTER.tf.num,SMOOTH_FILTER.tf.den,temp(3:STA_DATA_SI
ZE,8));


    % Add Acceleration
  dat(1:STA_DATA_SIZE,5) = smdat(1:STA_DATA_SIZE,6);
    % Add Differentiated Jerk


  temp(2:STA_DATA_SIZE,5) = (dat(2:STA_DATA_SIZE,5)-
dat(1:STA_DATA_SIZE-1,5))./SAMPLING_RATE;
    % Smooth Differentiated Jerk
  minitavg(19) = initavg(temp,5);
  temp(2:STA_DATA_SIZE,5) = temp(2:STA_DATA_SIZE,5)-minitavg(19);
  dat(2:STA_DATA_SIZE,6) =
filtfilt(SMOOTH_FILTER.tf.num,SMOOTH_FILTER.tf.den,temp(2:STA_DATA_SI
ZE,5));
```

```
    % Shear
  dat(1:STA_DATA_SIZE,7) = smdat(1:STA_DATA_SIZE,7);

    % Touch
  dat(1:STA_DATA_SIZE,8) = smdat(1:STA_DATA_SIZE,8);
    % Add APCOP
    % Add APCOP Velocity
    % Add MLCOP
    % Add MLCOP Velocity

  filenamecal = [Loc_ToBeProcessed,subject,trial,rawid,'1'];
  fpcal = calmod(filenamecal);

  [temp(:,13),temp(:,15)] =
apmlcop(smdat(:,1),smdat(:,2),smdat(:,3),smdat(:,4),fpcal);


  for i=13:2:15
    minitavg(i-12) = mean(temp(:,i));
    temp(1:STA_DATA_SIZE,i) = temp(1:STA_DATA_SIZE,i)-minitavg(i-12);
    dat(1:STA_DATA_SIZE,i-4) =
filtfilt(SMOOTH_FILTER.tf.num,SMOOTH_FILTER.tf.den,temp(1:STA_DATA_SI
ZE,i));
  end

  temp(2:STA_DATA_SIZE,14) = (dat(2:STA_DATA_SIZE,9)-
dat(1:STA_DATA_SIZE-1,9))./SAMPLING_RATE;
  temp(2:STA_DATA_SIZE,16) = (dat(2:STA_DATA_SIZE,11)-
dat(1:STA_DATA_SIZE-1,11))./SAMPLING_RATE;


  for i= 14:2:16
    minitavg(i-12) = mean(temp(:,i));
    temp(2:STA_DATA_SIZE,i) = temp(2:STA_DATA_SIZE,i)-minitavg(i-12);
    dat(2:STA_DATA_SIZE,i-4) =
filtfilt(SMOOTH_FILTER.tf.num,SMOOTH_FILTER.tf.den,temp(2:STA_DATA_SI
ZE,i));
  end

    % ADD RMS EMG RTA
    % ADD RMS EMG RGS
    % ADD RMS EMG LTA
    % ADD RMS EMG LGS
```

```
   dat(:,13:16)=smdat(:,9:12);

      %  Head Accel X
      %  Head Accel Y
      %  Head Accel Z
   for i = 21:23
      dat(1:STA_DATA_SIZE,i-4) = smdat(1:STA_DATA_SIZE,i-8);
   end

      %  Bell
   dat(1:STA_DATA_SIZE,20) = smdat(1:STA_DATA_SIZE,16);


   % Add Headings
   %      1  2        3                4     5     6
   A = {'Time' 'Position' 'Diff velocity' 'Diff Accel' 'Accel' 'Diff jerk'...
            'Shear' 'Touch' 'APCOP' 'APCOP Vel' 'MLCOP' 'MLCOP Vel' 'RTA'
'RGS' 'LTA' 'LGS' 'Head Accel X' 'Head Accel Y' 'Head Accel Z' 'Bell'};
      %     7     8     9     10        11     12        13     14  15     16  17
18          19          20

   %  Writes File
   cd([Loc_Processed,subject,'\',subject,trial,'\']);
%    save([subject,r,wrawid]);
    xlswrite([subject,trial,wrawid,'_sta'],A,'Sheet1','A1:T1');
    xlswrite([subject,trial,wrawid,'_sta'],dat,'Sheet1','A2:T20001');
else
   cd([Loc_Processed,subject,'\',subject,trial,'\']);
   save(['error_sta',trial],'filenameplate');
end
clear dat smdat convdata msmoothdata temp cop A trial wrawid subject

%  Calculates the initial average
%      By averaging first 180 Data points
function a = initavg(d,i)
   %  d is array
   %  i is column of data (type)
   a = mean(d(200:3600,i));

function [APCOP,MLCOP,mass] = apmlcop(l1,l2,l3,l4,fpcal)

%calculating Ap-COP and Ml-COP
         FP1=l1-fpcal(1);
         FP2=l2-fpcal(2);
         FP3=l3-fpcal(3);
         FP4=l4-fpcal(4);
```

```
        %Calculate AP and ML COP
        wght = FP3+FP4+FP1+FP2;  %in volts

        %   209.55 mm  174.625 mm

        APCOP=209.55*(FP3+FP4-FP1-FP2)./wght;
        MLCOP=174.625*(FP3+FP2-FP1-FP4)./wght;

        %  Conversion factor is linear
        %      (Sum of fpcal [Volts])/13.95 kg(mass of plate)

        cnvfact=-39.92;

        mass=wght.*cnvfact;  %  wght is in Volts
                             %  cnvfact is -39.92KG/V

%Get cal values

    function f = calmod(str)
      calstr=[str '.cal'];
      fid=fopen(calstr);
      CAL= fscanf(fid, '%f',[16 inf]);
      CAL=CAL';
      fclose(fid);
      %calculates the calibration
      mcal=mean(CAL(.10*length(CAL):.90*length(CAL),:));
      %Plate Weight is substracted from the calibration values
      f=mcal(:,1:4);%+.25*.347; %platewt 13.95kg = .347V
      clear mcal;

function QSmetrics(subject,rawid,move,row,trial)

global Loc_ToBeProcessed Loc_Processed

APCOP =
xlsread([Loc_ToBeProcessed,subject,trial,rawid,'_sta.xls'],'Sheet1','I2:I20001');
MLCOP =
xlsread([Loc_ToBeProcessed,subject,trial,rawid,'_sta.xls'],'Sheet1','K2:K20001');

%calculate resultant distance
rd=sqrt(APCOP.^2+MLCOP.^2);
mdist=sum(rd)/(length(rd));
mdistap=sum(abs(APCOP))/(length(APCOP));
mdistml=sum(abs(MLCOP))/(length(MLCOP));

%calculate rms distance from mean cop
```

```
rdist=sqrt((sum(rd.*rd))/(length(rd)));
rdistap=sqrt((sum(APCOP.*APCOP))/(length(APCOP)));
rdistml=sqrt((sum(MLCOP.*MLCOP))/(length(MLCOP)));

%calculation of total excursion
m=length(APCOP)-1;
totex=sum(sqrt(((APCOP(2:m+1)-APCOP(1:m)).^2)+((MLCOP(2:m+1)-
MLCOP(1:m)).^2)));
totexap=sum(abs(APCOP(2:m+1)-APCOP(1:m)));
totexml=sum(abs(MLCOP(2:m+1)-MLCOP(1:m)));
%calculate mean velocity
mvelo=totex/(length(APCOP)/1000);
mveloap=totexap/(length(APCOP)/1000);
mveloml=totexml/(length(APCOP)/1000);

%calculate mean, standard deviation and range of COP's
meanrd=mean(rd);
rng=range(rd);
meanap=mean(APCOP);
meanml=mean(MLCOP);
stddevrd=std(rd);
stddevap=std(APCOP);
stddevml=std(MLCOP);
rngap=range(APCOP);
rngml=range(MLCOP);

%calculate the 95% confedence circle area
areacc=pi*(mdist+1.645*(sqrt(rdist^2-mdist^2)))^2;

%calculate the 95% confidence ellipse area
stddevapml=(sum(APCOP.*MLCOP))/(length(APCOP));
areace=2*pi*3*(sqrt(stddevap^2*stddevml^2-stddevapml^2));

%calculate the sway area
n=length(APCOP)-1;
areasway=sum(abs((APCOP(2:n+1).*MLCOP(1:n))-
(MLCOP(2:n+1).*APCOP(1:n))))/(2*length(APCOP)/1000);

%calculate mean frequency
mfreq=mvelo/(2*pi*mdist);
mfreqml=mveloml/(4*sqrt(2)*mdistml);
mfreqap=mveloap/(4*sqrt(2)*mdistap);

%calculate fractal dimension based on 95% Confidence Circle
dcc=2*(mdist+(1.645*(sqrt(rdist^2-mdist^2))));
FD_cc=log10(length(APCOP))/log10((length(APCOP)*dcc)/totex);
```

```
%calculate fractal dimension based on 95% Confidence Ellipse
dce=sqrt(8*3*sqrt(stddevap^2*stddevml^2-stddevapml^2));
FD_ce=log10(length(APCOP))/log10((length(APCOP)*dce)/totex);

% Frequency domain calculations using Multitaper method
% Calculates total power for each
i=7;
while length(APCOP)>2^i
   i=i+1;
end
nfft=2^i;
m=n/2;
fs=1000;
fc=fs/2;
f = fc * [0:m]/m;
df=f(2);
LPS=6; % for 0.15 Hz cutoff for analysis
HPS=164; %for 5Hz cutoff for Analysis
% [G,w]=pmtm(rd,4.5,nfft,fs);
% [Gap,w]=pmtm(APCOP,4.5,nfft,fs);
% [Gml,w]=pmtm(MLCOP,4.5,nfft,fs);

MLCOPF=fft(MLCOP,n);
Gml=MLCOPF.*conj(MLCOPF) / n;

APCOPF=fft(APCOP,n);
Gap=APCOPF.*conj(APCOPF) / n;

rdF=fft(rd,n);
G=rdF.*conj(rdF) / n;

power=sum(G(LPS:HPS));
powerap=sum(Gap(LPS:HPS));
powerml=sum(Gml(LPS:HPS));
% powerap=sum(APCOP.^2);
% powerml=sum(MLCOP.^2);
%calculates 50% power for each
pfreq50=f(2)*find(cumsum(G(LPS:HPS))>=power*0.5,1,'first');
pfreq50ap=f(2)*find(cumsum(Gap(LPS:HPS))>=powerap*0.5,1,'first');
pfreq50ml=f(2)*find(cumsum(Gml(LPS:HPS))>=powerml*0.5,1,'first');
%calculates 95% power for each
pfreq95=f(2)*find(cumsum(G(LPS:HPS))>=power*0.95,1,'first');
pfreq95ap=f(2)*find(cumsum(Gap(LPS:HPS))>=powerap*0.95,1,'first');
pfreq95ml=f(2)*find(cumsum(Gml(LPS:HPS))>=powerml*0.95,1,'first');
%Calculates centroidal frequency
```

```
cfreq=(sum((((LPS:HPS)*df).^2).*G(LPS:HPS)')/power).^0.5;
cfreqap=(sum((((LPS:HPS).*df).^2).*Gap(LPS:HPS)')/powerap).^0.5;
cfreqml=(sum((((LPS:HPS).*df).^2).*Gml(LPS:HPS)')/powerml).^0.5;
%calculates frequency dispersion
freqd=(1-
sum(((LPS:HPS).*df).*G(LPS:HPS)')^2/(power*sum((((LPS:HPS).*df).^2).*G(LPS
:HPS)')))^0.5;
freqdap=(1-
sum(((LPS:HPS).*df).*Gap(LPS:HPS)')^2/(powerap*sum((((LPS:HPS).*df).^2).*G
ap(LPS:HPS)')))^0.5;
freqdml=(1-
sum(((LPS:HPS).*df).*Gml(LPS:HPS)')^2/(powerml*sum((((LPS:HPS).*df).^2).*G
ml(LPS:HPS)')))^0.5;


%   1    2     3      4        5    6    7    8
%                                          9    10     11      12  13
14     15   16      17    18     19    20    21    22     23     24    25
26       27   28    29    30    31  32     33    34      35      36
37      38      39     40   41     42     43   44     45
output = { move meanrd  meanap meanml stddevrd stddevap stddevml rng rngap
rngml mdist mdistap mdistml rdist rdistap rdistml totex totexap totexml mvelo
mveloap mveloml mfreq mfreqap mfreqml areacc areasway areace FD_cc
FD_ce power powerap powerml pfreq50 pfreq50ap pfreq50ml pfreq95 pfreq95ap
pfreq95ml cfreq cfreqap cfreqml freqd freqdap freqdml};
cd(Loc_Processed);
if row==2
   H = {'Move' 'meanrd' 'meanap' 'meanml' 'stddevrd' 'stddevap' 'stddevml' 'rng'
'rngap' 'rngml' 'mdist' 'mdistap' 'mdistml' 'rdist' 'rdistap' 'rdistml' 'totex' 'totexap'
'totexml' 'mvelo' 'mveloap' 'mveloml' 'mfreq' 'mfreqap' 'mfreqml' 'areacc'
'areasway' 'areace' 'FD_cc' 'FD_ce' 'power' 'powerap' 'powerml' 'pfreq50'
'pfreq50ap' 'pfreq50ml' 'pfreq95' 'pfreq95ap' 'pfreq95ml' 'cfreq' 'cfreqap' 'cfreqml'
'freqd' 'freqdap' 'freqdml'};
   xlswrite([subject,trial,'_QS.xls'],H,'Sheet1','A1:AS1');
end
xlswrite([subject,trial,'_QS.xls'],output,'Sheet1',['A',row,':AS',row]);

function QSmetrics_Analysis(subject,row_read,trial)

global Loc_ToBeProcessed Loc_Processed row_write

[qsmetrics, move_size] =
xlsread([Loc_ToBeProcessed,subject,trial,'_QS.xls'],'Sheet1',['A2:AS',num2str(ro
w_read+1)]);
```

```
if strcmp(trial,'')
   trial={'a'};
end
qsmetricsf(1,length(move_size)*length(qsmetrics)) = 0;
cd(Loc_Processed);


   H = {};
   Hf = {'Subject'};
   for (i=1:length(move_size))

      %  Write Header for QS_Analysis Spreadsheet
      H = {['meanrd_',char(move_size(i))]...
         ['meanap_',char(move_size(i))]...
         ['meanml_',char(move_size(i))]...
         ['stddevrd_',char(move_size(i))]...
         ['stddevap_',char(move_size(i))]...
         ['stddevml_',char(move_size(i))]...
         ['rng_',char(move_size(i))]...
         ['rngap_',char(move_size(i))]...
         ['rngml_',char(move_size(i))]...
         ['mdist_',char(move_size(i))]...
         ['mdistap_',char(move_size(i))]...
         ['mdistml_',char(move_size(i))]...
         ['rdist_',char(move_size(i))]...
         ['rdistap_',char(move_size(i))]...
         ['rdistml_',char(move_size(i))]...
         ['totex_',char(move_size(i))]...
         ['totexap_',char(move_size(i))]...
         ['totexml_',char(move_size(i))]...
         ['mvelo_',char(move_size(i))]...
         ['mveloap_',char(move_size(i))]...
         ['mveloml_',char(move_size(i))]...
         ['mfreq_',char(move_size(i))]...
         ['mfreqap_',char(move_size(i))]...
         ['mfreqml_',char(move_size(i))]...
         ['areacc_',char(move_size(i))]...
         ['areasway_',char(move_size(i))]...
         ['areace_',char(move_size(i))]...
         ['FD_cc_',char(move_size(i))]...
         ['FD_ce_',char(move_size(i))]...
         ['power',char(move_size(i))]...
         ['powerap_',char(move_size(i))]...
         ['powerml_',char(move_size(i))]...
         ['pfreq50_',char(move_size(i))]...
```

```
        ['pfreq50ap_',char(move_size(i))]...
        ['pfreq50ml_',char(move_size(i))]...
        ['pfreq95_',char(move_size(i))]...
        ['pfreq95ap_',char(move_size(i))]...
        ['pfreq95ml_',char(move_size(i))]...
        ['cfreq_',char(move_size(i))]...
        ['cfreqap_',char(move_size(i))]...
        ['cfreqml_',char(move_size(i))]...
        ['freqd_',char(move_size(i))]...
        ['freqdap_',char(move_size(i))]...
        ['freqdml_',char(move_size(i))]};
      Hf = [Hf H];
      qsmetricsf(1,1+(i-
1)*length(qsmetrics):i*length(qsmetrics))=qsmetrics(i,1:length(qsmetrics));
   end
if row_write==2
   xlswrite(['QS_Analysis_',char(trial),'.xls'],Hf,'Sheet1','A1');
end
xlswrite(['QS_Analysis_',char(trial),'.xls'],cellstr(subject),'Sheet1',['A',num2str(row
_write)]);
xlswrite(['QS_Analysis_',char(trial),'.xls'],qsmetricsf,'Sheet1',['B',num2str(row_writ
e)]);

function QSmetrics_Analysis_Sum(subject,row_read,trial)

global Loc_ToBeProcessed Loc_Processed row_write

qsmetrics(1:3,1:25)=0;
[qsmetrics, move_size] =
xlsread([Loc_ToBeProcessed,subject,trial,'_QS.xls'],'Sheet1',['A2:AS',num2str(ro
w_read+1)]);



if strcmp(trial,'')
   trial={'a'};
end

qsmetricsf_sum = sum(qsmetrics);
qsmetricsf_mean = mean(qsmetrics);

cd(Loc_Processed);

if row_write==2
   H = {};
   Hf = {'Subject'};
```

```
% Write Header for QS_Analysis Spreadsheet
H = {['meanrd']...
   ['meanap']...
   ['meanml']...
   ['stddevrd']...
   ['stddevap']...
   ['stddevml']...
   ['rng']...
   ['rngap']...
   ['rngml']...
   ['mdist']...
   ['mdistap']...
   ['mdistml']...
   ['rdist']...
   ['rdistap']...
   ['rdistml']...
   ['totex']...
   ['totexap']...
   ['totexml']...
   ['mvelo']...
   ['mveloap']...
   ['mveloml']...
   ['mfreq']...
   ['mfreqap']...
   ['mfreqml']...
   ['areacc']...
   ['areasway']...
   ['areace']...
   ['FD_cc']...
   ['FD_ce']...
   ['power']...
   ['powerap']...
   ['powerml']...
   ['pfreq50']...
   ['pfreq50ap']...
   ['pfreq50ml']...
   ['pfreq95']...
   ['pfreq95ap']...
   ['pfreq95ml']...
   ['cfreq']...
   ['cfreqap']...
   ['cfreqml']...
   ['freqd']...
   ['freqdap']...
   ['freqdml']};
Hf = [Hf H];
```

```
    xlswrite(['QS_Analysis_sum_',char(trial),'.xls'],Hf,'Sheet1','A1');
    xlswrite(['QS_Analysis_mean_',char(trial),'.xls'],Hf,'Sheet1','A1');
end

xlswrite(['QS_Analysis_sum_',char(trial),'.xls'],cellstr(subject),'Sheet1',['A',num2st
r(row_write)]);
xlswrite(['QS_Analysis_sum_',char(trial),'.xls'],qsmetricsf_sum,'Sheet1',['B',num2s
tr(row_write)]);


xlswrite(['QS_Analysis_mean_',char(trial),'.xls'],cellstr(subject),'Sheet1',['A',num2
str(row_write)]);
xlswrite(['QS_Analysis_mean_',char(trial),'.xls'],qsmetricsf_mean,'Sheet1',['B',nu
m2str(row_write)]);
```

APPENDIX N

ENGINEERING UNIT CONVERSION

ON-THE-FLY MATLAB® CODE

```
function [norm_EMG_COP,dat] =
datchanger(subject,rawid,pert,trial,cop,cal,TEKSCAN_SAMP)

Loc_Processed = 'E:\data\';
Accel_CF =1;
Shear_CF =-110;
load('SMOOTH_FILTER.mat');
load('Notch60Hz.mat');
SAMPLING_RATE  = 0.001;


[DAT_DATA_SIZE,COLs]=size(cop);
%   Initializations
msmoothdata=zeros(DAT_DATA_SIZE,COLs);
minitavg =0;
temp =zeros(DAT_DATA_SIZE,16);
convdata=zeros(DAT_DATA_SIZE,COLs);
dat =zeros(DAT_DATA_SIZE,COLs+5);
%   Tekscan File Directory
%   TEKSCAN_DIR =
%   Data Extraction from raw plate data

% tekscanfsx =
tekscan_processor(TEKSCAN_DIR,[subject,'_',trial,'_',rawid],filenum,1);

%   Zero Baseline
for i = 5:COLs
   minitavg(i) = initavg(cop,i);
   msmoothdata(1:DAT_DATA_SIZE,i)=cop(1:DAT_DATA_SIZE,i)-minitavg(i);
end

%msmoothdata=filtfilt(Notch60Hz.tf.num,Notch60Hz.tf.den,msmoothdata);

%   Conversions

 %   Load Cells
convdata(:,1:4) = cop(:,1:4);
%   Position
convdata(:,5) = msmoothdata(:,5) .* pert;
%   Acceleration
convdata(:,6) = msmoothdata(:,6) .* Accel_CF;
%   Shear
convdata(:,7) = msmoothdata(:,7) .* Shear_CF;
%   Touch
convdata(:,8) = msmoothdata(:,8);
%   Head Accel X,Y,Z
```

```
convdata(:,9:11) = msmoothdata(:,9:11) .* Accel_CF;

%  EMGs
% Always keep EMGs at End so can easily expand the number
convdata(:,12:COLs) = abs(msmoothdata(:,12:COLs));

%  Smoothing done after conversions to prevent roughening of data

smdat=filtfilt(SMOOTH_FILTER.tf.num,SMOOTH_FILTER.tf.den,convdata);


%  Make Output Array
%  Add milliseconds to first column
dat(1:DAT_DATA_SIZE,1) = (1:DAT_DATA_SIZE)';

%  Add Position

dat(1:DAT_DATA_SIZE,2) = smdat(1:DAT_DATA_SIZE,5);

%  Add differentiated velocity

temp(2:DAT_DATA_SIZE,7) = (smdat(2:DAT_DATA_SIZE,5)-
smdat(1:DAT_DATA_SIZE-1,5))./SAMPLING_RATE;

%  Smooth velocity
minitavg(7) = initavg(temp,7);
temp(2:DAT_DATA_SIZE,7) = temp(2:DAT_DATA_SIZE,7)-minitavg(7);
dat(2:DAT_DATA_SIZE,3) =
filtfilt(SMOOTH_FILTER.tf.num,SMOOTH_FILTER.tf.den,temp(2:DAT_DATA_SI
ZE,7));


%  Add differentiated Acceleration

temp(3:DAT_DATA_SIZE,8) = (dat(3:DAT_DATA_SIZE,3)-
dat(2:DAT_DATA_SIZE-1,3))./SAMPLING_RATE;

% Smooth Acceleration
minitavg(8) = initavg(temp,8);
temp(3:DAT_DATA_SIZE,8) = temp(3:DAT_DATA_SIZE,8)-minitavg(8);
dat(3:DAT_DATA_SIZE,4) =
filtfilt(SMOOTH_FILTER.tf.num,SMOOTH_FILTER.tf.den,temp(3:DAT_DATA_SI
ZE,8));


%  Add Acceleration
```

```
dat(1:DAT_DATA_SIZE,5) = smdat(1:DAT_DATA_SIZE,6);
%   Add Differentiated Jerk


temp(2:DAT_DATA_SIZE,5) = (dat(2:DAT_DATA_SIZE,5)-
dat(1:DAT_DATA_SIZE-1,5))./SAMPLING_RATE;
% Smooth Differentiated Jerk
minitavg(5) = initavg(temp,5);
temp(2:DAT_DATA_SIZE,5) = temp(2:DAT_DATA_SIZE,5)-minitavg(5);
dat(2:DAT_DATA_SIZE,6) =
filtfilt(SMOOTH_FILTER.tf.num,SMOOTH_FILTER.tf.den,temp(2:DAT_DATA_SI
ZE,5));


%   Shear
dat(1:DAT_DATA_SIZE,7) = smdat(1:DAT_DATA_SIZE,7);

%   Touch
dat(1:DAT_DATA_SIZE,8) = smdat(1:DAT_DATA_SIZE,8);
%   Add APCOP
%   Add APCOP Velocity
%   Add MLCOP
%   Add MLCOP Velocity

% 'Calculating COPs'
fpcal = calmod(cal);

[temp(:,13),temp(:,15),dat(:,9)] =
apmlcop(smdat(:,1),smdat(:,2),smdat(:,3),smdat(:,4),fpcal);

% 'APCOP & MLCOP'

for i=13:2:15
   minitavg(i) = initavg(temp,i);
   temp(1:DAT_DATA_SIZE,i) = temp(1:DAT_DATA_SIZE,i)-minitavg(i);
   dat(1:DAT_DATA_SIZE,i-3) =
filtfilt(SMOOTH_FILTER.tf.num,SMOOTH_FILTER.tf.den,temp(1:DAT_DATA_SI
ZE,i));
end

temp(2:DAT_DATA_SIZE,14) = (dat(2:DAT_DATA_SIZE,10)-
dat(1:DAT_DATA_SIZE-1,10))./SAMPLING_RATE;
temp(2:DAT_DATA_SIZE,16) = (dat(2:DAT_DATA_SIZE,12)-
dat(1:DAT_DATA_SIZE-1,12))./SAMPLING_RATE;
```

```
for i= 14:2:16
   minitavg(i) = initavg(temp,i);
   temp(2:DAT_DATA_SIZE,i) = temp(2:DAT_DATA_SIZE,i)-minitavg(i);
   dat(2:DAT_DATA_SIZE,i-3) =
filtfilt(SMOOTH_FILTER.tf.num,SMOOTH_FILTER.tf.den,temp(2:DAT_DATA_SI
ZE,i));
end

%  Head Accel X
%  Head Accel Y
%  Head Accel Z
for i = 14:16
   dat(1:DAT_DATA_SIZE,i) = smdat(1:DAT_DATA_SIZE,i-5);
end

%  ADD RMS EMG RTA
%  ADD RMS EMG RGS
%  ADD RMS EMG LTA
%  ADD RMS EMG LGS

dat(:,17:COLs+5)=smdat(:,12:COLs);


%  Create Normalization Array
%  EMGs
for i=17:20
   norm_EMG_COP(1,i-16) = mean(dat(2000:5000,i));
   norm_EMG_COP(2,i-16) = mean(dat(11000:14000,i));
   norm_EMG_COP(3,i-16) = mean(dat(16000:19000,i));
   norm_EMG_COP(4,i-16) = mean(dat(25000:28000,i));
end
%  COP
for i=10:2:12
   norm_EMG_COP(1,i-5-(i-10)./2) = mean(dat(2000:5000,i));
   norm_EMG_COP(2,i-5-(i-10)./2) = mean(dat(11000:14000,i));
   norm_EMG_COP(3,i-5-(i-10)./2) = mean(dat(16000:19000,i));
   norm_EMG_COP(4,i-5-(i-10)./2) = mean(dat(25000:28000,i));
end

A=cell(1,COLs+5);

% Add Headings
%      1  2         3                4      5      6
A(1,1:20) = {'Time' 'Position' 'Diff velocity' 'Diff Accel' 'Accel' 'Diff jerk'...
   'Shear' 'Touch' 'MASS' 'APCOP' 'APCOP Vel' 'MLCOP' 'MLCOP Vel' 'Head
Accel X' 'Head Accel Y' 'Head Accel Z' 'RTA' 'LTA' 'RGS' 'LGS'};
```

```
%     7     8     9     10        11     12        13     14        15        16
17   18   19   20


if COLs > 15
   for i=16:COLs
      % Follows convention that Even number are on the right side
      if mod(i,2) == 0
         leftright='R';
      else
         leftright='L';
      end
      if i==16
         t_head='RSCM';
      elseif i==17
         t_head='LSCM';
      elseif i==18
         t_head='R Soleus';
      elseif i==19
         t_head='L Soleus';
      else
         t_head=['EMG', leftright, num2str(i-11)];
      end
      A(1,20+i-15)=cellstr(t_head);
   end
end
xlspread=cell(DAT_DATA_SIZE+1,COLs+5);
xlspread(1,1:COLs+5)=A(1,1:COLs+5);
xlspread(2:DAT_DATA_SIZE+1,1:COLs+5)=num2cell(dat);

%   Writes File
mkdir([Loc_Processed,subject,'\',subject,'_',trial,'\ENGRUNITS\'])
cd([Loc_Processed,subject,'\',subject,'_',trial,'\ENGRUNITS\']);

xlswrite([subject,'_',trial,'_',rawid],xlspread,'Sheet1','A1');



%*******************************
%*****Tekscan .fsx processing Weight Even
tekdir=[Loc_Processed,subject,'\',subject,'_',trial,'\Tekscan\'];
[tekdat, feetcop,
pweight]=tekmat_processor([tekdir,subject,'_',trial,'_',strrep(rawid,'_emcp',''),num
2str(1,'%04d')],1);
tekdat=[tekdat feetcop pweight];
tekspread=cell(size(tekdat,1)+1,size(tekdat,2)+1);
```

```
tekspread(1,:)={'Time' 'APCOP' 'MLCOP' 'RAPCOP' 'RMLCOP' 'LAPCOP'
'LMLCOP' '% Right Foot' '% Left Foot'};
tekspread(2:size(tekdat,1)+1,1)=num2cell(1/TEKSCAN_SAMP:1/TEKSCAN_SA
MP:size(tekdat,1)/TEKSCAN_SAMP);
tekspread(2:size(tekdat,1)+1,2:size(tekdat,2)+1)=num2cell(tekdat);
xlswrite([subject,'_',trial,'_',rawid],tekspread,'TekscanEW1','A1');
%*******************************

%*******************************
%*****Tekscan .fsx processing on Toes
[tekdat, feetcop,
pweight]=tekmat_processor([tekdir,subject,'_',trial,'_',strrep(rawid,'_emcp',''),num
2str(2,'%04d')],1);
tekdat=[tekdat feetcop pweight];
tekspread=cell(size(tekdat,1)+1,size(tekdat,2)+1);
tekspread(1,:)={'Time' 'APCOP' 'MLCOP' 'RAPCOP' 'RMLCOP' 'LAPCOP'
'LMLCOP' '% Right Foot' '% Left Foot'};
tekspread(2:size(tekdat,1)+1,1)=num2cell(1/TEKSCAN_SAMP:1/TEKSCAN_SA
MP:size(tekdat,1)/TEKSCAN_SAMP);
tekspread(2:size(tekdat,1)+1,2:size(tekdat,2)+1)=num2cell(tekdat);
xlswrite([subject,'_',trial,'_',rawid],tekspread,'TekscanToes','A1');
%*******************************

%*******************************
%*****Tekscan .fsx processing on Heels
[tekdat, feetcop,
pweight]=tekmat_processor([tekdir,subject,'_',trial,'_',strrep(rawid,'_emcp',''),num
2str(3,'%04d')],1);
tekdat=[tekdat feetcop pweight];
tekspread=cell(size(tekdat,1)+1,size(tekdat,2)+1);
tekspread(1,:)={'Time' 'APCOP' 'MLCOP' 'RAPCOP' 'RMLCOP' 'LAPCOP'
'LMLCOP' '% Right Foot' '% Left Foot'};
tekspread(2:size(tekdat,1)+1,1)=num2cell(1/TEKSCAN_SAMP:1/TEKSCAN_SA
MP:size(tekdat,1)/TEKSCAN_SAMP);
tekspread(2:size(tekdat,1)+1,2:size(tekdat,2)+1)=num2cell(tekdat);
xlswrite([subject,'_',trial,'_',rawid],tekspread,'TekscanHeels','A1');
%*******************************

%*******************************
%*****Tekscan .fsx processing Weisht Even Again
[tekdat, feetcop,
pweight]=tekmat_processor([tekdir,subject,'_',trial,'_',strrep(rawid,'_emcp',''),num
2str(4,'%04d')],1);
tekdat=[tekdat feetcop pweight];
tekspread=cell(size(tekdat,1)+1,size(tekdat,2)+1);
```

```
tekspread(1,:)={'Time' 'APCOP' 'MLCOP' 'RAPCOP' 'RMLCOP' 'LAPCOP'
'LMLCOP' '% Right Foot' '% Left Foot'};
tekspread(2:size(tekdat,1)+1,1)=num2cell(1/TEKSCAN_SAMP:1/TEKSCAN_SA
MP:size(tekdat,1)/TEKSCAN_SAMP);
tekspread(2:size(tekdat,1)+1,2:size(tekdat,2)+1)=num2cell(tekdat);
xlswrite([subject,'_',trial,'_',rawid],tekspread,'TekscanEW2','A1');
%*******************************

%****************************************
%****Tekscan Sum File
teksum=cell(5,2);
teksum(1,:)={'Filename' 'Description'};
teksum(2,:)={[subject,'_',trial,'_',strrep(rawid,'_emcp',''),num2str(1,'%04d')] 'EMG
COP: Weight even on both Feet'};
teksum(3,:)={[subject,'_',trial,'_',strrep(rawid,'_emcp',''),num2str(2,'%04d')] 'EMG
COP: On Toes'};
teksum(4,:)={[subject,'_',trial,'_',strrep(rawid,'_emcp',''),num2str(3,'%04d')] 'EMG
COP: On Heels'};
teksum(5,:)={[subject,'_',trial,'_',strrep(rawid,'_emcp',''),num2str(4,'%04d')] 'EMG
COP: Weight even on both Feet'};
cd(tekdir);
xlswrite([subject,'_',trial,'_',strrep(rawid,'_emcp',''),'_tekscan_sum'],teksum,'Sheet
1','A1');
%****************************************

clear Loc_Processed smdat convdata msmoothdata leftright t_head temp cop A
clear Accel_CF Shear_CF Load_Cell_CF DAT_DATA_SIZE SMOOTH_FILTER
clear SAMPLING_RATE minitavg subject trial rawid xlspread
function  [dat] =
filechanger(subject,rawid,pert,trial,trialnum,cop,cal,norm_EMG_COP,sta_avg,fre
q,noise_amp,sumd,sinusoid_setup,TEKSCAN_SAMP,PEAK_NUM)

Loc_Processed = 'E:\data\';
Accel_CF = 1;
Shear_CF =-110;
load('SMOOTH_FILTER.mat');
SAMPLING_RATE  = 0.001; %Sampling Period

[RAW_DATA_SIZE,COLs]=size(cop);
%  Initializations
msmoothdata=zeros(RAW_DATA_SIZE,COLs);
minitavg=zeros(1,COLs+3);
temp =zeros(RAW_DATA_SIZE,COLs);
convdata=zeros(RAW_DATA_SIZE,COLs);
dat =zeros(RAW_DATA_SIZE,COLs+5);
%****************************************
```

```
%****Sum File Writer
%      Header Setup
filenamesum=[Loc_Processed,subject,'\',subject,'_',trial,'\ENGRUNITS\',subject,'_
',trial,'_',rawid,'_F',freq,'_sum'];
if trialnum == 1
   avg_h=cell(2,COLs+4);
   avg_h(1,1:16) ={'Trial' 'APCOP' 'APCOPV' 'MLCOP' 'MLCOPV' 'Position'
'Acceleration' ...
                 'Shear' 'Touch' 'Head Accel X' 'Head Accel Y' 'Head Accel Z' 'RTA'
'LTA' 'RGS' 'LGS'};
   if COLs > 15
      for i=16:COLs
         % Follows convention that Even number are on the right side
         if mod(i,2) == 0
            leftright='R';
         else
            leftright='L';
         end
         if i==16
            t_head='RSCM';
         elseif i==17
            t_head='LSCM';
         elseif i==18
            t_head='R Soleus';
         elseif i==19
            t_head='L Soleus';
         else
            t_head=['EMG', leftright, num2str(i-11)];
         end
         avg_h(1,i+1)={t_head};
      end
   end
   avg_h(1,COLs+2:COLs+4) = {'Diff velocity' 'Diff Accel' 'Diff jerk'};
   avg_h(2,1)={'QS'};
   avg_h(2,2:COLs+4)=num2cell(sta_avg);
   fsumh=cell(3,10);
   fsumh(1,1:6)={filenamesum ' ' 'Front' ' ' 'Sample Frequency = 1000 Hz'
['Sinusoidal Setup String: ',sinusoid_setup]};
   dtstr=datestr(now, 'mmmm dd, yyyy HH:MM:SS.FFF AM');
   fsumh(1,2)={dtstr};
   fsumh(1,4)=num2cell(noise_amp);
   fsumh(3,1:10)={'Trial #' 'Detection Code' 'Increment' 'Amplitude' 'Peak
Acceleration' 'Reversals' 'Consecutive Reversals' 'Detection' 'Tekscan Filename'
'Peak Filename'};
   xlswrite(filenamesum,fsumh,'Sheet1','A1');
   xlswrite(filenamesum,avg_h,'AVG','A1');
```

```
end
%*****************************************

% Zero Baseline
% 5 to 15
for i = 5:COLs
   minitavg(i) = initavg(cop,i);
   msmoothdata(1:RAW_DATA_SIZE,i)=cop(1:RAW_DATA_SIZE,i)-sta_avg(i);
end
% Conversions

 % Load Cells
convdata(:,1:4) = cop(:,1:4);
% Position
convdata(:,5) = msmoothdata(:,5) .* pert;
% Acceleration
convdata(:,6) = msmoothdata(:,6) .* Accel_CF;
% Shear
convdata(:,7) = msmoothdata(:,7) .* Shear_CF;
% Touch
convdata(:,8) = msmoothdata(:,8);
% Head Accel X,Y,Z
convdata(:,9:11) = msmoothdata(:,9:11) .* Accel_CF;

% EMGs
% ALways keep EMGs at End so can easily expand the number
convdata(:,12:COLs) = abs(msmoothdata(:,12:COLs));

% Smoothing done after conversions to prevent roughening of data

smdat=filtfilt(SMOOTH_FILTER.tf.num,SMOOTH_FILTER.tf.den,convdata);


% Make Output Array
% Add milliseconds to first column

dat(1:RAW_DATA_SIZE,1) = (1:RAW_DATA_SIZE)';


% Add Position

dat(1:RAW_DATA_SIZE,2) = smdat(1:RAW_DATA_SIZE,5);

% Add differentiated velocity
```

```
temp(2:RAW_DATA_SIZE,7) = (smdat(2:RAW_DATA_SIZE,5)-
smdat(1:RAW_DATA_SIZE-1,5))./SAMPLING_RATE;

%  Smooth velocity
minitavg(COLs+1) = initavg(temp,7);
temp(2:RAW_DATA_SIZE,7) = temp(2:RAW_DATA_SIZE,7)-sta_avg(7);
dat(2:RAW_DATA_SIZE,3) =
filtfilt(SMOOTH_FILTER.tf.num,SMOOTH_FILTER.tf.den,temp(2:RAW_DATA_SI
ZE,7));


%  Add differentiated Acceleration

temp(3:RAW_DATA_SIZE,8) = (dat(3:RAW_DATA_SIZE,3)-
dat(2:RAW_DATA_SIZE-1,3))./SAMPLING_RATE;

% Smooth Acceleration
minitavg(COLs+2) = initavg(temp,8);
temp(3:RAW_DATA_SIZE,8) = temp(3:RAW_DATA_SIZE,8)-sta_avg(8);
dat(3:RAW_DATA_SIZE,4) =
filtfilt(SMOOTH_FILTER.tf.num,SMOOTH_FILTER.tf.den,temp(3:RAW_DATA_SI
ZE,8));

%  Add Acceleration
dat(1:RAW_DATA_SIZE,5) = smdat(1:RAW_DATA_SIZE,6);

temp(2:RAW_DATA_SIZE,5) = (dat(2:RAW_DATA_SIZE,5)-
dat(1:RAW_DATA_SIZE-1,5))./SAMPLING_RATE;
% Smooth Jerk
minitavg(COLs+3) = initavg(temp,5);
temp(2:RAW_DATA_SIZE,5) = temp(2:RAW_DATA_SIZE,5)-sta_avg(5);
dat(2:RAW_DATA_SIZE,6) =
filtfilt(SMOOTH_FILTER.tf.num,SMOOTH_FILTER.tf.den,temp(2:RAW_DATA_SI
ZE,5));


%  Shear
dat(1:RAW_DATA_SIZE,7) = smdat(1:RAW_DATA_SIZE,7);

%  Touch
dat(1:RAW_DATA_SIZE,8) = smdat(1:RAW_DATA_SIZE,8);
%  Add APCOP
%  Add APCOP Velocity
%  Add MLCOP
%  Add MLCOP Velocity
```

```
% 'Calculating COPs'
fpcal = calmod(cal);


[temp(:,13),temp(:,15),dat(:,9)] =
apmlcop(smdat(:,1),smdat(:,2),smdat(:,3),smdat(:,4),fpcal);

% 'APCOP & MLCOP'

for i=13:2:15
   minitavg(i-12) = initavg(temp,i);
   temp(1:RAW_DATA_SIZE,i) = temp(1:RAW_DATA_SIZE,i)-sta_avg(i-12);
   dat(1:RAW_DATA_SIZE,i-3) =
filtfilt(SMOOTH_FILTER.tf.num,SMOOTH_FILTER.tf.den,temp(1:RAW_DATA_SI
ZE,i));
end

temp(2:RAW_DATA_SIZE,14) = (dat(2:RAW_DATA_SIZE,10)-
dat(1:RAW_DATA_SIZE-1,10))./SAMPLING_RATE;
temp(2:RAW_DATA_SIZE,16) = (dat(2:RAW_DATA_SIZE,12)-
dat(1:RAW_DATA_SIZE-1,12))./SAMPLING_RATE;


for i= 14:2:16
   minitavg(i-12) = initavg(temp,i);
   temp(2:RAW_DATA_SIZE,i) = temp(2:RAW_DATA_SIZE,i)-sta_avg(i-12);
   dat(2:RAW_DATA_SIZE,i-3) =
filtfilt(SMOOTH_FILTER.tf.num,SMOOTH_FILTER.tf.den,temp(2:RAW_DATA_SI
ZE,i));
end

%  Head Accel X
%  Head Accel Y
%  Head Accel Z
for i = 14:16
   dat(1:RAW_DATA_SIZE,i) = smdat(1:RAW_DATA_SIZE,i-5);
end

%  ADD RMS EMG RTA
%  ADD RMS EMG RGS
%  ADD RMS EMG LTA
%  ADD RMS EMG LGS

dat(:,17)=smdat(:,12)./norm_EMG_COP(3,1);
dat(:,18)=smdat(:,13)./norm_EMG_COP(2,3);
dat(:,19)=smdat(:,14)./norm_EMG_COP(3,3);
```

```
dat(:,20)=smdat(:,15)./norm_EMG_COP(2,4);

dat(:,21:COLs+5)=smdat(:,16:COLs);

A=cell(1,COLs+5);

% Add Headings
%      1  2          3                4      5      6
A(1,1:20) = {'Time' 'Position' 'Diff velocity' 'Diff Accel' 'Accel' 'Diff jerk'...
   'Shear' 'Touch' 'MASS' 'APCOP' 'APCOP Vel' 'MLCOP' 'MLCOP Vel' 'Head
Accel X' 'Head Accel Y' 'Head Accel Z' 'RTA' 'LTA' 'RGS' 'LGS'};
%      7      8      9      10         11      12         13      14          15          16
17    18    19    20


if COLs > 15
   for i=16:COLs
      % Follows convention that Even number are on the right side
      if mod(i,2) == 0
         leftright='R';
      else
         leftright='L';
      end
      if i==16
         t_head='RSCM';
      elseif i==17
         t_head='LSCM';
      elseif i==18
         t_head='R Soleus';
      elseif i==19
         t_head='L Soleus';
      else
         t_head=['EMG', leftright, num2str(i-11)];
      end
      A(1,20+i-15)={t_head};
   end
end

%  Builds Cell Array for Spread Sheet
xlspread=cell(RAW_DATA_SIZE+1,COLs+5);
xlspread(1,1:COLs+5)=A(1,1:COLs+5);
xlspread(2:RAW_DATA_SIZE+1,1:COLs+5)=num2cell(dat);

%  Writes File
cd([Loc_Processed,subject,'\',subject,'_',trial,'\ENGRUNITS\']);
if (trialnum<10)
```

```
xlswrite([subject,'_',trial,'_',rawid,'_F',freq,'_0',num2str(trialnum)],xlspread,'Sheet1'
,'A1');
else

xlswrite([subject,'_',trial,'_',rawid,'_F',freq,'_',num2str(trialnum)],xlspread,'Sheet1','
A1');
end

%*******************************
%****Sum File Writer
%      Add Trial Information

fsumd=cell(1,10);
fsumd(1,1)=num2cell(trialnum);
fsumd(1,2:7)=num2cell(sumd(1:6));
switch sumd(1)
   case 0
      fsumd(1,8)={'HIT'};
   case 1
      fsumd(1,8)={'MISS'};
   case 2
      fsumd(1,8)={'FALSE ALARM'};
   case 3
      fsumd(1,8)={'CORRECT REJECTION'};
   case -1
      error('Bad Detection')
end
fsumd(1,9)={[subject,'_',trial,'_',rawid,num2str(sumd(7),'%04d')]};
fsumd(1,10)={[subject,'_',trial,'_',rawid,num2str(PEAK_NUM,'%04d')]};
xlswrite(filenamesum,fsumd,'Sheet1',['A',num2str(trialnum+3)]);
avgd=cell(1,COLs+4);
avgd(1,1)=num2cell(trialnum);
avgd(1,2:COLs+4)=num2cell(minitavg);
xlswrite(filenamesum,avgd,'AVG',['A',num2str(trialnum+2)]);
%*******************************

%*******************************
%*****Tekscan .fsx processing
tekdir=[Loc_Processed,subject,'\',subject,'_',trial,'\Tekscan\'];
[tekdat, feetcop,
pweight]=tekmat_processor([tekdir,subject,'_',trial,'_',rawid,num2str(sumd(7),'%0
4d')],1);
tekdat=[tekdat feetcop pweight];
tekspread=cell(size(tekdat,1)+1,size(tekdat,2)+1);
```

```
tekspread(1,:)={'Time' 'APCOP' 'MLCOP' 'RAPCOP' 'RMLCOP' 'LAPCOP'
'LMLCOP' '% Right Foot' '% Left Foot'};
tekspread(2:size(tekdat,1)+1,1)=num2cell(1/TEKSCAN_SAMP:1/TEKSCAN_SA
MP:size(tekdat,1)/TEKSCAN_SAMP);
tekspread(2:size(tekdat,1)+1,2:size(tekdat,2)+1)=num2cell(tekdat);
xlswrite([subject,'_',trial,'_',rawid,'_F',freq,'_',num2str(trialnum,'%02d')],tekspread,'
Tekscan','A1');
%*******************************

%****************************************
%****Tekscan Sum File
teksum=cell(1,2);
teksum(1,:)={[subject,'_',trial,'_',rawid,num2str(sumd(7),'%04d')] ['Threshold Trial
', num2str(trialnum),' at ', freq, ' Frequency']};
cd(tekdir);
xlswrite([subject,'_',trial,'_',rawid,'_tekscan_sum'],teksum,'Sheet1',['A',num2str(su
md(7)+1)]);
%****************************************

%  Clear workspace
clear smdat temp convdata tekdat leftright t_head msmoothdata cop sta_avg
subject rawid pert trial trialnum fsumd fsumct fsumc fsumh fsuml A xlspread

function dat =
lockchanger(subject,rawid,pert,trial,cop,cal,norm_EMG_COP,Freq,sumd,trialnum
,TEKSCAN_SAMP,PEAK_NUM)

% Setup so all EMGs are the last columns

Loc_Processed = 'E:\data\';
Accel_CF =1;
Shear_CF =-110;
load('SMOOTH_FILTER.mat');
SAMPLING_RATE  = 0.001;
[LOCK_DATA_SIZE,COLs]=size(cop);

%  Initializations
msmoothdata=zeros(LOCK_DATA_SIZE,COLs);
minitavg =zeros(1,COLs+3);
temp =zeros(LOCK_DATA_SIZE,16);
convdata=zeros(LOCK_DATA_SIZE,COLs);
dat =zeros(LOCK_DATA_SIZE,COLs+5);

%****Sum File Writer
%      Header Setup
```

```
filenamesum=[Loc_Processed,subject,'\',subject,'_',trial,'\ENGRUNITS\',subject,'_
',trial,'_',rawid,'_sum'];
if trialnum == 1
   avg_h=cell(1,COLs+4);
   avg_h(1,1:16) ={'Trial' 'APCOP' 'APCOPV' 'MLCOP' 'MLCOPV' 'Position'
'Acceleration' ...
              'Shear' 'Touch' 'Head Accel X' 'Head Accel Y' 'Head Accel Z' 'RTA'
'LTA' 'RGS' 'LGS'};
   if COLs > 15
      for i=16:COLs
         % Follows convention that Even number are on the right side
         if mod(i,2) == 0
            leftright='R';
         else
            leftright='L';
         end
         if i==16
            t_head='RSCM';
         elseif i==17
            t_head='LSCM';
         elseif i==18
            t_head='R Soleus';
         elseif i==19
            t_head='L Soleus';
         else
            t_head=['EMG', leftright, num2str(i-11)];
         end
         avg_h(1,i+1)={t_head};
      end
   end
   avg_h(1,COLs+2:COLs+4) = {'Diff velocity' 'Diff Accel' 'Diff jerk'};
   fsumh=cell(3,6);
   fsumh(1,1:5)={filenamesum ' ' 'Front' 'No Noise at Start' 'Sample Frequency =
1000 Hz'};
   dtstr=datestr(now, 'mmmm dd, yyyy HH:MM:SS.FFF AM');
   fsumh(1,2)={dtstr};
   fsumh(3,1:6)={'Trial #' Freq 'Amplitude' 'Peak Acceleration' 'Tekscan Filename'
'PEAK File Number'};
   xlswrite(filenamesum,fsumh,'Sheet1','A1');
   xlswrite(filenamesum,avg_h,'AVG','A1');

end
%************************************

%  Zero Baseline
for i = 5:COLs
```

```
   minitavg(i) = mean(cop(200:4200,i));
   msmoothdata(1:LOCK_DATA_SIZE,i)=cop(1:LOCK_DATA_SIZE,i)-
minitavg(i);
end

%  Conversions

 %  Load Cells
convdata(:,1:4) = cop(:,1:4);
%  Position
convdata(:,5) = msmoothdata(:,5) .* pert;
%  Acceleration
convdata(:,6) = msmoothdata(:,6) .* Accel_CF;
%  Shear
convdata(:,7) = msmoothdata(:,7) .* Shear_CF;
%  Touch
convdata(:,8) = msmoothdata(:,8);
%  Head Accel X,Y,Z
convdata(:,9:11) = msmoothdata(:,9:11) .* Accel_CF;

%  EMGs
% ALways keep EMGs at End so can easily expand the number
convdata(:,12:COLs) = abs(msmoothdata(:,12:COLs));

%  Smoothing done after conversions to prevent roughening of data

disp('Smoothing')
smdat=filtfilt(SMOOTH_FILTER.tf.num,SMOOTH_FILTER.tf.den,convdata);


%  Make Output Array
%  Add milliseconds to first column
dat(1:LOCK_DATA_SIZE,1) = (1:LOCK_DATA_SIZE)';

%  Add Position

dat(1:LOCK_DATA_SIZE,2) = smdat(1:LOCK_DATA_SIZE,5);

%  Add differentiated velocity

temp(2:LOCK_DATA_SIZE,7) = (smdat(2:LOCK_DATA_SIZE,5)-
smdat(1:LOCK_DATA_SIZE-1,5))./SAMPLING_RATE;

%  Smooth velocity
minitavg(COLs+1) = initavg(temp,7);
```

```
temp(2:LOCK_DATA_SIZE,7) = temp(2:LOCK_DATA_SIZE,7)-
minitavg(COLs+1);
dat(2:LOCK_DATA_SIZE,3) =
filtfilt(SMOOTH_FILTER.tf.num,SMOOTH_FILTER.tf.den,temp(2:LOCK_DATA_
SIZE,7));


%   Add differentiated Acceleration

temp(3:LOCK_DATA_SIZE,8) = (dat(3:LOCK_DATA_SIZE,3)-
dat(2:LOCK_DATA_SIZE-1,3))./SAMPLING_RATE;

% Smooth Acceleration
minitavg(COLs+2) = initavg(temp,8);
temp(3:LOCK_DATA_SIZE,8) = temp(3:LOCK_DATA_SIZE,8)-
minitavg(COLs+2);
dat(3:LOCK_DATA_SIZE,4) =
filtfilt(SMOOTH_FILTER.tf.num,SMOOTH_FILTER.tf.den,temp(3:LOCK_DATA_
SIZE,8));

disp('Accelerating')
%   Add Acceleration
dat(1:LOCK_DATA_SIZE,5) = smdat(1:LOCK_DATA_SIZE,6);
%   Add Differentiated Jerk


temp(2:LOCK_DATA_SIZE,5) = (dat(2:LOCK_DATA_SIZE,5)-
dat(1:LOCK_DATA_SIZE-1,5))./SAMPLING_RATE;
% Smooth Differentiated Jerk
minitavg(COLs+3) = initavg(temp,5);
temp(2:LOCK_DATA_SIZE,5) = temp(2:LOCK_DATA_SIZE,5)-
minitavg(COLs+3);
dat(2:LOCK_DATA_SIZE,6) =
filtfilt(SMOOTH_FILTER.tf.num,SMOOTH_FILTER.tf.den,temp(2:LOCK_DATA_
SIZE,5));


%   Shear
dat(1:LOCK_DATA_SIZE,7) = smdat(1:LOCK_DATA_SIZE,7);

%   Touch
dat(1:LOCK_DATA_SIZE,8) = smdat(1:LOCK_DATA_SIZE,8);
%   Add APCOP
%   Add APCOP Velocity
%   Add MLCOP
%   Add MLCOP Velocity
```

```
% 'Calculating COPs'
fpcal = calmod(cal);

[temp(:,13),temp(:,15),dat(:,9)] =
apmlcop(smdat(:,1),smdat(:,2),smdat(:,3),smdat(:,4),fpcal);

% 'APCOP & MLCOP'

for i=13:2:15
   minitavg(i-12) = mean(temp(:,i));
   temp(1:LOCK_DATA_SIZE,i) = temp(1:LOCK_DATA_SIZE,i)-minitavg(i-12);
   dat(1:LOCK_DATA_SIZE,i-4) =
filtfilt(SMOOTH_FILTER.tf.num,SMOOTH_FILTER.tf.den,temp(1:LOCK_DATA_
SIZE,i));
end

temp(2:LOCK_DATA_SIZE,14) = (dat(2:LOCK_DATA_SIZE,9)-
dat(1:LOCK_DATA_SIZE-1,9))./SAMPLING_RATE;
temp(2:LOCK_DATA_SIZE,16) = (dat(2:LOCK_DATA_SIZE,11)-
dat(1:LOCK_DATA_SIZE-1,11))./SAMPLING_RATE;


for i= 14:2:16
   minitavg(i-12) = mean(temp(:,i));
   temp(2:LOCK_DATA_SIZE,i) = temp(2:LOCK_DATA_SIZE,i)-minitavg(i-12);
   dat(2:LOCK_DATA_SIZE,i-4) =
filtfilt(SMOOTH_FILTER.tf.num,SMOOTH_FILTER.tf.den,temp(2:LOCK_DATA_
SIZE,i));
end

%  Head Accel X
%  Head Accel Y
%  Head Accel Z
for i = 14:16
   dat(1:LOCK_DATA_SIZE,i) = smdat(1:LOCK_DATA_SIZE,i-5);
end

%  ADD RMS EMG RTA
%  ADD RMS EMG RGS
%  ADD RMS EMG LTA
%  ADD RMS EMG LGS

dat(:,17)=smdat(:,12)./norm_EMG_COP(3,1);
dat(:,18)=smdat(:,13)./norm_EMG_COP(2,3);
dat(:,19)=smdat(:,14)./norm_EMG_COP(3,3);
```

```
dat(:,20)=smdat(:,15)./norm_EMG_COP(2,4);
dat(:,21:COLs+5)=smdat(:,16:COLs);

A=cell(1,COLs+5);

% Add Headings
%      1  2         3                4      5      6
A(1,1:20) = {'Time' 'Position' 'Diff velocity' 'Diff Accel' 'Accel' 'Diff jerk'...
   'Shear' 'Touch' 'MASS' 'APCOP' 'APCOP Vel' 'MLCOP' 'MLCOP Vel' 'Head
Accel X' 'Head Accel Y' 'Head Accel Z' 'RTA' 'LTA' 'RGS' 'LGS'};
%      7      8      9      10         11      12         13      14          15          16
17    18    19    20


if COLs > 15
   for i=16:COLs
      % Follows convention that Even number are on the right side
      if mod(i,2) == 0
         leftright='R';
      else
         leftright='L';
      end
      if i==16
         t_head='RSCM';
      elseif i==17
         t_head='LSCM';
      elseif i==18
         t_head='R Soleus';
      elseif i==19
         t_head='L Soleus';
      else
         t_head=['EMG', leftright, num2str(i-11)];
      end
      A(1,20+i-15)={t_head};
   end
end


cd([Loc_Processed,subject,'\',subject,'_',trial,'\ENGRUNITS\']);
save([subject,'_',trial,'_',rawid,'_',Freq,'_sta'],'dat');

for i=1:(LOCK_DATA_SIZE-5000)/60000+1
   if i == 1
      xlspread=cell(5000+1,COLs+5);
      xlspread(1,1:COLs+5)=A(1,1:COLs+5);
      xlspread(2:5000+1,1:COLs+5)=num2cell(dat(1:5000,:));
```

```
   else
      xlspread=cell(60000+1,COLs+5);
      xlspread(1,1:COLs+5)=A(1,1:COLs+5);
      xlspread(2:60000+1,1:COLs+5)=num2cell(dat(5001+60000*(i-
2):65000+60000*(i-2),:));
   end
   %  Writes File

xlswrite([subject,'_',trial,'_',rawid,'_',Freq,'_sta'],xlspread,['Sheet',num2str(i)],'A1');
   clear xlspread

end

%*********************************
%****Sum File Writer
%      Add Trial Information
fsumd=cell(1,6);
fsumd(1,1)=num2cell(trialnum);
fsumd(1,2)={Freq};
fsumd(1,3:4)=num2cell(sumd(1:2));
fsumd(1,5)={[subject,'_',trial,'_',strrep(rawid,'_lock',''),num2str(sumd(3),'%04d')]};
fsumd(1,6)={[subject,'_',trial,'_',strrep(rawid,'_lock',''),num2str(PEAK_NUM,'%04d'
)]};
xlswrite(filenamesum,fsumd,'Sheet1',['A',num2str(trialnum+3)]);
avgd=cell(1,COLs+4);
avgd(1,1)=num2cell(trialnum);
avgd(1,2:COLs+4)=num2cell(minitavg);
xlswrite(filenamesum,avgd,'AVG',['A',num2str(trialnum+1)]);
%*********************************

%*********************************
%*****Tekscan .fsx processing
tekdir=[Loc_Processed,subject,'\',subject,'_',trial,'\Tekscan\'];
[tekdat, feetcop,
pweight]=tekmat_processor([tekdir,subject,'_',trial,'_',strrep(rawid,'_lock',''),num2s
tr(sumd(3),'%04d')],1);
tekdat=[tekdat feetcop pweight];
tekspread=cell(size(tekdat,1)+1,size(tekdat,2)+1);
tekspread(1,:)={'Time' 'APCOP' 'MLCOP' 'RAPCOP' 'RMLCOP' 'LAPCOP'
'LMLCOP' '% Right Foot' '% Left Foot'};
tekspread(2:size(tekdat,1)+1,1)=num2cell(1/TEKSCAN_SAMP:1/TEKSCAN_SA
MP:size(tekdat,1)/TEKSCAN_SAMP);
tekspread(2:size(tekdat,1)+1,2:size(tekdat,2)+1)=num2cell(tekdat);
xlswrite([subject,'_',trial,'_',rawid,'_',Freq,'_sta'],tekspread,'Tekscan','A1');
%*********************************
```

```
%****************************************
%****Tekscan Sum File
teksum=cell(1,2);
teksum(1,:)={[subject,'_',trial,'_',strrep(rawid,'_lock',''),num2str(sumd(3),'%04d')]
['Threshold Trial ', num2str(trialnum),' at ', Freq, ' Frequency']};
cd(tekdir);
xlswrite([subject,'_',trial,'_',strrep(rawid,'_lock',''),'_tekscan_sum'],teksum,'Sheet1',
['A',num2str(sumd(3)+1)]);
%****************************************

clear smdat convdata msmoothdata temp cop A trial subject rawid
clear Loc_Processed Accel_CF Shear_CF LOCK_DATA_SIZE
clear SMOOTH_FILTER SAMPLING_RATE i leftright t_head

function [minitavg,dat] =
stachanger(subject,rawid,pert,trial,cop,cal,norm_EMG_COP,Freq,teknum,TEKS
CAN_SAMP)

Loc_Processed = 'E:\data\';
Accel_CF =1;
Shear_CF =-110;
load('SMOOTH_FILTER.mat');
SAMPLING_RATE  = 0.001;
[STA_DATA_SIZE,COLs]=size(cop);

%  Initializations
msmoothdata=zeros(STA_DATA_SIZE,COLs);
minitavg =zeros(1,1:18);
temp =zeros(STA_DATA_SIZE,16);
convdata=zeros(STA_DATA_SIZE,COLs);
dat =zeros(STA_DATA_SIZE,COLs+5);

%  Zero Baseline
for i = 5:COLs
   minitavg(i) = mean(cop(:,i));
   msmoothdata(1:STA_DATA_SIZE,i)=cop(1:STA_DATA_SIZE,i)-minitavg(i);
end

%  Conversions

 %  Load Cells
convdata(:,1:4) = cop(:,1:4);
%  Position
convdata(:,5) = msmoothdata(:,5) .* pert;
%  Acceleration
convdata(:,6) = msmoothdata(:,6) .* Accel_CF;
```

```
% Shear
convdata(:,7) = msmoothdata(:,7) .* Shear_CF;
% Touch
convdata(:,8) = msmoothdata(:,8);
% Head Accel X,Y,Z
convdata(:,9:11) = msmoothdata(:,9:11) .* Accel_CF;

% EMGs
% ALways keep EMGs at End so can easily expand the number
convdata(:,12:COLs) = abs(msmoothdata(:,12:COLs));

% Smoothing done after conversions to prevent roughening of data

smdat=filtfilt(SMOOTH_FILTER.tf.num,SMOOTH_FILTER.tf.den,convdata);


% Make Output Array
% Add milliseconds to first column
dat(1:STA_DATA_SIZE,1) = (1:STA_DATA_SIZE)';

% Add Position

dat(1:STA_DATA_SIZE,2) = smdat(1:STA_DATA_SIZE,5);

% Add differentiated velocity

temp(2:STA_DATA_SIZE,7) = (smdat(2:STA_DATA_SIZE,5)-
smdat(1:STA_DATA_SIZE-1,5))./SAMPLING_RATE;

% Smooth velocity
minitavg(COLs+1) = initavg(temp,7);
temp(2:STA_DATA_SIZE,7) = temp(2:STA_DATA_SIZE,7)-minitavg(COLs+1);
dat(2:STA_DATA_SIZE,3) =
filtfilt(SMOOTH_FILTER.tf.num,SMOOTH_FILTER.tf.den,temp(2:STA_DATA_SI
ZE,7));


% Add differentiated Acceleration

temp(3:STA_DATA_SIZE,8) = (dat(3:STA_DATA_SIZE,3)-
dat(2:STA_DATA_SIZE-1,3))./SAMPLING_RATE;

% Smooth Acceleration
minitavg(COLs+2) = initavg(temp,8);
temp(3:STA_DATA_SIZE,8) = temp(3:STA_DATA_SIZE,8)-minitavg(COLs+2);
```

```
dat(3:STA_DATA_SIZE,4) =
filtfilt(SMOOTH_FILTER.tf.num,SMOOTH_FILTER.tf.den,temp(3:STA_DATA_SI
ZE,8));


%  Add Acceleration
dat(1:STA_DATA_SIZE,5) = smdat(1:STA_DATA_SIZE,6);
%  Add Differentiated Jerk


temp(2:STA_DATA_SIZE,5) = (dat(2:STA_DATA_SIZE,5)-
dat(1:STA_DATA_SIZE-1,5))./SAMPLING_RATE;
% Smooth Differentiated Jerk
minitavg(COLs+3) = initavg(temp,5);
temp(2:STA_DATA_SIZE,5) = temp(2:STA_DATA_SIZE,5)-minitavg(COLs+3);
dat(2:STA_DATA_SIZE,6) =
filtfilt(SMOOTH_FILTER.tf.num,SMOOTH_FILTER.tf.den,temp(2:STA_DATA_SI
ZE,5));


%  Shear
dat(1:STA_DATA_SIZE,7) = smdat(1:STA_DATA_SIZE,7);

%  Touch
dat(1:STA_DATA_SIZE,8) = smdat(1:STA_DATA_SIZE,8);
%  Add APCOP
%  Add APCOP Velocity
%  Add MLCOP
%  Add MLCOP Velocity

% 'Calculating COPs'
fpcal = calmod(cal);

[temp(:,13),temp(:,15),dat(:,9)] =
apmlcop(smdat(:,1),smdat(:,2),smdat(:,3),smdat(:,4),fpcal);

% 'APCOP & MLCOP'

for i=13:2:15
   minitavg(i-12) = mean(temp(:,i));
   temp(1:STA_DATA_SIZE,i) = temp(1:STA_DATA_SIZE,i)-minitavg(i-12);
   dat(1:STA_DATA_SIZE,i-4) =
filtfilt(SMOOTH_FILTER.tf.num,SMOOTH_FILTER.tf.den,temp(1:STA_DATA_SI
ZE,i));
end
```

```
temp(2:STA_DATA_SIZE,14) = (dat(2:STA_DATA_SIZE,9)-
dat(1:STA_DATA_SIZE-1,9))./SAMPLING_RATE;
temp(2:STA_DATA_SIZE,16) = (dat(2:STA_DATA_SIZE,11)-
dat(1:STA_DATA_SIZE-1,11))./SAMPLING_RATE;


for i= 14:2:16
   minitavg(i-12) = mean(temp(:,i));
   temp(2:STA_DATA_SIZE,i) = temp(2:STA_DATA_SIZE,i)-minitavg(i-12);
   dat(2:STA_DATA_SIZE,i-4) =
filtfilt(SMOOTH_FILTER.tf.num,SMOOTH_FILTER.tf.den,temp(2:STA_DATA_SI
ZE,i));
end

%  Head Accel X
%  Head Accel Y
%  Head Accel Z
for i = 14:16
   dat(1:STA_DATA_SIZE,i) = smdat(1:STA_DATA_SIZE,i-5);
end

%  ADD RMS EMG RTA
%  ADD RMS EMG RGS
%  ADD RMS EMG LTA
%  ADD RMS EMG LGS

dat(:,17)=smdat(:,12)./norm_EMG_COP(3,1);
dat(:,18)=smdat(:,13)./norm_EMG_COP(2,3);
dat(:,19)=smdat(:,14)./norm_EMG_COP(3,3);
dat(:,20)=smdat(:,15)./norm_EMG_COP(2,4);

dat(:,21:COLs+5)=smdat(:,16:COLs);

A=cell(1,COLs+5);

% Add Headings
%     1  2        3                4     5     6
A(1,1:20) = {'Time' 'Position' 'Diff velocity' 'Diff Accel' 'Accel' 'Diff jerk'...
   'Shear' 'Touch' 'MASS' 'APCOP' 'APCOP Vel' 'MLCOP' 'MLCOP Vel' 'Head
Accel X' 'Head Accel Y' 'Head Accel Z' 'RTA' 'LTA' 'RGS' 'LGS'};
%     7     8     9     10        11     12        13     14        15        16
17   18   19   20


if COLs > 15
   for i=16:COLs
```

```
        % Follows convention that Even number are on the right side
        if mod(i,2) == 0
           leftright='R';
        else
           leftright='L';
        end
        if i==16
           t_head='RSCM';
        elseif i==17
           t_head='LSCM';
        elseif i==18
           t_head='R Soleus';
        elseif i==19
           t_head='L Soleus';
        else
           t_head=['EMG', leftright, num2str(i-11)];
        end
        A(1,20+i-15)={t_head};
    end
end
xlspread=cell(STA_DATA_SIZE+1,COLs+5);
xlspread(1,1:COLs+5)=A(1,1:COLs+5);
xlspread(2:STA_DATA_SIZE+1,1:COLs+5)=num2cell(dat);

%   Writes File
cd([Loc_Processed,subject,'\',subject,'_',trial,'\ENGRUNITS\']);
xlswrite([subject,'_',trial,'_',rawid,'_',Freq,'_sta'],xlspread,'Sheet1','A1');

%*********************************
%*****Tekscan .fsx processing
tekdir=[Loc_Processed,subject,'\',subject,'_',trial,'\Tekscan\'];
[tekdat, feetcop,
pweight]=tekmat_processor([tekdir,subject,'_',trial,'_',strrep(rawid,'_QS',''),num2st
r(teknum,'%04d')],1);
tekdat=[tekdat feetcop pweight];
tekspread=cell(size(tekdat,1)+1,size(tekdat,2)+1);
tekspread(1,:)={'Time' 'APCOP' 'MLCOP' 'RAPCOP' 'RMLCOP' 'LAPCOP'
'LMLCOP' '% Right Foot' '% Left Foot'};
tekspread(2:size(tekdat,1)+1,1)=num2cell(1/TEKSCAN_SAMP:1/TEKSCAN_SA
MP:size(tekdat,1)/TEKSCAN_SAMP);
tekspread(2:size(tekdat,1)+1,2:size(tekdat,2)+1)=num2cell(tekdat);
xlswrite([subject,'_',trial,'_',rawid,'_',Freq, '_sta'],tekspread,'Tekscan','A1');
%*********************************

%****************************************
%****Tekscan Sum File
```

```
teksum=cell(1,2);
teksum(1,:)={[subject,'_',trial,'_',strrep(rawid,'_QS',''),num2str(teknum,'%04d')]
['QS Trial for ', Freq, ' Frequency']};
cd(tekdir);
xlswrite([subject,'_',trial,'_',strrep(rawid,'_QS',''),'_tekscan_sum'],teksum,'Sheet1',[
'A',num2str(teknum+1)]);
%****************************************

clear smdat convdata msmoothdata temp cop A trial subject rawid
clear Loc_Processed Accel_CF Shear_CF STA_DATA_SIZE
clear SMOOTH_FILTER SAMPLING_RATE xlspread t_head leftright

function [APCOP,MLCOP,mass] = apmlcop(l1,l2,l3,l4,fpcal)

%calculating Ap-COP and Ml-COP
        FP1=l1-fpcal(1);
        FP2=l2-fpcal(2);
        FP3=l3-fpcal(3);
        FP4=l4-fpcal(4);
        %Calculate AP and ML COP
        wght = FP3+FP4+FP1+FP2;  %in volts

        %   209.55 mm  174.625 mm

        APCOP=209.55*(FP3+FP4-FP1-FP2)./wght;

        % To the left is Positive
        MLCOP=174.625*(FP1+FP4-FP3-FP2)./wght;

        %  Conversion factor is linear
        %      (Sum of fpcal [Volts])/13.95 kg(mass of plate)

%          COnverted in Labview
        %cnvfact=-39.92;

        mass=wght;  %  wght is in Volts
                    %  cnvfact is -39.92KG/V

%Get cal values

    function f = calmod(CAL)

      %calculates the calibration
      mcal=mean(CAL(.10*length(CAL):.90*length(CAL),:));
      %Plate Weight is substracted from the calibration values
      f=mcal(1:4);%+.25*.347; %platewt 13.95kg = .347V
```

```
    clear mcal;

% Calculates the initial average
%     By averaging first 180 Data points
function a = initavg(d,i)
   % d is array
   % i is column of data (type)
   a = mean(d(200:3600,i));

function peak_Freq = peak_freq_det(subject,rawid,trial,dat,peak_num)

% Beginning of sway_frequency code
Loc_Processed = 'E:\data\';

freq_spec = figure;

STA_DATA_SIZE = size(dat,1);

i=1;
while 2^i < STA_DATA_SIZE
n=2^i;
i=i+1;
end

Upper_Freq_Limit=1;
Lower_Freq_Limit=.1;

m=n/2;
fs=1000;
fc=fs/2;
f = fc * (0:m)/m;

i=1;
while f(i) < Lower_Freq_Limit
   Hzp10=i;
   i=i+1;
end

while f(i) < Upper_Freq_Limit
   Hz2p5=i;
   i=i+1;
end

tot_pow=sum(dat(1:STA_DATA_SIZE,10).^2);
APCOPF=fft(dat(1:STA_DATA_SIZE,10),n);
PAPCOPF=APCOPF.*conj(APCOPF) / n;
```

```
PAPCOPF=20.*log10(PAPCOPF/max(PAPCOPF(Hzp10:Hz2p5)));


PAPCOPF(m+2:n) = [ ];
PAPCOPF(2:m+1) = 2*PAPCOPF(2:m+1);
plot(f(Hzp10:Hz2p5),PAPCOPF(Hzp10:Hz2p5),'Marker','o')

thresh = -30; %Threshold for detection of peaks


%  Summary (sum total and number) of all detected, to calculate average
mxtot=0;
nn=0;

peak_Freq = [];
peak_a = [];
peak_b = [];

for i = 1:peak_num

   mx = max(PAPCOPF(Hzp10:Hz2p5)); % find max value of entire array

   if mx>thresh

      % find max position
      [c]=find(PAPCOPF(Hzp10:Hz2p5)==mx);
      c=c(1);

      %Update summary info
      mxtot=mxtot+f(c+Hzp10-1);
      nn=nn+1;

      peak_Freq = [peak_Freq; f(c+Hzp10-1)];

      temp_a = [f(c+Hzp10-1); mx];

      peak_a = [peak_a temp_a];

      temp_b = [f(c+Hzp10-1) mx];

      peak_b = [peak_b temp_b];

      L_OK = 1;
      R_OK = 1;
      L_x = c+Hzp10-1;
      R_x = c+Hzp10;
```

```
        PAPCOPF(c+Hzp10-1)=thresh;
        old_l=mx;

        if c+Hzp10-1<=Hzp10
           L_OK=0;
        end
        old_r=mx;
        if c+Hzp10-1>=Hz2p5
           R_OK=0;
        end


        while L_OK
           if PAPCOPF(L_x) <= old_l
              old_l =PAPCOPF(L_x);
              PAPCOPF(L_x)=thresh;
              L_x=L_x-1;
           else
              L_OK =0;
           end
           if L_x<=Hzp10
              L_OK =0;
           end
        end

        while R_OK
           if PAPCOPF(R_x) <= old_r
              old_r =PAPCOPF(R_x);
              PAPCOPF(R_x)=thresh;
              R_x=R_x+1;
           else
              R_OK =0;
           end
           if R_x>=Hz2p5
              R_OK =0;
           end
        end

        % Mark peak with asterick
        text('position',[(f(Hz2p5)*c/Hz2p5+f(3)) mx],'fontsize',24,'string','*')

%       else
%          OK =0; %no peak above threshold
     end
end
```

```
if ~isempty(peak_a)

   %label line with the value
   text('position',[.11 0],'string',...
      ['Threshold=' num2str(thresh,2)],...
      'verticalalignment','top')
   text('position',[.11 -20],'string',...
      ['Total Power=' num2str(tot_pow,'%-8.2e\n')],...
      'verticalalignment','top')
   title([subject,rawid,' QS Frequency Power'])
   xlabel ('Frequency (Hz)')
   ylabel ('Power (dB)')
   set(gca,'XScale','log')

   str_arr_f = cell(size(peak_a,2)+1,1);
   str_arr_f(1)=cellstr('Frequency (Hz)');
   str_arr_f(2:size(peak_a,2)+1) = cellstr(num2str(peak_a(1,:)'));
   text(0.3981,peak_a(2,1),str_arr_f,'verticalalignment','top')

   str_arr_p = cell(size(peak_a,2)+1,1);
   str_arr_p(1)=cellstr('Power (dB)');
   str_arr_p(2:size(peak_a,2)+1) = cellstr(num2str(peak_a(2,:)'));
   text(0.6918,peak_a(2,1),str_arr_p,'verticalalignment','top')

   axis([Lower_Freq_Limit Upper_Freq_Limit -100 0])

   drawnow

   cd([Loc_Processed,subject,'\',subject,'_',trial,'\ENGRUNITS\']);
   saveas(freq_spec,[subject,'_',trial,'_',rawid,'_freq_spec_dB.jpg']);
   saveas(freq_spec,[subject,'_',trial,'_',rawid,'_freq_spec_dB.emf']);
   hgsave(freq_spec,[subject,'_',trial,'_',rawid,'_freq_spec_dB']);
   xlspread=cell(2,2+2*peak_num);
   xlspread(1,1:4)={'Total Power' 'Threshold' 'freq' 'peak'};
   xlspread(2,1:(2+length(peak_b)))=num2cell([tot_pow thresh peak_b]);
   xlswrite([subject,'_',trial,'_',rawid,'_freq_spec_dB.xls'],xlspread,'Sheet1','A1');
else
   xlspread=cell(2,3);
   xlspread(1,:)={'Threshold' 'Max Peak' 'Total Power'};
   xlspread(2,:)=num2cell([thresh max(PAPCOPF(Hzp10:Hz2p5)) tot_pow]);
   xlswrite([subject,'_',trial,'_',rawid,'_freq_spec_dB.xls'],xlspread,'Sheet1','A1');
end

close(freq_spec)
while length(peak_Freq) < peak_num
   peak_Freq = [peak_Freq; -1];
```

```
end

clear header pert thresh PAPCOPF APCOP APCOPF peak_a peak_b dat
subject trial rawid tot_pow str_arr_p str_arr_f f

function QSmetrics(subject,rawid,trial,move,row,dat)

Loc_Processed = 'E:\data\';

APCOP = dat(:,10);
MLCOP = dat(:,12);

%calculate resultant distance
rd=sqrt(APCOP.^2+MLCOP.^2);
mdist=sum(rd)/(length(rd));
mdistap=sum(abs(APCOP))/(length(APCOP));
mdistml=sum(abs(MLCOP))/(length(MLCOP));

%calculate rms distance from mean cop
rdist=sqrt((sum(rd.*rd))/(length(rd)));
rdistap=sqrt((sum(APCOP.*APCOP))/(length(APCOP)));
rdistml=sqrt((sum(MLCOP.*MLCOP))/(length(MLCOP)));

%calculation of total excursion
m=length(APCOP)-1;
totex=sum(sqrt(((APCOP(2:m+1)-APCOP(1:m)).^2)+((MLCOP(2:m+1)-
MLCOP(1:m)).^2)));
totexap=sum(abs(APCOP(2:m+1)-APCOP(1:m)));
totexml=sum(abs(MLCOP(2:m+1)-MLCOP(1:m)));

%calculate mean velocity
mvelo=totex/(length(APCOP)/1000);
mveloap=totexap/(length(APCOP)/1000);
mveloml=totexml/(length(APCOP)/1000);

%calculate mean, standard deviation and range of COP's
meanrd=mean(rd);
rng=range(rd);
meanap=mean(APCOP);
meanml=mean(MLCOP);
stddevrd=std(rd);
stddevap=std(APCOP);
stddevml=std(MLCOP);
rngap=range(APCOP);
rngml=range(MLCOP);
```

```
%calculate the 95% confedence circle area
areacc=pi*(mdist+1.645*(sqrt(rdist^2-mdist^2)))^2;

%calculate the 95% confidence ellipse area
stddevapml=(sum(APCOP.*MLCOP))/(length(APCOP));
areace=2*pi*3*(sqrt(stddevap^2*stddevml^2-stddevapml^2));

%calculate the sway area
n=length(APCOP)-1;
areasway=sum(abs((APCOP(2:n+1).*MLCOP(1:n))-
(MLCOP(2:n+1).*APCOP(1:n))))/(2*length(APCOP)/1000);

%calculate mean frequency
mfreq=mvelo/(2*pi*mdist);
mfreqml=mveloml/(4*sqrt(2)*mdistml);
mfreqap=mveloap/(4*sqrt(2)*mdistap);

%calculate fractal dimension based on 95% Confidence Circle
dcc=2*(mdist+(1.645*(sqrt(rdist^2-mdist^2))));
FD_cc=log10(length(APCOP))/log10((length(APCOP)*dcc)/totex);

%calculate fractal dimension based on 95% Confidence Ellipse
dce=sqrt(8*3*sqrt(stddevap^2*stddevml^2-stddevapml^2));
FD_ce=log10(length(APCOP))/log10((length(APCOP)*dce)/totex);

% Frequency domain calculations using Multitaper method
% Calculates total power for each
i=7;
while length(APCOP)>2^i
   i=i+1;
end
nfft=2^i;
m=n/2;
fs=1000;
fc=fs/2;
f = fc * [0:m]/m;
df=f(2);
LPS=6; % for 0.15 Hz cutoff for analysis
HPS=164; %for 5Hz cutoff for Analysis
% [G,w]=pmtm(rd,4.5,nfft,fs);
% [Gap,w]=pmtm(APCOP,4.5,nfft,fs);
% [Gml,w]=pmtm(MLCOP,4.5,nfft,fs);

MLCOPF=fft(MLCOP,n);
Gml=MLCOPF.*conj(MLCOPF) / n;
```

```
APCOPF=fft(APCOP,n);
Gap=APCOPF.*conj(APCOPF) / n;

rdF=fft(rd,n);
G=rdF.*conj(rdF) / n;

power=sum(G(LPS:HPS));
powerap=sum(Gap(LPS:HPS));
powerml=sum(Gml(LPS:HPS));
% powerap=sum(APCOP.^2);
% powerml=sum(MLCOP.^2);
%calculates 50% power for each
pfreq50=f(2)*find(cumsum(G(LPS:HPS))>=power*0.5,1,'first');
pfreq50ap=f(2)*find(cumsum(Gap(LPS:HPS))>=powerap*0.5,1,'first');
pfreq50ml=f(2)*find(cumsum(Gml(LPS:HPS))>=powerml*0.5,1,'first');
%calculates 95% power for each
pfreq95=f(2)*find(cumsum(G(LPS:HPS))>=power*0.95,1,'first');
pfreq95ap=f(2)*find(cumsum(Gap(LPS:HPS))>=powerap*0.95,1,'first');
pfreq95ml=f(2)*find(cumsum(Gml(LPS:HPS))>=powerml*0.95,1,'first');
%Calculates centroidal frequency
cfreq=(sum((((LPS:HPS)*df).^2).*G(LPS:HPS)')/power).^0.5;
cfreqap=(sum((((LPS:HPS).*df).^2).*Gap(LPS:HPS)')/powerap).^0.5;
cfreqml=(sum((((LPS:HPS).*df).^2).*Gml(LPS:HPS)')/powerml).^0.5;
%calculates frequency dispersion
freqd=(1-
sum(((LPS:HPS).*df).*G(LPS:HPS)')^2/(power*sum((((LPS:HPS).*df).^2).*G(LPS
:HPS)')))^0.5;
freqdap=(1-
sum(((LPS:HPS).*df).*Gap(LPS:HPS)')^2/(powerap*sum((((LPS:HPS).*df).^2).*G
ap(LPS:HPS)')))^0.5;
freqdml=(1-
sum(((LPS:HPS).*df).*Gml(LPS:HPS)')^2/(powerml*sum((((LPS:HPS).*df).^2).*G
ml(LPS:HPS)')))^0.5;


%   1    2     3      4        5    6    7    8
%                                          9    10     11      12  13
14      15   16      17    18     19    20    21    22     23     24    25
26        27   28    29    30    31  32     33    34      35       36
37      38      39      40   41      42     43   44     45
output = { move meanrd  meanap meanml stddevrd stddevap stddevml rng rngap
rngml mdist mdistap mdistml rdist rdistap rdistml totex totexap totexml mvelo
mveloap mveloml mfreq mfreqap mfreqml areacc areasway areace FD_cc
FD_ce power powerap powerml pfreq50 pfreq50ap pfreq50ml pfreq95 pfreq95ap
pfreq95ml cfreq cfreqap cfreqml freqd freqdap freqdml};
cd([Loc_Processed,subject,'\',subject,'_',trial,'\ENGRUNITS\']);
```

```
if row==2
   H = {'Move' 'meanrd' 'meanap' 'meanml' 'stddevrd' 'stddevap' 'stddevml' 'rng'
'rngap' 'rngml' 'mdist' 'mdistap' 'mdistml' 'rdist' 'rdistap' 'rdistml' 'totex' 'totexap'
'totexml' 'mvelo' 'mveloap' 'mveloml' 'mfreq' 'mfreqap' 'mfreqml' 'areacc'
'areasway' 'areace' 'FD_cc' 'FD_ce' 'power' 'powerap' 'powerml' 'pfreq50'
'pfreq50ap' 'pfreq50ml' 'pfreq95' 'pfreq95ap' 'pfreq95ml' 'cfreq' 'cfreqap' 'cfreqml'
'freqd' 'freqdap' 'freqdml'};
   xlswrite([subject,'_',trial,'_',rawid,'_metrics.xls'],H,'Sheet1','A1:AS1');
end
xlswrite([subject,'_',trial,'_',rawid,'_metrics.xls'],output,'Sheet1',['A',row,':AS',row]);

clear

function [dat, feetcop, pweight]=tekmat_processor(filename,calflag)

X_ML=1;
Y_AP=2;
calflag=calflag*0;
%Note: this loadfsx2 is modified from the original to store data in 3d
%   array
[ m_data, m_Rows, m_Cols, m_frame] = loadfsx2( [filename,'.fsx'], calflag);

% Saves Raw Data
rm_data=m_data;

%*********************************************************
%   Remove Saturated frames and interpolate
if isempty(find(m_data>254,1))
   badr=[];
else
   badr=find(histc(floor((find(m_data>254)-
1)./(m_Rows*m_Cols))+1,0.5:size(m_data,3)+0.5));
end

if ~isempty(badr)
   i=0;

   %   Eliminates Bad Frames at beginning
   if badr(1) == 1
      i=i+1;
      j=0;
      while badr(i+j)+1 == badr(i+j+1)
         j=j+1;
      end
      for c=i:i+j
         m_data(:,:,c)=m_data(:,:,i+j+1);
```

```
      end
      i=i+j;
   end

   % Eliminates bad frames at end
   if badr(length(badr)) == size(m_data,3)
      j=length(badr);
      while badr(j)-1 == badr(j-1)
         j=j-1;
      end
      for c=length(badr):-1:j
         m_data(:,:,badr(c))=m_data(:,:,badr(j)-1);
      end
      badr=badr(1:j-1);
   end

   while i < length(badr)
      i=i+1;
      %  Eliminates other bad frames
      j=0;
      flg_badc=1;
      while i+j<length(badr) && flg_badc
         if badr(i+j)+1 == badr(i+j+1)
            flg_badc=1;
            j=j+1;
         else
            flg_badc=0;
         end
      end

      for c=i:i+j
         m_data(:,:,badr(c))=(m_data(:,:,badr(i)-1)*(i+j-
c+1)+m_data(:,:,badr(i+j)+1)*(c-i+1))./(j+2);
      end
      i=i+j;
   end
end

%*******************************************************

%*******************************************************
% Eliminate stray cells
%_____________________________________________
%|_17|_11|_____________3_____________|_19|_25|
%|_16|_10|_____________2_____________|_18|_24|
%|  |  |                |  |  |
```

```
%| 7 | 6 |        1        | 8 | 9 |
%|   |   |                 |   |   |
%|___|___|_________________________|___|___|
%|_15|_12|_____________4___________|_20|_22|
%|_14|_13|_____________5___________|_21|_23|
%
%  The above map of tekmat display number that correspond to if statements
%  below. Therefor the corresponding code checks that section of the map
%  for stray sensels
%


for k=1:size(m_data,3)

   if ~isempty(find(m_data(:,:,k)<255 & m_data(:,:,k)>0,1))

      [r,c,v]=find(m_data(:,:,k)<255 & m_data(:,:,k)>0);
      sr=sortrows([r c v],1);
      hsr=histc(sr(:,1),0.5:m_Rows+.5);
      hsc=histc(sr(:,2),0.5:m_Cols+.5);
      rhsr=find(hsr<5 & hsr>0);
      rhsc=find(hsc<5 & hsc>0);
      dr=[rhsr;rhsc];
      for m=1:length(dr)
         if m>length(rhsr)
            rdr=find(sr(:,2)==dr(m));
         else
            rdr=find(sr(:,1)==dr(m));
         end
         for n=1:length(rdr)


            i=sr(rdr(n),1);
            j=sr(rdr(n),2);
            %     for i=1:m_Rows
            %
            %        for j=1:m_Cols

            % 1
            if i > 2 && i < m_Rows-1 && j > 2 && j < m_Cols-1
               A = m_data(i-2,j-2,k)==0 && m_data(i-2,j-1,k)==0 && m_data(i-
2,j,k)==0 && m_data(i-2,j+1,k)==0 && m_data(i-2,j+2,k)==0;
               B = m_data(i-1,j-2,k)==0 && m_data(i-1,j-1,k)==0 && m_data(i-
1,j,k)==0 && m_data(i-1,j+1,k)==0 && m_data(i-1,j+2,k)==0;
               C = m_data(i,j-2,k)==0 && m_data(i,j-1,k)==0 && m_data(i,j,k)~=0
&& m_data(i,j+1,k)==0 && m_data(i,j+2,k)==0;
```

```
            D = m_data(i+1,j-2,k)==0 && m_data(i+1,j-1,k)==0 &&
m_data(i+1,j,k)==0 && m_data(i+1,j+1,k)==0 && m_data(i+1,j+2,k)==0;
            E = m_data(i+2,j-2,k)==0 && m_data(i+2,j-1,k)==0 &&
m_data(i+2,j,k)==0 && m_data(i+2,j+1,k)==0 && m_data(i+2,j+2,k)==0;
            % 2
        elseif i > 1 && i < m_Rows-1 && j > 2 && j < m_Cols-1
            A = 1;
            B = m_data(i-1,j-2,k)==0 && m_data(i-1,j-1,k)==0 && m_data(i-
1,j,k)==0 && m_data(i-1,j+1,k)==0 && m_data(i-1,j+2,k)==0;
            C = m_data(i,j-2,k)==0 && m_data(i,j-1,k)==0 && m_data(i,j,k)~=0
&& m_data(i,j+1,k)==0 && m_data(i,j+2,k)==0;
            D = m_data(i+1,j-2,k)==0 && m_data(i+1,j-1,k)==0 &&
m_data(i+1,j,k)==0 && m_data(i+1,j+1,k)==0 && m_data(i+1,j+2,k)==0;
            E = m_data(i+2,j-2,k)==0 && m_data(i+2,j-1,k)==0 &&
m_data(i+2,j,k)==0 && m_data(i+2,j+1,k)==0 && m_data(i+2,j+2,k)==0;
            %3
        elseif i == 1 && i < m_Rows-1 && j > 2 && j < m_Cols-1
            A = 1;
            B = 1;
            C = m_data(i,j-2,k)==0 && m_data(i,j-1,k)==0 && m_data(i,j,k)~=0
&& m_data(i,j+1,k)==0 && m_data(i,j+2,k)==0;
            D = m_data(i+1,j-2,k)==0 && m_data(i+1,j-1,k)==0 &&
m_data(i+1,j,k)==0 && m_data(i+1,j+1,k)==0 && m_data(i+1,j+2,k)==0;
            E = m_data(i+2,j-2,k)==0 && m_data(i+2,j-1,k)==0 &&
m_data(i+2,j,k)==0 && m_data(i+2,j+1,k)==0 && m_data(i+2,j+2,k)==0;
            %4
        elseif i > 2 && i < m_Rows && j > 2 && j < m_Cols-1
            A = m_data(i-2,j-2,k)==0 && m_data(i-2,j-1,k)==0 && m_data(i-
2,j,k)==0 && m_data(i-2,j+1,k)==0 && m_data(i-2,j+2,k)==0;
            B = m_data(i-1,j-2,k)==0 && m_data(i-1,j-1,k)==0 && m_data(i-
1,j,k)==0 && m_data(i-1,j+1,k)==0 && m_data(i-1,j+2,k)==0;
            C = m_data(i,j-2,k)==0 && m_data(i,j-1,k)==0 && m_data(i,j,k)~=0
&& m_data(i,j+1,k)==0 && m_data(i,j+2,k)==0;
            D = m_data(i+1,j-2,k)==0 && m_data(i+1,j-1,k)==0 &&
m_data(i+1,j,k)==0 && m_data(i+1,j+1,k)==0 && m_data(i+1,j+2,k)==0;
            E = 1;
            %5
        elseif i > 2 && i == m_Rows && j > 2 && j < m_Cols-1
            A = m_data(i-2,j-2,k)==0 && m_data(i-2,j-1,k)==0 && m_data(i-
2,j,k)==0 && m_data(i-2,j+1,k)==0 && m_data(i-2,j+2,k)==0;
            B = m_data(i-1,j-2,k)==0 && m_data(i-1,j-1,k)==0 && m_data(i-
1,j,k)==0 && m_data(i-1,j+1,k)==0 && m_data(i-1,j+2,k)==0;
            C = m_data(i,j-2,k)==0 && m_data(i,j-1,k)==0 && m_data(i,j,k)~=0
&& m_data(i,j+1,k)==0 && m_data(i,j+2,k)==0;
            D = 1;
            E = 1;
```

```
            %6
        elseif i > 2 && i < m_Rows-1 && j > 1 && j < m_Cols-1
            A = m_data(i-2,j-1,k)==0 && m_data(i-2,j,k)==0 && m_data(i-
2,j+1,k)==0 && m_data(i-2,j+2,k)==0;
            B = m_data(i-1,j-1,k)==0 && m_data(i-1,j,k)==0 && m_data(i-
1,j+1,k)==0 && m_data(i-1,j+2,k)==0;
            C = m_data(i,j-1,k)==0 && m_data(i,j,k)~=0 && m_data(i,j+1,k)==0
&& m_data(i,j+2,k)==0;
            D = m_data(i+1,j-1,k)==0 && m_data(i+1,j,k)==0 &&
m_data(i+1,j+1,k)==0 && m_data(i+1,j+2,k)==0;
            E = m_data(i+2,j-1,k)==0 && m_data(i+2,j,k)==0 &&
m_data(i+2,j+1,k)==0 && m_data(i+2,j+2,k)==0;

            %7
        elseif i > 2 && i < m_Rows-1 && j == 1 && j < m_Cols-1
            A = m_data(i-2,j,k)==0 && m_data(i-2,j+1,k)==0 && m_data(i-
2,j+2,k)==0;
            B = m_data(i-1,j,k)==0 && m_data(i-1,j+1,k)==0 && m_data(i-
1,j+2,k)==0;
            C = m_data(i,j,k)~=0 && m_data(i,j+1,k)==0 && m_data(i,j+2,k)==0;
            D = m_data(i+1,j,k)==0 && m_data(i+1,j+1,k)==0 &&
m_data(i+1,j+2,k)==0;
            E = m_data(i+2,j,k)==0 && m_data(i+2,j+1,k)==0 &&
m_data(i+2,j+2,k)==0;

            %8
        elseif i > 2 && i < m_Rows-1 && j > 2 && j < m_Cols
            A = m_data(i-2,j-2,k)==0 && m_data(i-2,j-1,k)==0 && m_data(i-
2,j,k)==0 && m_data(i-2,j+1,k)==0;
            B = m_data(i-1,j-2,k)==0 && m_data(i-1,j-1,k)==0 && m_data(i-
1,j,k)==0 && m_data(i-1,j+1,k)==0;
            C = m_data(i,j-2,k)==0 && m_data(i,j-1,k)==0 && m_data(i,j,k)~=0
&& m_data(i,j+1,k)==0;
            D = m_data(i+1,j-2,k)==0 && m_data(i+1,j-1,k)==0 &&
m_data(i+1,j,k)==0 && m_data(i+1,j+1,k)==0;
            E = m_data(i+2,j-2,k)==0 && m_data(i+2,j-1,k)==0 &&
m_data(i+2,j,k)==0 && m_data(i+2,j+1,k)==0;

            %9
        elseif i > 2 && i < m_Rows-1 && j > 2 && j == m_Cols
            A = m_data(i-2,j-2,k)==0 && m_data(i-2,j-1,k)==0 && m_data(i-
2,j,k)==0;
            B = m_data(i-1,j-2,k)==0 && m_data(i-1,j-1,k)==0 && m_data(i-
1,j,k)==0;
            C = m_data(i,j-2,k)==0 && m_data(i,j-1,k)==0 && m_data(i,j,k)~=0;
```

```
            D = m_data(i+1,j-2,k)==0 && m_data(i+1,j-1,k)==0 &&
m_data(i+1,j,k)==0;
            E = m_data(i+2,j-2,k)==0 && m_data(i+2,j-1,k)==0 &&
m_data(i+2,j,k)==0;

            %10
        elseif i > 1 && i < m_Rows-1 && j > 1 && j < m_Cols-1
            A = 1;
            B = m_data(i-1,j-1,k)==0 && m_data(i-1,j,k)==0 && m_data(i-
1,j+1,k)==0 && m_data(i-1,j+2,k)==0;
            C = m_data(i,j-1,k)==0 && m_data(i,j,k)~=0 && m_data(i,j+1,k)==0
&& m_data(i,j+2,k)==0;
            D = m_data(i+1,j-1,k)==0 && m_data(i+1,j,k)==0 &&
m_data(i+1,j+1,k)==0 && m_data(i+1,j+2,k)==0;
            E = m_data(i+2,j-1,k)==0 && m_data(i+2,j,k)==0 &&
m_data(i+2,j+1,k)==0 && m_data(i+2,j+2,k)==0;

            %11
        elseif i == 1 && i < m_Rows-1 && j > 1 && j < m_Cols-1
            A = 1;
            B = 1;
            C = m_data(i,j-1,k)==0 && m_data(i,j,k)~=0 && m_data(i,j+1,k)==0
&& m_data(i,j+2,k)==0;
            D = m_data(i+1,j-1,k)==0 && m_data(i+1,j,k)==0 &&
m_data(i+1,j+1,k)==0 && m_data(i+1,j+2,k)==0;
            E = m_data(i+2,j-1,k)==0 && m_data(i+2,j,k)==0 &&
m_data(i+2,j+1,k)==0 && m_data(i+2,j+2,k)==0;

            %12
        elseif i > 2 && i < m_Rows && j > 1 && j < m_Cols-1
            A = m_data(i-2,j-1,k)==0 && m_data(i-2,j,k)==0 && m_data(i-
2,j+1,k)==0 && m_data(i-2,j+2,k)==0;
            B = m_data(i-1,j-1,k)==0 && m_data(i-1,j,k)==0 && m_data(i-
1,j+1,k)==0 && m_data(i-1,j+2,k)==0;
            C = m_data(i,j-1,k)==0 && m_data(i,j,k)~=0 && m_data(i,j+1,k)==0
&& m_data(i,j+2,k)==0;
            D = m_data(i+1,j-1,k)==0 && m_data(i+1,j,k)==0 &&
m_data(i+1,j+1,k)==0 && m_data(i+1,j+2,k)==0;
            E = 1;

            %13
        elseif i > 2 && i == m_Rows && j > 1 && j < m_Cols-1
            A = m_data(i-2,j-1,k)==0 && m_data(i-2,j,k)==0 && m_data(i-
2,j+1,k)==0 && m_data(i-2,j+2,k)==0;
            B = m_data(i-1,j-1,k)==0 && m_data(i-1,j,k)==0 && m_data(i-
1,j+1,k)==0 && m_data(i-1,j+2,k)==0;
```

```
            C = m_data(i,j-1,k)==0 && m_data(i,j,k)~=0 && m_data(i,j+1,k)==0
&& m_data(i,j+2,k)==0;
            D = 1;
            E = 1;

            %14
        elseif i > 2 && i == m_Rows && j ==1 && j < m_Cols-1
            A = m_data(i-2,j,k)==0 && m_data(i-2,j+1,k)==0 && m_data(i-
2,j+2,k)==0;
            B = m_data(i-1,j,k)==0 && m_data(i-1,j+1,k)==0 && m_data(i-
1,j+2,k)==0;
            C = m_data(i,j,k)~=0 && m_data(i,j+1,k)==0 && m_data(i,j+2,k)==0;
            D = 1;
            E = 1;

            %15
        elseif i > 2 && i < m_Rows && j == 1 && j < m_Cols-1
            A = m_data(i-2,j,k)==0 && m_data(i-2,j+1,k)==0 && m_data(i-
2,j+2,k)==0;
            B = m_data(i-1,j,k)==0 && m_data(i-1,j+1,k)==0 && m_data(i-
1,j+2,k)==0;
            C = m_data(i,j,k)~=0 && m_data(i,j+1,k)==0 && m_data(i,j+2,k)==0;
            D = m_data(i+1,j,k)==0 && m_data(i+1,j+1,k)==0 &&
m_data(i+1,j+2,k)==0;
            E = 1;

            %16
        elseif i > 1 && i < m_Rows-1 && j == 1 && j < m_Cols-1
            A = 1;
            B = m_data(i-1,j,k)==0 && m_data(i-1,j+1,k)==0 && m_data(i-
1,j+2,k)==0;
            C = m_data(i,j,k)~=0 && m_data(i,j+1,k)==0 && m_data(i,j+2,k)==0;
            D = m_data(i+1,j,k)==0 && m_data(i+1,j+1,k)==0 &&
m_data(i+1,j+2,k)==0;
            E = m_data(i+2,j,k)==0 && m_data(i+2,j+1,k)==0 &&
m_data(i+2,j+2,k)==0;

            %17
        elseif i == 1 && i < m_Rows-1 && j == 1 && j < m_Cols-1
            A = 1;
            B = 1;
            C = m_data(i,j,k)~=0 && m_data(i,j+1,k)==0 && m_data(i,j+2,k)==0;
            D = m_data(i+1,j,k)~=0 && m_data(i+1,j+1,k)==0 &&
m_data(i+1,j+2,k)==0;
            E = m_data(i+2,j,k)==0 && m_data(i+2,j+1,k)==0 &&
m_data(i+2,j+2,k)==0;
```

```
            %18
        elseif i > 1 && i < m_Rows-1 && j > 2 && j < m_Cols
            A = 1;
            B = m_data(i-1,j-2,k)==0 && m_data(i-1,j-1,k)==0 && m_data(i-
1,j,k)==0 && m_data(i-1,j+1,k)==0;
            C = m_data(i,j-2,k)==0 && m_data(i,j-1,k)==0 && m_data(i,j,k)~=0
&& m_data(i,j+1,k)==0;
            D = m_data(i+1,j-2,k)==0 && m_data(i+1,j-1,k)==0 &&
m_data(i+1,j,k)==0 && m_data(i+1,j+1,k)==0;
            E = m_data(i+2,j-2,k)==0 && m_data(i+2,j-1,k)==0 &&
m_data(i+2,j,k)==0 && m_data(i+2,j+1,k)==0;

            %19
        elseif i == 1 && i < m_Rows-1 && j > 2 && j < m_Cols
            A = 1;
            B = 1;
            C = m_data(i,j-2,k)==0 && m_data(i,j-1,k)==0 && m_data(i,j,k)~=0
&& m_data(i,j+1,k)==0;
            D = m_data(i+1,j-2,k)==0 && m_data(i+1,j-1,k)==0 &&
m_data(i+1,j,k)==0 && m_data(i+1,j+1,k)==0;
            E = m_data(i+2,j-2,k)==0 && m_data(i+2,j-1,k)==0 &&
m_data(i+2,j,k)==0 && m_data(i+2,j+1,k)==0;

            %20
        elseif i > 2 && i < m_Rows && j > 2 && j < m_Cols
            A = m_data(i-2,j-2,k)==0 && m_data(i-2,j-1,k)==0 && m_data(i-
2,j,k)==0 && m_data(i-2,j+1,k)==0;
            B = m_data(i-1,j-2,k)==0 && m_data(i-1,j-1,k)==0 && m_data(i-
1,j,k)==0 && m_data(i-1,j+1,k)==0;
            C = m_data(i,j-2,k)==0 && m_data(i,j-1,k)==0 && m_data(i,j,k)~=0
&& m_data(i,j+1,k)==0;
            D = m_data(i+1,j-2,k)==0 && m_data(i+1,j-1,k)==0 &&
m_data(i+1,j,k)==0 && m_data(i+1,j+1,k)==0;
            E = 1;

            %21
        elseif i > 2 && i == m_Rows && j > 2 && j < m_Cols
            A = m_data(i-2,j-2,k)==0 && m_data(i-2,j-1,k)==0 && m_data(i-
2,j,k)==0 && m_data(i-2,j+1,k)==0;
            B = m_data(i-1,j-2,k)==0 && m_data(i-1,j-1,k)==0 && m_data(i-
1,j,k)==0 && m_data(i-1,j+1,k)==0;
            C = m_data(i,j-2,k)==0 && m_data(i,j-1,k)==0 && m_data(i,j,k)~=0
&& m_data(i,j+1,k)==0;
            D = 1;
            E = 1;
```

```
            %22
        elseif i > 2 && i < m_Rows && j > 2 && j == m_Cols
            A = m_data(i-2,j-2,k)==0 && m_data(i-2,j-1,k)==0 && m_data(i-
2,j,k)==0;
            B = m_data(i-1,j-2,k)==0 && m_data(i-1,j-1,k)==0 && m_data(i-
1,j,k)==0;
            C = m_data(i,j-2,k)==0 && m_data(i,j-1,k)==0 && m_data(i,j,k)~=0;
            D = m_data(i+1,j-2,k)==0 && m_data(i+1,j-1,k)==0 &&
m_data(i+1,j,k)==0;
            E = 1;

            %23
        elseif i > 2 && i == m_Rows && j > 2 && j == m_Cols
            A = m_data(i-2,j-2,k)==0 && m_data(i-2,j-1,k)==0 && m_data(i-
2,j,k)==0;
            B = m_data(i-1,j-2,k)==0 && m_data(i-1,j-1,k)==0 && m_data(i-
1,j,k)==0;
            C = m_data(i,j-2,k)==0 && m_data(i,j-1,k)==0 && m_data(i,j,k)~=0;
            D = 1;
            E = 1;

            %24
        elseif i > 1 && i < m_Rows-1 && j > 2 && j == m_Cols
            A = 1;
            B = m_data(i-1,j-2,k)==0 && m_data(i-1,j-1,k)==0 && m_data(i-
1,j,k)==0;
            C = m_data(i,j-2,k)==0 && m_data(i,j-1,k)==0 && m_data(i,j,k)~=0;
            D = m_data(i+1,j-2,k)==0 && m_data(i+1,j-1,k)==0 &&
m_data(i+1,j,k)==0;
            E = m_data(i+2,j-2,k)==0 && m_data(i+2,j-1,k)==0 &&
m_data(i+2,j,k)==0;

            %25
        elseif i == 1 && i < m_Rows-1 && j > 2 && j == m_Cols
            A = 1;
            B = 1;
            C = m_data(i,j-2,k)==0 && m_data(i,j-1,k)==0 && m_data(i,j,k)~=0;
            D = m_data(i+1,j-2,k)==0 && m_data(i+1,j-1,k)==0 &&
m_data(i+1,j,k)==0;
            E = m_data(i+2,j-2,k)==0 && m_data(i+2,j-1,k)==0 &&
m_data(i+2,j,k)==0;

            %Default for Error SHould never get here
        elseif 1
```

```
                error(['Bad Program: i = ',num2str(i), ' j = ', num2str(j), ' k = ',
num2str(k)])
            end
            if A && B && C && D && E
                m_data(i,j,k)=0;
            end
        end
    end
  end
end
%*************************************************************

%*************************************************************
%  Vectorized Calculation of APCOP and MLCOP
FRAMEs=1:m_frame;

COLs=1:m_Cols;
ROWs=1:m_Rows;

rower(1:m_frame)=1;

COLs_3d=COLs'*rower;
ROWs_3d=ROWs'*rower;


MLCOP=sum(squeeze(sum(m_data(:,:,FRAMEs),X_ML)).*(COLs_3d),1)./sum(sq
ueeze(sum(m_data(:,:,FRAMEs),X_ML)),1);
APCOP=sum(squeeze(sum(m_data(:,:,FRAMEs),Y_AP)).*(ROWs_3d),1)./sum(s
queeze(sum(m_data(:,:,FRAMEs),Y_AP)),1);

dat=[APCOP; MLCOP]';
dat=dat.*5.08; % Conversion to mm
%*************************************************************


%*****************************************************
%  Foot Analysis


%  Seperate Feet

right_side_left_foot=zeros(size(m_data,3),1);
left_side_left_foot=zeros(size(m_data,3),1);
front_side_left_foot=zeros(size(m_data,3),1);
back_side_left_foot=zeros(size(m_data,3),1);
right_side_right_foot=zeros(size(m_data,3),1);
```

```
left_side_right_foot=zeros(size(m_data,3),1);
front_side_right_foot=zeros(size(m_data,3),1);
back_side_right_foot=zeros(size(m_data,3),1);
for k=1:size(m_data,3)

   if ~isempty(find(m_data(:,:,k),1))
      [r,c,v]=find(m_data(:,:,k));
      feet_division=(max(c)-min(c))/2+min(c);
      c=sort(c);
   end
   if exist('feet_division','var')==1
      if ~isempty(find(c>feet_division,1))
         xr=find(c>feet_division,1,'first');
         right_side_left_foot(k)=c(xr);
      end

      if ~isempty(find(c>feet_division,1))
         xr=find(c>feet_division,1,'last');
         left_side_left_foot(k)=c(xr);
      end

      if ~isempty(find(c<feet_division,1))
         xr=find(c<feet_division,1,'first');
         right_side_right_foot(k)=c(xr);
      end

      if ~isempty(find(c<feet_division,1))
         xr=find(c<feet_division,1,'last');
         left_side_right_foot(k)=c(xr);
      end
   end

   leftfoot=imcrop(m_data(:,:,k),[right_side_left_foot(k) 1 left_side_left_foot(k)-
right_side_left_foot(k) m_Rows]);
   rightfoot=imcrop(m_data(:,:,k),[right_side_right_foot(k) 1
left_side_right_foot(k)-right_side_right_foot(k) m_Rows]);

   if ~isempty(find(leftfoot,1))
      [r,c,v]=find(leftfoot);
      r=sort(r);


      if ~isempty(find(r,1,'first'))
         xr=find(r,1,'first');
         back_side_left_foot(k)=r(xr);
      end
```

```
        if ~isempty(find(r,1,'last'))
            xr=find(r,1,'last');
            front_side_left_foot(k)=r(xr);
        end
    end
    if ~isempty(find(rightfoot,1))
        [r,c,v]=find(rightfoot);
        r=sort(r);


        if ~isempty(find(r,1,'first'))
            xr=find(r,1,'first');
            back_side_right_foot(k)=r(xr);
        end

        if ~isempty(find(r,1,'last'))
            xr=find(r,1,'last');
            front_side_right_foot(k)=r(xr);
        end
    end
end

left_foot_row_size=max(front_side_left_foot)-min(back_side_left_foot)+1;
if left_foot_row_size > m_Rows
    left_foot_row_size=m_Rows;
end

left_foot_col_size=max(left_side_left_foot)-min(right_side_left_foot)+1;
if left_foot_col_size > m_Cols
    left_foot_col_size=m_Cols;
end

right_foot_row_size=max(front_side_right_foot)-min(back_side_right_foot)+1;
if right_foot_row_size > m_Rows
    right_foot_row_size=m_Rows;
end

right_foot_col_size=max(left_side_right_foot)-min(right_side_right_foot)+1;
if right_foot_col_size > m_Cols
    right_foot_col_size=m_Cols;
end

leftfoot=zeros(left_foot_row_size,left_foot_col_size,m_frame);
rightfoot=zeros(right_foot_row_size,right_foot_col_size,m_frame);
for k=1:size(m_data,3)
```

```
   if min(right_side_left_foot)==0 && min(back_side_left_foot)==0
      leftfoot(:,:,k)=imcrop(m_data(:,:,k),[min(right_side_left_foot)+1
min(back_side_left_foot)+1 max(left_side_left_foot)-min(right_side_left_foot)
max(front_side_left_foot)-min(back_side_left_foot)]);
   elseif min(back_side_left_foot)==0
      leftfoot(:,:,k)=imcrop(m_data(:,:,k),[min(right_side_left_foot)
min(back_side_left_foot)+1 max(left_side_left_foot)-min(right_side_left_foot)
max(front_side_left_foot)-min(back_side_left_foot)]);
   elseif min(right_side_left_foot)==0
      leftfoot(:,:,k)=imcrop(m_data(:,:,k),[min(right_side_left_foot)+1
min(back_side_left_foot) max(left_side_left_foot)-min(right_side_left_foot)
max(front_side_left_foot)-min(back_side_left_foot)]);
   else
      leftfoot(:,:,k)=imcrop(m_data(:,:,k),[min(right_side_left_foot)
min(back_side_left_foot) max(left_side_left_foot)-min(right_side_left_foot)
max(front_side_left_foot)-min(back_side_left_foot)]);
   end

   if min(right_side_right_foot)==0 && min(back_side_right_foot)==0
      rightfoot(:,:,k)=imcrop(m_data(:,:,k),[min(right_side_right_foot)+1
min(back_side_right_foot)+1 max(left_side_right_foot)-min(right_side_right_foot)
max(front_side_right_foot)-min(back_side_right_foot)]);
   elseif min(back_side_right_foot)==0
      rightfoot(:,:,k)=imcrop(m_data(:,:,k),[min(right_side_right_foot)
min(back_side_right_foot)+1 max(left_side_right_foot)-min(right_side_right_foot)
max(front_side_right_foot)-min(back_side_right_foot)]);
   elseif min(right_side_right_foot)==0
      rightfoot(:,:,k)=imcrop(m_data(:,:,k),[min(right_side_right_foot)+1
min(back_side_right_foot) max(left_side_right_foot)-min(right_side_right_foot)
max(front_side_right_foot)-min(back_side_right_foot)]);
   else
      rightfoot(:,:,k)=imcrop(m_data(:,:,k),[min(right_side_right_foot)
min(back_side_right_foot) max(left_side_right_foot)-min(right_side_right_foot)
max(front_side_right_foot)-min(back_side_right_foot)]);
   end
end

if size(leftfoot,1)==1 || size(leftfoot,2)==1
   leftfoot=zeros(10,10,size(leftfoot,3));
end

if size(rightfoot,1)==1 || size(rightfoot,2)==1
   rightfoot=zeros(10,10,size(rightfoot,3));
end
```

```
%*********************************************************
%   Vectorized Calculation of APCOP and MLCOP for Each Foot
rower(1:m_frame)=1;

R_COLs=1:size(rightfoot,2);
R_ROWs=1:size(rightfoot,1);

R_COLs_3d=R_COLs'*rower;
R_ROWs_3d=R_ROWs'*rower;

L_COLs=1:size(leftfoot,2);
L_ROWs=1:size(leftfoot,1);

L_COLs_3d=L_COLs'*rower;
L_ROWs_3d=L_ROWs'*rower;

LMLCOP=sum(squeeze(sum(leftfoot,X_ML)).*(L_COLs_3d),1)./sum(squeeze(su
m(leftfoot,X_ML)),1);
LAPCOP=sum(squeeze(sum(leftfoot,Y_AP)).*(L_ROWs_3d),1)./sum(squeeze(su
m(leftfoot,Y_AP)),1);

RMLCOP=sum(squeeze(sum(rightfoot,X_ML)).*(R_COLs_3d),1)./sum(squeeze(s
um(rightfoot,X_ML)),1);
RAPCOP=sum(squeeze(sum(rightfoot,Y_AP)).*(R_ROWs_3d),1)./sum(squeeze(
sum(rightfoot,Y_AP)),1);

feetcop=[RAPCOP; RMLCOP; LAPCOP; LMLCOP]';
feetcop=feetcop.*5.08; % Conversion to mm


%*****************************************************

%*****************************************************
%   Subject Weight Feet Distrubution

% Total Weights
totalweight=squeeze(sum(sum(m_data,1),2));
leftweight=squeeze(sum(sum(leftfoot,1),2));
rightweight=squeeze(sum(sum(rightfoot,1),2));

% Percentages between feet
pleftweight=leftweight./totalweight;
prightweight=rightweight./totalweight;
pweight=[prightweight pleftweight];
```

```
%*****************************************************

save(filename,'APCOP', 'MLCOP', 'm_data', 'rm_data', 'm_Rows', 'm_Cols',
'leftfoot', 'rightfoot', 'm_frame', 'filename', 'RAPCOP', 'RMLCOP', 'LAPCOP',
'LMLCOP', 'totalweight', 'leftweight', 'rightweight', 'pleftweight', 'prightweight');

clear X_ML Y_AP filename m_data m_Rows m_Cols m_frame smdat sm_data i j
clear calflag FRAMEs COLs ROWs rower COLs_3d ROWs_3d APCOP MLCOP
rm_data
clear RMLCOP RAPCOP LAPCOP LMLCOP totalweight leftweight rightweight
clear pleftweight prightweight R_COLs R_ROWs L_COLs L_ROWs R_COLs_3d
clear R_ROWs_3d L_COLs_3d L_ROWs_3d leftfoot rightfoot feet_division
clear right_side_right_foot front_side_right_foot back_side_right_foot
clear left_side_right_foot right_side_left_foot front_side_left_foot
clear back_side_left_foot left_side_left_foot r c v A B C D E m n sr hsr
clear hsc dr xr badr rhsr rhsc k
function                    [ m_data, m_Rows, m_Cols, m_frame, m_RowSpacing,
m_ColSpacing] = loadfsx2( filename, calflag)

% load fsx, faster
% mov = loadfsx2( filename, calflag)
% calflag = 0  for loading of raw values
% calflag = 1  for loading calibrated values

if ( exist('calflag','var') == 0)
   calflag = 1 ;
end

FALSE = 0 ;
TRUE = 1 ;

MOVIE_END_OF_FRAME = 255 ;
NORMAL_HEADER_END_MARK = 186 ;
HISPEED_HEADER_END_MARK = 187;

% wait for file to be written
iji=0;
while exist(filename,'file')==0 && iji < 100
   iji=iji+1;
   pause(0.1)
end
fid = fopen( filename, 'r');

if ( fid == -1)
   error(['File ' filename ' not found']);
```

```
end

bd = fread( fid, Inf) ;

bdi = 1 ;

fclose(fid);

head = '' ;
b = 0 ;
while ( b ~= NORMAL_HEADER_END_MARK && b ~=
HISPEED_HEADER_END_MARK)
   b = bd(bdi) ; bdi=bdi+1 ;
   %disp([ num2str(b)]);
   head = [ head  sprintf('%c', b)] ;
end

%head
%disp('End of header found');
% b = bd(bdi) ;
bdi=bdi+1 ;

m_Rows                          = str2double( exstr( head, 'ROWS')) ;
m_Cols                          = str2double( exstr( head, 'COLS')) ;
m_RowSpacing                = str2double( exstr( head, 'ROW_SPACING')) ;
m_ColSpacing                = str2double( exstr( head, 'COL_SPACING')) ;
% m_DesiredAspect    = str2double( exstr( head, 'DESIRED_ASPECT'));
m_SenselArea                = str2double( exstr( head, 'SENSEL_AREA'));
% m_NoiseThreshold   = str2double( exstr( head, 'NOISE_THRESHOLD'));
m_FramesFromHeader = str2double( exstr( head, 'FRAMES'));
m_ScaleFactor      = str2double( exstr( head, 'SCALE_FACTOR'));
m_Exponent         = str2double( exstr( head, 'EXPONENT'));
% m_SecondsPerFrame  = str2double( exstr( head,
'SECONDS_PER_FRAME'));
m_FrameInfo  = str2double( exstr( head, 'FRAME_INFO'));
m_CAL_FPI_1 = str2double( exstr( head, 'CAL_FPI_1'));
m_CAL_RPI_1 = str2double( exstr( head, 'CAL_RSI_1'));
m_Units = exstr( head, 'UNITS');

m_frame = m_FramesFromHeader;

if(m_Units(1) == 'r')
   calflag = 0;
end

if ( calflag == 0 )
```

```
    %disp(['Loading raw - ignoring calibration']);
    scale = 1.0 ;
    exponent = 1 ;
else
    if(~isempty(m_CAL_FPI_1) && ~isempty(m_CAL_RPI_1))
        exponent = 1 ;
        scale = m_CAL_FPI_1/(m_CAL_RPI_1 * m_SenselArea);
    end

    if(~isempty(m_ScaleFactor) && ~isempty(m_Exponent))
        scale = m_ScaleFactor ;
        exponent = m_Exponent ;
    end
end

if isempty(m_FrameInfo)
    m_FrameInfo = 0;
end

m_data=zeros( m_Rows, m_Cols, m_FramesFromHeader);

%disp(['Frames to load: ' num2str(m_FramesFromHeader)]);
%disp('Loading... ');
pause(0.0001);

for f=0:m_FramesFromHeader-1
    %disp(['     Frame: ' num2str(f)]);
    PreviousEndOfFrame = FALSE ;
    IsFrameInfo = FALSE ;
    cont = TRUE ;
    while ( cont == TRUE)
        low = bd(bdi) ; bdi=bdi+1 ;

        if ( low ~= MOVIE_END_OF_FRAME)
            PreviousEndOfFrame = FALSE ;
            hi = bd(bdi) ; bdi=bdi+1 ;
            loc = hi * 256 + low ;

            if (loc > (m_Cols * m_Rows))
                hi
                loc
                low
                cont
                f
                m_Cols
                m_Rows
```

```
            return;
            %error('Bad Location Data: 1');
         else
            t_elements = bd(bdi);
            bdi=bdi+1 ;
            if ( f>=3000)
               %disp(['t_elements = ' num2str(t_elements)]);
               %pause
            end

            for i=loc:(loc+t_elements-1)
               r = floor(i/m_Cols) ;
               c = i - r * m_Cols ;

               if ( f>=3000)
                  %disp(['i = ' num2str(i)]);
                  %disp(['Row = ' num2str(r) '  Col = ' num2str(c)]);
               end

               sensel = bd(bdi) ;
               bdi=bdi+1 ;
               sensel = scale * (sensel^exponent)  ;

               if ( f>=3000)
                  %disp(['first']);
%                    m_Rows;
%                    f * m_Rows + r + 1;
%                    c+1;
%                    size( m_data);
%                    sensel;
               end
               m_data( r + 1, c+1,f+1) = sensel ;
            end % for i
         end % else
         % end if low != end of frame
      else
         if (PreviousEndOfFrame == FALSE)
            PreviousEndOfFrame = TRUE ;
            hi = bd(bdi) ; bdi=bdi+1 ;
            if (hi ~= MOVIE_END_OF_FRAME)
               PreviousEndOfFrame = FALSE ;
               loc = hi * 256 + low ;
               if ( loc > (m_Cols * m_Rows))
                  hi
                  loc
                  low
```

```
                cont
                f
                m_Cols
                m_Rows
                return;
                %error('Bad Location Data: 2');
            else
                t_elements = bd(bdi) ; bdi=bdi+1 ;

                for i=loc:(loc+t_elements-1)
                    r = floor(i/m_Cols) ;
                    c = i - r * m_Cols ;
                    sensel = bd(bdi) ; bdi=bdi+1 ;
                    sensel = scale * (sensel^exponent);
                    m_data(  r + 1, c+1,f+1) = sensel  ;
                end % for i
            end % else
        elseif (m_FrameInfo == 1 && IsFrameInfo == FALSE) %Skip frame info
if any
            low = bd(bdi) ; bdi=bdi+1 ;
            hi = bd(bdi) ; bdi=bdi+1 ;
            IsFrameInfo = TRUE;
            while (low ~= MOVIE_END_OF_FRAME || hi ~=
MOVIE_END_OF_FRAME) && bdi <= length(bd)
                low = bd(bdi) ; bdi=bdi+1 ;
                hi = bd(bdi) ; bdi=bdi+1 ;
            end
            if low ~= MOVIE_END_OF_FRAME && hi ~=
MOVIE_END_OF_FRAME
                error('Bad frame info')
            end
        end % /** end if hi != MOVIE_END_OF_FRAME **/
    end %  /** PreviousEndOfFrame == FALSE **/
end %  /** end else **/

cont =  FALSE ;
if ( low ~= MOVIE_END_OF_FRAME || PreviousEndOfFrame ~= TRUE)
    cont = TRUE ;
end

end % while( low ~= MOVIE_END_OF_FRAME | PreviousEndOfFrame ~=
TRUE) ;
end % end % for f

%disp([ 'Done ... ' num2str(m_FramesFromHeader) ' frames loaded']);
```

```
return;
% Modified By Chris Storey
% $Header:  G:/CORE/LOGFILES/MATLAB/loadfsx2.m_v  1.1  Sep 20 2000
16:44:18  FCHEN  $
%
% $Log:  G:/CORE/LOGFILES/MATLAB/loadfsx2.m_v  $
%
%   Rev 1.1  Sep 20 2000 16:44:18  FCHEN
% Modified to read the movies with frameinfo and multi-tile
% calibration info.  Use the first tile cal info as the whole.
%
%   Rev 1.0  Sep 19 2000 15:16:14  FCHEN
% Initial revision.

function                    str = exstr( line, s1)


i = findstr( line, s1);

if ( length(i)>0)
                            start = i + length(s1(1,:)) + 1 ;
                            j = start ;
  c = line(j) ;
  while( ~isspace(c))
                              j = j + 1 ;
    c = line(j) ;
                              end
                            str = line(start:(j)) ;
else
                            str = '';
                            end

  return;
% $Header:  G:/CORE/LOGFILES/MATLAB/exstr.m_v  1.1  Sep 20 2000
16:15:08  FCHEN  $
%
% $Log:  G:/CORE/LOGFILES/MATLAB/exstr.m_v  $
%
%   Rev 1.1  Sep 20 2000 16:15:08  FCHEN
% Fixed the bug of extracting extra 2 chars.
%
%   Rev 1.0  Sep 19 2000 15:16:20  FCHEN% Initial revision.
```

APPENDIX O

mSIAM SIMULATION MATLAB® CODE

```
% function montecarlo(n,s)

n=1000;
s=10000;

% Monte Carlo Simulation in Matlab
% n is number of trials
% s is number of subjects

% --- Generate vectors of random inputs
% x ~ Uniform distribution of integers 0-3

x = rem(round(rand(n,s)*4),4);

% Initial Increment

incr = 1;

% Initial Amplitude

Amp = 4;

% Hit change setting

hit = -1;

% Miss change setting

miss = 1;

% False Alarm change setting

fls_alm = 2;

% Correct Rejection change setting

cor_rej = 0;

% Minimum number of hits before 80% rule goes into effect

hit_total = 5;

% --- Run the simulation
% Note the use of element-wise multiplication

[Amps,stoprules] = t2IFCmPESTh(x,incr,n,s, Amp);
```

```
% --- Create a histogram of the results (50 bins)

edges = (0:5:1000);


histc023 = figure;
histc02v=histc(stoprules(1:s,1),edges);
bar(edges,histc02v)
axis([0 1000 0 500])
title('mPEST 2% Rule')
% hist02h3y1n2r3 = figure;
% hist(stoprulesh3y1n2r3(1:s,1),edges)
% axis([0 500 0 1500])



histc05 = figure;
histc05v=histc(stoprules(1:s,2),edges);
bar(edges,histc05v)
axis([0 1000 0 500])
title('mPEST 5% Rule')
% hist05h3y1n2r3 = figure;
% hist(stoprulesh3y1n2r3(1:s,2),edges)
% axis([0 500 0 1500])

% hist80h = figure;
% histc(stoprulesh(1:s,3),edges)

% --- Calculate summary statistics

% y_mean = mean(y)
% y_std = std(y)
% y_median = median(y)

mean02 = mean(stoprules(1:s,1))
mean05 = mean(stoprules(1:s,2))
mean02A = mean(stoprules(1:s,3))
mean05A = mean(stoprules(1:s,4))
% mean80h = mean(stoprulesh(1:s,3))

std02 = std(stoprules(1:s,1))
std05 = std(stoprules(1:s,2))
std02A = std(stoprules(1:s,3))
std05A = std(stoprules(1:s,4))
% std80h = std(stoprulesh(1:s,3))
```

```
% d_efficiency = (norm(sum(d))./30)

save('mPEST')

function [Amps,stoprules] = mSIAM_Implemented(x,incr,n,s, Amp,hit, miss,
fls_alm,cor_rej)

% 0 => HIT
% 1 => MISS
% 2 => FALSE ALARM
% 3 => CORRECT REJECTION

% x contains the uniformaly random detections
% incr contains inital increment
% n contains number of trials
% s contains number of subjects
% Amp contains Intial Amplitude
% hit contains Hit change setting
% miss contains Miss change setting
% fls_alm = False Alarm Change setting
% cor_rej = Correct Rejection Change Setting

% stoprules=zeros(s,3); % Include 80% rule

stoprules=zeros(s,2);
Amps=zeros(n,s);



h1=waitbar(0,['Monte Carlo Simulation of mSIAM_Implemented ',num2str(s),'
subjects']);

tt=0;
ttot=0;
for i = 1:s
   ttot=ttot+tt;
   tic
   waitbar(i/s,h1,{['Monte Carlo Simulation of mSIAM_shr_Implemented
',num2str(s),' subjects.'] ['Estimated time remaining: ',num2str(ttot/i*(s-
i)/60,'%6.2f')]});
   j=1;
   % Flag that stops while loop
   flg=0;
   % Flag that indicates when 2% rule met
   flg02 = 0;
```

```
% Flag that indicates when 5% rule met
flg05 = 0;
% Counts the number of Reversals
rvrsl = 0;
crvrsl = 0;
newincr = incr;
newAmp = Amp;
y(1,i)=newAmp;
h2=waitbar(0,['Monte Carlo Simulation of subject: ',num2str(i)]);
while (j<=n && flg==0)
   oldAmp=newAmp;
   if j >1
      waitbar(j/n,h2,{['Monte Carlo Simulation of subject: ',num2str(i),' Trial:
',num2str(j),] ['2% Flag: ',num2str(flg02), ' 5% Flag: ',num2str(flg05), ' Average
Stop: ', num2str(mean(stoprules(1:i-1,1)))]});
   end
   if x(j,i) ~= 3

      if j >1
         none_3_indx = 1;
         last_none_3 = 3;
         while last_none_3 == 3
            if x(j-none_3_indx,i) ~= 3
               last_none_3 = x(j-none_3_indx,i);
            end

            none_3_indx = none_3_indx + 1;

            if j-none_3_indx == 0 && last_none_3 == 3
               last_none_3 = -1;
            end
         end
      end

      if j > 2 && j > none_3_indx
         nlast_none_3 = 3;
         while nlast_none_3 == 3
            if x(j-none_3_indx,i) ~=3
               nlast_none_3 = x(j-none_3_indx,i);
            end

            none_3_indx = none_3_indx + 1;

            if j-none_3_indx == 0 && nlast_none_3 == 3
               nlast_none_3 = -1;
            end
```

```
            end
        end
%**************Current HIT
        if j>2 && x(j,i) == 0
            switch last_none_3
                case 0
                    if rvrsl >=2
                        switch nlast_none_3
                            case 0
                                if hit_jump == 1
                                    newincr=newincr*2;
                                end
                            case 1
                                newincr=newincr/2;
                                rvrsl = rvrsl+1;
                                crvrsl= crvrsl+1;
                            case 2
                                newincr=newincr/2;
                                rvrsl = rvrsl+1;
                                crvrsl= crvrsl+1;
                            case -1
                            otherwise
                                error(['Bad Program: 0 : ',num2str(last_none_3)])
                        end
                    else
                        newincr=newincr*2;
                    end

                case 1
                    if rvrsl < 2
                        rvrsl = rvrsl+1;
                        crvrsl= crvrsl+1;
                    end
                case 2
                    if rvrsl < 2
                        rvrsl = rvrsl+1;
                        crvrsl= crvrsl+1;
                    end
                case -1

                otherwise
                    error(['Bad Program: 0 : ',num2str(last_none_3)])
            end
        end
%***********END of Current HIT
```

```
if j>2 && x(j,i)==1
   switch last_none_3
      case 0
         if rvrsl >=2
            if hit_jump
               newincr=newincr/2;
            end
         else
            if nlast_none_3 == 0
               newincr=newincr/2;
            end
         end
         rvrsl = rvrsl+1;
         crvrsl= crvrsl+1;
      case 1
         newincr=newincr*2;

      case 2
         newincr=newincr*2;
      case -1
      otherwise
         error(['Bad Program: 1 : ',num2str(last_none_3)])
   end
end

if j>2 && x(j,i)==2
   switch last_none_3
      case 0
         if rvrsl >=2
            if hit_jump
               newincr=newincr/2;
            end
         else
            if nlast_none_3 == 0
               newincr=newincr/2;
            end
         end
         rvrsl = rvrsl+1;
         crvrsl= crvrsl+1;
      case 1
         newincr=newincr*2;

      case 2
         newincr=newincr*2;
      case -1
      otherwise
```

```
            error(['Bad Program: 1 : ',num2str(last_none_3)])
        end
    end
end
if crvrsl >=4
    newincr=newincr/2;
    crvrsl=0;
end
switch x(j,i)
    case 0
        if j>1
            if last_none_3 == 0
                if rvrsl >=2
                    if nlast_none_3 == 0
                        if newAmp+newincr*hit < 0
                            newincr=newAmp/2;
                        end
                        newAmp=newAmp+newincr*hit;
                        hit_jump=1;
                    else
                        if newAmp+newincr*hit < 0
                            newincr=newAmp/2;
                        end
                        newAmp=newAmp+newincr*hit;
                    end
                else
                    if newAmp+newincr*hit < 0
                        newincr=newAmp/2;
                    end
                    newAmp=newAmp+newincr*hit;
                end
            else
                if newAmp+newincr*hit < 0
                    newincr=newAmp/2;
                end
                newAmp=newAmp+newincr*hit;
            end
        else
            if newAmp+newincr*hit < 0
                newincr=newAmp/2;
            end
            newAmp=newAmp+newincr*hit;
        end
    case 1
        newAmp=newAmp+newincr*miss;
        hit_jump=0;
```

```
        case 2
          newAmp=newAmp+newincr*fls_alm;
          hit_jump=0;
        case 3
          newAmp=newAmp+newincr*cor_rej;
        otherwise
          error('Bad Program')
      end
      if newAmp <=0
        newAmp=oldAmp/2;
        newincr=oldAmp/2;
      end
      y(j+1,i)=newAmp;
%       plot(y(:,i));
%       drawnow;
%       if j==30
%         disp('Hi');
%       end
      %       for k = 1:j+1
      %         if y(k,i)==newAmp
      %           total=total+1;
      %           if x(k,i)==0
      %             hits=hits+1;
      %           end
      %         end
      %       end
      %       if total > hit_total
      %         if hits/total > 0.8
      %           stoprules(i,3)=j;
      %           flghits=1;
      %         end
      %       end
      %       if flghits && flg02 && flg05
      %         flg = 1;
      %       end
      if (newincr/incr < .02 && flg02==0)
        stoprules(i,1)=j;
        stoprules(i,3)=newAmp;
        flg02=1;
      end
      if (newincr/incr < .05 && flg05==0)
        stoprules(i,2)=j;
        stoprules(i,4)=newAmp;
        flg05=1;
      end
      if flg02 && flg05
```

```
            flg = 1;
        end
        j=j+1;
    end
    if j>n
        if flg02 ~=1
            stoprules(i,1)=j;
            stoprules(i,3)=newAmp;
        end
        if flg05 ~=1
            stoprules(i,2)=j;
            stoprules(i,4)=newAmp;
        end
    end
    close(h2);
    tt=toc;
end
close(h1);

function [Amps,stoprules] = mSIAM_shr_Implemented(x,incr,n,s, Amp,hit, miss,
fls_alm,cor_rej)

% 0 => HIT
% 1 => MISS
% 2 => FALSE ALARM
% 3 => CORRECT REJECTION

% x contains the uniformaly random detections
% incr contains inital increment
% n contains number of trials
% s contains number of subjects
% Amp contains Intial Amplitude
% hit contains Hit change setting
% miss contains Miss change setting
% fls_alm = False Alarm Change setting
% cor_rej = Correct Rejection Change Setting

% stoprules=zeros(s,3); % Include 80% rule

stoprules=zeros(s,2);
Amps=zeros(n,s);

% Simulated Subjects Threshold
thresh=3;
```

```
h1=waitbar(0,['Monte Carlo Simulation of mSIAM_shr_Implemented ',num2str(s),'
subjects']);
tt=0;
ttot=0;
for i = 1:s
   ttot=ttot+tt;
   tic
   waitbar(i/s,h1,{['Monte Carlo Simulation of mSIAM_shr_Implemented
',num2str(s),' subjects.'] ['Estimated time remaining: ',num2str(ttot/i*(s-
i)/60,'%6.2f')]});
   j=1;
   % Flag that stops while loop
   flg=0;
   % Flag that indicates when 2% rule met
   flg02 = 0;
   % Flag that indicates when 5% rule met
   flg05 = 0;
   % Counts the number of Reversals
   rvrsl = 0;
   crvrsl = 0;
   newincr = incr;
   newAmp = Amp;
   h2=waitbar(0,['Monte Carlo Simulation of subject: ',num2str(i)]);
   while (j<=n && flg==0)
      oldAmp=newAmp;
      if j >1
         waitbar(j/n,h2,{['Monte Carlo Simulation of subject: ',num2str(i),' Trial:
',num2str(j),] ['2% Flag: ',num2str(flg02), ' 5% Flag: ',num2str(flg05), ' Average
Stop: ', num2str(mean(stoprules(1:i-1,1)))]});
      end
%****************************************
%***   Simulated Human Response CODE

      if x(j,i) == 1
         prob = newAmp*3/thresh;
         if rand < prob
            x(j,i)=0;
         end
      end

%****************************************
      if x(j,i) ~= 3

         if j >1
            none_3_indx = 1;
            last_none_3 = 3;
```

```
            while last_none_3 == 3
               if x(j-none_3_indx,i) ~= 3
                  last_none_3 = x(j-none_3_indx,i);
               end

               none_3_indx = none_3_indx + 1;

               if j-none_3_indx == 0 && last_none_3 == 3
                  last_none_3 = -1;
               end
            end
         end

         if j > 2 && j > none_3_indx
            nlast_none_3 = 3;
            while nlast_none_3 == 3
               if x(j-none_3_indx,i) ~=3
                  nlast_none_3 = x(j-none_3_indx,i);
               end

               none_3_indx = none_3_indx + 1;

               if j-none_3_indx == 0 && nlast_none_3 == 3
                  nlast_none_3 = -1;
               end
            end
         end
%**************Current HIT
         if j>2 && x(j,i) == 0
            switch last_none_3
               case 0
                  if rvrsl >=2
                     switch nlast_none_3
                        case 0
                           if hit_jump == 1
                              newincr=newincr*2;
                           end
                        case 1
                           newincr=newincr/2;
                           rvrsl = rvrsl+1;
                           crvrsl= crvrsl+1;
                        case 2
                           newincr=newincr/2;
                           rvrsl = rvrsl+1;
                           crvrsl= crvrsl+1;
                        case -1
```

```
                    otherwise
                        error(['Bad Program: 0 : ',num2str(last_none_3)])
                    end
                else
                    newincr=newincr*2;
                end

            case 1
                if rvrsl < 2
                    rvrsl = rvrsl+1;
                    crvrsl= crvrsl+1;
                end
            case 2
                if rvrsl < 2
                    rvrsl = rvrsl+1;
                    crvrsl= crvrsl+1;
                end
            case -1

            otherwise
                error(['Bad Program: 0 : ',num2str(last_none_3)])
        end
    end
%***********END of Current HIT

    if j>2 && x(j,i)==1
        switch last_none_3
            case 0
                if rvrsl >=2
                    if hit_jump
                        newincr=newincr/2;
                    end
                else
                    if nlast_none_3 == 0
                        newincr=newincr/2;
                    end
                end
                rvrsl = rvrsl+1;
                crvrsl= crvrsl+1;
            case 1
                newincr=newincr*2;

            case 2
                newincr=newincr*2;
            case -1
            otherwise
```

```
            error(['Bad Program: 1 : ',num2str(last_none_3)])
        end
    end

    if j>2 && x(j,i)==2
        switch last_none_3
            case 0
                if rvrsl >=2
                    if hit_jump
                        newincr=newincr/2;
                    end
                else
                    if nlast_none_3 == 0
                        newincr=newincr/2;
                    end
                end
                rvrsl = rvrsl+1;
                crvrsl= crvrsl+1;
            case 1
                newincr=newincr*2;

            case 2
                newincr=newincr*2;
            case -1
            otherwise
                error(['Bad Program: 1 : ',num2str(last_none_3)])
        end
    end
end
if crvrsl >= 4
    newincr=newincr/2;
    crvrsl=0;
end
switch x(j,i)
    case 0
        if j>1
            if last_none_3 == 0
                if rvrsl >=2
                    if nlast_none_3 == 0
                        if newAmp+newincr*hit < 0
                            newincr=newAmp/2;
                        end
                        newAmp=newAmp+newincr*hit;
                        hit_jump=1;
                    else
                        if newAmp+newincr*hit < 0
```

```
                    newincr=newAmp/2;
                 end
                 newAmp=newAmp+newincr*hit;
              end
           else
              if newAmp+newincr*hit < 0
                 newincr=newAmp/2;
              end
              newAmp=newAmp+newincr*hit;
           end
        else
           if newAmp+newincr*hit < 0
              newincr=newAmp/2;
           end
           newAmp=newAmp+newincr*hit;
        end
     else
        if newAmp+newincr*hit < 0
           newincr=newAmp/2;
        end
        newAmp=newAmp+newincr*hit;
     end
  case 1
     newAmp=newAmp+newincr*miss;
     hit_jump=0;
  case 2
     newAmp=newAmp+newincr*fls_alm;
     hit_jump=0;
  case 3
     newAmp=newAmp+newincr*cor_rej;
  otherwise
     error('Bad Program')
end
if newAmp <=0
  newAmp=oldAmp/2;
  newincr=oldAmp/2;
end
%       for k = 1:j+1
%          if y(k,i)==newAmp
%             total=total+1;
%             if x(k,i)==0
%                hits=hits+1;
%             end
%          end
%       end
%       if total > hit_total
```

```
        %           if hits/total > 0.8
        %              stoprules(i,3)=j;
        %              flghits=1;
        %           end
        %        end
        %        if flghits && flg02 && flg05
        %           flg = 1;
        %        end
        if (newincr/incr < .02 && flg02==0)
           stoprules(i,1)=j;
           stoprules(i,3)=newAmp;
           flg02=1;
        end
        if (newincr/incr < .05 && flg05==0)
           stoprules(i,2)=j;
           stoprules(i,4)=newAmp;
           flg05=1;
        end
        if flg02 && flg05
           flg = 1;
        end
        j=j+1;
     end
     if j>n
        if flg02 ~=1
           stoprules(i,1)=j;
           stoprules(i,3)=newAmp;
        end
        if flg05 ~=1
           stoprules(i,2)=j;
           stoprules(i,4)=newAmp;
        end
     end
     close(h2);
     tt=toc;
  end
  close(h1);

  function [Amps,stoprules] = t2IFCmPESTh(x,incr,n,s, Amp)

  % 0 - Detect First Period
  % 1 - Detect Second Period
  % 2 - Non-detect First Period
  % 3 - Non-detect Second Period
  % stoprules=zeros(s,3); % Include 80% rule
  stoprules=zeros(s,2);
```

```
Amps=zeros(n,s);
h1=waitbar(0,['Monte Carlo Simulation of 2IFC with mPEST for',num2str(s),'
subjects']);

for i = 1:s
   waitbar(i/s,h1);
   j=1;
   flg=0;
   flghits = 0;
   flgcor = 0;
   flg02 = 0;
   flg05 = 0;
   newincr = incr;
   newAmp = Amp;
   h2=waitbar(0,['Monte Carlo Simulation of subject: ',num2str(i)]);
   while (j<=n && flg==0)
      waitbar(j/n,h2,{['Monte Carlo Simulation of subject: ',num2str(i),' Trial:
',num2str(j),] ['0.02% Flag: ',num2str(flg02), ' 0.05% Flag: ',num2str(flg05), '
0.80% Flag: ',num2str(flghits)]});

      if j == 1
         if x(j,i) < 2
            newAmp = newAmp + newincr;
         end
      end
      if j>1 && j<=10
         if x(j,i) > 1
            if x(j-1,i) > 1
               if flgcor == 1
                  newincr = newincr*2;
               elseif flgcor == 0
                  newincr = newincr/2;
               end
               flgcor = 1;
               if (newAmp - newincr) < 0
                  newincr = newAmp/2;
               end
               newAmp = newAmp - newincr;
            end
         else
            if flgcor == 0
               newincr = newincr*2;
            end
            newAmp = newAmp + newincr;
            flgcor = 0;
         end
```

```
end
if j > 10
   if x(j,i) > 1
      if x(j-1,i) > 1
         if x(j-2,i) > 1
            if flgcor == 1
               newincr = newincr*2;
            elseif flgcor == 0
               newincr = newincr/2;
            end
            flgcor = 1;
            if (newAmp - newincr) < 0
               newincr = newAmp/2;
            end
            newAmp = newAmp - newincr;
         end
      end
   else
      if flgcor == 0
         newincr = newincr*2;
      end
      newAmp = newAmp + newincr;
      flgcor = 0;
   end
end

%        for k = 1:j+1
%           if y(k,i)==newAmp
%              total=total+1;
%              if x(k,i)==0
%                 hits=hits+1;
%              end
%           end
%        end
%        if total > hit_total
%           if hits/total > 0.8
%              stoprules(i,3)=j;
%              flghits=1;
%           end
%        end
%        if flghits && flg02 && flg05
%           flg = 1;
%        end
if (newincr/incr < .02 && flg02==0)
   stoprules(i,1)=j;
   stoprules(i,3)=newAmp;
```

```
            flg02=1;
        end
        if (newincr/incr < .05 && flg05==0)
            stoprules(i,2)=j;
            stoprules(i,4)=newAmp;
            flg05=1;
        end
        if flg02 && flg05
            flg = 1;
        end
        j=j+1;
    end
    if j>n
        if flg02 ~=1
            stoprules(i,1)=j;
            stoprules(i,3)=newAmp;
        end
        if flg05 ~=1
            stoprules(i,2)=j;
            stoprules(i,4)=newAmp;
        end
    end
    close(h2);
end
close(h1);

function [Amps,stoprules] = t2IFCmPESTh_shr(x,incr,n,s, Amp)

% 2 - Detect First Period
% 3 - Detect Second Period
% 0 - Non-detect First Period
% 1 - Non-detect Second Period
% stoprules=zeros(s,3); % Include 80% rule

stoprules=zeros(s,2);
Amps=zeros(n,s);
thresh = 3;
h1=waitbar(0,['Monte Carlo Simulation of 2IFC with mPEST for',num2str(s),'
subjects']);

for i = 1:s
    waitbar(i/s,h1);
    j=1;
    flg=0;
    flgcor = -1;
    flg02 = 0;
```

```
   flg05 = 0;
   newincr = incr;
   newAmp = Amp;
   h2=waitbar(0,['Monte Carlo Simulation of subject: ',num2str(i)]);
   while (j<=n && flg==0)
      waitbar(j/n,h2,{['Monte Carlo Simulation of subject: ',num2str(i),' Trial:
',num2str(j),] ['0.02% Flag: ',num2str(flg02), ' 0.05% Flag: ',num2str(flg05), '
Average Stop: ', num2str(mean(stoprules(1:i-1,1)))]});

%****************************************
%***   Simulated Human Response CODE
      if x(j,i) < 2
         prob = newAmp*3/thresh;
         if rand < prob
            if x(j,i) == 0
               x(j,i)=2;
            end
            if x(j,i) == 1
               x(j,i)=3;
            end
         end
      end
%****************************************
      if j == 1
         if x(j,i) < 2
            newAmp = newAmp + newincr;
         end
      end
      if j>1 && j<=10
         if x(j,i) > 1
            if x(j-1,i) > 1
               if flgcor == 1
                  newincr = newincr*2;
               elseif flgcor == 0
                  newincr = newincr/2;
               end
               flgcor = 1;
               if (newAmp - newincr) < 0
                  newincr = newAmp/2;
               end
               newAmp = newAmp - newincr;
            end
         else
            if flgcor == 0
               newincr = newincr*2;
            end
```

```
        newAmp = newAmp + newincr;
        flgcor = 0;
    end
end
if j > 10
    if x(j,i) > 1
        if x(j-1,i) > 1
            if x(j-2,i) > 1
                if flgcor == 1
                    newincr = newincr*2;
                elseif flgcor == 0
                    newincr = newincr/2;
                end
                flgcor = 1;
                if (newAmp - newincr) < 0
                    newincr = newAmp/2;
                end
                newAmp = newAmp - newincr;
            end
        end
    else
        if flgcor == 0
            newincr = newincr*2;
        end
        newAmp = newAmp + newincr;
        flgcor = 0;
    end
end

%       for k = 1:j+1
%           if y(k,i)==newAmp
%               total=total+1;
%               if x(k,i)==0
%                   hits=hits+1;
%               end
%           end
%       end
%       if total > hit_total
%           if hits/total > 0.8
%               stoprules(i,3)=j;
%               flghits=1;
%           end
%       end
%       if flghits && flg02 && flg05
%           flg = 1;
%       end
```

```
        if (newincr/incr < .02 && flg02==0)
            stoprules(i,1)=j;
            stoprules(i,3)=newAmp;
            flg02=1;
        end
        if (newincr/incr < .05 && flg05==0)
            stoprules(i,2)=j;
            stoprules(i,4)=newAmp;
            flg05=1;
        end
        if flg02 && flg05
            flg = 1;
        end
        j=j+1;
    end
    if j>n
        if flg02 ~=1
            stoprules(i,1)=j;
            stoprules(i,3)=newAmp;
        end
        if flg05 ~=1
            stoprules(i,2)=j;
            stoprules(i,4)=newAmp;
        end
    end
    close(h2);
end
close(h1);
```

APPENDIX P

ANKLE MODEL MATLAB® CODE

```
% main_Ankle.m
clear all
clear classes

global DEBUG_F Project_Folder Picture_Folder BW_flg Color_flg Grayscale_flg
File_Folder sim_name
Picture_Folder='Ankle_Pictures_Grayscale\';
File_Folder='E:\Current Projects\ASME\';
Project_Folder ='E:\Current Projects\Multi-Linked Systems';
addpath Project_Folder
DEBUG_F = 0;

sim_name='Ankle';
Grayscale_flg=1;
Color_flg=0;
BW_flg=0;

flnm='Ankle_2006082301';
dspfig=0;

%  Setup Limbs by length, width and height
%     Along repective axis as follows:
%              x     y     z

tibia=limb([474 20 39]);
talus=limb([20 25 39]);
calcaneus=limb([50 80 30]);

% l1=limb([474 39 20]);
% l2=limb([25 39 20]);
% l3=limb([13 32 80]);
% l4=limb([29 48 19]);

%  Setup joints by x,y,z translations from prox limb
%  Setup joints by psi(x), phi(y) rotations from prox limb
%  Setup final rotation about the revolute joint theta(z)
%  Setup joints by x,y,z translations to dist limb
%  Setup joints by psi(x), phi(y) rotations to dist limb
%  Setup final rotation about the revolute joint theta(z)

%j=joint(x,  y,  z,psi,phi,Theta,x,y,z,psi,phi,theta);
talocrural=joint(237,0,0,-16,-20,0,10,0,0,16,20,0);
subtalar=joint(10,0,0,-67,-41,0,25,0,5,67,41,0);
% j3=joint(7.5,0,-17,-80,0,0,18,-26,-20,-10,0,0);

rfoot=ml_sys(tibia,talocrural,talus,subtalar,calcaneus);
```

```
write_limb_joint_info(rfoot,flnm);

% Rotate To position 0
disp('Position ')
rfoot=build_v3(rfoot,0);
write_vertices_rotation(rfoot,0,0,0,flnm,3);

% Rotate To position 1
disp('Position 1')
rfoot=rotate_v4(rfoot,15,2,0);
write_vertices_rotation(rfoot,1,15,2,flnm,3);

% Rotate To position 2
disp('Position 2')
rfoot=rotate_v4(rfoot,-20,1,0);
write_vertices_rotation(rfoot,2,-20,1,flnm,3);

% Rotate To position 3
disp('Position 3')
rfoot=rotate_v4(rfoot,5,1,0);
write_vertices_rotation(rfoot,3,5,1,flnm,3);

% Rotate To position 4
disp('Position 4')
rfoot=rotate_v4(rfoot,-20,2,0);
write_vertices_rotation(rfoot,4,-20,2,flnm,3);

% Rotate To position 5
disp('Position 5')
rfoot=rotate_v4(rfoot,10,1,0);
write_vertices_rotation(rfoot,5,10,1,flnm,3);

% Rotate To position 6
disp('Position 6')
rfoot=rotate_v4(rfoot,-10,2,0);
write_vertices_rotation(rfoot,6,-10,2,flnm,3);

% Rotate To position 7
disp('Position 7')
rfoot=rotate_v4(rfoot,15,2,0);
write_vertices_rotation(rfoot,7,15,2,flnm,3);

% Rotate To position 8
disp('Position 8')
rfoot=rotate_v4(rfoot,5,1,0);
```

```
write_vertices_rotation(rfoot,8,5,1,flnm,3);

rfoot=rotate_movie(rfoot,'rotate_30_both_ankle',30,2,-30,1);
% % %
% % % rfoot=rotate_movie(rfoot,'rotate_30_back',30,1,-30,3);
rfoot=rotate_movie(rfoot,'rotate_30_back_ankle',-30,2,30,1);

%compare yaw pitch and role for all rotations
clc
clear all
clear classes

global DEBUG_F Project_Folder

Project_Folder ='E:\Current Projects\Multi-Linked Systems';
addpath Project_Folder
DEBUG_F = 0;

%  Setup Limbs by length, width and height
%     Along repective axis as follows:
%              x     y     z

l1=limb([100 40 40]);
l2=limb([80 30 30]);
l3=limb([60 20 20]);
l4=limb([30 10 10]);

% l1=limb([474 39 20]);
% l2=limb([25 39 20]);
% l3=limb([13 32 80]);
% l4=limb([29 48 19]);

%  Setup joints by x,y,z translations from prox limb
%  Setup joints by psi(x), phi(y) rotations from prox limb
%  Setup final rotation about the revolute joint theta(z)
%  Setup joints by x,y,z translations to dist limb
%  Setup joints by psi(x), phi(y) rotations to dist limb
%  Setup final rotation about the revolute joint theta(z)

%j=joint(x,  y,  z,psi,phi,Theta,x,y,z,psi,phi,theta);
j1=joint(237,0,-10,-15,-35,0,12.5,0,10,15,35,0);
j2=joint(12.5,0,0,0,0,0,7.5,0,0,0,0,0);
j3=joint(7.5,0,-17,-80,0,0,18,-26,-20,-10,0,0);

ml=ml_sys(l1,j1,l2,j2,l3,j3,l4);
```

```
m2 = ml_sys(ml);
ml=build_v3(ml,0);

% Creating a second multi linked system variable to run rotate without
% translations on
% compare_ml_2(ml,m2,1);
% compare_ml_2(ml,m2,2);
% compare_ml_2(ml,m2,3);
% compare_ml_2(ml,m2,4);


% ml=build(ml);
%
% ml=rotate(ml,-30,1);
%
% ml=rotate_v4(ml,30,1,0);
% compare_ml_2(ml,m2,1);
% compare_ml_2(ml,m2,2);
% compare_ml_2(ml,m2,3);
% compare_ml_2(ml,m2,4);
%
% ml=rotate_v4(ml,30,3,0);
%
% compare_ml_2(ml,m2,1);
% compare_ml_2(ml,m2,2);
% compare_ml_2(ml,m2,3);
% compare_ml_2(ml,m2,4);


% ml = rotate(ml,-30,3);

h1=waitbar(0/1,'Checking Rotations');
lim_d=180;
for i = -lim_d:1:lim_d
   waitbar((i+lim_d+1)/(2*lim_d+1),h1,['Checking Rotations:  ',num2str(i),'
degrees.'])
   ml=rotate_v4(ml,i,1,0);
   h2=waitbar(0/1,'Checking Rotations');
   for j = -lim_d:1:lim_d
      waitbar((j+lim_d+1)/(2*lim_d+1),h2,['Checking Rotations:  ',num2str(j),'
degrees.'])
      ml=rotate_v4(ml,j,3,0);
      for c=2:4
         f_flag = compare_ml_2(ml,m2,c);
         if f_flag == 0
```

```
            error(['At Joint 1: ',num2str(i),' degrees and Joint 3: ',num2str(j),'
degrees. ',...
                'There was an error in limb: ',num2str(c)])
          end
       end
       ml=rotate_v4(ml,-j,3,0);
    end
    close(h2)
    ml=rotate_v4(ml,-i,3,0);
end
close(h1)



%       A second different script that translates to origin but does not
%       store data

%       Run rotate_notrans

%       Translate back to original using previously stored translation
%       matrix

%
% ml=rotate(ml,30,3,-30,1);
%
% %   Find Bug with order
%
% ml=rotate(ml,30,1,-30,3);

%ml=rotate_movie(ml,'rotate_30_both',30,3,-30,1);
%
%ml=rotate_movie(ml,'rotate_30_back',30,1,-30,3);
% ml=rotate_movie(ml,'rotate_30_back',-30,3,30,1);

function ML  = build_v3(ML,displayf)
%   builds multi-linked system.
%   ML = build(v) creates a ml_sys object from the vector v,
%   containing: Contains
%

global DEBUG_F

if DEBUG_F
   disp('Entering Build_v3');
end
```

```
rotations = eye(4);

for count=1:ML.limb_num-1

   % Calc Yaw pitch and roll from Rotations

   center = get(get(ML.limbs(count), 'center'), 'vert_array');
   z_dc_y = get(get(ML.limbs(count),'y_unit'),'z')-center(3);
   z_dc_x = get(get(ML.limbs(count),'x_unit'),'z')-center(3);

   pitch = asin(rotations(1,2));
   yaw = -acos(rotations(1,1)/cos(asin(rotations(1,2))))*(z_dc_x/abs(z_dc_x));
   roll = -acos(rotations(2,2)/cos(asin(rotations(1,2))))*(z_dc_y/abs(z_dc_y));

   ML.limbs(count)=set(ML.limbs(count),'yaw',yaw,'pitch',pitch,'roll',roll);

   rotations=rotations*...
      (get(ML.joints(count),'x_axis_rotate_from_prox')* ...
      (get(ML.joints(count),'y_axis_rotate_from_prox')* ...
      (get(ML.joints(count),'z_axis_rotate_from_prox')* ...
      (get(ML.joints(count),'z_axis_rotate_to_dist')* ...
      (get(ML.joints(count),'y_axis_rotate_to_dist')* ...
      (get(ML.joints(count),'x_axis_rotate_to_dist')))))));

   % Limbs are translated and rotated from initial position

   ML.limb_vertices(1:4,(count)* ...
      ML.Points_per_Limb+1:ML.limb_num*ML.Points_per_Limb) = ...
      get(ML.joints(count),'Translate_from_prox')* ...
      (get(ML.joints(count),'x_axis_rotate_from_prox')* ...
      (get(ML.joints(count),'y_axis_rotate_from_prox')* ...
      (get(ML.joints(count),'z_axis_rotate_from_prox')* ...
      (get(ML.joints(count),'z_axis_rotate_to_dist')* ...
      (get(ML.joints(count),'y_axis_rotate_to_dist')* ...
      (get(ML.joints(count),'x_axis_rotate_to_dist')* ...
      (get(ML.joints(count),'Translate_to_dist')* ...
      ML.limb_vertices(1:4,(count)*ML.Points_per_Limb+1 ...
      :ML.limb_num*ML.Points_per_Limb))))))));
   ML=find_rpy_dc(ML,count);

end

ML=find_rpy_dc(ML,ML.limb_num);

center = get(get(ML.limbs(count), 'center'), 'vert_array');
```

```
z_dc_y = get(get(ML.limbs(count),'y_unit'),'z')-center(3);
z_dc_x = get(get(ML.limbs(count),'x_unit'),'z')-center(3);

pitch = asin(rotations(1,2));
yaw = -acos(rotations(1,1)/cos(asin(rotations(1,2))))*(z_dc_x/abs(z_dc_x));
roll = -acos(rotations(2,2)/cos(asin(rotations(1,2))))*(z_dc_y/abs(z_dc_y));

ML.limbs(ML.limb_num)=set(ML.limbs(ML.limb_num),'yaw',yaw,'pitch',pitch,'roll',r
oll);

ML=set(ML,'limb_vertices',ML.limb_vertices);

if displayf==1

   display_ml(ML,1);
end

if DEBUG_F
   disp('Leaving Build_v3');
end

function f_flag = compare_ml_2 (m1, m2, limb_num)

global DEBUG_F

% Constructs the translation matrix to take the rotate_notrans limb
% center to the origin.
Translate_Origin = eye(4);
Translate_Origin(1:4,4) = get(get(m1.limbs(limb_num),'center'),'vert_array');

% Translate the limb's center to the origin

limb_array2= get(m2.limbs(limb_num),'vertex_array_v');
limb_array3=limb_array2;

% disp('Back Calculated yaw pitch and roll')

bc_yaw = get(m1.limbs(limb_num),'bc_yaw');
bc_pitch = get(m1.limbs(limb_num),'bc_pitch');
bc_roll = get(m1.limbs(limb_num),'bc_roll');

y_axis_rotate = [ ...
   cos(bc_yaw),0,sin(bc_yaw),0; ...
   0,1,0,0; ...
   -sin(bc_yaw),0,cos(bc_yaw),0;0,0,0,1];
```

```
z_axis_rotate = [ ...
   cos(bc_pitch),-sin(bc_pitch),0,0; ...
   sin(bc_pitch),cos(bc_pitch),0,0; ...
   0,0,1,0;0,0,0,1];

x_axis_rotate = [1,0,0,0; ...
   0,cos(bc_roll),-sin(bc_roll),0; ...
   0,sin(bc_roll),cos(bc_roll),0;0,0,0,1];

limb_array2 = ...
   Translate_Origin * ...
   (inv(x_axis_rotate) * ...
   (inv(z_axis_rotate) * ...
   (inv(y_axis_rotate) * ...
   limb_array2)));

limb_array1 = get_limb_array(m1,limb_num);

test_1 = round(limb_array1*1000) == round(limb_array2*1000);

% disp('Rotation Yaw pitch and roll')

yaw = get(m1.limbs(limb_num),'yaw');
pitch = get(m1.limbs(limb_num),'pitch');
roll = get(m1.limbs(limb_num),'roll');

y_axis_rotate = [ ...
   cos(yaw),0,sin(yaw),0; ...
   0,1,0,0; ...
   -sin(yaw),0,cos(yaw),0;0,0,0,1];

z_axis_rotate = [ ...
   cos(pitch),-sin(pitch),0,0; ...
   sin(pitch),cos(pitch),0,0; ...
   0,0,1,0;0,0,0,1];

x_axis_rotate = [1,0,0,0; ...
   0,cos(roll),-sin(roll),0; ...
   0,sin(roll),cos(roll),0;0,0,0,1];

limb_array3 = ...
   Translate_Origin * ...
   (inv(x_axis_rotate) * ...
   (inv(z_axis_rotate) * ...
   (inv(y_axis_rotate) * ...
   limb_array3)));
```

```
test_2 = round(limb_array1*1000) == round(limb_array3*1000);

test_3 = round(limb_array2*1000) == round(limb_array3*1000);

% if test_2 == test_1
if test_2
   f_flag=1;
else
   disp('boo')
   bc_yaw
   bc_pitch
   bc_roll
   limb_array2
   test_1
   limb_array1
   test_2
   limb_array3
   yaw
   pitch
   roll
   f_flag=0;
   test_3
end

function display_ml(ML,flg,rot)
%  display multi-linked system.
%
%
global  sim_name DEBUG_F
%      Position of Vertices of Distal Limb with respect to the joint

if (flg == 1)
   figure
end
for count=1:ML.limb_num

   sim_horz((count-1)*8+1:(count-1)* ...
      8+8,1:3) = ...
      get(ML.limbs(count), ...
      'vertex_array_h');

   sim_face((count-1)*6+1:(count-1)*6+6,1:4) = get(ML.limbs(count), ...
      'faces')+8*(count-1);

end
```

```
% Color
patch('Vertices',sim_horz,'Faces',sim_face,...
   'FaceVertexCData',hsv(ML.limb_num*6),'FaceColor','flat')

% h=axes('CameraPosition',[350 125 70]);
% %set(h,'YDir','rev');
% set(h,'NextPlot','replace');
switch sim_name
   case 'Ankle'
      % Ankle
      axis([120 320 -100 100 -100 100 0 1])
      %  Back of Ankle
      view(21+rot,44+rot);
      % Front of ANkle
      %view(-148+rot,-43+rot);
      % view(-128+rot,-50+rot);

   case 'Crab'
      % Crab axis
      axis([-5 15 -5 15 -5 15 0 1])
      % axis([-300 300 -300 300 -300 300 0 1])
      % Crab Leg
      view(-55+rot,-31+rot);
      %view(150+rot,-23+rot);

   otherwise
      error('Bad sim_name');
end

xlabel('X')
ylabel('Y')
zlabel('Z')
drawnow

function display_save_ml(ML,flg,rot,flnm,pos)
%   display multi-linked system.
%
%
global DEBUG_F Project_Folder Picture_Folder BW_flg Color_flg Grayscale_flg
File_Folder sim_name
%      Position of Vertices of Distal Limb with respect to the joint

if (flg == 1 || flg == 2)
   h1=figure;
end
```

```
for count=1:ML.limb_num

   sim_horz((count-1)*8+1:(count-1)* ...
      8+8,1:3) = ...
      get(ML.limbs(count), ...
      'vertex_array_h');

   sim_face((count-1)*6+1:(count-1)*6+6,1:4) = get(ML.limbs(count), ...
      'faces')+8*(count-1);

end
% h=axes('CameraPosition',[350 125 70]);
%set(h,'YDir','rev');
% set(h,'NextPlot','replace');
% axis([-10 10 -10 10 -10 10 0 1])
% axis([-17 17 -17 17 -17 17 0 1])

if Color_flg

   % Color
   patch('Vertices',sim_horz,'Faces',sim_face,...
      'FaceVertexCData',hsv(ML.limb_num*6),'FaceColor','flat')

end

% Black and White
if BW_flg
   patch('Vertices',sim_horz,'Faces',sim_face,...
      'FaceVertexCData',white(ML.limb_num*6),'FaceColor','flat')

end

%  Gray Scale
if Grayscale_flg

   patch('Vertices',sim_horz,'Faces',sim_face,...
      'FaceVertexCData',gray(ML.limb_num*6),'FaceColor','flat')
end
switch sim_name
   case 'Ankle'
      % Ankle
      axis([120 320 -100 100 -100 100 0 1])
      %  Back of Ankle
      view(21+rot,44+rot);
      % Front of ANkle
```

```
        %view(-148+rot,-43+rot);
        % view(-128+rot,-50+rot);

    case 'Crab'
        % Crab axis
        axis([-5 15 -5 15 -5 15 0 1])
        % axis([-300 300 -300 300 -300 300 0 1])
        % Crab Leg
        view(-55+rot,-31+rot);
        %view(127+rot,-23+rot);

    otherwise
        error('Bad sim_name');
end



xlabel('X')
ylabel('Y')
zlabel('Z')
drawnow


if (flg == 3 || flg == 2)
    saveas(gcf,[File_Folder,Picture_Folder,flnm,'_Pos_',num2str(pos),'.emf']);
    saveas(gcf,[File_Folder,Picture_Folder,flnm,'_Pos_',num2str(pos),'.jpg']);
    saveas(gcf,[File_Folder,Picture_Folder,flnm,'_Pos_',num2str(pos),'.tif']);
    if flg ==3
        close(gcf)
    end
end

function ML  = display_vert(ML)
%   builds multi-linked system.
%   ML = build(v) creates a ml_sys object from the vector v,
%   containing: Contains
%

global DEBUG_F



for count=1:ML.limb_num
```

```
   disp(['Limb: ',num2str(count)])
   list_vertices(ML.limbs(count))

end

function display_vert_conf(ML,pos)
%  writes multi-linked system.
%  display_vert_conf(ML,pos) writes limb coord to file
%

global DEBUG_F



header= {'Position' 'End Segment 1' ' ' ' ' ' 'Joint #1' ' ' ' ' ' 'Segment #2 Center' ' ' ' '
'Joint #2' ' ' ' ' 'Segment #3 Center' ' ' ' '; ' ' 'x' 'y' 'z' 'x' 'y' 'z' 'x' 'y' 'z' 'x' 'y' 'z' 'x' 'y'
'z'};

sprdsht = cell(1,16);



   sprdsht(1,1)= cellstr(num2str(pos));
   sprdsht(1,2:4)=num2cell(get(get(ML.limbs(10),'x_face'),'horz_array'));
   sprdsht(1,5:7)=num2cell(get(get(ML.limbs(8),'x_face'),'horz_array'));
   sprdsht(1,8:10)=num2cell(get(get(ML.limbs(7),'center'),'horz_array'));
   sprdsht(1,11:13)=num2cell(get(get(ML.limbs(5),'x_face'),'horz_array'));
   sprdsht(1,14:16)=num2cell(get(get(ML.limbs(4),'center'),'horz_array'));


xlswrite('E:\Current Projects\ASME\BioKinWorkbook2006.xls',header,'Conf
1','A1');
xlswrite('E:\Current Projects\ASME\BioKinWorkbook2006.xls',sprdsht,'Conf
1',['A',num2str(3+pos)]);

function ML = find_rpy_dc(ML, limb_num)
global DEBUG_F
outpt = get(ML.limbs(limb_num), 'center');
center = get(outpt, 'vert_array');

global DEBUG_F

if DEBUG_F
   disp('Entering find_rpy_dc');
end
```

```
% Constructs the translation matrix to take the rotate_notrans limb
% center to the origin.
Translate_Origin = eye(4);
Translate_Origin(1:4,4) = center;

% Translate the limb's center to the origin
limb_vertices = get(ML.limbs(limb_num),'vertex_array_v');
limb_vertices = inv(Translate_Origin) * limb_vertices;

if DEBUG_F
   disp('find_rpy_dc');
   limb_vertices
end

%*****************************************************
%  Main yaw, Pitch and roll Find
%      must be done in order:
%          roll, pitch, and yaw
% axis_vector=limb_vertices(1:3,11);
%
% x_dc_o = axis_vector(1)/norm(axis_vector)
% y_dc_o = axis_vector(2)/norm(axis_vector)
% z_dc_o = axis_vector(3)/norm(axis_vector)


x_dc = get(get(ML.limbs(limb_num),'y_unit'),'x')-center(1);
y_dc = get(get(ML.limbs(limb_num),'y_unit'),'y')-center(2);
z_dc = get(get(ML.limbs(limb_num),'y_unit'),'z')-center(3);

u_prime_mag = norm([y_dc,z_dc]);

%  Negative sign added so that a clockwise rotation occurs for positve
%  angle instead of counterclockwise
roll = -acos(dot([0,y_dc,z_dc],[0,1,0])/norm([0,y_dc,z_dc]))*(z_dc/abs(z_dc));

x_axis_rotate = [1,0,0,0; ...
   0,cos(roll),-sin(roll),0; ...
   0,sin(roll),cos(roll),0;0,0,0,1];

limb_vertices = ...
   (x_axis_rotate * ...
   limb_vertices);

if DEBUG_F == 1
   disp('find_rpy_dc: X-axis rotation: Align y_unit with xy plane')
```

```
   limb_vertices
end

pitch =
acos(dot([x_dc,u_prime_mag,0],[0,1,0])/norm([x_dc,u_prime_mag,0]))*(x_dc/abs(
x_dc));

z_axis_rotate = [ ...
   cos(pitch),-sin(pitch),0,0; ...
   sin(pitch),cos(pitch),0,0; ...
   0,0,1,0;0,0,0,1];

limb_vertices = ...
   (z_axis_rotate * ...
   limb_vertices);

if DEBUG_F == 1
   disp('find_rpy_dc: Z-axis rotation: Align y_unit with Y axis and x_unit with xz
plane')
   limb_vertices
end

% axis_vector=limb_vertices(1:3,10);
%
% x_dc = axis_vector(1)/norm(axis_vector);
% y_dc = axis_vector(2)/norm(axis_vector);
% z_dc = axis_vector(3)/norm(axis_vector);


x_dc = limb_vertices(1,13);
% y_dc = limb_vertices(2,13);
z_dc = limb_vertices(3,13);

yaw = acos(dot([x_dc,0,z_dc],[1,0,0])/norm([x_dc,0,z_dc]))*(z_dc/abs(z_dc));

y_axis_rotate = [ ...
   cos(yaw),0,sin(yaw),0; ...
   0,1,0,0; ...
   -sin(yaw),0,cos(yaw),0;0,0,0,1];

limb_vertices = ...
   (y_axis_rotate * ...
   limb_vertices);

if DEBUG_F == 1
   disp('find_rpy_dc: Y-axis rotation: Align x_unit with X axis')
```

```
   limb_vertices
end

ML.limbs(limb_num)=set(ML.limbs(limb_num),'bc_yaw',yaw,'bc_pitch',pitch,'bc_r
oll',roll);

if DEBUG_F
   disp('Leaving find_rpy_dc');
end

function outpt = get(Var_ML_sys, data_req)
%ML_sys  get function.
%  Returns variable depending on request.
%
global DEBUG_F
switch data_req
   case 'limb_vertices'
      outpt = Var_ML_sys.limb_vertices;

   otherwise
      error([data_req,' Is not a valid asset property'])
end

function outpt = get_limb_array(Var_ML_sys, limb_num)
% Retrieves the vertex_array_v of the desired limb and outputs it.
global DEBUG_F
outpt = get(Var_ML_sys.limbs(limb_num),'vertex_array_v');

function list_vertices(ML)
%  list all variables and values

global DEBUG_F

disp('Vertices: (x, y, z)')
disp(['L.topface_ul: ',list_xyz(L.topface_ul)])
disp(['L.topface_ur: ',list_xyz(L.topface_ur)])
disp(['L.topface_bl: ',list_xyz(L.topface_bl)])
disp(['L.topface_br: ',list_xyz(L.topface_br)])
disp(['L.bottomface_ul: ',list_xyz(L.bottomface_ul)])
disp(['L.bottomface_ub: ',list_xyz(L.bottomface_ur)])
disp(['L.bottomface_bl: ',list_xyz(L.bottomface_bl)])
disp(['L.bottomface_br: ',list_xyz(L.bottomface_br)])
disp('Center')
disp(['L.center: ',list_xyz(L.center)])
disp('Center of Faces on positive axis')
disp(['L.x_face: ',list_xyz(L.x_face)])
```

```
disp(['L.y_face: ',list_xyz(L.y_face)])
disp(['L.z_face: ',list_xyz(L.z_face)])

function ML  = ml_sys(varargin)
%ml_sys class constructor.
%   ML = ml_sys(v) creates a ml_sys object from the vector v,
%   containing: Contains ml_sys
%
global DEBUG_F
if nargin == 0
   ML.c = [];
   ML = class(ML,'ml_sys');
else
   if isa(varargin{1},'ml_sys')
      ML = varargin{1};
   else
      ML.Points_per_Limb = 16;
      Var_Updates = varargin;

      ML.limbs(1) = Var_Updates{1};
      ML.joints(1) = Var_Updates{2};
      ML.limbs(2) = Var_Updates{3};
      Var_Updates = Var_Updates(4:end);
      ML.limbs(1) = set(ML.limbs(1),'dist_joint',get(ML.joints(1),'dist_joint'));

      ind = 2;

      while length(Var_Updates) >=2
         ML.joints(ind) = Var_Updates{1};
         ML.limbs(ind) =
set(ML.limbs(ind),'dist_joint',get(ML.joints(ind),'dist_joint'));
         ind=ind+1;
         ML.limbs(ind) = Var_Updates{2};
         Var_Updates = Var_Updates(3:end);

      end

      ML.limb_num = ind;



      for count=1:ind
         ML.limb_vertices(1:4,1+(ML.Points_per_Limb*(count-1)): ...
            ML.Points_per_Limb+(ML.Points_per_Limb*(count-1)))= ...
            get(ML.limbs(count),'vertex_array_v');
      end
```

```
      ML = class(ML,'ml_sys');
   end

end

function write_vertices_rotation(ML,pos,rot,jnt,flnm,flg)
%  writes multi-linked system.
%  display_vert_conf(ML,pos) writes limb coord to file
%

global DEBUG_F File_Folder

h_h=cell(3+ML.limb_num,16);


header_l1= {'Position:'  num2str(pos) 'Rotation: ' num2str(rot) 'Joint: '
num2str(jnt)};
header_l2= {'Segment' 'Center' ' ' ' ' 'X vector' ' ' ' ' 'Y Vector' ' ' ' ' 'Z vector' ' ' ' '
'Orientation' ' ' ' ' 'Distal Joint'};
header_l3= {' ' 'x' 'y' 'z' 'x' 'y' 'z' 'x' 'y' 'z' 'x' 'y' 'z' 'Yaw' 'Pitch' 'Roll' 'x' 'y' 'z'};

h_h(1,1:6) = header_l1;
h_h(2,1:17) = header_l2;
h_h(3,1:19) = header_l3;

for i = 1:ML.limb_num

   h_h(i+3,1)= cellstr(num2str(i));
   h_h(i+3,2:4)=num2cell(get(get(ML.limbs(i),'center'),'horz_array'));
   h_h(i+3,5:7)=num2cell(get(get(ML.limbs(i),'x_face'),'horz_array'));
   h_h(i+3,8:10)=num2cell(get(get(ML.limbs(i),'y_face'),'horz_array'));
   h_h(i+3,11:13)=num2cell(get(get(ML.limbs(i),'z_face'),'horz_array'));
   h_h(i+3,17:19)=num2cell(get(get(ML.limbs(i),'dist_joint'),'horz_array'));
   h_h(i+3,14)=num2cell(get(ML.limbs(i),'yaw')*180/pi);
   h_h(i+3,15)=num2cell(get(ML.limbs(i),'pitch')*180/pi);
   h_h(i+3,16)=num2cell(get(ML.limbs(i),'roll')*180/pi);

end

xlswrite([File_Folder,flnm,'.xls'],h_h,['Pos', num2str(pos)],'A1');

if (flg >=1 && flg <=3)
   display_save_ml(ML,flg,0,flnm,pos);
end
```

```
function Var_ML_sys = rotate_movie_EMBC(Var_ML_sys,name)
%Joint Rotator movie maker about the revolu Joint.
%   J = rotate(Var_ML_sys,degrees) Rotates distal limb
%   containing: Contains degrees
%
global DEBUG_F Project_Folder
folder = 'E:\Current Projects\Multi-Linked Systems\movies\';

movie = avifile([folder,name,'.avi']);
fig=figure;
set(fig,'DoubleBuffer','on');

incr=1/4;

for i=0:incr:90
   for j=1:Var_ML_sys.limb_num-1
      switch j
         case 1
            degrees=incr;
         case 2
            if i<30
               degrees=-incr;
            elseif i<45
               degrees=0;
            elseif i<70
               degrees=incr;
            else
               degrees=0;
            end
         case 3
            if i<10
               degrees=0;
            elseif i<30
               degrees=-incr;
            elseif i<60
               degrees=0;
            else
               degrees=incr;
            end
         otherwise
            error('Error: rotate movie_EMBC.m - No Such Joint');
      end

      joint=j;

      if degrees>0
```

```
            for k=incr:incr:degrees
                Var_ML_sys = rotate_v4(Var_ML_sys, incr, joint,0);
                display_ml(Var_ML_sys,0,0);
                drawnow
                f = getframe(gca);
                movie = addframe(movie,f);
                cla
            end
        end
        if degrees<0
            for k=-incr:-incr:degrees
                Var_ML_sys = rotate_v4(Var_ML_sys, -incr,joint,0);
                display_ml(Var_ML_sys,0,0);
                drawnow
                f = getframe(gca);
                movie = addframe(movie,f);
                cla
            end
        end
    end
end
for rep=1:3
    for i=1:2

        if i==1
            degrees=75;
        else
            degrees=-75;
        end

        joint=3;

        if degrees>0
            for k=incr:incr:degrees
                Var_ML_sys = rotate_v4(Var_ML_sys, incr, joint,0);
                display_ml(Var_ML_sys,0,0);
                drawnow
                f = getframe(gca);
                movie = addframe(movie,f);
                cla
            end
        end
        if degrees<0
            for k=-incr:-incr:degrees
                Var_ML_sys = rotate_v4(Var_ML_sys, -incr,joint,0);
                display_ml(Var_ML_sys,0,0);
```

```
            drawnow
            f = getframe(gca);
            movie = addframe(movie,f);
            cla
          end
        end

    end
end
movie = close(movie);
close

function Var_ML_sys = rotate_v4(Var_ML_sys,varargin)
%Joint Rotator about the revolute Joint.
%  J = rotate(Var_ML_sys,degrees,joint) Rotates distal limb
%  containing: Contains degrees,joint
%

global DEBUG_F

if DEBUG_F
   disp('Entering rotate_v4');
end

Var_Updates = varargin;
while length(Var_Updates) >=2

   axis_position = eye(4);


   displayf=Var_Updates{length(Var_Updates)};
   theta=Var_Updates{1}*pi/180;
   joint=Var_Updates{2};
   Var_Updates = Var_Updates(3:end);
   rev_rotate = [ ...
      cos(theta),-sin(theta),0,0; ...
      sin(theta),cos(theta),0,0; ...
      0,0,1,0;0,0,0,1];

   axis_position(1,4) =
Var_ML_sys.limb_vertices(1,(joint)*Var_ML_sys.Points_per_Limb);
   axis_position(2,4) =
Var_ML_sys.limb_vertices(2,(joint)*Var_ML_sys.Points_per_Limb);
   axis_position(3,4) =
Var_ML_sys.limb_vertices(3,(joint)*Var_ML_sys.Points_per_Limb);
```

```
Var_ML_sys.limb_vertices(1:4,(joint)*Var_ML_sys.Points_per_Limb+1 ...
   :Var_ML_sys.limb_num*Var_ML_sys.Points_per_Limb) = ...
   (inv(axis_position)* ...
   Var_ML_sys.limb_vertices(1:4,(joint)*Var_ML_sys.Points_per_Limb+1 ...
   :Var_ML_sys.limb_num*Var_ML_sys.Points_per_Limb));

for count=1:joint


   % Translate to Joint

   Var_ML_sys.limb_vertices(1:4,(joint)*Var_ML_sys.Points_per_Limb+1 ...
      :Var_ML_sys.limb_num*Var_ML_sys.Points_per_Limb) = ...
      (inv(get(Var_ML_sys.joints(count),'y_axis_rotate_from_prox'))* ...
      (inv(get(Var_ML_sys.joints(count),'x_axis_rotate_from_prox'))* ...
      Var_ML_sys.limb_vertices(1:4,(joint)*Var_ML_sys.Points_per_Limb+1 ...
      :Var_ML_sys.limb_num*Var_ML_sys.Points_per_Limb)));

   if count==joint

      %  Rotates around Arbitrary Axis then Translates back to Proximal
Member

      Var_ML_sys.limb_vertices(1:4,(joint)*Var_ML_sys.Points_per_Limb+1 ...
         :Var_ML_sys.limb_num*Var_ML_sys.Points_per_Limb) = ...
         (get(Var_ML_sys.joints(joint),'x_axis_rotate_from_prox')* ...
         (get(Var_ML_sys.joints(joint),'y_axis_rotate_from_prox')* ...
         (rev_rotate* ...
         Var_ML_sys.limb_vertices(1:4,(joint)*Var_ML_sys.Points_per_Limb+1
...
         :Var_ML_sys.limb_num*Var_ML_sys.Points_per_Limb))));

      % Sets the new Rotation about the Z-axis into Joint Specs

      theta=get(Var_ML_sys.joints(joint),'R_theta_from_prox')+theta;
      rev_rotate = [ ...
         cos(theta),-sin(theta),0,0; ...
         sin(theta),cos(theta),0,0; ...
         0,0,1,0;0,0,0,1];
      Var_ML_sys.joints(joint)=set(Var_ML_sys.joints(joint), ...
         'z_axis_rotate_from_prox',rev_rotate,'R_theta_from_prox',theta);

   else

      % Continues Propagation to Joint to be rotated
```

```
        Var_ML_sys.limb_vertices(1:4,(joint)*Var_ML_sys.Points_per_Limb+1 ...
          :Var_ML_sys.limb_num*Var_ML_sys.Points_per_Limb) = ...
          (inv(get(Var_ML_sys.joints(count),'x_axis_rotate_to_dist'))* ...
          (inv(get(Var_ML_sys.joints(count),'y_axis_rotate_to_dist'))* ...
          (inv(get(Var_ML_sys.joints(count),'z_axis_rotate_to_dist'))* ...
          (inv(get(Var_ML_sys.joints(count),'z_axis_rotate_from_prox'))* ...
          Var_ML_sys.limb_vertices(1:4,(joint)*Var_ML_sys.Points_per_Limb+1
...
          :Var_ML_sys.limb_num*Var_ML_sys.Points_per_Limb)))));
      end
    end

    for count=joint-1:-1:1

      % Translate back from Rotated Joint

      Var_ML_sys.limb_vertices(1:4,(joint)*Var_ML_sys.Points_per_Limb+1 ...
        :Var_ML_sys.limb_num*Var_ML_sys.Points_per_Limb) = ...
        (get(Var_ML_sys.joints(count),'x_axis_rotate_from_prox')* ...
        (get(Var_ML_sys.joints(count),'y_axis_rotate_from_prox')* ...
        (get(Var_ML_sys.joints(count),'z_axis_rotate_from_prox')* ...
        (get(Var_ML_sys.joints(count),'z_axis_rotate_to_dist')* ...
        (get(Var_ML_sys.joints(count),'y_axis_rotate_to_dist')* ...
        (get(Var_ML_sys.joints(count),'x_axis_rotate_to_dist')* ...
        Var_ML_sys.limb_vertices(1:4,(joint)*Var_ML_sys.Points_per_Limb+1 ...
        :Var_ML_sys.limb_num*Var_ML_sys.Points_per_Limb)))))));

    end

    Var_ML_sys.limb_vertices(1:4,(joint)*Var_ML_sys.Points_per_Limb+1 ...
      :Var_ML_sys.limb_num*Var_ML_sys.Points_per_Limb) = ...
      (axis_position* ...
      Var_ML_sys.limb_vertices(1:4,(joint)*Var_ML_sys.Points_per_Limb+1 ...
      :Var_ML_sys.limb_num*Var_ML_sys.Points_per_Limb));

    Var_ML_sys=set(Var_ML_sys,'limb_vertices',Var_ML_sys.limb_vertices);

    if displayf==1
      display_ml(Var_ML_sys,1,0);
    end

    rotations = eye(4);
    Translate_Origin = eye(4);

    for count=1:Var_ML_sys.limb_num
```

```
Var_ML_sys=find_rpy_dc(Var_ML_sys,count);

center = get(get(Var_ML_sys.limbs(count), 'center'), 'vert_array');
limb_vertices = get(Var_ML_sys.limbs(count),'vertex_array_v');
Translate_Origin = eye(4);
Translate_Origin(1:4,4) = center;

limb_vertices = inv(Translate_Origin) * limb_vertices;
if DEBUG_F
   disp('Entering Rotate_v4: ypr section');
   limb_vertices
end


z_dc_y = get(get(Var_ML_sys.limbs(count),'y_unit'),'z')-center(3);
z_dc_x = get(get(Var_ML_sys.limbs(count),'x_unit'),'z')-center(3);

pitch = asin(rotations(1,2));
roll = -acos(rotations(2,2)/cos(asin(rotations(1,2))))*(z_dc_y/abs(z_dc_y));

x_axis_rotate = [1,0,0,0; ...
   0,cos(roll),-sin(roll),0; ...
   0,sin(roll),cos(roll),0;0,0,0,1];
limb_vertices = ...
   (x_axis_rotate * ...
   limb_vertices);

if DEBUG_F
   disp('Rotate_v4: X-axis rotation: Align y_unit with xy plane')
   limb_vertices

end

z_axis_rotate = [ ...
   cos(pitch),-sin(pitch),0,0; ...
   sin(pitch),cos(pitch),0,0; ...
   0,0,1,0;0,0,0,1];
limb_vertices = ...
   (z_axis_rotate * ...
   limb_vertices);

if DEBUG_F
   disp('Rotate_v4: Z-axis rotation: Align y_unit with Y axis and x_unit with
xz plane')
   limb_vertices
end
```

```
        x_dc_x = limb_vertices(1,13);
        % y_dc_x = limb_vertices(2,13);
        z_dc_x = limb_vertices(3,13);

        yaw = acos(rotations(1,1)/cos(asin(rotations(1,2))))*(z_dc_x/abs(z_dc_x));

        if DEBUG_F
           disp('Rotate_v4: Y-axis rotation: Align x_unit with X axis')
           y_axis_rotate = [ ...
              cos(yaw),0,sin(yaw),0; ...
              0,1,0,0; ...
              -sin(yaw),0,cos(yaw),0;0,0,0,1];

           limb_vertices = ...
              (y_axis_rotate * ...
              limb_vertices)
        end


Var_ML_sys.limbs(count)=set(Var_ML_sys.limbs(count),'yaw',yaw,'pitch',pitch,'ro
ll',roll);

        if count<Var_ML_sys.limb_num

           rotations=rotations*...
              (get(Var_ML_sys.joints(count),'x_axis_rotate_from_prox')* ...
              (get(Var_ML_sys.joints(count),'y_axis_rotate_from_prox')* ...
              (get(Var_ML_sys.joints(count),'z_axis_rotate_from_prox')* ...
              (get(Var_ML_sys.joints(count),'z_axis_rotate_to_dist')* ...
              (get(Var_ML_sys.joints(count),'y_axis_rotate_to_dist')* ...
              (get(Var_ML_sys.joints(count),'x_axis_rotate_to_dist')))))));
        end

     end

  end

  if DEBUG_F
     disp('leaving rotate_v4');
  end

  function Var_ML_sys = set(Var_ML_sys, varargin)
  %ML_sys  set function.
  %   Sets Variable depending on request.
  %
```

```
global DEBUG_F
Var_Updates = varargin;
while length(Var_Updates) >=2
   data_type = Var_Updates{1};
   data_in = Var_Updates{2};
   Var_Updates = Var_Updates(3:end);
   switch data_type
      case 'limb_vertices'
         for count=1:Var_ML_sys.limb_num;

            Var_ML_sys.limbs(count) = set(Var_ML_sys.limbs(count), ...
               'vertex_array_v', ...
               data_in(1:3,1+(count-1)*Var_ML_sys.Points_per_Limb: ...
               Var_ML_sys.Points_per_Limb+(count-1)* ...
               Var_ML_sys.Points_per_Limb));

         end
      otherwise
         error([data_type,' Is not a valid asset property'])
   end
end

function outpt = set_limb_array(Var_ML_sys, limb_num,vert_arr_v)
% Retrieves the vertex_array_v of the desired limb and outputs it.
global DEBUG_F
set(Var_ML_sys.limbs(limb_num),'vertex_array_v',vert_arr_v);
outpt=Var_ML_sys;

function write_limb_joint_info(ML,flnm)
%  builds multi-linked system.
%  ML = build(v) creates a ml_sys object from the vector v,
%  containing: Contains
%

global DEBUG_F Project_Folder File_Folder



header_l= {'Limb Number' 'Length' 'Width' 'Height'};
header_j= {'Joint Number' 'x from prox' 'y from prox' 'z from prox' 'psi from prox'
'phi from prox' 'theta from prox' 'x to dist' 'y to dist' 'z to dist' 'psi to dist' 'phi to dist'
'theta to dist'};

sprdsht_l = cell(1+ML.limb_num,4);
sprdsht_j = cell(ML.limb_num,13);
```

```
sprdsht_l(1,1:4)=header_l;
sprdsht_j(1,1:13)=header_j;

sprdsht_l(2,1)= cellstr(num2str(1));
sprdsht_l(2,2)=num2cell(get(ML.limbs(1),'length'));
sprdsht_l(2,3)=num2cell(get(ML.limbs(1),'width'));
sprdsht_l(2,4)=num2cell(get(ML.limbs(1),'height'));

for i = 2:ML.limb_num

   sprdsht_l(i+1,1)= cellstr(num2str(i));
   sprdsht_j(i,1)= cellstr(num2str(i-1));

   sprdsht_l(i+1,2)=num2cell(get(ML.limbs(i),'length'));
   sprdsht_l(i+1,3)=num2cell(get(ML.limbs(i),'width'));
   sprdsht_l(i+1,4)=num2cell(get(ML.limbs(i),'height'));

   sprdsht_j(i,2)=num2cell(get(ML.joints(i-1),'Tx_from_prox'));
   sprdsht_j(i,3)=num2cell(get(ML.joints(i-1),'Ty_from_prox'));
   sprdsht_j(i,4)=num2cell(get(ML.joints(i-1),'Tz_from_prox'));

   sprdsht_j(i,5)=num2cell(get(ML.joints(i-1),'R_psi_from_prox')*180/pi);
   sprdsht_j(i,6)=num2cell(get(ML.joints(i-1),'R_phi_from_prox')*180/pi);
   sprdsht_j(i,7)=num2cell(get(ML.joints(i-1),'R_theta_from_prox')*180/pi);

   sprdsht_j(i,8)=num2cell(get(ML.joints(i-1),'Tx_to_dist'));
   sprdsht_j(i,9)=num2cell(get(ML.joints(i-1),'Ty_to_dist'));
   sprdsht_j(i,10)=num2cell(get(ML.joints(i-1),'Tz_to_dist'));

   sprdsht_j(i,11)=num2cell(get(ML.joints(i-1),'R_psi_to_dist')*180/pi);
   sprdsht_j(i,12)=num2cell(get(ML.joints(i-1),'R_phi_to_dist')*180/pi);
   sprdsht_j(i,13)=num2cell(get(ML.joints(i-1),'R_theta_to_dist')*180/pi);


end

   xlswrite([File_Folder,flnm,'.xls'],sprdsht_l,'Limbs','A1');
   xlswrite([File_Folder,flnm,'.xls'],sprdsht_j,'Joints','A1');


% xlswrite('E:\Current Projects\ASME\BioKinWorkbook2006.xls',header,'Conf
1','A1');
% xlswrite('E:\Current Projects\ASME\BioKinWorkbook2006.xls',sprdsht,'Conf
1',['A',num2str(3+pos)]);
```

```
function write_vertices_rotation(ML,pos,rot,jnt,flnm,flg)
%  writes multi-linked system.
%  display_vert_conf(ML,pos) writes limb coord to file
%

global DEBUG_F File_Folder

h_h=cell(3+ML.limb_num,16);


header_l1= {'Position:'  num2str(pos) 'Rotation: ' num2str(rot) 'Joint: '
num2str(jnt)};
header_l2= {'Segment' 'Center' ' ' ' ' 'X vector' ' ' ' ' 'Y Vector' ' ' ' ' 'Z vector' ' ' ' '
'Orientation' ' ' ' ' 'Distal Joint'};
header_l3= {' ' 'x' 'y' 'z' 'x' 'y' 'z' 'x' 'y' 'z' 'x' 'y' 'z' 'Yaw' 'Pitch' 'Roll' 'x' 'y' 'z'};

h_h(1,1:6) = header_l1;
h_h(2,1:17) = header_l2;
h_h(3,1:19) = header_l3;

for i = 1:ML.limb_num

   h_h(i+3,1)= cellstr(num2str(i));
   h_h(i+3,2:4)=num2cell(get(get(ML.limbs(i),'center'),'horz_array'));
   h_h(i+3,5:7)=num2cell(get(get(ML.limbs(i),'x_face'),'horz_array'));
   h_h(i+3,8:10)=num2cell(get(get(ML.limbs(i),'y_face'),'horz_array'));
   h_h(i+3,11:13)=num2cell(get(get(ML.limbs(i),'z_face'),'horz_array'));
   h_h(i+3,17:19)=num2cell(get(get(ML.limbs(i),'dist_joint'),'horz_array'));
   h_h(i+3,14)=num2cell(get(ML.limbs(i),'yaw')*180/pi);
   h_h(i+3,15)=num2cell(get(ML.limbs(i),'pitch')*180/pi);
   h_h(i+3,16)=num2cell(get(ML.limbs(i),'roll')*180/pi);

end

xlswrite([File_Folder,flnm,'.xls'],h_h,['Pos', num2str(pos)],'A1');

if (flg >=1 && flg <=3)
   display_save_ml(ML,flg,0,flnm,pos);
end

function outpt = get(Var_limb, data_req)
%limb  get function.
%  Returns variable depending on request.
%
global DEBUG_F
switch data_req
```

```
case 'length'
   outpt = Var_limb.length;
case 'width'
   outpt = Var_limb.width;
case 'height'
   outpt = Var_limb.height;
case 'global_pos'
   outpt = Var_limb.global_pos;
case 'topface_ul'
   outpt = Var_limb.topface_ul;
case 'topface_ur'
   outpt = Var_limb.topface_ur;
case 'topface_bl'
   outpt = Var_limb.topface_bl;
case 'topface_br'
   outpt = Var_limb.topface_br;
case 'bottomface_ul'
   outpt = Var_limb.bottomface_ul;
case 'bottomface_ur'
   outpt = Var_limb.bottomface_ur;
case 'bottomface_bl'
   outpt = Var_limb.bottomface_bl;
case 'bottomface_br'
   outpt = Var_limb.bottomface_br;
case 'center'
   outpt = Var_limb.center;
case 'x_face'
   outpt = Var_limb.x_face;
case 'y_face'
   outpt = Var_limb.y_face;
case 'z_face'
   outpt = Var_limb.z_face;
case 'x_unit'
   outpt = Var_limb.x_unit;
case 'y_unit'
   outpt = Var_limb.y_unit;
case 'z_unit'
   outpt = Var_limb.z_unit;
case 'dist_joint'
   outpt = Var_limb.dist_joint;
case 'yaw'
   outpt = Var_limb.yaw;
case 'pitch'
   outpt = Var_limb.pitch;
case 'roll'
   outpt = Var_limb.roll;
```

```
    case 'bc_yaw'
      outpt = Var_limb.bc_yaw;
    case 'bc_pitch'
      outpt = Var_limb.bc_pitch;
    case 'bc_roll'
      outpt = Var_limb.bc_roll;
%    case 'rect'
%       outpt = Var_limb.rect;
    case 'vertex_array_h'
      outpt = [get(Var_limb.topface_ul,'horz_array'); ...
        get(Var_limb.topface_ur,'horz_array'); ...
        get(Var_limb.topface_bl,'horz_array'); ...
        get(Var_limb.topface_br,'horz_array'); ...
        get(Var_limb.bottomface_ul,'horz_array'); ...
        get(Var_limb.bottomface_ur,'horz_array'); ...
        get(Var_limb.bottomface_bl,'horz_array'); ...
        get(Var_limb.bottomface_br,'horz_array')];
    case 'vertex_array_v'
      outpt = [get(Var_limb.topface_ul,'vert_array') ...
        get(Var_limb.topface_ur,'vert_array') ...
        get(Var_limb.topface_bl,'vert_array') ...
        get(Var_limb.topface_br,'vert_array') ...
        get(Var_limb.bottomface_ul,'vert_array') ...
        get(Var_limb.bottomface_ur,'vert_array') ...
        get(Var_limb.bottomface_bl,'vert_array') ...
        get(Var_limb.bottomface_br,'vert_array') ...
        get(Var_limb.center,'vert_array') ...
        get(Var_limb.x_face,'vert_array') ...
        get(Var_limb.y_face,'vert_array') ...
        get(Var_limb.z_face,'vert_array') ...
        get(Var_limb.x_unit,'vert_array') ...
        get(Var_limb.y_unit,'vert_array') ...
        get(Var_limb.z_unit,'vert_array') ...
        get(Var_limb.dist_joint,'vert_array')];
    case 'faces'
      outpt = Var_limb.faces;

    otherwise
      error([data_req,' Is not a valid asset property'])
end

function L = limb(v)
%LIMB class constructor.
%  L = LIMB(v) creates a Limb object from the vector v,
%  containing: Contains dimensions (length, width, and height).
%
```

```
% Calulations Inherited:
%          Center of Mass will be true center assumer constant density
%          Yaw, Pitch, and Roll

global DEBUG_F

if nargin == 0
  L.c = [];
  L = class(L,'limb');
elseif isa(v,'limb')
  L = v;
else
   L.length = v(1);
   L.width = v(2);
   L.height = v(3);

   L.global_pos = coord([0 0 0]);

   L.faces=[1,2,4,3;5,6,8,7;1,3,7,5;2,4,8,6;1,2,6,5;3,4,8,7];

% Defines Coordinates of corners
%
%     %face%_%corner_description% = coord([x y z]);

   L.topface_ul = coord([-L.length/2 L.width/2 L.height/2]);
   L.topface_ur = coord([L.length/2 L.width/2 L.height/2]);
   L.topface_bl = coord([-L.length/2 -L.width/2 L.height/2]);
   L.topface_br = coord([L.length/2 -L.width/2 L.height/2]);
   L.bottomface_ul = coord([-L.length/2 L.width/2 -L.height/2]);
   L.bottomface_ur = coord([L.length/2 L.width/2 -L.height/2]);
   L.bottomface_bl = coord([-L.length/2 -L.width/2 -L.height/2]);
   L.bottomface_br = coord([L.length/2 -L.width/2 -L.height/2]);


% Defines rectangle by corners


%    L.rect=[L.topface_ul L.topface_ur L.topface_bl L.topface_br ...
%       L.bottomface_ul L.bottomface_ur L.bottomface_bl L.bottomface_br];
   L.yaw = 0;
   L.pitch = 0;
   L.roll = 0;

   L.bc_yaw = 0;
   L.bc_pitch = 0;
   L.bc_roll = 0;
```

```
    L.center = coord([0 0 0]);
    L.dist_joint = coord([0 0 0]);
    L.x_face = coord([0 0 0]);
    L.y_face = coord([0 0 0]);
    L.z_face = coord([0 0 0]);
    L.x_face =
set(L.x_face,'vert_array',(get(L.topface_ur,'vert_array')+get(L.bottomface_br,'vert
_array'))./2);
    L.y_face =
set(L.y_face,'vert_array',(get(L.topface_ul,'vert_array')+get(L.bottomface_ur,'vert
_array'))./2);
    L.z_face =
set(L.z_face,'vert_array',(get(L.topface_ul,'vert_array')+get(L.topface_br,'vert_arr
ay'))./2);

    L.x_unit = coord([1 0 0]);
    L.y_unit = coord([0 1 0]);
    L.z_unit = coord([0 0 1]);


    L = class(L,'limb');


end
function list(a)
%   list all variables and values

global DEBUG_F

disp(['length = ',num2str(a.length)])
disp(['width = ',num2str(a.width)])
disp(['height = ',num2str(a.height)])

function list_vertices(L)
%   list all variables and values

global DEBUG_F

disp('Vertices: (x, y, z)')
disp(['L.topface_ul: ',list_xyz(L.topface_ul)])
disp(['L.topface_ur: ',list_xyz(L.topface_ur)])
disp(['L.topface_bl: ',list_xyz(L.topface_bl)])
disp(['L.topface_br: ',list_xyz(L.topface_br)])
disp(['L.bottomface_ul: ',list_xyz(L.bottomface_ul)])
disp(['L.bottomface_ub: ',list_xyz(L.bottomface_ur)])
```

```
disp(['L.bottomface_bl: ',list_xyz(L.bottomface_bl)])
disp(['L.bottomface_br: ',list_xyz(L.bottomface_br)])
disp('Center')
disp(['L.center: ',list_xyz(L.center)])
disp('Face center on postive axis')
disp(['L.x_face: ',list_xyz(L.x_face)])
disp(['L.y_face: ',list_xyz(L.y_face)])
disp(['L.z_face: ',list_xyz(L.z_face)])

function Var_limb = set(Var_limb, varargin)
%limb  set function.
%   Set variable depending on request.

global DEBUG_F

Var_Updates = varargin;
while length(Var_Updates) >=2
   data_type = Var_Updates{1};
   data_in = Var_Updates{2};
   Var_Updates = Var_Updates(3:end);
   switch data_type
      case 'length'
         error([data_type ,' cannot be set'])
      case 'width'
         error([data_type ,' cannot be set'])
      case 'height'
         error([data_type ,' cannot be set'])
      case 'global_pos'
         Var_limb.global_pos = data_in;
      case 'global_pos_v'
         Var_limb.global_pos = ...
            set(Var_limb.global_pos,'vert_array',data_in);
      case 'topface_ul'
         error([data_type ,' cannot be set'])
      case 'topface_ur'
         error([data_type ,' cannot be set'])
      case 'topface_bl'
         error([data_type ,' cannot be set'])
      case 'topface_br'
         error([data_type ,' cannot be set'])
      case 'bottomface_ul'
         error([data_type ,' cannot be set'])
      case 'bottomface_ur'
         error([data_type ,' cannot be set'])
      case 'bottomface_bl'
         error([data_type ,' cannot be set'])
```

```
        case 'bottomface_br'
           error([data_type ,' cannot be set'])
        case 'center'
           error([data_type ,' cannot be set'])
        case 'x_face'
           error([data_type ,' cannot be set'])
        case 'y_face'
           error([data_type ,' cannot be set'])
        case 'z_face'
           error([data_type ,' cannot be set'])
        case 'dist_joint'
           Var_limb.dist_joint = set(Var_limb.dist_joint,'vert_array',data_in(1:3,1));
        case 'yaw'
           Var_limb.yaw=data_in;
        case 'pitch'
           Var_limb.pitch=data_in;
        case 'roll'
           Var_limb.roll=data_in;
        case 'bc_yaw'
           Var_limb.bc_yaw=data_in;
        case 'bc_pitch'
           Var_limb.bc_pitch=data_in;
        case 'bc_roll'
           Var_limb.bc_roll=data_In;
%          case 'rect'
%             error([data_type ,' cannot be set'])
        case 'vertex_array_v'

           Var_limb.topface_ul =
set(Var_iimb.topface_ul,'vert_array',data_in(1:3,1));
           Var_limb.topface_ur =
set(Var_limb.topface_ur,'vert_array',data_in(1:3,2));
           Var_limb.topface_bl =
set(Var_limb.topface_bl,'vert_array',data_in(1:3,3));
           Var_iimb.topface_br =
set(Var_iimb.topface_br,'vert_array',data_in(1:3,4));
           Var_limb.bottomface_ul =
set(Var_limb.bottomface_ul,'vert_array',data_in(1:3,5));
           Var_limb.bottomface_ur =
set(Var_limb.bottomface_ur,'vert_array',data_in(1:3,6));
           Var_limb.bottomface_bl =
set(Var_iimb.bottomface_bl,'vert_array',data_in(1:3,7));
           Var_limb.bottomface_br =
set(Var_limb.bottomface_br,'vert_array',data_in(1:3,8));
           Var_limb.center = set(Var_limb.center,'vert_array',data_In(1:3,9));
           Var_limb.x_face = set(Var_limb.x_face,'vert_array',data_in(1:3,10));
```

```
        Var_limb.y_face = set(Var_limb.y_face,'vert_array',data_in(1:3,11));
        Var_limb.z_face = set(Var_limb.z_face,'vert_array',data_in(1:3,12));
        Var_limb.x_unit = set(Var_limb.x_face,'vert_array',data_in(1:3,13));
        Var_limb.y_unit = set(Var_limb.y_face,'vert_array',data_in(1:3,14));
        Var_limb.z_unit = set(Var_limb.z_face,'vert_array',data_in(1:3,15));
        Var_limb.dist_joint = set(Var_limb.dist_joint,'vert_array',data_in(1:3,16));

      otherwise
        error([data_type,' Is not a valid asset property'])
    end
end

function outpt = get(Var_Joint, data_req)
%COORD  get function.
%  Returns Variable depending on request.
%

global DEBUG_F

switch data_req

   case 'Tx_from_prox'
      outpt = Var_Joint.Tx_from_prox;
   case 'Ty_from_prox'
      outpt = Var_Joint.Ty_from_prox;
   case 'Tz_from_prox'
      outpt = Var_Joint.Tz_from_prox;

   case 'R_psi_from_prox'
      outpt = Var_Joint.R_psi_from_prox;
   case 'R_phi_from_prox'
      outpt = Var_Joint.R_phi_from_prox;
   case 'R_theta_from_prox'
      outpt = Var_Joint.R_theta_from_prox;

   case 'Tx_to_dist'
      outpt = Var_Joint.Tx_to_dist;
   case 'Ty_to_dist'
      outpt = Var_Joint.Ty_to_dist;
   case 'Tz_to_dist'
      outpt = Var_Joint.Tz_to_dist;

   case 'R_psi_to_dist'
      outpt = Var_Joint.R_psi_to_dist;
   case 'R_phi_to_dist'
      outpt = Var_Joint.R_phi_to_dist;
```

```
   case 'R_theta_to_dist'
      outpt = Var_Joint.R_theta_to_dist;

   case 'Translate_from_prox'
      outpt = Var_Joint.Translate_from_prox;
   case 'x_axis_rotate_from_prox'
      outpt = Var_Joint.x_axis_rotate_from_prox;
   case 'y_axis_rotate_from_prox'
      outpt = Var_Joint.y_axis_rotate_from_prox;
   case 'z_axis_rotate_from_prox'
      outpt = Var_Joint.z_axis_rotate_from_prox;

   case 'Translate_to_dist'
      outpt = Var_Joint.Translate_to_dist;
   case 'x_axis_rotate_to_dist'
      outpt = Var_Joint.x_axis_rotate_to_dist;
   case 'y_axis_rotate_to_dist'
      outpt = Var_Joint.y_axis_rotate_to_dist;
   case 'z_axis_rotate_to_dist'
      outpt = Var_Joint.z_axis_rotate_to_dist;

   case 'dist_joint'
      outpt = [Var_Joint.Tx_from_prox; Var_Joint.Ty_from_prox;
Var_Joint.Tz_from_prox];

   otherwise
      error([data_req,' Is not a valid asset property'])
end

function j = joint(varargin)
%joint class constructor.
%  j = joint(v) creates a joint object from the vector v,
%  containing:
%           Offset from center of both limbs Tx, Ty, Tz
%           Offset in radians for rotation of both limbs
%              R_phi, R_psi,
%            ***ALL above is constant***
%              R_theta just one since the same for both
%

global DEBUG_F

switch nargin
   case 0
      j.j = [];
      j = class(j,'joint');
```

```
case 1
   if isa(v,'joint')
      j = varargin{1};
   else
      error ('Not a Joint Object')
   end
case 12

   j.Tx_from_prox = varargin{1};
   j.Ty_from_prox = varargin{2};
   j.Tz_from_prox = varargin{3};

   j.Translate_from_prox = [1,0,0,j.Tx_from_prox; ...
      0,1,0,j.Ty_from_prox;0,0,1,j.Tz_from_prox;0,0,0,1];

   j.R_psi_from_prox = varargin{4}*pi/180;
   j.x_axis_rotate_from_prox = [1,0,0,0; ...
      0,cos(j.R_psi_from_prox),-sin(j.R_psi_from_prox),0; ...
      0,sin(j.R_psi_from_prox),cos(j.R_psi_from_prox),0;0,0,0,1];

   j.R_phi_from_prox = varargin{5}*pi/180;
   j.y_axis_rotate_from_prox = [ ...
      cos(j.R_phi_from_prox),0,sin(j.R_phi_from_prox),0; ...
      0,1,0,0; ...
      -sin(j.R_phi_from_prox),0,cos(j.R_phi_from_prox),0;0,0,0,1];


   j.R_theta_from_prox = varargin{6}*pi/180;
   j.z_axis_rotate_from_prox = [ ...
      cos(j.R_theta_from_prox),-sin(j.R_theta_from_prox),0,0; ...
      sin(j.R_theta_from_prox),cos(j.R_theta_from_prox),0,0; ...
      0,0,1,0;0,0,0,1];

   j.Tx_to_dist = varargin{7};
   j.Ty_to_dist = varargin{8};
   j.Tz_to_dist = varargin{9};

   j.Translate_to_dist = [1,0,0,j.Tx_to_dist; ...
      0,1,0,j.Ty_to_dist;0,0,1,j.Tz_to_dist;0,0,0,1];

   j.R_psi_to_dist = varargin{10}*pi/180;
   j.x_axis_rotate_to_dist = [1,0,0,0; ...
      0,cos(j.R_psi_to_dist),-sin(j.R_psi_to_dist),0; ...
      0,sin(j.R_psi_to_dist),cos(j.R_psi_to_dist),0;0,0,0,1];

   j.R_phi_to_dist = varargin{11}*pi/180;
```

```
        j.y_axis_rotate_to_dist = [ ...
           cos(j.R_phi_to_dist),0,sin(j.R_phi_to_dist),0; ...
           0,1,0,0; ...
           -sin(j.R_phi_to_dist),0,cos(j.R_phi_to_dist),0;0,0,0,1];

        j.R_theta_to_dist = varargin{12}*pi/180;
        j.z_axis_rotate_to_dist = [ ...
           cos(j.R_theta_to_dist),-sin(j.R_theta_to_dist),0,0; ...
           sin(j.R_theta_to_dist),cos(j.R_theta_to_dist),0,0; ...
           0,0,1,0;0,0,0,1];

        j = class(j,'joint');

    otherwise
        error ('Incorrect Number of Inputers for Joint Class')
end

function list(j)
%  list all variables and values

global DEBUG_F

disp(sprintf('\n'))

disp(['Tx_from_prox = ',num2str(j.Tx_from_prox)])
disp(['Ty_from_prox = ',num2str(j.Ty_from_prox)])
disp(['Tz_from_prox = ',num2str(j.Tz_from_prox)])

disp(sprintf('\n'))

disp(['R_psi_from_prox = ',num2str(j.R_psi_from_prox)])
disp(['R_phi_from_prox = ',num2str(j.R_phi_from_prox)])
disp(['R_theta_from_prox = ',num2str(j.R_theta_from_prox)])

disp(sprintf('\n'))

disp(['Tx_to_dist = ',num2str(j.Tx_to_dist)])
disp(['Ty_to_dist = ',num2str(j.Ty_to_dist)])
disp(['Tz_to_dist = ',num2str(j.Tz_to_dist)])

disp(sprintf('\n'))

disp(['R_psi_to_dist = ',num2str(j.R_psi_to_dist)])
disp(['R_phi_to_dist = ',num2str(j.R_phi_to_dist)])
disp(['R_theta_to_dist = ',num2str(j.R_theta_to_dist)])
```

```
disp(sprintf('\n'))

function Var_Joint = set(Var_Joint, varargin)
%COORD  set function.
%   Sets Variable depending on request.
%

global DEBUG_F

Var_Updates = varargin;
while length(Var_Updates) >=2
   data_type = Var_Updates{1};
   data_in = Var_Updates{2};
   Var_Updates = Var_Updates(3:end);
   switch data_type
      case 'Tx_from_prox'
         Var_Joint.Tx_from_prox = data_in;
      case 'Ty_from_prox'
         Var_Joint.Ty_from_prox = data_in;
      case 'Tz_from_prox'
         Var_Joint.Tz_from_prox = data_in;

      case 'R_psi_from_prox'
         Var_Joint.R_psi_from_prox = data_in;
      case 'R_phi_from_prox'
         Var_Joint.R_phi_from_prox = data_in;
      case 'R_theta_from_prox'
         Var_Joint.R_theta_from_prox = data_in;

      case 'Tx_to_dist'
         Var_Joint.Tx_to_dist = data_in;
      case 'Ty_to_dist'
         Var_Joint.Ty_to_dist = data_in;
      case 'Tz_to_dist'
         Var_Joint.Tz_to_dist = data_in;

      case 'R_psi_to_dist'
         Var_Joint.R_psi_to_dist = data_in;
      case 'R_phi_to_dist'
         Var_Joint.R_phi_to_dist = data_in;
      case 'R_theta_to_dist'
         Var_Joint.R_theta_to_dist = data_in;

      case 'Translate_from_prox'
         Var_Joint.Translate_from_prox = data_in;
      case 'x_axis_rotate_from_prox'
```

```
        Var_Joint.x_axis_rotate_from_prox = data_in;
      case 'y_axis_rotate_from_prox'
        Var_Joint.y_axis_rotate_from_prox = data_in;
      case 'z_axis_rotate_from_prox'
        Var_Joint.z_axis_rotate_from_prox = data_in;

      case 'Translate_to_dist'
        Var_Joint.Translate_to_dist = data_in;
      case 'x_axis_rotate_to_dist'
        Var_Joint.x_axis_rotate_to_dist = data_in;
      case 'y_axis_rotate_to_dist'
        Var_Joint.y_axis_rotate_to_dist = data_in;
      case 'z_axis_rotate_to_dist'
        Var_Joint.z_axis_rotate_to_dist = data_in;

      otherwise
        error([data_type,' Is not a valid asset property'])
    end
end

function C = coord(v)
%COORD class constructor.
%   C = COORD(v) creates a COORD object from the vector v,
%   containing: Contains coordinate in the form (x, y, and z).
%

global DEBUG_F

if nargin == 0
  C.c = [];
  C = class(C,'coord');
elseif isa(v,'coord')
  C = v;
else
   C.x = v(1);
   C.y = v(2);
   C.z = v(3);
   C = class(C,'coord');

end

function outpt = get(Var_Coord, data_req)
%COORD  get function.
%   Returns x, y, or z depending on request.
%
```

```
global DEBUG_F

switch data_req
   case 'x'
      outpt = Var_Coord.x;
   case 'y'
      outpt = Var_Coord.y;
   case 'z'
      outpt = Var_Coord.z;
   case 'vert_array'
      outpt = [Var_Coord.x;Var_Coord.y;Var_Coord.z;1];
   case 'horz_array'
      outpt = [Var_Coord.x,Var_Coord.y,Var_Coord.z];

   otherwise
      error([data_req,' Is not a valid asset property'])
end

function list(a)
%  list all variables and values

global DEBUG_F

disp(['x = ',num2str(a.x)])
disp(['y = ',num2str(a.y)])
disp(['z = ',num2str(a.z)])

function outpt = list_xyz(a)
%  list all variables and values

global DEBUG_F

outpt = ['(',num2str(a.x),', ',num2str(a.y),', ',num2str(a.z),')'];

function Var_Coord = set(Var_Coord, varargin)
%COORD  set function.
%  Returns x, y, or z depending on request.
%

global DEBUG_F

Var_Updates = varargin;
while length(Var_Updates) >=2
   data_type = Var_Updates{1};
   data_in = Var_Updates{2};
   Var_Updates = Var_Updates(3:end);
```

```
    switch data_type
      case 'x'
        Var_Coord.x = data_in;
      case 'y'
        Var_Coord.y = data_in;
      case 'z'
        Var_Coord.z = data_in;
      case 'horz_array'
        Var_Coord.x = data_in(1);
        Var_Coord.y = data_in(2);
        Var_Coord.z = data_in(3);
      case 'vert_array'
        Var_Coord.x = data_in(1);
        Var_Coord.y = data_in(2);
        Var_Coord.z = data_in(3);

      otherwise
        error([data_type,' Is not a valid asset property'])
    end
end
```

APPENDIX Q

INTERMEDIATE ANKLE MODE

CALCULATION DATA

Table Q.1. Calculated Linked system.

Position		0	1	2	3	4
Segment #1	x	35.73	3.81	5.88	5.88	10.01
	y	4.13	27.79	27.79	20.65	-20.65
	z	0.00	0.00	2.07	9.21	9.21
Joint #1	x	28.59	3.81	5.88	5.88	10.01
	y	4.13	20.65	20.65	20.65	-20.65
	z	0.00	0.00	2.07	2.07	2.07
Segment #2	x	21.60	3.81	5.88	5.88	10.01
	y	4.13	13.66	13.66	13.66	-13.66
	z	0.00	0.00	2.07	2.07	2.07
Joint #2	x	16.68	5.88	5.88	5.88	10.01
	y	2.07	8.74	8.74	8.74	-8.74
	z	0.00	0.00	0.00	0.00	0.00
Segment #3	x	13.34	7.94	7.94	7.94	7.94
	y	0.00	5.40	5.40	5.40	-5.40
	z	0.00	0.00	0.00	0.00	0.00

All lengths in cm

Table Q.2. Calculations with offsets.

Position		0	1	2	3	4
Segment #1	x	41.61	9.69	11.75	11.75	15.88
	y	4.13	27.79	27.79	20.65	-20.65
	z	3.49	3.49	5.56	12.70	12.70
Joint #1	x	34.46	9.69	11.75	11.75	15.88
	y	4.13	20.65	20.65	20.65	-20.65
	z	3.49	3.49	5.56	5.56	5.56
Segment #2	x	27.47	9.69	11.75	11.75	15.88
	y	4.13	13.66	13.66	13.66	-13.66
	z	3.49	3.49	5.56	5.56	5.56
Joint #2	x	22.55	11.75	11.75	11.75	15.88
	y	2.07	8.74	8.74	8.74	-8.74
	z	3.49	3.49	3.49	3.49	3.49
Segment #3	x	19.22	13.82	13.82	13.82	13.82
	y	0.00	5.40	5.40	5.40	-5.40
	z	3.49	3.49	3.49	3.49	3.49

All lengths in cm

Table Q.3 Measurement and Calculation Differences.

Difference		0	1	2	3	4
Segment #1	x	-0.33	0.16	-0.32	-0.32	-0.01
	y	-0.07	-0.49	-0.49	-0.07	0.07
	z	0.00	0.00	0.16	0.00	0.00
Joint #1	x	-0.17	0.16	-0.32	-0.32	-0.01
	y	-0.07	-0.07	-0.07	-0.07	0.07
	z	0.00	0.00	0.16	0.16	0.16
Segment #2	x	-0.29	0.16	-0.32	-0.32	-0.01
	y	-0.07	-0.20	-0.20	-0.20	0.20
	z	0.00	0.00	0.16	0.16	0.16
Joint #2	x	-0.20	-0.32	-0.32	-0.32	-0.01
	y	-0.03	-0.48	-0.48	-0.48	0.48
	z	0.00	0.00	0.00	0.00	0.00
Segment #3	x	-0.17	0.15	0.15	0.15	0.15
	y	0.00	-0.32	-0.32	-0.32	0.32
	z	-0.33	0.16	-0.32	-0.32	-0.01

All differences in cm

Table Q.4. Measured Linked System.

Confirmation Measured Values		0	1	2	3	4
Segment #1	x	41.28	9.84	11.43	11.43	15.88
	y	4.06	27.31	27.31	20.57	-20.57
	z	3.49	3.49	5.72	12.70	12.70
Joint #1	x	34.29	9.84	11.43	11.43	15.88
	y	4.06	20.57	20.57	20.57	-20.57
	z	3.49	3.49	5.72	5.72	5.72
Segment #2	x	27.18	9.84	11.43	11.43	15.88
	y	4.06	13.46	13.46	13.46	-13.46
	z	3.49	3.49	5.72	5.72	5.72
Joint #2	x	22.35	11.43	11.43	11.43	15.88
	y	2.03	8.26	8.26	8.26	-8.26
	z	3.49	3.49	3.49	3.49	3.49
Segment #3	x	19.05	13.97	13.97	13.97	13.97
	y	0.00	5.08	5.08	5.08	-5.08
	z	3.49	3.49	3.49	3.49	3.49

Values in cm

Table Q.5. Crab Position Measurements.

Crab 1				
Pos 2	Point	X (cm)	Y (cm)	Z (cm)
	A	11.3	16.5	24.3
	B	0.0	16.5	24.3
	C	0.0	16.5	28.3
	D	0.0	16.5	35.0
	E	3.4	16.5	35.0
Crab 3				
Pos 1	Point	X (cm)	Y (cm)	Z (cm)
	A	12.3	12.2	26.0
	B	0.0	12.2	26.0
	C	0.0	12.2	29.3
	D	0.0	12.2	36.5
	E	3.8	12.2	36.5

Table Q.6. Differences in vector and measured length.

	Vector		Measured	Difference	
Crab 1	Pos 1	Pos 2		Pos 1	Pos 2
AB	11.3	11.3	11.3	0.0	0.0
BC	3.9	4.0	3.9	0.0	-0.1
CD	6.8	6.7	7.0	0.2	0.3
DE	3.8	3.4	3.4	-0.4	0.0
Crab 3	Pos 1	Pos 2		Pos 1	Pos 2
AB	12.3	12.3	12.3	0.0	0.0
BC	3.3	3.3	3.5	0.2	0.2
CD	7.2	7.2	7.1	-0.1	-0.1
DE	3.8	4.7	3.5	-0.3	-1.2

Table Q.7. Calculated Crab Limb Positions.

Crab 1				
Pos 2	Point	X (cm)	Y (cm)	Z (cm)
	B	5.7	0.0	0.0
	C	5.7	0.3	3.9
	D	5.7	0.9	10.9
	E	9.1	0.9	10.9
Crab 3				
Pos 1	Point	X (cm)	Y (cm)	Z (cm)
	B	6.2	0.0	0.0
	C	6.2	0.3	3.5
	D	6.1	-0.4	10.6
	E	9.7	0.5	10.6

Table Q.8. Calculated Crab Limb Position with Offsets.

Crab 1				
Pos 2	Point	X (cm)	Y (cm)	Z (cm)
	B	0.0	16.5	24.3
	C	0.0	16.8	28.2
	D	0.1	17.4	35.2
	E	3.5	17.4	35.2
Crab 3				
Pos 1	Point	X (cm)	Y (cm)	Z (cm)
	B	0.0	12.2	26.0
	C	0.0	12.5	29.5
	D	0.0	11.8	36.6
	E	3.5	12.7	36.6

Table Q.9. Differences between Calculated and Measured Crab Limb Position.

Crab 1				
Pos 2	Point	X (cm)	Y (cm)	Z (cm)
	B	0.0	0.0	0.0
	C	0.0	0.3	-0.1
	D	0.1	0.9	0.2
	E	0.1	0.9	0.2
Crab 3				
Pos 1	Point	X (cm)	Y (cm)	Z (cm)
	B	0.0	0.0	0.0
	C	0.0	0.3	0.2
	D	0.0	-0.4	0.1
	E	-0.3	0.5	0.1

Table Q.10. Local Reference Frame Vector Coordinates for Ankle Model.

		Center (mm)			X Vector (mm)			Y Vector (mm)			Z Vector (mm)		
Pos	Limb	x	y	z	x	y	z	x	y	z	x	y	z
0	tibia	0.0	0.0	0.0	237.0	0.0	0.0	0.0	10.0	0.0	0.0	0.0	19.5
	talus	247.0	0.0	0.0	257.0	0.0	0.0	247.0	12.5	0.0	247.0	0.0	19.5
	calcaneus	282.0	0.0	5.0	307.0	0.0	5.0	282.0	40.0	5.0	282.0	0.0	20.0
1	tibia	0.0	0.0	0.0	237.0	0.0	0.0	0.0	10.0	0.0	0.0	0.0	19.5
	talus	247.0	0.0	0.0	257.0	0.0	0.0	247.0	12.5	0.0	247.0	0.0	19.5
	calcaneus	282.4	2.4	0.2	306.9	3.9	-4.5	278.7	41.7	-6.3	285.0	5.1	14.7
2	tibia	0.0	0.0	0.0	237.0	0.0	0.0	0.0	10.0	0.0	0.0	0.0	19.5
	talus	246.5	-3.1	0.7	255.9	-6.3	1.4	250.3	8.7	2.3	244.4	-5.1	20.0
	calcaneus	280.7	-12.0	3.7	304.8	-17.8	1.0	289.8	26.9	2.1	282.4	-11.8	18.6
3	tibia	0.0	0.0	0.0	237.0	0.0	0.0	0.0	10.0	0.0	0.0	0.0	19.5
	talus	246.7	-2.4	0.6	256.4	-4.7	1.1	249.6	9.7	1.8	245.2	-3.9	19.9
	calcaneus	281.6	-8.4	3.0	306.0	-12.4	-0.1	287.6	31.0	0.1	283.6	-7.7	17.8
4	tibia	0.0	0.0	0.0	237.0	0.0	0.0	0.0	10.0	0.0	0.0	0.0	19.5
	talus	246.7	-2.4	0.6	256.4	-4.7	1.1	249.6	9.7	1.8	245.2	-3.9	19.9
	calcaneus	279.6	-12.0	8.9	303.5	-18.7	11.7	289.5	26.2	15.1	277.3	-13.8	23.6
5	tibia	0.0	0.0	0.0	237.0	0.0	0.0	0.0	10.0	0.0	0.0	0.0	19.5
	talus	247.0	-0.8	0.2	256.9	-1.6	0.4	247.9	11.7	0.6	246.5	-1.4	19.7
	calcaneus	281.3	-4.7	7.4	306.0	-7.4	9.4	285.3	35.0	11.0	279.9	-5.9	22.3
6	tibia	0.0	0.0	0.0	237.0	0.0	0.0	0.0	10.0	0.0	0.0	0.0	19.5
	talus	247.0	-0.8	0.2	256.9	-1.6	0.4	247.9	11.7	0.6	246.5	-1.4	19.7
	calcaneus	280.0	-6.8	10.0	304.1	-11.2	14.8	285.3	31.9	18.3	276.7	-9.4	24.4
7	tibia	0.0	0.0	0.0	237.0	0.0	0.0	0.0	10.0	0.0	0.0	0.0	19.5
	talus	247.0	-0.8	0.2	256.9	-1.6	0.4	247.9	11.7	0.6	246.5	-1.4	19.7
	calcaneus	281.7	-3.7	6.0	306.6	-5.7	6.5	284.9	36.2	7.2	281.4	-4.1	20.9
8	tibia	0.0	0.0	0.0	237.0	0.0	0.0	0.0	10.0	0.0	0.0	0.0	19.5
	talus	247.0	0.0	0.0	257.0	0.0	0.0	247.0	12.5	0.0	247.0	0.0	19.5
	calcaneus	282.0	0.0	5.0	307.0	0.0	5.0	282.0	40.0	5.0	282.0	0.0	20.0

Table Q.11. Limb Orientations in Ankle Model.

Pos	Limb	Yaw	Pitch	Roll
0	tibia	0.0°	0.0°	0.0°
	talus	0.0°	0.0°	0.0°
	calcaneus	0.0°	0.0°	0.0°
1	tibia	0.0°	0.0°	0.0°
	talus	0.0°	0.0°	0.0°
	calcaneus	-10.0°	-5.3°	9.4°
2	tibia	0.0°	0.0°	0.0°
	talus	6.5°	17.7°	-7.9°
	calcaneus	-6.7°	13.2°	2.3°
3	tibia	0.0°	0.0°	0.0°
	talus	4.6°	13.3°	-5.7°
	calcaneus	-7.8°	8.6°	4.2°
4	tibia	0.0°	0.0°	0.0°
	talus	4.6°	13.3°	-5.7°
	calcaneus	8.9°	14.4°	-9.2°
5	tibia	0.0°	0.0°	0.0°
	talus	1.4°	4.5°	-1.8°
	calcaneus	5.1°	5.8°	-5.1°
6	tibia	0.0°	0.0°	0.0°
	talus	1.4°	4.5°	-1.8°
	calcaneus	12.9°	7.7°	-12.1°
7	tibia	0.0°	0.0°	0.0°
	talus	1.4°	4.5°	-1.8°
	calcaneus	1.4°	4.5°	-1.8°
8	tibia	0.0°	0.0°	0.0°
	talus	0.0°	0.0°	0.0°
	calcaneus	0.0°	0.0°	0.0°

APPENDIX R

SUBMITTED IEEE ROBOTICS PAPER

A representation for multilinked systems with arbitrary revolute joints in human and arthropod limbs

Christopher M Storey, Student *Member, IEEE*, Anne M. Hollister, *Associate Member, IEEE*, Charles J. Robinson, *Fellow, IEEE*, Norman M. Witriol, Dale O. Anderson

***Abstract*—Arthropod and human limbs are multilinked systems in which the revolute joints are not orthogonal to the limb segments or to each other. The Denavit-Hartenberg (DH) representation is the traditional model used for orthogonal systems such as industrial robots. When applied to systems with non-orthogonal linkages, the DH representation projects the reference frames outside of the limb segments and presents other computational difficulties. A new method to represent kinematics of multilinked lower-pair mechanisms is proposed. Three-dimensional computer graphics techniques act on arrays of points describing bodies that move about arbitrary revolute joints. This computational model has been adapted to represent multilinked systems such as animal limbs to calculate both position (X, Y, Z) and orientation (yaw, pitch, and roll) of individual limb segments and joints for measurement comparisons. The linkage parameters are explicitly stated. This method allows a simplified representation for the kinematics of human and animal limbs by maintaining reference frames within the limb segments. It reduces errors such as the arc sine errors associated with Euler calculations and the azimuth errors seen with the DH representation. A common computational system is provided for simulation, design, measurement and animation.**

***Index Terms*—Biomechanics, spatial linkage Kinematics, Robotics, Biometrics**

I. Introduction

There has been a recent increase in interest in the simulation of arthropod or human limbs in robot design [1-14]. These multilinked robotic limbs use orthogonal mechanisms, usually revolute joints for their mechanisms [15]. The kinematics and kinetics of the limb segments are calculated with the Denavit-Hartenberg (DH) representation, a simplified system that uses only four of six joint parameters for motion, that has worked well for planar and orthogonal mechanisms for over fifty years by reducing matrix size and the number of matrix multiplications [16].

Arthropod and human limbs are multilinked systems with revolute joints that are not orthogonal to each other or to the limb segments [17-40]. Such revolute joints, known as arbitrary revolute joints, produce three-dimensional spatial motion with only one degree of freedom, thus the revolute joints reduce the limb's number of degrees of freedom and control complexity. A vector (d) and two angles of offset, the twist (α) and cant (β) angles shown in Fig. 1, define the location and orientation of arbitrary revolute joints. The resulting limb movements are in different planes at each revolute. The simplification of these linkages with the DH representation produces several problems [18] If the twist and cant angles are not 0 or 90, the reference frames are projected outside of the limb segments by DH representation. If the mechanisms are nearly parallel to one of the coordinate axes, DH incurs large azimuth errors [18].

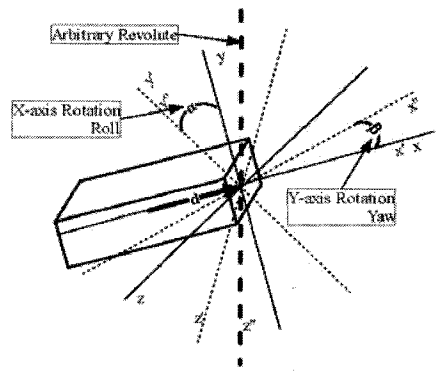

Fig. 1. The α and β offset axes and d offset position.

We propose a representation based on computer graphics techniques for rotation about an arbitrary axis that is suitable

Manuscript received November 21, 2006. A VA Rehab Research Career Scientist Award provided partial funding for his participation in this project.

This paper has supplementary downloadable material available at http://ieeexplore.ieee.org, provided by the authors. This includes two multimedia Mpeg format movie clips, which show animations of human and animal limbs. This material is 2.4 MB in size.

C. M. Storey is with the Biomedical Engineering Department at Louisiana Tech University, Ruston, LA 71272 USA (phone: 504-782-3280; fax: 318-213-8856; e-mail: cstorey@ieee.org).

A. M. Hollister is with Louisiana State University Health Sciences Center, Shreveport, LA, 71103 USA (e-mail: annahans@mac.com).

C. J. Robinson is with the Center for Rehabilitation Engineering, Science, and Technology, Clarkson University, Potsdam, NY 13699 USA and The Syracuse VAMC Research Service, Syracuse, NY 13210 (e-mail: crobinson@ieee.org).

N. M. Witriol is with the Witriol Scientific Consulting Service, Ruston, LA 71270 USA (e-mail: witriol@cox.net).

D. O. Anderson is a consultant, Ruston, LA 71272 USA (e-mail: drdoanderson@cox.net).

for analysis and display of kinematic chains connected by nonorthogonal and/or orthogonal revolute joints and is optimized to reduce computational cost over traditional methods [41-44]. These three-dimensional techniques have been used successfully in human limb simulations; (Buford, et al., 2005 has expanded them to the whole human body) [45-49]. As with the DH system, a limb is modeled as a hierarchical kinematic chain from the ground (support) to the end effector. Each child link moves with its parent. In this system, the revolute joint to be rotated is translated to the origin, the twist (alpha) and cant (beta) angles are de-rotated and the arbitrary axis is aligned with the global *z*-axis. The dependent points for this joint are then rotated through a specified joint actuation angle about the revolute; the twist and cant angles are re-rotated and the revolute and dependent points are then translated back into position. Thus, the method is more robust than either DH or multibody because it includes all six joint parameters calculates both position and orientation of each link relative to the joints between them, and permits the origin of each revolute to lie within the joint itself. Modern computer capabilities allow this more robust method to be used easily on personal computers.

Our proposed system places the limb segment and joint reference frames within the segments or joints to facilitate the measurement, design, modeling, simulation, and control of these natural systems. Many design engineers prefer to compute and measure the motion of reference frames for each limb segment or revolute relative to the body and global reference frames with calculated values of x, y, and z displacements and yaw, pitch ,and roll rotations [50, 51]. Our method facilitates this with outputs of x, y, and z displacements with yaw, pitch, and roll rotations if desired by the user. The parameters that determine the limb and joint orientation and motion are stated explicitly to facilitate accurate measurement in animal limbs. We simulated models of the human ankle calculated from Inman's data and on data taken from crab legs [31-33].

II. Methods

A. Software

Analysis routines were written in Matlab® to have access of the matrix mathematics functions. The program was object-oriented to allow for ease and robustness of expansion [52]. The software provided text (Excel Spreadsheet), jpg (picture), and avi (Video) output representing motion.

B. System representation

The simplest system has two segments and a single revolute joint. The reference frame for the first link is placed at the origin of a Cartesian coordinate system. The displacement vector ($\mathbf{d}_1$), the *x*, *y*, and *z* coordinates, represent the distance from the first segment's reference frame to the center of the first revolute. The limb local coordinates may be placed anywhere, including a location along the revolute axis. The α_1 and β_1 angles are the twist and cant angles of offset from the preceding segment's reference frame that are needed to align the revolute axis of motion with the *z*-axis of the preceding limb. In relation to the second limb, the α_2, β_2, and $\mathbf{d}_2$ are the variables defined that are needed to rotate the axis of rotation to align with *z*-axis of the next segment and to find the distance from the joint center to the following segment's center. Setting subsequent displacement vectors to zero simulates saddle (2-orthogonal revolute joints) and ball and socket joints (3-othogonal revolute joints).

III. Definitions

A vertices matrix ([V_n], (1)) is defined by the joint number to be rotated, *n*; therefore, all limbs distal to it (limbs [*n*+1:*d*]) are operated on or accessed in the matrix. The subscript *d* is equal to the number of the most distal limb. Each limb requires 12 columns of the matrix (expandable for more vertices). The first eight columns are the limb vertices. The ninth column is the limb center, and the 10th, 11th, and 12th columns are the local *x*, *y*, and *z*-unit vectors of the local coordinate system relative to global Cartesian coordinate system. The 13th column contains the position of the distal revolute joint of each respective limb, (*jp*).

$$\begin{bmatrix} x_{1,1} & x_{1,2} & \cdots & x_{n+1,1} & \cdots & x_{d,13} \\ y_{1,1} & y_{1,2} & \cdots & y_{n+1,1} & \cdots & y_{d,13} \\ z_{1,1} & z_{1,2} & \cdots & z_{n+1,1} & \cdots & z_{d,13} \\ 1 & 1 & 1 & 1 & 1 & 1 \end{bmatrix} \tag{1}$$

A translation matrix ([$T_{n,r}$], (2)) is defined by *n* (same as above) and *r*, such that the offset as "from proximal" (*fp*) or "to distal" (*td*) is defined in reference to the joint in relation to the limb.

$$\begin{bmatrix} 1 & 0 & 0 & \Delta x \\ 0 & 1 & 0 & \Delta y \\ 0 & 0 & 1 & \Delta z \\ 0 & 0 & 0 & 1 \end{bmatrix} \tag{2}$$

Rotation matrices ([$R_{n,a,r}$]) are defined by *n*, *a*, and *r*, where *a* is the axis of rotation. Equations (3)-(5) show the rotation matrices for rotating about the *x*, *y*, and *z*-axes respectively. Roll (α) is defined by the rotation about the *x*-axis. Yaw (β) provides the rotation about the *y*-axis. Pitch (θ) describes the rotation about the *z*-axis.

$$\begin{bmatrix} 1 & 0 & 0 & 0 \\ 0 & \cos(\alpha) & -\sin(\alpha) & 0 \\ 0 & \sin(\alpha) & \cos(\alpha) & 0 \\ 0 & 0 & 0 & 1 \end{bmatrix} \tag{3}$$

$$\begin{bmatrix} \cos(\beta) & 0 & \sin(\beta) & 0 \\ 0 & 1 & 0 & 0 \\ -\sin(\beta) & 0 & \cos(\beta) & 0 \\ 0 & 0 & 0 & 1 \end{bmatrix} \tag{4}$$

$$\begin{bmatrix} \cos(\theta) & -\sin(\theta) & 0 & 0 \\ \sin(\theta) & \cos(\theta) & 0 & 0 \\ 0 & 0 & 1 & 0 \\ 0 & 0 & 0 & 1 \end{bmatrix} \tag{5}$$

A joint rotation matrix ([Rev]) defines the amount of rotation about the arbitrary axis of the revolute joint. The α and β angles of offset are calculated from the *z*-axis to allow for the rotation of the joint to be about the *z*-axis as in (5). A single rotation matrix ([RM (row, column)]) is used to define

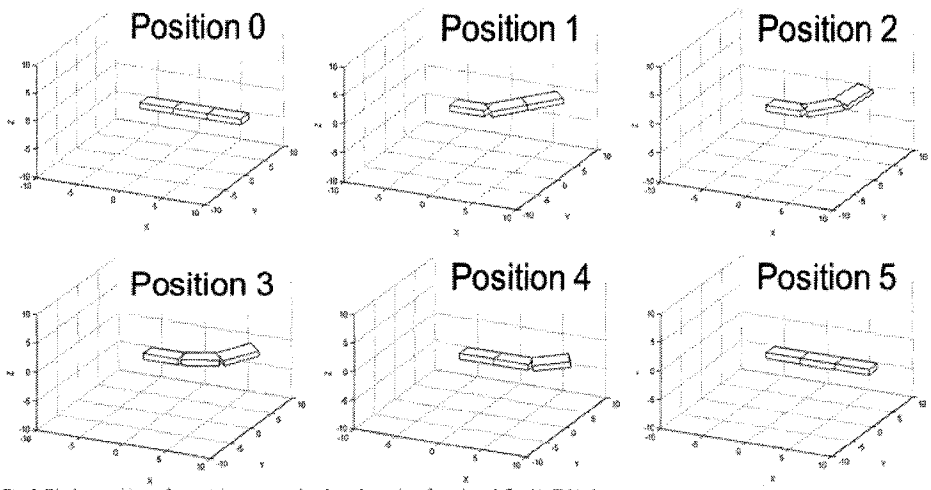

Fig. 2. Displays positions of a two joint system going through a series of rotations defined in Table 1.

the orientation of a limb in space through a single rotation once the yaw, pitch, and roll have been tabulated.

$$\begin{bmatrix} c(\beta)c(\theta) & s(\theta) & -c(\theta)s(\beta) & 0 \\ -c(\alpha)s(\theta)c(\beta)+s(\alpha)s(\beta) & c(\alpha)c(\theta) & c(\alpha)s(\beta)s(\theta)+s(\alpha)c(\beta) & 0 \\ c(\beta)s(\theta)s(\alpha)+s(\beta)c(\alpha) & -c(\theta)s(\alpha) & -s(\alpha)s(\beta)s(\theta)+c(\theta)c(\beta) & 0 \\ 0 & 0 & 0 & 1 \end{bmatrix} \quad (6)$$

In Equation (6), c refers to cosine and s to sine.

A. System Description

A relative object-oriented design utilizing limb, joint, and system objects facilitates the setup of the model using global positions and angles. The global origin and axis are designated at the local origin of the most proximal limb segment. The limb is modeled as a cuboid defined by length, width, and height for simplicity, but any shape with any number of vertices can be used. The local reference frame for each limb segment is located arbitrarily at the segment's geometric center. The joint is defined in relation to the proximal and distal limbs. Due to the sequential operation in traversing the limb, the program progresses arbitrarily proximal to distal. The displacement offset for each joint is the x_{jp}, y_{jp}, and z_{jp} offset from the geometric center of the proximal limb. These define its position in space in relation to proximal limb. Next, the α_{jp} (x-axis), β_{jp} (y-axis), and θ_{jp} (z-axis) are defined as the offset orientations from the local axis of the proximal limb. Then a similar set of offset orientations (α_{jd}, β_{jd}, and θ_{jd}) are defined to allow the rotation of the revolute joint to align it with the z-axis of the distal limb. Finally, the offset is defined from the center of the revolute joint to the geometric center of the distal limb, x_{jd}, y_{jd}, and z_{jd}. No range limitation is enabled to allow axis positions or orientations that are considered out of the range of natural joint motion as in fractures or dislocations.

IV. Kinematics of the Multi-Linked System

A multi-linked system assembled to the specifications of an initial state and followed by a series of rotations is shown in Fig. 2. The local coordinate systems are set at the origin for all limbs. Therefore, the limbs are moved to their positions and orientations in space via the matrix multiplications shown in the pseudocode below:

1. $[V_1] = [T_{1,jp}]\,[R_{1,x,jp}]\,[R_{1,y,jp}]\,[R_{1,z,jp}]\,[R_{1,z,jd}]\,[R_{1,y,jd}]\,[R_{1,x,jd}]\,[T_{1,jd}]\,[V_1]$
2. $[V_2] = [T_{2,jp}]\,[R_{2,x,jp}]\,[R_{2,y,jp}]\,[R_{2,z,jp}]\,[R_{2,z,jd}]\,[R_{2,y,jd}]\,[R_{2,x,jd}]\,[T_{2,jd}]\,[V_2]$
3. . . . . .
4. . . . . .
5. . . . . .
6. $[V_n] = [T_{n,jp}]\,[R_{n,x,jp}]\,[R_{n,y,jp}]\,[R_{n,z,jp}]\,[R_{n,z,jd}]\,[R_{n,y,jd}]\,[R_{n,x,jd}]\,[T_{n,jd}]\,[V_n]$.

To rotate the distal limbs around a respective joint (n), the joint axis is translated to the global origin and the axis of rotation is aligned with the z-axis. The convention for local z-axis rotations has been designated as the rotation for each arbitrary joint. All other axes are held constant at the initial specification.

Once the system is built, it can be optimized from the pure computer graphics framework. By using the position (jp) of the revolute joint stored in the vertex matrix, we can use one translation to bring the joint to the origin. This optimization creates a reduction in translational matrix multiplications by a factor of 2*(n-1) if n is the number of the joint to be rotated. In addition, the optimization provides less overhead as the number of vertices to be operated is reduced by c*n where c is the number of vertices per limb and n is the number of the joint to be rotated. The optimization is detailed in the pseudocode below:

1. $[V_n] = [T_{n,ip}]^{-1} [V_n]$
2. $[V_n] = [R_{1,y,fp}]^{-1} [R_{1x,ip}]^{-1} [V_n]$
   a. If the joint is the joint of rotation, jump to step nine.
3. $[V_n] = [R_{1x,id}]^{-1} [R_{1y,id}]^{-1} [R_{1z,id}]^{-1} [R_{1x,fp}]^{-1} [V_n]$
4. $[V_n] = [R_{2y,fp}]^{-1} [R_{2x,ip}]^{-1} [V_n]$
   a. If the joint is the joint of rotation, jump to step nine.
5. $[V_n] = [R_{2x,id}]^{-1} [R_{2y,id}]^{-1} [R_{2z,id}]^{-1} [R_{2x,fp}]^{-1} [V_n]$
6. . . . . .
7. . . . . .
8. . . . . .
9. $[V_n] = [R_{n,x,fp}] [R_{n,y,fp}] [Rev] [V_n]$.

After joint is rotated, the system is returned to its proper global coordinates as follows:

1. $[V_n] = [R_{n,x,fp}] [R_{n,y,fp}] [R_{n,z,fp}] [R_{n,z,id}] [R_{n,y,id}] [R_{n,x,id}] [V_n]$
2. . . . . .
3. . . . . .
4. . . . . .
5. $[V_n] = [R_{2,x,fp}] [R_{2,y,fp}] [R_{2,z,fp}] [R_{2,z,id}] [R_{2,y,id}] [R_{2,x,id}] [V_n]$
6. $[V_n] = [R_{1,x,fp}] [R_{1,y,fp}] [R_{1,z,fp}] [R_{1,z,id}] [R_{1,y,id}] [R_{1,x,id}] [V_n]$
7. $[V_n] = [T_{n,ip}] [V_n]$

V. Yaw, Pitch, and Roll of Limbs

The rotation about an arbitrary revolute joint in a multilinked system allows joint motion to include displacements in all three dimensions and rotations about all three coordinate axes. In mechanisms with orthogonal revolute joints, three revolute joints would be required to achieve the same rotations. Changes in link yaw, pitch, and roll Euler angles occur from rotation about a single revolute joint. Therefore, the new yaw, pitch, and roll are calculated after proximal joints are rotated. To avoid errors in back calculation of the orientation via position coordinates in real data, the yaw, pitch, and roll are calculated via the rotation sequence through multiplication of only the rotation matrices. The sequence necessary for rotation using Euler angles required that the orientations be calculated in the order roll, pitch, and yaw as in (6). The calculation of yaw, pitch, and roll is tabulated both ways so that each method could verify the other. The method of back calculation is accomplished by first translating the limb back to the global origin of the coordinates system by using the limb center as the offset for the translation matrix in (7).

$$\begin{bmatrix} 1 & 0 & 0 & x_{c,p} \\ 0 & 1 & 0 & y_{c,p} \\ 0 & 0 & 1 & z_{c,p} \\ 1 & 1 & 1 & 1 \end{bmatrix} \tag{7}$$

Roll (α) is calculated by projecting the local y-axis unit vector (x_uy, y_uy, z_uy) onto the yz-plane (11) and calculating the angle of rotation (α) between u' and the global y-axis (12).

$$u' = [0, y\_uy, z\_uy] \tag{11}$$

$$\alpha = \frac{\cos^{-1}(u' \cdot [0,1,0])}{|u'|} \times \frac{z\_uy}{|z\_uy|} \tag{12}$$

The arc cosine function only returns values between zero and π radians so it is multiplied by a factor that is -1 or 1 depending on z_uy in respect to the xy-plane. A similar respective factor is multiplied to determine angle direction for yaw and pitch. The computer animation standard rotations used designate positive angles as counter-clockwise rotations [2]. For α, a positive angle requires a clockwise rotation to align u' with the global y-axis. Therefore, the calculated α is inverted. The remaining calculations of pitch (θ) and yaw (β) follow the standard convention of positive angles for counter-clockwise rotations. Using α, an x-axis rotation matrix is used to rotate the limb so that the local y-axis vector lies in the xy-plane.

Since u'' already lies within the xy-plane but was calculated with the absolute value of u' (13), the pitch (θ) must be calculated from the angle of rotation between u'' and the global y-axis (14).

$$u'' = [x\_uy, 0, |u'|] \tag{13}$$

$$\theta = \frac{\cos^{-1}(u'' \cdot [0,1,0])}{|u''|} \times \frac{x\_uy}{|x\_uy|} \tag{14}$$

Yaw (β) requires the use of a separate local axis since the local y-axis unit vector is aligned with the global y-axis. The local x-axis unit vector (x_ux, y_ux, z_ux) is projected onto the xz-plane (17) so that the angle between the x-axis vector (x_ux) and the global x-axis is calculated as the yaw of the limb (18).

$$u''' = [x\_ux, 0, z\_ux] \tag{17}$$

$$\beta = \frac{\cos^{-1}(u''' \cdot [1,0,0])}{|u'''|} \times \frac{z\_ux}{|z\_ux|} \tag{18}$$

Utilizing the calculated yaw, pitch, and roll, one is able to move and orient the limb without resorting to sequential steps as in (19).

$$[V_n] = [T] [R_\alpha] [R_\theta] [R_\beta] [V_n] \tag{19}$$

Inability to make small, precise measurements for the position of limbs introduces the possibility for large errors when back calculating the yaw, pitch, and roll for a limb, especially at the asymptotes. So in addition to back calculating the yaw, pitch, and roll from the limb's position relative to global axis, the yaw, pitch, and roll are calculated solely with the inputted rotation matrices. The rotation matrices are ordered as they would be for the multiplication to build a limb as previously shown in pseudocode above, but no translations are used. The rotation matrix of (6) is then obtained. By using an ordered sequence of rotation matrix multiplications, the pseudocode is given to back-calculate yaw, pitch, and roll from the values in the rotation matrix as follows:

1. $[RM_1] = [R_{1,x,fp}] [R_{1,y,fp}] [R_{1,z,fp}] [R_{1,z,id}] [R_{1,y,id}] [R_{1,x,id}]$
2. $[RM_2] = [R_{2,x,fp}] [R_{2,y,fp}] [R_{2,z,fp}] [R_{2,z,id}] [R_{2,y,id}] [R_{2,x,id}]$
3. . . . . .
4. . . . . .
5. . . . . .
6. $[RM_n] = [R_{n,x,fp}] [R_{n,y,fp}] [R_{n,z,fp}] [R_{n,z,id}] [R_{n,y,id}] [R_{n,x,id}]$

Pitch is calculated first, since (6) has one unknown. Because the arc-sine function's range is $[-\pi/2, \pi/2]$, roll is rotated first; this guarantees that the pitch will always be less than $\pi/2$ via the order to calculate Euler's yaw, pitch, and role.

$$\theta = \sin^{-1}(RM(1,2)) \tag{20}$$

Roll as in (12) is negated to provide the correct rotation direction. The z component of the y and x unit vectors is the same for roll and yaw in (14) and (18).

$$\alpha = -\cos^{-1}\left(\frac{RM(2,2)}{\cos(\theta)}\right) * \left(\frac{z\_uy}{|z\_uy|}\right) \tag{21}$$

$$\beta = \cos^{-1}\left(\frac{RM(1,1)}{\cos(\theta)}\right) * \left(\frac{z\_ux}{|z\_ux|}\right) \tag{22}$$

This method allows one to track the yaw, pitch, and roll of the limbs without the need for position data (except to track the sign for yaw and roll).

VI. Results

To verify our methods we rotated to an end position and then back to an initial home position with different rotations on the way back to the home position. Our final vertices matrix equaled the initial one thus verifying our method, since a closed loop rotation is the identity matrix. Table 1 shows the sequence of rotations and initial offsets that are illustrated in Fig. 2. Figure 2 shows a simple system of only two arbitrary revolute joints; however it is given as an example as it is simple to expand to a matrix of vertices representing detailed objects. The yaw, pitch, and roll are calculated both through rotations and by back-calculation from the end position of each limb for both joints with rotations from -180° to 180° in 1° increments. The angles were found to be equal.

Table 1
Offsets and Rotations of a Simple System with Nonorthogonal Revolute Hinges

Joint	α_{fp}	β_{fp}	θ_{fp}	α_{td}	β_{td}	θ_{td}
1	5°	10°	0°	-5°	-10°	0°
2	15°	20°	0°	-15°	-20°	0°
Position	**Rotated Joint**			**Degrees**		
0	None					
1	1			45°		
2	2			30°		
3	1			-25°		
4	1			-20°		
5	2			-30°		

A. Orthogonal Rotations

To compare our methodology to real physical data, a mechanical linkage system (restricted to orthogonal axes) using joints with adjustable twist, cant, and joint angles has been devised and fabricated. Measurements were made with respect to right-hand Cartesian coordinate system using a grid on drafting paper and a ruler for the vertical z-axis. The drafting paper was taped to a flat tabletop, and one end of the multi-linked system was secured to the tabletop. The system was offset since it was above the tabletop. Adding 2.313 to the x values and 1.375 to the z values adjusted the calculations. An offset was used since the our method takes the global zero to be at the center of the most proximal limb, while the test apparatus begins at the end of the most proximal limb, whose center is located at 1.375 inches on the positive z-axis. After measurements and adjustments were finalized, the data were converted to centimeters. The differences were calculated between the confirmation values and the modified calculated values. Error was calculated as the Root Mean Square (RMS) of the difference between the measured and calculated coordinates. Table 2 shows a maximum 6 mm error, which is within the experimental error of the measurement method used.

Table 2
Root Mean Square Difference of Calculation and Measurements (cm)

RMS	0	1	2	3	4
Segment #1	0.34	0.51	0.60	0.33	0.07
Joint #1	0.18	0.17	0.36	0.36	0.17
Segment #2	0.30	0.25	0.41	0.41	0.25
Joint #2	0.20	0.58	0.58	0.58	0.48
Segment #3	0.17	0.36	0.36	0.36	0.36

B. Nonorthogonal Rotations

Measurements were also performed on snow crab legs (*Chionoecetes opilio*) to verify rotations for nonorthogonal biological revolute crab joints as seen in Table 3 [33]. Two different crab legs were used and measurements were performed on each crab leg in two different positions. The measurements were made using methods of the orthogonal section above. One of the positions of the Crab legs is shown in Fig. 3; the results are given in Table 3.

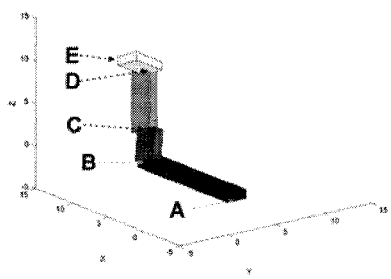

Fig. 3. Position one of crab leg three.

Table 3
Rotations and Offsets of Crab Limb Joints

Crab 1	Joint	α_{fp}	β_{fp}	θ_{fp}	α_{td}	β_{td}	θ_{td}
Pos 2	1	-5°	90°	90°	5°	-90°	0°
	2	-35°	90°	0°	35°	-90°	0°
	3	-5°	90°	-90°	5°	-90°	0°
Crab 3	**Joint**	α_{fp}	β_{fp}	θ_{fp}	α_{td}	β_{td}	θ_{td}
Pos 1	1	-5°	90°	90°	5°	-90°	0°
	2	-40°	90°	0°	35°	-90°	0°
	3	-3°	90°	-90°	5°	-90°	0°

The methods used to make the measurements were similar to those of the orthogonal axes measurements. The level of

accuracy in the measurements was determined by comparing the vector lengths of the limbs compared to the measured length of the limb (accuracy within 0.3 cm required, which allows for ±1.5 mm error for each axis coordinate). Measurements meeting this requirement attained comparable results (Table 4) with our simulation shown in Fig. 2. Since the measurements were carried out similar to the orthogonal linkage measurements with measurements taken in centimeters instead of inches, the errors were the same. All the nonorthogonal measurements that met the required accuracy had RMS error less than 6 mm.

TABLE 4
RMS OF DIFFERENCES IN CRAB LIMB POSITION (CM)

RMS	B	C	D	E
Crab 1 Pos 2	0.0	0.2	0.6	0.6
Crab 3 Pos 1	0.0	0.2	0.2	0.4

VII. A MODEL FOR CALIBRATION OF ANKLE ANGLE MEASUREMENTS

A model of the human ankle was developed based on three segments with two arbitrary revolute joints (Table 5). The segments are the calcaneus, talus, and mortise (comprised of the tibia, fibula and ligaments). The talocrural joint (upper ankle joint) and the subtalar joint (lower ankle joint) are arbitrary revolute joints [31, 32, 39]. Isman and Inman measured the locations of the axes in the bones relative to each other (Table 5) [31, 32]. A computer animation of the ankle joints' was made as seen in Fig. 4.

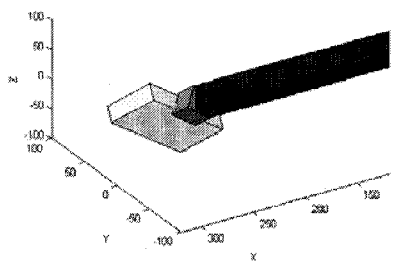

Fig. 4. The ankle model in the second position of our simulation to show both a slight plantarflexion and supination.

TABLE 5
OFFSET OF THE HUMAN ANKLE JOINT

Joint	α_{fp}	β_{fp}	θ_{fp}	α_{td}	β_{td}	θ_{td}
talocrural	-20°	-16°	0°	20°	16°	0°
subtalar	-41°	-67°	0°	41°	67°	0°

VIII. DISCUSSION

The DH representation has been used to measure the movements of animal joints with a six revolute orthogonal mechanism [53, 54] and represents the mechanics of the arthropod limbs with their arbitrary revolute joints [23, 34]. Albright, et al., described the difficulties encountered using DH for linkages with arbitrary axes and suggested a more flexible method, which utilized directional cosines [18]. Buford, et al., used computer graphics techniques and arbitrary revolute joints for computer simulation of human hand joints' motions [45, 48, 49].

Our proposed model is a more complete method for multilinked systems than the DH representation or Albright's method, but requires more computational power for motion simulation. These computations, whose complexity presented difficulties in past years, are now feasible because of the increases in desktop computing capabilities. Programming in Matlab®, a common software program, allows for flexibility in a variety of settings. Outputs for motion of limb segments can be in yaw, pitch, roll, x, y, and z values; a representation commonly used by engineers. The method is three-dimensional and has the same computational approach used in computer graphics and CAD software, thereby providing a common language to modeler, designers, engineers, and biologists. The technique involves translating and rotating the limb joint mechanism to align with a reference coordinate axis, rotating the joint revolute, and then the mechanism is de-rotated and de-translated back to its correct position. There is no order dependence for joint rotations. This approach reduces the azimuth errors and keeps the limb or joint reference frames within the limb segments. The parameters describing each limb segment and revolute are clearly defined, simplifying the limb's mechanical description and kinematic modeling. The errors between the measured data and our technique are within the experimental errors of our measurement process. Thus, it is reasonable to assume that our methods of calculating the positions of the limbs are correct for orthogonal and non-orthogonal rotations. The identity matrix that is attained from the closed loop rotation also validates the methodology. Our method can be generalized to represent linkages with any lower pair mechanism.

The method can also be used to compute limb dynamics and control. Giurintano, et al., used sophisticated non-linear optimization to resolve static thumb joint forces using a five arbitrary revolute manipulator [46]. The solutions of static and dynamic forces in a non-orthogonal system are much more difficult than in the more common orthogonal robot designs. A design advantage of our method is that the resultant forces are three-dimensional and can project out of the plane of the limb segments. Solutions for the dynamics of non-orthogonal systems are also more complicated than for orthogonal systems. In addition to centripetal forces, Coriolis forces become real factors for each moving linkage and may project out of the plane of the limb segments or the limb itself. These forces can be additive and are of great use to the moving crab or human. They are probably an important factor in the evolutionary design of limbs and their joints. Robotic designs exploiting such forces could improve robot efficacy including more rapid motion, improved efficiency of motion, increased dynamic torque, and increased (or decreased) impact forces.

A better representation of the forward kinematics of animal limbs should assist in the understanding of limb motion, in

limb and joint design, and to better solutions for inverse kinematics. Lupichuk developed a method for finding the position and orientation of an arbitrary revolute from three-dimensional data (x, y, z, yaw, pitch, and roll) with application to the elbow [36]. The method was very accurate and precise, but was limited to joints with only one degree of freedom, a relatively long limb segment, and an arc of motion of at least 60 degrees. Moore, et al., used configuration space analysis of human wrist three-dimensional data to determine the number of degrees of freedom in the joint and to determine the paths of motion within the space, which showed only one degree of freedom [37]. Future research will improve our measurement of joint motion and the analysis and design of joint and limb kinematic mechanisms.

IX. Conclusion

Animal limb mechanisms are three-dimensional kinematic chains with nonorthogonal revolute joints. We proposed a more complete method for the representation and analysis of the movements of these and other three dimensional linkages. Our SEA (Storey, et al.) representation is similar to that used in computer animation and provides a common and clear language for designers, modelers, animators and biologists.

X. Acknowledgements

We would like to thank Dr. William Buford Jr. of UTMB for his insight and help with this paper.

XI. References

[1] A. Banos, M. A. Jimenez, and P. Gonzalez de Santos, "Dynamic simulation of a four-legged gait," in *Systems, Man and Cybernetics, IEEE International Conference on* 1992, pp. 498-503.

[2] J. Estremera and P. Gonzalez de Santos, "Generating continuous free crab gaits for quadruped robots on irregular terrain," *Robotics, IEEE Transactions on*, vol. 21, pp. 1067- 1076, 2005.

[3] Z. Fuhai, W. Weiguo, L. Yuedong, and R. Bingyin, "Omni-directional quadruped walking gaits and simulation for a gorilla robot," in *Intelligent Robots and Systems, Proceedings of the 2005 IEEE/RSJ International Conference on*, 2005, pp. 1121-1126.

[4] T. Geng, B. Porr, and F. Worgotter, "Self-stabilized biped walking under control of a novel reflexive network," in *Intelligent Robots and Systems, Proceedings of the 2005 IEEE/RSJ International Conference on*, 2005, pp. 3269- 3274.

[5] C. Hwang and K. Sasaki, "Evaluation of robotic fingers based on kinematic analysis," in *Intelligent Robots and Systems, Proceedings of the 2003 IEEE/RSJ International Conference on*, 2003, pp. 3318- 3324.

[6] W. Li-quan, C. Dong-liang, S. Lei, M. Qing-xin, and Z. Ling, "The research on bionic crab-liked robot prototype," in *Mechatronics and Automation, 2005 IEEE International Conference*, 2005, pp. 2017-2021.

[7] Y. Matsuoka and P. Afshar, "Neuromuscular strategies for dynamic finger movements: a robotic approach," in *Engineering in Medicine and Biology Society, 26th Annual International Conference of the*, 2004, pp. 4649- 4652.

[8] S. Peng, C. P. Lam, and G. R. Cole, "A biologically inspired four legged walking robot," in *Robotics and Automation, Proceedings of the 2003 IEEE International Conference on*, 2003, pp. 2024- 2030.

[9] A. Schneider, H. Cruse, and J. Schmitz, "A biologically inspired active compliant joint using local positive velocity feedback (LPVF)," *Systems, Man and Cybernetics, Part B, IEEE Transactions on*, vol. 35, pp. 1120- 1130, 2005.

[10] W. Weiguo, L. Yuedong, Z. Fuhai, and R. Bingyin, "Design, simulation and walking experiments for a humanoid and gorilla robot with multiple locomotion modes," in *Intelligent Robots and Systems, Proceedings of the 2005 IEEE/RSJ International Conference on*, 2005, pp. 1157- 1162.

[11] J. Yamaguchi and A. Takanishi, "Design of biped walking robots having antagonistic driven joints using nonlinear spring mechanism," in *Intelligent Robots and Systems, Proceedings of the 1997 IEEE/RSJ International Conference on*, 1997, pp. 251-259.

[12] J. Yamaguchi, A. Takanishi, and I. Kato, "Development of a biped walking robot compensating for three-axis moment by trunk motion," in *Intelligent Robots and Systems, Proceedings of the 1993 IEEE/RSJ International Conference on*, Yokohama, Japan, 1993, pp. 561-566.

[13] J. Yang and K. J., "A strategy of optimal fault tolerant gait for the hexapod robot in crab walking," in *Robotics and Automation, Proceedings of the 1998 IEEE International Conference on*, 1998, pp. 1695-1700.

[14] A. Torige, M. Noguchi, and N. Ishizawa, "Centipede type multi-legged walking robot," in *Intelligent Robots and Systems, Proceedings of the 1993 IEEE/RSJ International Conference on*, 1993, pp. 567-571.

[15] M. W. Spong and M. Vidyasagar, in *Robot Dynamics and Control* New York: John Wiley and Sons, 1989, pp. 32-72.

[16] J. Denavit and R. S. Hartenberg, "A kinematic notation for lower-pair mechanisms based on matrices," *ASME Journal of Applied Mechanics*, vol. 22, pp. 215–221, 1955.

[17] J. Agee, A. Hollister, and F. King, "The Longitudinal Axes of Rotation of the Metacarpophalangeal Joint of the Finger," *J Hand Surg*, vol. 11, p. 767, 1986.

[18] S. L. Albright, E. F. Fichter, and B. L. Fichter, "Kinematic Model for Arthropod Legs and Other Manipulators," *Journal of Mechanical Design, Transaction of ASME*, vol. 116, pp. 22-27, 1994.

[19] S. G. Elias, M. A. R. Freeman, and E. I. Gokcay, "A correlative study of the geometry and anatomy of the

distal femur," *Clin Orthop Relat Res*, vol. 260, pp. 98-103, 1990.

[20] A. Fick, "Die Gelenke mit sattelformigen Flachen," in *Zeitschrift fur Rationelle Medicin* Heidelberg: Akademische Verlagshandlung von C. F. Winter, 1854, pp. 314-21.

[21] A. Fick, "Lehrbuck der Physik," in *Medicinische Physik* Brunchweig: Verlag Friedrich Vieweg und Sohn, 1866.

[22] R. Fick, "Handbuch der Anatomie und Mechanik der Gelenke unter Berucksichtigung der bewegenden Muskeln," in *Specielle Gelenk und Muskelmechanik*. vol. 2 Jena: Verlag von Gustav Fisher, 1908.

[23] E. F. Fitcher and B. L. Fichter, "A survey of legs of insects and spiders from a kinematic perspective," in *Robotics and Automation, Proceedings of the 1988 IEEE International Conference on*, 1988, pp. 984-986.

[24] M. Freeman, "Knee Flexion: The cruciate ligaments and posterior stability in the flexed knee," in *Total Arthroplasty of the Knee. Proceedings of the Knee Society 1985-1986*, 1986.

[25] A. Hollister, W. L. Buford, L. M. Myers, D. J. Giurintano, and A. Novick, "The Axes of Rotation of the Thumb Carpometacarpal Joint," *J Orthop Res*, vol. 10, pp. 454-60, 1992.

[26] A. Hollister and D. J. Giurintano, "Thumb Movements, Motions, and Moments," *J Hand Therapy*, vol. 8, pp. 106-114, 1995.

[27] A. Hollister, D. J. Giurintano, W. L. Buford, L. M. Myers, and A. Novick, "The Axes of Rotation of the Thumb Interphalangeal and Metacarpophalangeal Joints," *Clin Orthop Relat Res*, vol. 320, pp. 188-93, 1995.

[28] A. M. Hollister, H. Gellman, and R. L. Waters, "The Relationship of the Interosseus Membrane to the Axis of Rotation of the Forearm," *Clin Orthop Relat Res*, vol. 298, pp. 272-276, 1994.

[29] A. M. Hollister and D. G. Giruintano, "How Joints Move," in *Clinical Mechanics of the Hand*, P. W. Brand, Hollister, A. M., Ed. Chicago Mosby 1999.

[30] A. M. Hollister, S. Jatana, A. K. Singh, W. W. Sullivan, and A. G. Lupichuk, "The Axes of Rotation of the Knee," *Clin Orthop Relat Res*, vol. 290, pp. 259-268, 1993.

[31] V. T. Inman, *The joints of the ankle*. Baltimore: Williams & Wilkins, 1976.

[32] R. E. Isman and V. T. Inman, "Anthropometric studies of the human foot and ankle," *Bulletin of Prosthetics Research*, pp. 97-129, 1969.

[33] N. Koti, "Design of a biomimetic manipulator with nonorthogonal Joint Axes." vol. Masters Ruston, LA: Louisiana Tech University, 2005.

[34] A. F. Krause and V. Dürr, "Tactile efficiency of insect antennae with two hinge joints," *Biol. Cybern.*, vol. 91, pp. 168-81, 2004.

[35] J. T. London, "Kinematics of the Elbow," *J Bone Joint Surg*, vol. 63, pp. 529-35, 1981.

[36] A. G. Lupichuk, "Determining the axis of rotation from 3-D motion data," in *College of Engineering*. vol. Masters Long Beach: California State University, 1995.

[37] J. A. Moore, C. F. Small, J. T. Bryant, R. E. Ellis, D. R. Pichora, and A. M. Hollister, "A Kinematic Technique for Describing Wrist Joint Motion: Analysis of Configuration Space Plots," *Proc Instn Mech Eng*, vol. 207, pp. 211-218, 1993.

[38] V. Moyer, E. Fichter, and B. Fichter, "Analyzing dynamics of arthropod walking," in *Medicine and Biology Society, Proceedings of the 1988 Annual International Conference of the IEEE Engineering in*, 1988, pp. 710- 711.

[39] A. K. Singh, K. D. Starkweather, A. M. Hollister, S. Jatana, and A. G. Lupichuk, "Kinematics of the ankle: a hinge axis model," *Foot and Ankle*, vol. 13, pp. 439-446, 1992.

[40] W. Weber and E. Weber, in *Mechanik der Menschlichen Gehwerkzeuge* Berlin: Springer Verlag, 1836, pp. 75-97.

[41] D. Hearn and M. P. Baker, in *Computer graphics C version*: Prentice Hall, 1997, pp. 408-423.

[42] D. F. Rogers and J. A. Adams, in *Mathematical Elements for Computer Graphics* New York: McGraw-Hill, 1990, pp. 101-30.

[43] D. F. Rogers and R. A. Earnshaw, *Techniques for computer graphics*. New York: Springer-Verlag, 1987.

[44] C. M. Storey, A. M. Hollister, C. Robinson, N. Witriol, D. O. Anderson, J. C. London, and W. L. Buford, "A System for Measurement and Calibration of Nonorthogonal Joints and Limbs in Humans," in *in Proceedings of the 28th Annual International Conference IEEE EMBS*, New York, NY, USA, 2006.

[45] W. L. Buford, A. M. Hollister, and L. M. Myers, "A Modeling and Simulation System for the Human Hand," *J Clin Engr*, vol. 15, pp. 445-451, 1990.

[46] D. J. Giurintano, A. M. Hollister, W. L. Buford, D. E. Thompson, and L. M. Myers, "A virtual five-link model of the thumb," *Med Eng Phys*, vol. 17, pp. 297-303, 1995.

[47] D. E. Thompson and D. J. Giurintano, "A Kinematic Model of the Flexor Tendons of the Hand," *J Biomech*, vol. 22, pp. 327-34, 1989.

[48] W. L. Buford, Jr. and D. E. Thompson, "A System for Three-Dimensional Interactive Simulation of Hand Biomechanics," *IEEE Transactions on Biomedical Engineering*, vol. 34, pp. 444-453, 1987.

[49] W. L. Buford, Jr. and C. R. Andersen, "Definition of the kinematic plant for the human musculoskeletal system," in *Systems, Man and Cybernetics, 2005 IEEE International Conference on*, 2005, pp. 1246-1251.

[50] E. D. Pohl and H. Lipkin, "Kinematics of complex joint angles in robotics," in *Robotics and Automation, 1990 IEEE International Conference on*, 1990, pp. 86-91.

[51] J. Ziegert and P. Datseris, "Basic considerations for robot calibration," in *Robotics and Automation, Proceedings of the 1988 IEEE International Conference on*, 1988, pp. 932-938.

[52] D. L. Kunz, "An object oriented approach to multibody systems analysis," *Computers and Structures*, vol. 69, pp. 209-217, 1998.

[53] G. L. Kinzell and L. J. Gutkowski, "Joint models, degrees of freedom, and anatomical measurement," *J Biomech Eng*, vol. 105, pp. 55-62, 1979.

[54] G. L. Kinzell, A. S. Hall, and B. M. Hillberry, "Measurement of total motion between two body segments - I Analytical development," *J Biomech*, vol. 5, pp. 93-105, 1972.

APPENDIX S

SUBMITTED JOURNAL OF REHABILITATION RESEARCH AND DEVELOPMENT PAPER

Balance and Diabetes in Mature Adults

Storey, Christopher M., MSc[a,b], Robinson, Charles J., DSc[a,b,c,d], Hollister, Anne, MD[e],and The SLIP-FALLS Study Team[a,d,*]

[a]Louisiana Tech University, Department of Biomedical Engineering

[b]Clarkson University, Center for Rehabilitation Engineering, Science and Technology

[c]Dept. of Physical Med. & Rehab, Upstate Med Univ., Syracuse, NY

[d]Syracuse, NY, Research Service, VA Medical Center

[e]Louisiana State University Health Sciences Center, Department of Orthopaedic Surgery

Corresponding Author:	Christopher M. Storey	Clarkson University - CREST
	Cell: 504-782-3280	8 Clarkson Ave.
	Fax: 315-268-6654	Box 5730 CAMP 225
	storeytime@hotmail.com	Potsdam, NY 13699

* The SLIP-FALLS-STEPm study team consisted of students at the University of Pittsburgh and Louisiana Tech University, and staff at the Shreveport, Louisiana, VA Medical Center, who helped with the collection of these data, and whose PhD dissertations and MS theses addressed different aspects of these experiments. The team members in alphabetical order are Venketesh Balasubramanian, Vikram Darbhe, Shruti Deshmuhk, Charlotte Eichelberger, Larry Faulkner, Scott Morstatt, Senthilnathan Nakappan, Kristopher K. O'Neal, Gloria Patrick, and Samantha J. Richerson.

Abbreviations: Diabetic mature adult with Peripheral Neuropathy (DPN), Diabetic mature adult who is Neurally Intact (DNI), Healthy Mature Adult (HMA), Sliding Linear Investigative Platform For Assessing Lower Limb Stability with Simultaneous Tracking, EMG and Pressure measurements (SLIP-FALLS-STEPm), Semmes-Weinstein monofilaments (SWM), Short Form 36-item health survey (SF-36), Nerve conduction velocities (NCV), total excursion (TOTEX), resultant distance (RD), 95% confidence circular area (AREA-CC), 95% confidence elliptical area (AREA-CE)

Funding: State of Louisiana Board of Regents Fellowship; Merit Review grants from VA Rehabilitation R&D Service Grants #E91-355AP, #E2143PC, #E01-2097R, and a VA Senior Rehabilitation Research Career Scientist Award to Dr. Charles Robinson.

Abstract

Our objective was to show that detriments to postural control exist prior to the development of peripheral neuropathy in type 2 diabetes with no fall history. This study tested diabetic mature adults with peripheral neuropathy (DPN: n=17, nerve conduction velocity < 40 m/s) and without peripheral neuropathy (DNI: n=11) and healthy mature adults (HMA: n=34); all aged 50 to 74 years. No nerve conduction or latency differences existed between HMA and DNI. All underwent static and quasi-static postural assessments, with the latter assessed by short anterior platform perturbations. DPN's anterior-posterior center-of-pressure static metrics differed from HMA's. Both diabetic groups had higher thresholds for acceleration than HMA at 1 and 4 mm anterior perturbations. Both had higher plantar touch thresholds than did HMA. Since both had markedly higher thresholds to detect short perturbations, we conclude that

peripheral neuropathy in diabetic individuals is not solely the cause of decreased postural control.

Introduction

Postural instability and diabetes are leading risk factors for falls, which are a common source of morbidity and mortality in those over 65 years old (1, 2). Elders who fall frequently have an unsteady gait (3) or poor postural control (4). Falls lead to a fear of falling in the elderly, which increases the likelihood that one becomes homebound or bed-bound, thus resulting in a poorer quality of life (5). Diabetic individuals can also develop subtly impaired cognition, have lower reaction times to perturbations, and have a higher incidence of falls than their age–matched cohorts (4, 6-9). People with diabetes who have lower limb peripheral neuropathy show increased postural instability over diabetic subjects without peripheral neuropathy (10), and have increased likelihood of falls (11).

Postural control in elderly and diabetic individuals has been studied during quiet standing and has shown decreased stability in (10, 12-15). Prieto, et al., has shown that significant differences exists in a large array of posture metrics between young adults and the elderly (12). Lafond, et al., has shown that significant instabilities exist between diabetic individuals without history of falls and their elderly cohorts (14). We want to show that same instabilities can be seen though a large array of quiet standing metrics. Also we felt that our test that characterizes the response to small transient platform movements would be a more sensitive method for testing dynamic postural instabilities than methods that use waist-pulls at the hip, large perturbations, and tilts (16-24). Thus we developed a series of test protocols that use the Sliding Linear Investigative Platform for Assessing Lower Limb Stability with Synchronized Tracking, EMG and Pressure measurement (SLIP-FALLS-STEPm) (25-29). Our novel platform and its test protocols focus on quantifying differences between groups in their ability to detect small movements (≈1 mm). These small movements that are within the normal sway range provide the

mechanism to study how humans stand, as opposed to how humans prevent falls to discover deficiencies in postural control that could lead to an increased likelihood of falls.

By studying diabetic individuals both with and without lower limb peripheral neuropathy, who have no history of falls in either group, we have are able to study people who are at high risk for falls but have not become symptomatic. The aim of our study was to investigate whether large fiber lower limb neuropathy secondary to diabetes was the sole cause of increased postural instability.

Research Design and Methods:

Subjects

Our subjects were well-controlled diabetic mature adults with peripheral neuropathy (DPN: 4 female and 13 male) and without peripheral neuropathy (DNI: 4 female and 7 male). Healthy mature adults (HMA: 14 female and 20 male), all who had normal lower-limb peripheral nerve conduction tests, volunteered for the control group. To enable a precise comparison, only subjects who completed our entire electrophysiological and acceleration threshold test protocol were used for this paper. Their primary care physician had previously diagnosed each DPN or DNI with type 2 diabetes. Subject recruiting took place via flyer advertising at the Overton Brooks VA hospital in Shreveport, Louisiana, and in the local area. Individuals from 50 to 75 years of age, inclusive, were labeled as mature adults. Our test protocol was approved by the IRBs of the Shreveport VAMC and Louisiana Tech University.

Screening

A medical history questionnaire was given to each potential subject. Individuals were not further tested if they had a medical history of cardiovascular and/or respiratory disease,

neurological problems such as cerebrovascular disease, stroke, head or spine injury, vestibular ailments and dizziness, memory and concentration deficits, muscle activity deficits, or non-healing skin ulcers. Orthopaedic problems such as lower back pain or spasms, arthritis or joint disease, and deformations of joints or bones led to exclusion of individuals from the study. Those with past or current drug or alcohol dependence were also excluded.

All consented subjects were screened with the Berg Balance Scale and Sharpened Romberg Test to assure that they were able to operate independently from assistance, and vision was tested (Snellen Eye Chart correctable vision required). In addition, the subjects were tested with the Mini-Mental State Exam to insure that they were mentally competent to follow instructions during the experiment. Patellar and Achilles' reflexes were tested to confirm that they were present and normal. The DPN and DNI groups had hemoglobin A1c values below 9%., with no group differences seen in values, or in number of subjects with values >7.0 (4 DPN, 2 DNI). A temporary classification of Healthy Mature Adult (HMA) was made for all consented subjects who reported no history of diabetes or neurological impairment. Perturbation testing on all of our subjects commenced before, during or after the nerve conduction tests were carried out, as the scheduling of the NCV tests by the Neurology Service were on a fill-in basis between clinical tests. Once the NCV results were in, a final classification into an HMA group could be made. Of the 46 individuals without a history of diabetes that went through our protocol, 34 were classed as HMA, and are studied here. The remaining twelve were positive for peripheral neuropathy during the NCV testing. These individuals were excluded from this analysis since we did not know the cause or the extent of the neuropathy, as Nardone, et al., showed that different types of peripheral neuropathy affect postural stability to different degrees,

and we could not rule out diabetes, given the epidemic prevalence of undiagnosed diabetes in mature adults (21, 30, 31).

Testing Procedures

The preceding tests provide physiological backgrounds on individuals for our posture test protocol. The 2-Alternate Forced Choice acceleration thresholds to forward perturbations of constant displacement were carried out on the SLIP-FALLS-STEPm platform while blindfolded (25). Air bearings insure that the ultra-low vibration, frictionless platform provides no movement cues and allows for the test of movements within the range of sway. The subjected is presented via wireless headphones prerecorded commands with white masking noise of "Ready", "One", "Two", and "Decide". During the four second decision period, the subject must in which period they perceived the perturbation to have occurred, by a single (interval 1) or double (interval 2) bell press. The subject needed to accrue a correct detection percentage of 79% for an acceleration to be considered threshold. The platform moves in a 100% smoothed s-curve, which allows for symmetrical acceleration and deceleration of which the peaks are used as the measurement for threshold (25, 26). The peak imparted kinetic energy (PIKE) was calculated by Eq. 1, where m is the subject's mass, PAT is the peak acceleration threshold, and PD is the platform displacement. The peak imparted kinetic energy accounts for individuals' mass in relation to each individual's peak acceleration threshold.

$$PIKE = \frac{m * PAT * PD}{2} \qquad (1)$$

Prior to each threshold detection session, twenty seconds of quiet standing data were recorded to assess an individual's natural sway. This yielded three quiet standing observations periods per individual. Sway parameters are calculated from the four

load cells of the force-plate. The anterior-posterior center of pressure (APCoP) and medial-lateral center of pressure (MLCoP) time-series profiles were derived from the load cell data (25), with the convention that forward and rightward were the positive directions. The time series were filtered using a 10Hz type 2 Chebyshev low-pass filter, and the means subtracted out. From these time-series, another is calculated - the resultant distance (RD) - to provide a time series of the vector distance combining each APCoP and MLCoP pair. Based on these time-series, we calculated metrics suggested by Prieto, et al., who had shown differences in aged and young adult groups (12). They are broken up into four categories: time-domain distance, time-domain area, time-domain hybrid, and frequency domain measures. From the time-domain distance metrics, mean and RMS distances were calculated for RD, APCoP, and MLCoP (12), along with the standard deviation and range of each time series. The total excursion (TOTEX), a summation of the changes in distance, was calculated for APCoP, MLCoP, and the vector distance change of both (12). The mean velocity is calculated from the TOTEX, $TOTEX_{ap}$, and $TOTEX_{ml}$ (12). The two time-domain area measures that are calculated are the 95% confidence circular area (AREA-CC) and 95% confidence elliptical area (AREA-CE) with 95% confidence level coming from the z and F statistic respectively (12). The hybrid measures include sway area (estimates area enclosed by COP path per unit of time), mean frequency (both rotational and in the respective APCoP and MLCoP planes), and fractal dimension (based on TOTEX, AREA-CC, AREA-CE) (12). For the frequency domain, the total power, 50% power frequency (median power frequency), 95% power frequency (95% percentile power frequency), centroidal frequency, and frequency dispersion were calculated using discrete Fourier transform and not the sinusoidal multi-taper estimate (12).

All subjects were given the RAND 36-item (with Depression Screener) health survey, a modified version of the short form 36-item (SF-36) health survey, which has shown correlations of poor health scores with individuals who had diabetes (32-36). The RAND evaluates a person's s self-reported physical and mental health on their quality of life. Jenkins, et al., and Lyons, et al., verified the validity and reliability of SF-36 health survey in an elderly population (37, 38). Lower scores were correlated with elderly who have a fall risk (5). Post-test scoring was performed automatically within an Excel spreadsheet.

Semmes-Weinstein Monofilaments (SWM) were used to assess sensory thresholds on the sole of the foot by exerting a constant force based on buckling strength of the monofilament pressed to the foot. The monofilaments are marked with a log of the force exerted in grams by the monofilament. These threshold measurements were taken on the plantar surface at the great toe, metatarsal at the first and fourth digit, and heel. The procedure required that two out of three touches be detected for a given monofilament to be at threshold at a location. For simplicity, with eyes closed, subjects were asked to respond when they felt the probe. For the SWM test, a discrepancy in sample size exists across the test sites, because we did not begin taking measurements at the heel and fourth metatarsal until after a number of subjects had been recruited.

Surface lower-limb nerve conduction tests, performed by Overton Brooks VA Medical Center Neurology Service by a technician supervised by a neurologist, determined the presence of peripheral neuropathy. NCV were measured for the peroneal, tibial, and sural nerves bilaterally. In fifteen subjects (4 DNI, 5 DPN, and 6 HMA), no sural nerve conduction velocity could be obtained. Inferences cannot be made from the inability to find sural nerve CVs via surface electrodes as sural nerve studies often require the use of needle electrodes (39-42). M-

wave and F-wave latency tests were performed on the peroneal and tibial nerves. Marked audiological differences were noted between those with diabetes and the HMA group (43). This analysis will be presented later due to space limitations here.

Analysis

Electrophysiological and subject screening results were analyzed in SPSS via an ANOVA with Games-Howell post-hoc correction to compensate for the unequal group sizes and variances. Quiet standing metrics also used a post-hoc Games-Howell after ANOVA with repeated measures. Statistics on Mini-Mental Exam, Berg Balance Scale, RAND, acceleration thresholds, and SWM were performed in SPSS with Kruskal-Wallis one-way ANOVA. The Kruskal-Wallis one-way ANOVA allowed us to account for the subjects who did not reach threshold but went to the maximum allowed acceleration of the test for acceleration thresholds. The Kruskal-Wallis was performed pair-wise on groups as a post-hoc test. For SWM tests, geometric means are reported instead of the log values because of the power law nature of tactile perception (44, 45).

Results

We hypothesized the peripheral neuropathy secondary to type 2 diabetes would cause decreased ability to detect platform perturbations. We found instead that the ability to detect platform perturbations is diminished in diabetic mature adults with peripheral neuropathy (DPN) and without peripheral neuropathy (DNI), both as compared to healthy mature adults (HMA), suggesting that the presence of diabetes itself was major factor in an increased detection threshold.

Subjects

There was no significant difference in age, height, or body mass index between DNIs, DPNs, and HMAs. While mass was not significantly different between HMA and DNI or DNI and DPN, it was significantly different ($p < 0.05$) between HMA (83.2 kg) and DPN (98.3 kg), as shown in Table 1.

[Insert Table 1 Near Here]

[Insert Figure 1 Near Here]

Peak Acceleration Thresholds

A difference exists in DNI and DPN acceleration threshold values for all move displacements (Figure 1). Both DNI and DPN had significantly higher thresholds than HMA at 1 mm ($p<0.01$) and 4 mm ($p<0.01$ and $p<0.05$, respectively) displacements (table 2). A strong trend was also noted for significantly increased threshold of DNI over HMA ($p=0.054$).

[Insert Table 2 Near Here]

Using the calculated peak energy imparted on the subject, we gain significantly higher peak energies ($p<0.05$) for DNI over HMA for all displacements. While significantly higher imparted peak energies were seen in DPN over HMA for 1 mm ($p<0.01$) and 4 mm ($p<0.05$) displacements, only a strong trend was noted for the 16 mm displacement. Due to safety constraints of our system, we set a maximal peak acceleration value at 200 mm/s^2 for 1 mm moves and 100 mm/s^2 for 4 mm and 16 mm moves. A number of subjects reached these values (rail condition). Analysis of the negative power-law relationship (29, 44-47) between acceleration and displacement values provided reason to raise the maximum peak acceleration test values to 256 mm/s^2, 181 mm/s^2, and 128 mm/s^2 respectively for 1 mm, 4 mm, and 16 mm perturbations. HMA subjects reaching the rail (11%, 3%, and 0%) were fewer than both DPN

(41%, 18%, and 6%) and DNI (63%, 36%, and 18%) at 1 mm, 4 mm and 16 mm displacement respectively as seen in Table 3.

[Insert Table 3 Near Here]

Quiet Standing Metrics

In the anterior-posterior time-series, significant ($p < 0.05$) differences were seen in range, standard deviation, and RMS distance for HMA versus DPN (Table 4). The total power for anterior-posterior was significantly increased ($p < 0.01$) for the DPN versus HMA. Trends in HMA versus DPN groups were seen with increased mean resultant distance, mean anterior-posterior distance, RMS distance, anterior-posterior total excursion, and anterior-posterior mean velocity. No differences were seen between DNI and either DPN or HMA groups.

[Insert Table 4 Near Here]

Health Surveys

The mean scores on all health survey results (except for the RAND emotional well-being) score were better for HMA than for DNI and DPN, but not all mean differences were significant (Table 5). Although the scores on the Berg Balance Scale were within an acceptable range for DNI and DPN (they showed no risk of falls and could operate independently), these latter scores were still significantly lower than those of HMA. The only significant group difference gained from the RAND survey was in general health. Both DPN and DNI showed significant decreased feelings of general health ($p<0.05$ and $p<0.01$, respectively). Strong trends were observed in RAND measures of pain and physical health [Pain in HMA vs. DPN ($p=0.06$) and in HMA vs. DNI ($p=0.051$); physical health in HMA vs. DPN ($p=0.06$)]. No significance was seen between diabetic subjects with or without lower limb peripheral neuropathy.

[Insert Table 5 Near Here]

Foot Sensitivity

Semmes-Weinstein Monofilaments (SWM) testing displayed several significant differences in the geometric mean among the groups (Table 6). Bilateral significant differences provide a more significant measure of tactile sensory acuity. The first and fourth metatarsals had significantly different bilateral thresholds between HMA and DPN. The significance at the first metatarsal is higher ($p<0.01$) than at the fourth metatarsal ($p<0.05$). SWM of HMA had geometric means of thresholds less than 0.77 g for both first and fourth metatarsal bilaterally, while DPN had thresholds greater than 1.49 g. None of the geometric means is above the threshold for developing diabetic ulcers (>10.0 g) in either HMA, DNI, or DPN groups, however two DNI and five DPN subjects did have thresholds at risk for developing ulcers, while no HMA did. Thresholds of the fourth metatarsal differed bilaterally, significant and trend respectively for the left ($p<0.05$) and right ($p=0.062$) feet, between HMA and DNI. DPN had a significantly higher ($p<0.05$) SWM threshold at the left heel versus HMA, but none was seen in the right heel. DNI had a significant bilateral decrease in thresholds versus HMA at the heel.

[Insert Table 6 Near Here]

Lower Limb Electrophysiology

Both DNI and HMA have higher ($p<0.01$) NCVs than DPN bilaterally for the peroneal, tibial, and sural nerves (Table 7). No difference was observed in NCVs between HMA and DNI. No bilateral difference was observed for the M-wave latency test. The weaker significance in the tibial M-wave latency test can be attributed to the increased variance as seen in Table 7 by the 95% confidence interval, which for both DPN and DNI was greater than double the 95% confidence interval of HMA. Between HMA and DPN, bilateral significance ($p<0.01$ for all except left peroneal $p<0.05$) was seen for both peroneal and tibial nerves in the F-wave latency

test. Significant lower ($p<0.05$) latencies were seen in DPN versus DNI for all F-wave latencies except left peroneal.

[Insert Table 7 Near Here]

Discussion

The comprehensive study allowed us to look at alterations in both static and dynamic posture caused by Type-2 diabetes in mature adults. Lower limb peripheral neuropathy, prevalent among those with Type-2 diabetes, has been assumed the cause of the increased likelihood of falls and instability (2, 11). Our study was able to compare perception thresholds of movement and static postural metrics in people who have diabetes with and without lower limb peripheral neuropathy.

The acceleration threshold tests showed a distinct decrease in the ability to sense forward platform movement in both DPN and DNI as compared to HMA. Our electrophysiology examinations could not account for the decrease, since HMA and DNI did not significantly differ in NCV yet DNI had significantly increased detection thresholds at both 1 mm and 4 mm displacements. The SWM examination did not reveal any significant differences between DPN and DNI, but did show a bilateral significant difference in the heel and a significant difference with a trend on the left and right fourth metatarsal respectively between DNI and HMA. These physiological differences provide a cause for decreased sensitivity of DNI to motion, since the DNI have higher mean thresholds than the DPN, and the geometric mean of SWM at both heels was higher in the DNI than the DPN. More DPN (5) than DNI (2) had SWM greater than 10.0g, but none had any history of ulceration or vascular problems. The decreased sensation at the heel provides a reason why both DNI and DPN scored significantly lower than HMA on the Berg Scale. The DPN and DNI self-reported in the RAND poorer general health, and also had trends

at more pain and poorer physical health, which could be attributed to the increased SWM thresholds of both DPN and DNI groups.

Simmons, et al., studied diabetic individuals both with and without cutaneous sensory deficit versus controls. Our data confirms that DPN who had significantly different SWM thresholds from HMA, also had significantly larger anterior-posterior sway lengths than our control (HMA) for quiet standing analysis (15). Our data also shows that our DNI subjects who also had significantly different SWM thresholds did not significantly differ from HMA for any quiet standing posture metric. Lafond, et al., also studied quiet standing diabetics individuals with sensory neuropathy versus healthy elderly. His data and ours confirmed the increased anterior-posterior sway, but our data did not observe different medial-lateral sway between groups (14). Nardone, et al., studied both dynamic and static postural stability in subjects with polyneuropathy diagnosed by nerve conduction testing. They proposed that the increase in sway could be attributed to the loss of group II spindle fibers instead of group Ia motor fibers (21). Improper functioning of spindle fibers has decreased efficacy of muscle stretch receptors, which could lead to postural instability. Our HMA and DPN subjects had similar NCV scores as Nardone, et al., and our DPN group corresponds with Nardone, et al., by the increased sway over HMA, especially in anterior-posterior plane (21). Simoneau, et al., found that sensory neuropathy found by SWM threshold was more sensitive to quiet standing postural instability, where our data provides that the decreased NCVs of the DPN group cause their significant postural instability (10). The metric that Simoneau, et al., used to quantify stability was total excursion, which we found a trend in the anterior-posterior direction only (10).

Conclusion

The DMAs with and without peripheral neuropathy show increased threshold for the detection of movement, which is believed to increase their risk of falls since they would be less likely to detect an initiation of a fall. However, only DPN display significantly different quiet standing metrics compared to HMA, which leads to nerve conduction as a cause to the instability. Further studies focusing on diabetic individuals with cutaneous sensory neuropathy, with lower limb neuropathy, and those with both will help better define the cause for instability in diabetic individuals. In addition, further studies on individuals with peripheral neuropathy, but who are confirmed to not have diabetes or be glucose-intolerant will better define peripheral neuropathy's and type 2 diabetes' contribution to postural instability.

Acknowledgements

Support provided by a State of Louisiana Board of Regents Fellowship, Merit Review grants from VA Rehabilitation R&D Service Grants #E91-355AP, #E2143PC, #E01-2097R, and a Senior Rehabilitation Research Career Scientist Award to Dr. Charles Robinson.

References

1. Masud T, Morris RO. Epidemiology of falls. Age & Ageing 2001;30(suppl_4):3-7.
2. Schwartz AV, Hillier TA, Sellmeyer DE, Resnick HE, Gregg E, Ensrud KE, et al. Older Women With Diabetes Have a Higher Risk of Falls: A prospective study. Diabetes Care 2002;25(10):1749-1754.
3. Alexander NB. Gait disorders in older adults. Journal of the American Geriatrics Society 1996;44(4):434-51.
4. Lord SR, Clark RD, Webster IW. Postural stability and associated physiological factors in a population of aged persons. Journal of Gerontology 1991;46(3):M69-76.
5. Suzuki M, Ohyama N, Yamada K, Kanamori M. The relationship between fear of falling, activities of daily living and quality of life among elderly individuals. Nursing and Health Sciences 2002;4(4):155-161.
6. Gispen WH, Biessels G-J. Cognition and synaptic plasticity in diabetes mellitus. Trends in Neurosciences 2000;23(11):542-549.
7. Stewart R, Liolitsa D. Type 2 diabetes mellitus, cognitive impairment and dementia. Diabetic Medicine 1999;16(2):93-112.
8. Allen KV, Frier BM, Strachan MWJ. The relationship between type 2 diabetes and cognitive dysfunction: longitudinal studies and their methodological limitations. European Journal of Pharmacology 2004;490(1):169-175.
9. Cosway R, Strachan MWJ, Dougall A, Frier BM, Deary IJ. Cognitive function and information processing in Type 2 diabetes. Diabetic Medicine 2001;18(10):803-810.

10. Simoneau GG, Ulbrecht JS, Derr JA, Becker MB, Cavanagh PR. Postural instability in patients with diabetic sensory neuropathy. Diabetes Care 1994;17(12):1411-1421.
11. Powell MW, Carnegie DH, Burke TJ. Reversal of diabetic peripheral neuropathy with phototherapy (MIRE) decreases falls and the fear of falling and improves activities of daily living in seniors. Age & Ageing 2006;35(1):11-16.
12. Prieto TE, Myklebust JB, Hoffmann RG, Lovett EG, Myklebust BM. Measures of postural steadiness: differences between healthy young and elderly adults. Biomedical Engineering, IEEE Transactions on 1996;43(9):956-966.
13. Balasubramanian V, Arasu KA, Robinson CJ. Analysis of Postural Stability in Diabetes/Peripheral Neuropathy during Threshold Level Acceleration Perturbation. In: The First UAE International Conference on Biological and Medical Physics; 2005 March 27 -30; 2005. p. 77-93.
14. Lafond D, Corriveau H, Prince F. Postural Control Mechanisms During Quiet Standing in Patients With Diabetic Sensory Neuropathy. Diabetes Care 2004;27(1):173-178.
15. Simmons RW, Richardson C, Pozos R. Postural stability of diabetic patients with and without cutaneous sensory deficit in the foot. Diabetes Research & Clinical Practice 1997;36(3):153-60.
16. Pai Y-C, Rogers MW, Patton J, Cain TD, Hanke TA. Static versus dynamic predictions of protective stepping following waist-pull perturbations in young and older adults. Journal of Biomechanics 1998;31(12):1111-1118.
17. Pidcoe PE, Rogers MW. A closed-loop stepper motor waist-pull system for inducing protective stepping in humans. Journal of Biomechanics 1998;31(4):377-381.
18. Schulz BW, Ashton-Miller JA, Alexander NB. Compensatory stepping in response to waist pulls in balance-impaired and unimpaired women. Gait & Posture 2005;22(3):198-209.
19. Mille M-L, Johnson ME, Martinez KM, Rogers MW. Age-dependent differences in lateral balance recovery through protective stepping. Clinical Biomechanics 2005;20(6):607-616.
20. Rogers MW, Hedman LD, Johnson ME, Martinez KM, Mille M-L. Triggering of protective stepping for the control of human balance: age and contextual dependence. Cognitive Brain Research 2003;16(2):192-198.
21. Nardone A, Grasso M, Schieppati M. Balance control in peripheral neuropathy: Are patients equally unstable under static and dynamic conditions? Gait & Posture 2006;23(3):364-373.
22. Nardone A, Grasso M, Tarantola J, Corna S, Schieppati M. Postural coordination in elderly subjects standing on a periodically moving platform. Archives of Physical Medicine and Rehabilitation 2000;81(9):1217-1223.
23. Nardone A, Tarantola J, Miscio G, Pisano F, Schenone A, Schieppati M. Loss of large-diameter spindle afferent fibres is not detrimental to the control of body sway during upright stance: evidence from neuropathy. Experimental Brain Research 2000;135(2):155-62.
24. Nardone A, Siliotto R, Grasso M, Schieppati M. Influence of aging on leg muscle reflex responses to stance perturbation. Archives of Physical Medicine and Rehabilitation 1995;76(2):158-165.
25. Robinson CJ, Purucker MC, Faulkner LW. Design, control, and characterization of a sliding linear investigative platform for analyzing lower limb stability (SLIP-FALLS). Rehabilitation Engineering, IEEE Transactions on [see also IEEE Trans. on Neural Systems and Rehabilitation] 1998;6(3):334-350.
26. Richerson SJ, Faulkner LW, Robinson CJ, Redfern MS, Purucker MC. Acceleration threshold detection during short anterior and posterior perturbations on a translating platform. Gait & Posture 2003;18(2):11-9.
27. Richerson SJ, Morstatt SG, Vanya RD, Hollister AM, Robinson CJ. Factors affecting reaction times to short anterior postural disturbances. Medical Engineering & Physics 2004;26(7):581-6.
28. Richerson SJ, Robinson CJ, Shum J. A comparative study of reaction times between type II diabetics and non-diabetics. Biomedical Engineering Online 2005;4(1):12.
29. Richerson S, Morstatt S, O'Neal K, Patrick G, Robinson C. Effect of lateral perturbations on psychophysical acceleration detection thresholds. Journal of Neuroengineering and Rehabilitation 2006;3(1):2.
30. Simmons D, Thompson CF, Engelgau MM. Controlling the diabetes epidemic: how should we screen for undiagnosed diabetes and dysglycaemia? In: Diabetic Medicine: Blackwell Publishing Limited; 2005. p. 207-212.
31. Thomas MC, Walker MK, Emberson JR, Thomson AG, Lawlor DA, Ebrahim S, et al. Prevalence of undiagnosed TypeÂ 2 diabetes and impaired fasting glucose in older B ritish men and women. In: Diabetic Medicine: Blackwell Publishing Limited; 2005. p. 789-793.

32. Hays RD, Sherbourne CD, Mazel RM, Hays RD, Sherbourne CD, Mazel RM. The RAND 36-Item Health Survey 1.0.[see comment]. Health Economics 1993;2(3):217-27.
33. Burnam MA, Wells KB, Leake B, Landsverk J. Development of a brief screening instrument for detecting depressive disorders. Medical Care 1988;26(8):775-89.
34. Ware JE, Jr., Sherbourne CD. The MOS 36-item short-form health survey (SF-36). I. Conceptual framework and item selection. Medical Care 1992;30(6):473-83.
35. McHorney CA, Ware JE, Jr., Raczek AE. The MOS 36-Item Short-Form Health Survey (SF-36): II. Psychometric and clinical tests of validity in measuring physical and mental health constructs. Medical Care 1993;31(3):247-63.
36. McHorney CA, Ware JE, Jr., Lu JF, Sherbourne CD. The MOS 36-item Short-Form Health Survey (SF-36): III. Tests of data quality, scaling assumptions, and reliability across diverse patient groups. Medical Care 1994;32(1):40-66.
37. Jenkinson C, Wright L, Coulter A, Jenkinson C, Wright L, Coulter A. Criterion validity and reliability of the SF-36 in a population sample. Quality of Life Research 1994;3(1):7-12.
38. Lyons RA, Perry IM, Littlepage BNC. Evidence for the Validity of the Short-form 36 Questionnaire (SF-36) in an Elderly Population. Age & Ageing 1994;23(3):182-184.
39. Strobl W, Reisecker F, Koltringer P, Leblhuber F, Strobl W, Reisecker F, et al. [A comparative study of the sensory conduction velocity of the sural nerve using surface and needle electrodes]. EEG-EMG Zeitschrift fur Elektroenzephalographie Elektromyographie und Verwandte Gebiete 1992;23(3):135-9.
40. Husstedt IW, Grotemeyer KH, Schlake HP, Husstedt IW, Grotemeyer KH, Schlake HP. [The effect of the lead electrodes on the conduction velocity of the sural nerve]. EEG-EMG Zeitschrift fur Elektroenzephalographie Elektromyographie und Verwandte Gebiete 1991;22(3):152-6.
41. Ewert T, Hielscher H, Grotemeyer KH, Hermanns M, Ewert T, Hielscher H, et al. [Sural nerve neurography using surface and needle electrodes in polyneuropathies. Comparative study]. EEG-EMG Zeitschrift fur Elektroenzephalographie Elektromyographie und Verwandte Gebiete 1985;16(2):114-9.
42. Neundorfer B, Kompf D, Dedden J, Neundorfer B, Kompf D, Dedden J. [Sural neurography: comparative study in stimulation with surface and needle electrodes]. EEG-EMG Zeitschrift fur Elektroenzephalographie Elektromyographie und Verwandte Gebiete 1983;14(1):39-42.
43. Storey CM, Robinson CJ, Hollister A, Magee TD, Redman DE, Darbhe VA, et al. High Frequency Hearing Loss Related to Type-2 Diabetes. In: Audiology Now! Minneapolis, MN; 2006.
44. McBurney DH, Collings VB. Introduction to Sensation / Perception. 2nd edition ed. Englewood Cliffs, NJ: Prentice-Hall Inc; 1984.
45. Webb CH, McBurney DH. Salivary Habituation: Quantitative Similarities to Sensory Adaptation. The American Journal of Psychology 1971;84(4):501-512.
46. Deshmukh S. Physiological Correlates of Anterior Platform Perturbations. Ruston, LA: Louisiana Tech University; 2005.
47. Richerson S. Effects of Diabetes and Aging on Posture and Acceleration Thresholds during Lateral Translations. Ruston, LA: Louisiana Tech University; 2003.

Table 1

Subject Information

	HMA (n=34)			DNI (n=11)			DPN (n=17)		
	Mean	95% CI		Mean	95% CI		Mean	95% CI	
Age (yrs)	57.4	±	2.16	59.1	±	5.31	60.9	±	2.72
Height (m)	1.68	±	0.03	1.69	±	0.06	1.74	±	0.05
Mass (kg)	83.2*	±	5.6	97.8	±	17.12	98.3	±	9.28
Body Mass Index	29.5	±	1.71	33.7	±	4.22	32.7	±	3.18

* HMA vs. DPN $p<0.05$

Table 2

Detection Thresholds

	HMA (n=34)		DNI (n=11)		DPN (n=17)	
	gMean	aMean	gMean	aMean	gMean	aMean
Acceleration	mm/s^2					
1 mm	78.4[*][†]	97.7	158.2	177.4	143.4	157.9
4 mm	34.1[†][‡]	46.5	59.4	75.6	54.8	70.4
16 mm	16.4[§]	22.5	32.0	48.0	23.4	34.1
Peak Kinetic Energy	mJ					
1 mm	3.20[¶]	4.14	7.48	8.58	6.94	7.85
4 mm	1.39[¶]	2.05	2.81	3.85	2.65	3.51
16 mm	0.67[‖]	0.95	1.51	2.44	1.13	1.71

[*] HMA vs. DPN $p<0.01$ [†] HMA vs. DNI $p<0.01$ [‡] HMA vs. DPN $p<0.05$ [¶] HMA vs. DNI $p<0.05$ [‖] HMA vs. DPN $p=0.058$

[§] HMA vs. DNI $p=0.054$. gMean is the geometric mean of the SWM due to their log nature. The arithmetic means, aMean, are including solely for comparison.

Table 3

Rail Conditions

	1mm	4mm	16mm
HMA	4 (11%)	3 (9%)	0 (0%)
	2 @ 200 mm/s^2	1 @ 100 mm/s^2	0
	2 @ 256 mm/s^2	2 @ 181 mm/s^2	0
DNI	7 (63%)	4 (36%)	2 (18%)
	2 @ 200 mm/s^2	4 @ 100 mm/s^2	2 @ 100 mm/s^2
	2 @ 200 mm/s^2		
DPN	7 (41%)	3 (18%)	1 (6%)
	2 @ 200 mm/s^2	3 @ 100 mm/s^2	1 @ 100 mm/s^2
	2 @ 200 mm/s^2		

Table 4
Quiet Standing Metrics

	HMA (n=34)			DNI (n=11)			DPN (n=17)		
	Mean	95% CI		Mean	95% CI		Mean	95CI	
Standard Deviation-RD	2.5	±	0.6	3.2	±	3.1	3.1	±	1.0
Standard Deviation-AP	4.0*	±	0.7	4.7	±	2.6	5.0	±	1.4
Standard Deviation-ML	2.7	±	0.9	3.6	±	5.2	3.5	±	1.6
Range-RD	13.1	±	3.4	16.4	±	17.2	15.5	±	5.7
Range-AP	19.2*	±	3.5	23.4	±	13.4	24.6	±	7.6
Range-ML	14.7	±	5.6	17.7	±	25.5	17.1	±	8.2
Mean Distance-RD	4.2†	±	0.9	5.3	±	4.5	5.3	±	1.8
Mean Distance-AP	3.2†	±	0.6	3.8	±	2.1	3.9	±	1.1
Mean Distance-ML	2.1	±	0.6	2.8	±	3.7	2.7	±	1.3
RMS Distance-RD	4.9†	±	1.1	6.2	±	5.5	6.2	±	2.0
RMS Distance-AP	4.0*	±	0.7	4.7	±	2.6	5.0	±	1.4
RMS Distance-ML	2.7	±	0.9	3.6	±	5.2	3.5	±	1.6
Total Excursion-RD	230.2	±	64.0	288.0	±	189.1	295.6	±	121.1
Total Excursion-AP	178.3†	±	47.0	221.7	±	100.4	235.0	±	97.7
Total Excursion-ML	111.1	±	40.3	134.7	±	149.9	132.1	±	60.4
Mean Velocity-RD	11.5	±	3.2	14.4	±	9.5	14.8	±	6.1
Mean Velocity-AP	8.9†	±	2.4	11.1	±	5.0	11.7	±	4.9
Mean Velocity-ML	5.6	±	2.0	6.7	±	7.5	6.6	±	3.0
Mean Frequency-RD	0.5	±	0.1	0.5	±	0.1	0.5	±	0.1
Mean Frequency-AP	0.5	±	0.1	0.6	±	0.1	0.5	±	0.2
Mean Frequency-ML	0.5	±	0.1	0.5	±	0.2	0.5	±	0.1
95% Confidence Area Circle	269.5	±	138.0	571.1	±	1370.9	395.8	±	259.2
Sway Area	17.8	±	9.5	34.6	±	81.3	26.3	±	18.3
95% Confidence Area Ellipse	225.3	±	117.4	437.2	±	1036.8	339.8	±	240.9
Fractal Dimension Circle	1.4	±	0.0	1.4	±	0.1	1.4	±	0.1
Fractal Dimension Ellipse	1.4	±	0.0	1.4	±	0.0	1.4	±	0.1
Total Power-RD	42400.1	±	26235.7	94362.7	±	234490.9	60375.5	±	36617.0
Total Power-AP	67467.9‡	±	26878.5	122807.8	±	184208.8	121177.8	±	59236.5
Total Power-ML	50774.5	±	58018.8	183355.7	±	696399.1	60522.6	±	61366.7
Median Frequency-RD	0.3	±	0.1	0.4	±	0.1	0.4	±	0.2
Median Frequency-AP	0.2	±	0.1	0.3	±	0.1	0.3	±	0.1
Median Frequency-ML	0.2	±	0.1	0.2	±	0.1	0.2	±	0.1
95% peak frequency-RD	1.6	±	0.4	1.8	±	0.4	1.7	±	0.5
95% peak frequency-AP	1.4	±	0.4	1.4	±	0.4	1.3	±	0.3
95% peak frequency-ML	1.2	±	0.3	1.3	±	0.4	1.3	±	0.4
Centroid Frequency-RD	1.0	±	0.1	1.1	±	0.2	1.1	±	0.2
Centroid Frequency-AP	0.9	±	0.1	0.9	±	0.2	0.9	±	0.1
Centroid Frequency-ML	0.9	±	0.1	0.9	±	0.2	0.9	±	0.2
Frequency Dispersion-RD	0.6	±	0.0	0.6	±	0.1	0.6	±	0.0
Frequency Dispersion-AP	0.6	±	0.0	0.6	±	0.1	0.6	±	0.0
Frequency Dispersion-ML	0.7	±	0.0	0.7	±	0.1	0.7	±	0.0

* HMA vs. DPN $p<0.05$, † HMA vs. DPN $p<0.1$, ‡ HMA vs. DPN $p<0.01$ All metrics based on mm. Frequency metrics are in Hz.

Mean Velocity is in mm/s. Area metrics are in mm^2.

Table 5

Health Surveys

	HMA			DNI			DPN		
	n	Mean	Rank	n	Mean	Rank	n	Mean	Rank
Mini-Mental Exam	34	29.6	34.91	11	29.0	26.32	17	29.3	28.03
BERG	34	56.0*†	34.00	11	55.5	23.18	16	55.7	30.00
RAND	Modified SF-36 with depression screener								
Physical Function	32	84.0	32.72	11	78.5	26.86	16	75.9	26.72
Physical Health	32	85.2*	33.56	11	73.8	27.09	16	67.6	24.88
Emotional Health	32	84.4	31.48	11	78.4	28.55	16	78.0	28.03
Emotional Well-Being	32	76.4	30.69	11	77.6	27.82	16	75.9	30.13
Energy/ Fatigue	32	67.3	32.42	11	63.3	30.00	16	56.6	25.16
Social Function	32	87.1	33.25	11	82.2	26.77	16	80.2	25.72
Pain	32	83.4*¶	34.77	11	69.8	23.23	16	70.6	25.13
General Health	32	76.9*†	36.47	11	58.5	20.91	16	63.0	23.31

* HMA vs. DPN $p<0.05$ † HMA vs. DNI $p<0.01$ ‡ HMA vs. DPN $p=0.06$ ¶ HMA vs. DNI $p=0.051$

Table 6

Semmes Weinstein Monofilament Test

	HMA			DNI			DPN		
	n	gMean	aMean	n	gMean	aMean	n	gMean	aMean
Left Great Toe	34	0.45*	0.99	11	0.59	0.81	17	1.72	3.18
Left 1st Metatarsal	34	0.44†	0.79	11	0.74‡	2.11	17	2.10	7.74
Left 4th Metatarsal	20	0.59*¶	0.96	8	2.15	4.02	11	1.64	3.24
Left Heel	21	1.91*‖	3.34	8	9.94	41.11	12	8.41	21.55
Right Great Toe	34	0.44	0.78	11	0.78	1.02	17	1.32	2.59
Right 1st Metatarsal	34	0.51†	0.76	11	0.70	1.16	17	1.49	3.91
Right 4th Metatarsal	20	0.77*§	1.15	8	1.20	2.02	11	2.75	11.20
Right Heel	21	2.30¶	3.08	8	6.33	7.75	12	5.45	14.74

* HMA vs. DPN $p<0.05$ † HMA vs. DPN $p<0.01$ ‡ DNI vs. DPN $p=0.07$ ¶ HMA vs. DNI $p<0.05$ ‖ HMA vs. DNI $p<0.01$

§ HMA vs. DNI $p=0.062$. gMean is the geometric mean of the thresholds due to their power law relationship between displacement and acceleration threshold. All units are in grams. The arithmetic means, aMean, are including solely for comparison.

Table 7

Electrophysiology Results

	HMA				DNI				DPN			
	n	Mean	95% CI		n	Mean	95% CI		n	Mean	95% CI	
Conduction Velocity	m/s											
L. Peroneal	34	46.9*	±	1.31	11	45.4†	±	1.86	17	40.5	±	1.89
L. Tibial	34	45.8*	±	1.30	11	46.4†	±	1.88	17	39.6	±	1.92
L. Sural	28	45.1*	±	1.30	7	44.7†	±	3.36	12	39.3	±	2.72
R. Peroneal	34	46.9*	±	1.28	11	46.1†	±	2.18	17	40.3	±	2.03
R. Tibial	34	45.6*	±	1.71	11	45.9†	±	2.41	16	40.5	±	2.37
R. Sural	28	44.9*	±	1.39	7	46.0†	±	2.62	12	38.9	±	2.26
Conduction Latency	Ms											
M-wave L. Peroneal	34	4.5	±	0.37	11	4.5	±	0.44	16	5.1	±	0.48
M-wave L. Tibial	33	4.3‡	±	0.41	11	4.7	±	1.21	16	5.8	±	1.09
M-wave R. Peroneal	33	4.7*	±	0.34	11	4.6†	±	0.27	15	5.8	±	0.51
M-wave R. Tibial	33	4.5	±	0.52	11	5.4	±	1.12	15	5.5	±	1.09
F-wave L. Peroneal	33	50.1‡	±	1.78	11	51.9	±	3.00	16	56.9	±	4.22
F-wave L. Tibial	33	51.9*	±	1.86	11	55.3¶	±	2.65	16	60.9	±	3.14
F-wave R. Peroneal	33	49.8*	±	2.62	11	51.0¶	±	3.10	15	57.2	±	4.03
F-wave R. Tibial	31	53.1*	±	1.56	11	53.5¶	±	3.87	15	60.8	±	4.10

* HMA vs. DPN $p<0.01$ † DNI vs. DPN $p<0.01$ ‡ HMA vs. DPN $p<0.05$ ¶ DNI vs. DPN $p<0.05$

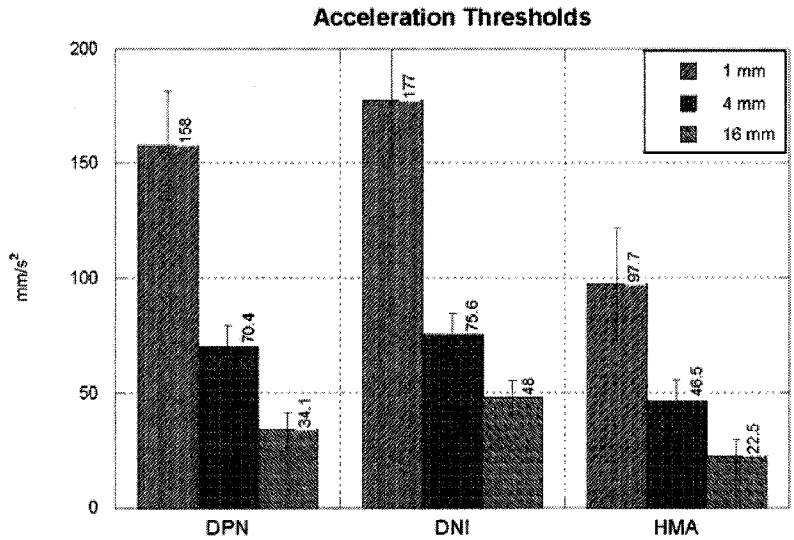

Figure 1: The left-slanting lines refer a 1mm move. The cross-hatched lines refer to a 4 mm move. The right-slanting lines refer to a 16 mm move. Error bars provide the standard error. DPN and DNI show pronounced decreased acuity in detecting small anterior perturbations as compared to HMA at 1 and 4 mm movements. Values are the arithmetic means.

APPENDIX T

ACCEPTED IEEE ENGINEERING IN MEDICINE AND BIOLOGY 2006 CONFERENCE PAPER

A system for measurement and calibration of nonorthogonal joints and limbs in humans

Christopher M. Storey, *Member, IEEE*, Anne M Hollister, Charles J. Robinson, *Fellow, IEEE*, Norman M. Witriol, Dale O. Anderson, John C. London, and William L. Buford, *Member, IEEE*

***Abstract*—Human limbs are a multilinked system in which the revolute joints are not orthogonal to the limb segments or to each other. The standard method for movements of multilinked systems is the Denavit-Hartenberg (DH) Representation, which is useful for orthogonal systems. When applied to non-orthogonal systems, the DH representation projects the reference frames outside of the limb segments. Computer graphics techniques move arrays of points in bodies that move about arbitrary revolute joints. This computational model has been modified to calculate both position (X, Y, Z) and orientation (yaw, pitch, and roll) of limbs and their individual segments. This method allows a simplified representation for the kinematics of animal limbs.**

I. Introduction

Many mechanical systems are composed of rigid segments linked by simple kinematic mechanisms such as revolute joints. Knowledge of positions and orientations of the links and revolute joints is essential for machine control. The current standard for calculating the position and orientation for the reference frames of these linked mechanisms is the Denavit-Hartenberg (DH) Representation [1]. The DH Representation assumes rigid links between limbs but to simplifies from the defined position and orientation with displacement and Euler angles to four numbers requires orthogonality between limbs and links [1]. The DH is a relatively simple system that works well when the mechanisms are orthogonal. The simplification is the result of choosing coordinate frames for the links that do not have to lie within link or limb [1]. Humans and animals have revolute joints that are not usually perpendicular to each other or to the limb segments, and do not parallel a global reference frame coordinate [2]. Such joints are known as arbitrary revolute joints and can be described as twist and crank angles, a vector from the origin, and the degrees of rotation (pitch – θ) about the revolute joint. DH representation of non-orthogonal systems project the local reference frames outside of the limb segments. Our proposed representation places the limb segment and joint reference frames within the segments or joints, facilitating the measurement, design, modeling, movements and control of these systems via methods developed for computer animation [3]. The parameters, which must be measured in the animal limb, are explicitly stated and are variables in the generalized equations.

Manuscript received April 24, 2006.

C. M. Storey is with the Biomedical Engineering Department at Louisiana Tech University, Ruston, LA 71272 USA (phone: 504-782-3280; fax: 318-213-8856; e-mail: cms043@latech.edu).

A. M. Hollister is with Louisiana State University Health Sciences Center, Shreveport, LA, 71103 USA (e-mail: annahans@mac.com).

C. J. Robinson is with the Center for Rehabilitation Engineering, Science, and Technology, Clarkson University, Potsdam, NY 13699 USA and The Syracuse VAMC Research Service, Syracuse, NY 13210 (e-mail: c.robinson@ieee.org).

N. M. Witriol is with the Physics Department at Louisiana Tech University, Ruston, LA 71272 USA (e-mail: witriol@latech.edu).

D. O. Anderson is with the Mechanical Engineering Department at Louisiana Tech University, Ruston, LA 71272 USA (e-mail: andersonfam@cox-internet.com).

J. C. London is with the Mathematics Department at Tulane University, New Orleans, LA 70118 USA (e-mail: jlondon@tulane.edu).

W. L. Buford, Jr. is with the Research Division of the Department of Orthopaedic Surgery and Rehabilitation at The University of Texas Medical Branch, Galveston, TX, 77555 USA (e-mail: wbuford@utmb.edu)

II. Methods

A. Software

The program was written in Matlab® to have access of the matrix mathematics functions. The program was object-oriented to allow for ease and robustness of expansion. The software provided text (Excel Spreadsheet), jpg (picture), and avi (Video) output representing motion.

B. System representation

The simplest system consisted of two segments and a single joint. The reference frame for the first link was placed at the origin of a Cartesian coordinate system. The displacement vector (D_1), the x, y, and z measurements from the first segment's reference frame to the center of the first revolute, were recorded. The limb local coordinates may be placed anywhere, including a location along the revolute axis. In biological systems, the center of mass in the stationary limb segment is difficult to establish and it changes as the muscles lengthen and contract. The φ_1 and ψ_1 angles were the twist and crank angles of offset from the preceding segment's reference frame needed to align the revolute axis of motion with the z-axis of the preceding limb. In relation to the second limb, the φ_2, ψ_2, and D_2 were the variables measured that were needed to rotate the axis of rotation so as to align with z-axis of the next segment and to find the distance from the joint center to the following segment's center. There for the method provides a definition of the orientation of limbs relative to their joint.

C. Definitions:

A vertices matrix ([$V_\#$], Eq. (1)) was defined by the joint number, "#", therefore, all limbs distal to it were are

operated on or accessed in the matrix. The subscript d is equal to the number of the most distal limb. Each limb requires 12 columns of the matrix (expandable for more vertices). The first eight columns were the limb vertices. The ninth column was the limb center, and the 10th, 11th, and 12th columns were the local x, y, and z vectors (not unit vectors) of the local coordinate system relative to global Cartesian coordinate system.

$$\begin{bmatrix} x_{1,1} & x_{1,2} & \cdots & x_{8,1} & \cdots & x_{d,12} \\ y_{1,1} & y_{1,2} & \cdots & y_{8,1} & \cdots & y_{d,12} \\ z_{1,1} & z_{1,2} & \cdots & z_{8,1} & \cdots & z_{d,12} \\ 1 & 1 & 1 & 1 & 1 & 1 \end{bmatrix} \quad (1)$$

A translation matrix ([$T_{\#,l}$], Eq. (2)) was defined by a subscript # and l, which defined the offset as "from proximal" (fp) or "to distal" (td) to the limb.

$$\begin{bmatrix} 1 & 0 & 0 & \Delta x \\ 0 & 1 & 0 & \Delta y \\ 0 & 0 & 1 & \Delta z \\ 0 & 0 & 0 & 1 \end{bmatrix} \quad (2)$$

Rotation matrices ([$R_{\#,a,l}$]) were defined by #, l, and a, which was the axis of rotation. Equations (3)-(5) show the rotation matrices for rotating about the x, y, and z-axes respectively. Roll (ψ) was defined by the rotation about the x-axis. Yaw (φ) provided the rotation about y-axis. Pitch (θ) described the rotation about the z-axis.

$$\begin{bmatrix} 1 & 0 & 0 & 0 \\ 0 & \cos(\psi) & -\sin(\psi) & 0 \\ 0 & \sin(\psi) & \cos(\psi) & 0 \\ 0 & 0 & 0 & 1 \end{bmatrix} \quad (3)$$

$$\begin{bmatrix} \cos(\varphi) & 0 & \sin(\varphi) & 0 \\ 0 & 1 & 0 & 0 \\ -\sin(\varphi) & 0 & \cos(\varphi) & 0 \\ 0 & 0 & 0 & 1 \end{bmatrix} \quad (4)$$

$$\begin{bmatrix} \cos(\theta) & -\sin(\theta) & 0 & 0 \\ \sin(\theta) & \cos(\theta) & 0 & 0 \\ 0 & 0 & 1 & 0 \\ 0 & 0 & 0 & 1 \end{bmatrix} \quad (5)$$

A joint rotation matrix ([Rev]) defined the amount of rotation about the arbitrary axis of the revolute joint. The ψ and φ angles of offset are calculated from the z-axis to allow for the define rotation of the joint to be about the z-axis as in Eq. (5). A single rotation matrix ([RM (row, column)]) was used to define the orientation of a limb in space through a single rotation once the yaw, pitch, and roll was tabulated.

$$\begin{bmatrix} c(\varphi)c(\theta) & s(\theta) & -c(\theta)s(\varphi) & 0 \\ -c(\psi)s(\theta)c(\varphi)+s(\psi)s(\varphi) & c(\psi)c(\theta) & c(\psi)s(\varphi)s(\theta)+s(\psi)c(\varphi) & 0 \\ c(\psi)s(\theta)s(\psi)+s(\varphi)c(\psi) & -c(\theta)s(\psi) & -s(\psi)s(\varphi)s(\theta)+c(\theta)c(\varphi) & 0 \\ 0 & 0 & 0 & 1 \end{bmatrix} \quad (6)$$

In Equation (6), c refers to cosine and s to sine.

D. System Description

To ease the difficulty in setting up the model with global positions and angles, a relative system was used through an object-oriented design utilizing limb, joint, and system objects. The global origin and axis were designated to be the local origin and axis of the most proximal limb of the system. The limb was modeled as a cuboid, which can easily be changed to any shape to any shaped by adding and/or removing vertices. The cuboid was used to simplify the program and was defined by length, width, and height. The local origin for each limb was defined as its geometric center. The joint was a single axis revolute joint. The center of the revolute joint was at the local origin and aligned with the z-axis. The joint was defined in relation to the proximal and distal limbs. Due to the sequential operation in traversing the limb, the program was designed arbitrarily in a proximal to distal method. The measure made for each joint was the x_{fp}, y_{fp}, and z_{fp} offset from the proximal limb. These defined its position in space in relation to proximal limb. Next, the ψ_{fp} (x-axis), φ_{fp} (y-axis), and θ_{fp} (z-axis) was measured as the offset orientation from the local axis of the proximal limb. Then the same offset orientations (ψ_{td}, φ_{td}, and θ_{td}) were measured to rotate the revolute joint to align with the z-axis of the distal limb. Finally, the offset was measured from the center of the revolute joint to the geometric center of the distal limb, which provided x_{td}, y_{td}, and z_{td}. No range limitation was enabled to allow coordinates or orientations that are considered out of the range of natural joint motion as in fractures or dislocations.

III. Building the Multi-Linked System

A multi-linked system was assembled to the specifications of an initial state. The local coordinate systems were set at the origin for all limbs. Therefore, the limbs were moved to their appropriate positions and orientations in space via a sequence of matrix multiplications as shown below:

1. $[V_1] = [T_{1,fp}]\,[R_{1,x,fp}]\,[R_{1,y,fp}]\,[R_{1,z,fp}]\,[R_{1,z,td}]\,[R_{1,y,td}]\,[R_{1,x,td}]\,[T_{1,td}]\,[V_1]$
2. $[V_2] = [T_{2,fp}]\,[R_{2,x,fp}]\,[R_{2,y,fp}]\,[R_{2,z,fp}]\,[R_{2,z,td}]\,[R_{2,y,td}]\,[R_{2,x,td}]\,[T_{2,td}]\,[V_2]$
3. . . . . .
4. . . . . .
5. . . . . .
6. $[V_8] = [T_{8,fp}]\,[R_{8,x,fp}]\,[R_{8,y,fp}]\,[R_{8,z,fp}]\,[R_{8,z,td}]\,[R_{8,y,td}]\,[R_{8,x,td}]\,[T_{8,td}]\,[V_8]$.

IV. Rotation about a Selected Joint

The lack of orthogonality between the joint axes and the global coordinate system presents a problem with joint rotation. To rotate the distal limbs around a respective joint (#), the joint was translated to the global origin and the axis of rotation was aligned with the z-axis. The z-axis has been designated as the as the only axis of rotation for all limbs. All other axes were held constant at initial specifications as shown in the following sequence:

1. $[V_1] = [R_{1,y,fp}]^{-1}\,[R_{1,x,fp}]^{-1}\,[T_{1,fp}]^{-1}\,[V_1]$
   a. If joint is joint of rotation, jump to step eight.
2. $[V_1] = [T_{1,td}]^{-1}\,[R_{1,z,td}]^{-1}\,[R_{1,y,td}]^{-1}\,[R_{1,x,td}]^{-1}\,[R_{1,z,fp}]^{-1}\,[V_1]$
3. $[V_2] = [R_{2,y,fp}]^{-1}\,[R_{2,x,fp}]^{-1}\,[T_{2,fp}]^{-1}\,[V_2]$
   a. If joint is joint of rotation, jump to step eight.

4. $[V_2] = [T_{2,id}]^{-1} [R_{2,x,id}]^{-1} [R_{2,y,id}]^{-1} [R_{2,z,id}]^{-1} [R_{2,z,fp}]^{-1} [V_2]$
5. . . . . .
6. . . . . .
7. . . . . .
8. $[V_8] = [T_{8,fp}] [R_{8,x,fp}] [R_{8,y,fp}] [Rev] [V_8]$.

After joint was rotated, the system was returned to their proper global coordinates as follows:

1. $[V_8] = [T_{8,fp}] [R_{8,x,fp}] [R_{8,y,fp}] [R_{8,z,fp}] [R_{8,z,id}] [R_{8,y,id}] [R_{8,x,id}] [T_{8,id}] [V_8]$
2. . . . . .
3. . . . . .
4. . . . . .
5. $[V_2] = [T_{2,fp}] [R_{2,x,fp}] [R_{2,y,fp}] [R_{2,z,fp}] [R_{2,z,id}] [R_{2,y,id}] [R_{2,x,id}] [T_{2,id}] [V_2]$
6. $[V_1] = [T_{1,fp}] [R_{1,x,fp}] [R_{1,y,fp}] [R_{1,z,fp}] [R_{1,z,id}] [R_{1,y,id}] [R_{1,x,id}] [T_{1,id}] [V_1]$.

V. Yaw, Pitch, and Roll of Limbs

The rotation about an arbitrary angle in the multilinked system of limbs allowed distal limbs to have changes in their spatial rotations about more than one axis simultaneously. Therefore, the new yaw, pitch, and roll was calculated after proximal joints have been rotated, but to avoid errors in back calculation of the orientation via position coordinates in real data, the yaw, pitch, and roll were calculated on the fly with rotations through multiplication of only the rotation matrices. Due to the sequence necessary for rotation using Euler angles, the orientations were calculated in the order roll, pitch, and yaw in the back calculation from Cartesian coordinates so the Euler angle multiplication sequence for rotations can take place in the order of yaw, pitch, and roll. The same order was used to calculate in (6). The calculation of yaw, pitch, and roll was tabulated both ways so that each method could verify the other. The method of back calculation was accomplished by first translating the limb back to the global origin of the coordinates system by using the limb center as the offset for the translation matrix (7).

$$\begin{bmatrix} 1 & 0 & 0 & x_{a,\delta} \\ 0 & 1 & 0 & y_{a,\delta} \\ 0 & 0 & 1 & z_{a,\delta} \\ 1 & 1 & 1 & 1 \end{bmatrix} \tag{7}$$

The limb number (α) describes the limb to be translated and later rotated. Once the limb was at the origin, the local axis vectors were converted to their respective unit vector coordinates for the y-axis (8)-(10).

$$x\_dc = \frac{x_{a,11}}{\sqrt{x_{a,11}^2 + y_{a,11}^2 + z_{a,11}^2}} \tag{8}$$

$$y\_dc = \frac{y_{a,11}}{\sqrt{x_{a,11}^2 + y_{a,11}^2 + z_{a,11}^2}} \tag{9}$$

$$z\_dc = \frac{z_{a,11}}{\sqrt{x_{a,11}^2 + y_{a,11}^2 + z_{a,11}^2}} \tag{10}$$

Roll (ψ) was calculated by projecting the local *y*-axis unit vector onto *yz*-plane (11) and calculating the angle of rotation (ψ) between *u'* and the global *y*-axis (12).

$$u' = [0, y\_dc, z\_dc] \tag{11}$$

$$\psi = -\frac{\cos^{-1}(u' \cdot [0,1,0])}{|u'|} \times \frac{z\_dc}{|z\_dc|} \tag{12}$$

The arc cosine function only returned values between zero and π radians so it was multiplied by a factor that was -1 or 1 depending on *z_dc* (*z*-component of *y*-axis unit vector) in respect to the *xy*-plane. A similar respective factor was multiplied to determine angle direction for yaw and pitch, also. The computer animation standard rotations utilized for the methodology designate positive angles as counter-clockwise rotations [2]. For ψ, a positive angle required a clockwise rotation to align *u'* with the global *y*-axis. Therefore, the calculated ψ was inverted. The remaining calculations of pitch (θ) and yaw (φ) followed the standard convention of positive angles are for counterclockwise rotations. Using ψ, an *x*-axis rotation matrix was used to rotate the limb so that the local *y*-axis vector lies in the *xy*-plane.

Since *u''* already lied within the *xy*-plane, but it was calculated with the absolute value of *u'* (13), Pitch (θ) was calculated from the angle of rotation between *u''* and the global *y*-axis (14).

$$u'' = [x\_dc, 0, |u'|] \tag{13}$$

$$\theta = \frac{\cos^{-1}(u'' \cdot [0,1,0])}{|u''|} \times \frac{x\_dc}{|x\_dc|} \tag{14}$$

Yaw (φ) required the use of a separate local axis since the local *y*-axis unit vector was aligned with the global *y*-axis. The local *x*-axis unit vector was calculated (only x and z coordinates; (15) and (16)) to project onto the *xz*-plane (17) and the angle between the *x*-axis vector and the global *x*-axis provides one with the yaw of the limb (18).

$$x\_dc = \frac{x_{a,10}}{\sqrt{x_{a,10}^2 + y_{a,10}^2 + z_{a,10}^2}} \tag{15}$$

$$z\_dc = \frac{z_{a,10}}{\sqrt{x_{a,10}^2 + y_{a,10}^2 + z_{a,10}^2}} \tag{16}$$

$$u''' = [x\_dc, 0, z\_dc] \tag{17}$$

$$\varphi = \frac{\cos^{-1}(u''' \cdot [1,0,0])}{|u'''|} \times \frac{z\_dc}{|z\_dc|} \tag{18}$$

Utilizing the calculated yaw, pitch, and roll, one is able to move and orient the limb without sequential steps as in (19).

$$[V_a] = [T] [R_\varphi] [R_\theta] [R_\psi] [V_a] \tag{19}$$

The lack of ability to make small measurements for the position of limbs introduces the possibility for large errors when back calculating the yaw, pitch, and roll for a limb, especially at the asymptotes. So in addition to back calculating the yaw, pitch, and roll from the limb's position relative to global axis, the yaw pitch and roll was calculated

by only using the inputted rotation matrices. The rotation matrices were ordered as they would for multiplication for building of limb as previously shown, but no translations are used. A rotation matrix in (6) is obtained and by using an ordered sequence of rotation matrix multiplications equations are given to back calculate yaw, pitch, and roll from the values in the rotation matrix as follows:

1. $[RM_1] = [R_{1,x,fp}]\,[R_{1,y,fp}]\,[R_{1,z,fp}]\,[R_{1,z,td}]\,[R_{1,y,td}]\,[R_{1,x,td}]$
2. $[RM_2] = [R_{2,x,fp}]\,[R_{2,y,fp}]\,[R_{2,z,fp}]\,[R_{2,z,td}]\,[R_{2,y,td}]\,[R_{2,x,td}]$
3. . . . . .
4. . . . . .
5. . . . . .
6. $[RM_{\#}] = [R_{\#,x,fp}]\,[R_{\#,y,fp}]\,[R_{\#,z,fp}]\,[R_{\#,z,td}]\,[R_{\#,y,td}]\,[R_{\#,x,td}]$

The pitch was calculated first, since it is in the equation from the (6) that has one unknown. The arc-sine function has a range $[-\pi/2, \pi/2]$, but since the order of yaw, pitch, and roll, roll was rotated first this guarantees that the pitch will always be less than 90°.

$$\theta = \sin^{-1}\left(RM(1,2)\right) \tag{20}$$

Roll as in (12) was negated to provide the correct rotation direction. The *z_dc* vector value was the same for roll and yaw as calculated in (10) and (16) respectively. Since the arc cosine's range was $[0, \pi]$, the *z_dc* vector value was used to determine the sign and the direction of the rotation.

$$\psi = -\cos^{-1}\left(\frac{RM(2,2)}{\cos(\theta)}\right) * \left(\frac{z\_dc}{|z\_dc|}\right) \tag{21}$$

$$\varphi = \cos^{-1}\left(\frac{RM(1,1)}{\cos(\theta)}\right) * \left(\frac{z\_dc}{|z\_dc|}\right) \tag{22}$$

This method allows one to track the yaw, pitch, and roll of the limbs without the need for position data (except to track the sign for yaw and roll).

A. Results

To verify our methods we rotated to position and then back to initial position with different rotations on the way back to the home position. Our final vertices matrix equaled the initial to verify our method since a closed loop rotation is an identity matrix. Table 1 shows the sequence of rotations and the initial offsets that are illustrated in Fig. 1. Fig. 1 is the display of a simple system of only two arbitrary revolute joints since it the points were rotated as a matrix of vertices, which makes it simple to expand to detailed objects. The yaw, pitch, and roll was calculated both through rotations and by back calculation from position in both joint with rotations from -180° to 180° in 1° increments and were found equal when compared.

VI. A Model for Calibration of Ankle Angle Measurements

A model of the ankle was developed based on three segments with two arbitrary revolute joints. The segments are the calcaneus, talus, and mortise (comprised of the leg bones and ligaments). The arbitrary revolute joints consist of the talocrural joint and the subtalar joint [4], [5]. This allows us to view the ankle bones as they rotate naturally instead of about the assumed single orthogonal axis of most models [6]. This will help to increase the accuracy of measurements of ankle rotation. The determination of joint moments and reaction forces make it possible for more realistic and natural ankle prostheses.

VII. Conclusion

This computational approach provides calculations for the position and orientation of limbs and revolute joints throughout the system's motion. The method facilitates modeling of kinetics and kinematics of joint in human and animal limbs and further force analysis. The ability to calibrate accurately small rotations of nonorthogonal joints improves the measurement of orientation of limbs. The methodology allows for measurements and calculations of joints without the need for any mutually orthogonal axes that could lie outside the body of rotation.

References

[1] Spong, M. and Vidyasagar, M., *Robot dynamics and control*. 1989, John Wiley & Sons, pp. 62-72.

[2] Koti, N., "Design of a biomimetic manipulator with nonorthogonal Joint Axes." Louisiana Tech University, Thesis, 2005, unpublished.

[3] Hearn, D. and Baker, M. P., *Computer graphics C version*. 1997, Prentice Hall, pp. 408-423.

[4] Isman, R. E. and Inman, V. T., "Anthropometric studies of the human foot and ankle," Bulletin of Prosthetics Research, 1969, 97-129.

[5] Inman, V. T., *The joints of the ankle*. Baltimore: Williams & Wilkins, 1976.

[6] Singh, A. K., Starkweather, K. D., Hollister, A. M., Jatana, S., Lupichuk, A. G., "Kinematics of the ankle: a hinge axis model," *Foot & Ankle* Vol. 13 No. 3 pp. 439-446, October 1992.

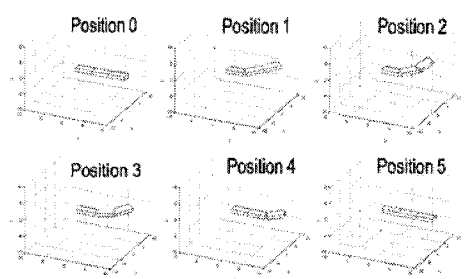

Fig. 1. Displays positions of a two joint system going through a series of rotations defined in Table 1.

TABLE 1
SERIES OF ROTATIONS

Joint Offsets	φ_0	ψ_0	θ_0	φ_{12}	ψ_{12}	θ_{12}
1	10°	5°	0°	-10°	-5°	0°
2	20°	15°	0°	-20°	-15°	0°
Position	**Rotated Joint**			**Degrees**		
0	None					
1	1			45°		
2	2			30°		
3	1			-25°		
4	1			-20°		
5	2			-30°		

APPENDIX U

ACCEPTED AMERICAN SOCIETY FOR ENGINEERING EDUCATION ST. LAWRENCE REGION CONFERENCE STUDENT PAPER

Using Server Architecture and Multi-Threaded Processors and Software to Time-Lock Multiple Data Streams in Time-Critical Physiological Experiments

Christopher M. Storey[1,2] and Charles J. Robinson[1-4]

[1]Center for Rehabilitation, Engineering, Science and Technology, Clarkson University, Potsdam, NY / [2]Dept. of Bioengineering, Louisiana Tech Univ., Ruston, LA / [3]Dept. of Electrical and Computer Engineering, Clarkson University, Potsdam, NY / [4]Research Service, Syracuse VA Medical Center, Syracuse, NY.

Abstract

To ferret our subtle clues in the data that we collect, we need highly stable and reliable instrumentation, and a way to link disparate data streams together. In a typical laboratory such as ours, collecting a variety of physiological data in time-synced fashion has in the past required a number of desktop computers, each one handling a different aspect of data collection. This wealth of data required us to do laborious off-line file conversion and synchronizing of three main data streams. Since new technologies such as hyper-threading and dual-core technologies have brought enormous power to desktop systems, we opted to use a server-style system to be able to multitask in a network environment, but still maintain Windows XP as the operating system. The server platform provides us the means necessary to combine our various data collection schemes into a single unit, and for on-line data calibration and conversion, while still allowing us an easy transition from our previous hardware and software.

Introduction

A wealth of multi-dimensional data can now be collected during biomechanical studies of human motion and postural reactions to perturbation. These include biomechanical measures like AP and ML Centers-of-Pressure (COP), weight on platform versus weight supported by harness, horizontal ground reaction forces, head and foot accelerations in multiple dimensions, distributions of pressures under the foot, and joint and limb trajectories as measured by motion-capture marker systems. Multi-channel EMG data and psychophysical responses collected simultaneously add richness to any control model built.

Collecting all of this data in time-synced fashion in the past has required using a number of computers, each one handling a different aspect of data collection, where one computer serves as the master and triggers the other slave computers to begin data collection. Yet many of the vendors of propriety data collection interfaces (like a pressure mat or a motion capture system) supply there own proprietary software to act as a master, with other data slaved in. For large-scale observations, this feature results in a number of datasets collected over the same epoch, but does not necessarily create datasets that are time synchronized with one another. Using each device as a master, with data from other devices imported into each setup's data collection, the already large size of the data for a single experiment rapidly grows due to the storage of duplicate data in multiple systems. However, the datasets are not truly duplicate, as each was processed a different way, with possible variations in amplitude and noise and certainly offsets in timing.

Parallel processing requires systems capable of running thread simultaneously. While parallel processing required multiprocessor systems, new technologies such as hyper-threading and dual-core technologies have brought this power to many desktop and laptop systems. These

technologies provide the ability to increase multiprocessor systems exponentially, which is the basis of many new server platforms on the market.

Time-Series Data

Like most research laboratories, our lab uses computers to control our experiments, collect data, analyze the results, and write up any resultant manuscripts. Our studies investigate the psychophysics of balance and postural control.

All people sway. We make very short perturbations of a platform on which a subjects stands that are generally of a length less than that a person's sway, as measured at the foot and ankle, and hence should be and are near the ability of a subject to detect them. Using psychophysical techniques, we apply peri-threshold perturbations to iteratively find the detection limit, and attempt to figure out what physiological or biomechanical variable(s) was (were) used by the subjects in making a correct detection, or led them to a false detection. Details of our experimental set-up and procedure have been described adequately elsewhere. Here we note that our Sliding Platform For Assessing Lower Limb Stability with Synced Tracking, EMG and Pressure measurement (SLIP-FALLS-STEPm) is a vibration-free, translating platform that rides on air bearings[1]. Our typical protocol has a subject picking in which of two 4s intervals that the perturbation occurred, with data collection occurring in thirty 15s windows. This protocol is repeated 2 to 4 times.

To ferret our subtle clues in the data that we collect, we need highly stable and reliable instrumentation, and a way to link disparate data streams together. During the build-up years in our lab, we grew the experiment by adding hardware as a system. For instance, we started with a single computer for experimental control and data collection. We added another data collection computer when we introduced the measurement of the distribution of pressure under the foot from an HR TekMat. We also later added a motion capture system that used retro-reflective markers to trace the movement of the joints and other body reference points that could be caused by the perturbation. This system also had its own computer. We used digital out signals from the controlling computer to trigger data collection routines in the other two computers. Fig. 1 details the setup and the outputs.

In the past, this wealth of data required us to do laborious off-line file conversion and synchronizing of the three main data streams. We wished that all of this conversion could occur simultaneously during data collection, but the computers in our original implementation lacked the processing power to process data efficiently without testing delays. The outdated technology could not take advantage of multithreading to parallel process.

Specifications for a New Lab

With a move to another university, we have had the chance to set up a second SLIP-FALLS-STEPm research lab for fundamental studies, while maintaining the original lab in a clinical setting within the VA research service. Based on >10 yrs experience with the original SLIP-FALLS lab, we set down a series of specifications for the new lab:

1. The essential elements of the user interface needed to remain the same as seen from the clinical environment.
2. The command and control aspects of the platform had to be functionally equivalent to previous implementations, and previous code had to be reused when possible.
3. The operator should be provided a user-friendly interface with which to monitor the progress and output of all these processes in real-time during a testing sequence.
4. The number of channels of data collected by the FALLS protocol must be increased to allow for additional sensor and EMG inputs. The EMG channels were to be increased from the original four to a user-selectable between four and sixteen. The amount of support the safety harness provides to the subject should also be collected and calculated.
5. The motion analysis system should be upgraded from a single camera, 2-D system to a multi-camera, 3-D system.
6. The FALLS data should be immediately stored in engineering units, rather than in raw voltages that required post-possessing. EMG potentials should be converted on-line and

stored as RMS time-series data, with a further conversion to a percentage of that seen under maximal contraction if possible.

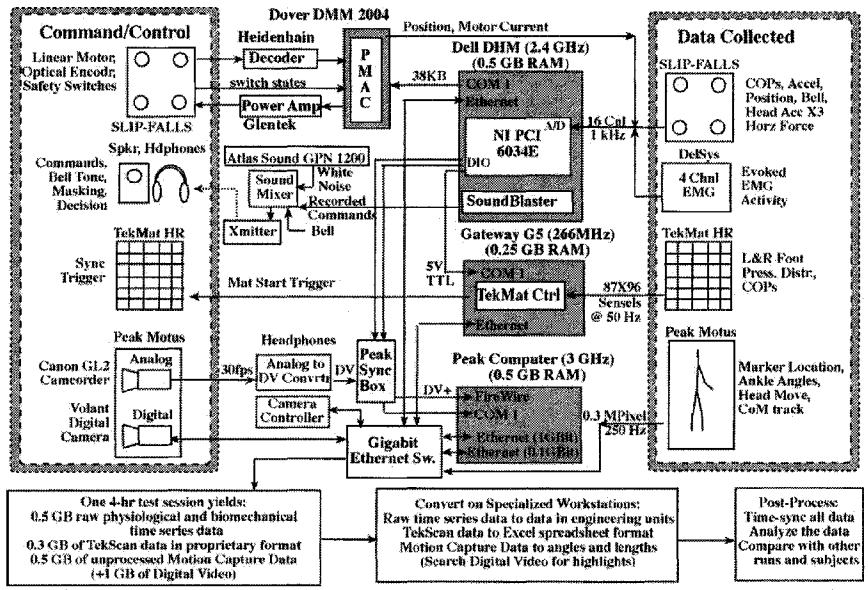

Figure 1: The original SLIP-FALLS-STEPm lab consists of a sliding platform (SLIP), hardware and software routines (FALLS) for collecting neurophysiological, biomechanical (Position, Acceleration, Centers-of-Pressure), EMG and psychophysical data, and equipment and software to simultaneously measure position markers, and foot pressure distributions (STEPm). The SLIP is controlled by a single board Programmable Multi-Axis Controller (PMAC) that receives commands from the FALLS computer (Dell DHM). This computer also relays pre-recording instructions to the subject via a SoundBlaster card and headphones. A Tekscan HRMat (TekMat) measures foot pressure distribution with an array of 87 by 96 sensels (4 per cm^2). A separate computer controls the TekMat. Its data collects starts with an external RS232 trigger. Motion capture of the location of retro-reflective markers is achieved by a single digital camera Peak-Motus system, along with a back-up analog camcorder. The peak computer is triggered also by the FALLS computer with an additional sync signal generated at the start of a platform move. A single 4-hr test session generates over 2 GB of data, all of which has to be processed offline after the completion of the experiment.

Solution

As our current setup was incapable of performing the required computations without testing delays, we focused on what was needed to meet these objectives. We needed a system that would remain under the Windows XP operating system to maintain current software and equipment drivers, which satisfied the first through third specifications. The remaining specifications require additional new or replacement equipment.

To meet the third specification we had to upgrade our multifunction data acquisition card (NI PCI 6034E) from a 16 analog inputs to 32 analog inputs (NI PCIe 6259M). We also achieved additional input be routing subject response (bell) to the digital inputs instead of counting peaks of analog input. To provide signal conditioning and signal access we used NI SC-2345 and NI BNC 2090 for I/O. The NI BNC has a dual functionality of allowing us access to EMG signals so they can be inputted into Peak Motion capture system. To acquire these signal in the Peak system and to meet the fifth specification the hardware had to be upgraded. Since the purchase of our previous system Peak-Motus was acquired by VICON, which allowed us to upgrade to VICON's superior cameras and hardware while maintaining same user interface with updated Peak software.

For the final specification, the data had to be converted on the fly to engineering units without causing any testing delays. A computer was needed that could parallel process threads, and not only utilize preemptive multitasking. New compact multi-processor server technologies were our focus for a new FALLS computer. We decided to purchase a Gateway E-9515-R series server to meet the fourth specific.

Implementation

Traditionally, for computers to be able to multitask in a network environment required a server style operating system. Due to such a small consumer base, there was very poor hardware support, which has left a mark on those who had endeavored to utilize its power in the past. With the advent of Windows XP to the general consumer, which is based off Microsoft's original server platform, the ability for user-friendly server platform was launched. Windows XP was chosen due to its widespread use and familiarity. Yet it remained stymied by its everyday use on desktops that it could handle computers that are more powerful and efficient.

Windows XP has both great hardware and software support, but if you try to purchase it with a server from major computer manufacturers, they will turn you down, or let you purchase separately with no support. They want you to purchase one of their newly branded server operating systems, which keep with the old tradition of having poor hardware and support for the everyday user and researcher. These server operating systems are expensive, which comes at the cost of paying per user license that allows for a true multi-user environment. Although this provides a limitation to the consumer, a multi-user environment would be a seldom-used feature in the lab environment. Since companies want the consumer to pay hundreds to thousands of dollars more for official server operating systems, they place limits on the software so it can only use a certain amount of the computer's resources.

Windows XP has a limit of two physical processors, but thanks to new technologies in the central processing unit (CPU), the limitation has become less stifling. Our new server class machine in Fig. 2 is composed of two Intel Xeon 2.8 GHz Dual-Core Processors. Each core also contains hyper-threading technology that is similar to dual-core but shares resources. Therefore, the software limitation imposed on us is met since we only have two physical processors. That limitation is surpassed by the fact that we have eight logical processors on which programs run.

To take advantage of extra processors software today is multithreaded, which translates into breaking up the program into smaller operations that can run independently and asynchronously. New multithreaded programs are able to push the processing envelope by distributing the work-load across all the logical CPUs. For our SLIP-FALLS-STEPm platform, we use LabVIEW® to run our experiment, record data, process data, and synch with other research systems. LabVIEW® provides a nice graphical programming interface so novice programmers can use it. It also allows for the flexibility in advanced programming for creating threaded applications, with communication streams between each, and for communicating with third party software.

The majority of our data analysis is performed in the Matlab package. With LabVIEW 8.0, you have an easy to script object to communicate and process data in Matlab. Given that we integrated and threaded our data acquisition and analysis, we have virtually eliminated offline processing time. In addition, Matlab can take advantage of Intel's Extended Memory 64-bit Technology (EM64T). The EM64T permits us to run Matlab 64-bit on our server, which also requires a 64-bit operating system (Windows XP 64-bit). With 64-bit software, the EM64T allows one to address over 4GB of memory to which will dramatically decrease the processing time by removing hard drive reads and writes due to virtual memory usage. In addition, the EM64T provides 64 bits of precision for accurate calculations. Nonetheless, we still have not reached the potential of our server. Therefore, we decided to run simultaneously the data acquisition hardware and software for Tekscan foot-pressure mat in the server.

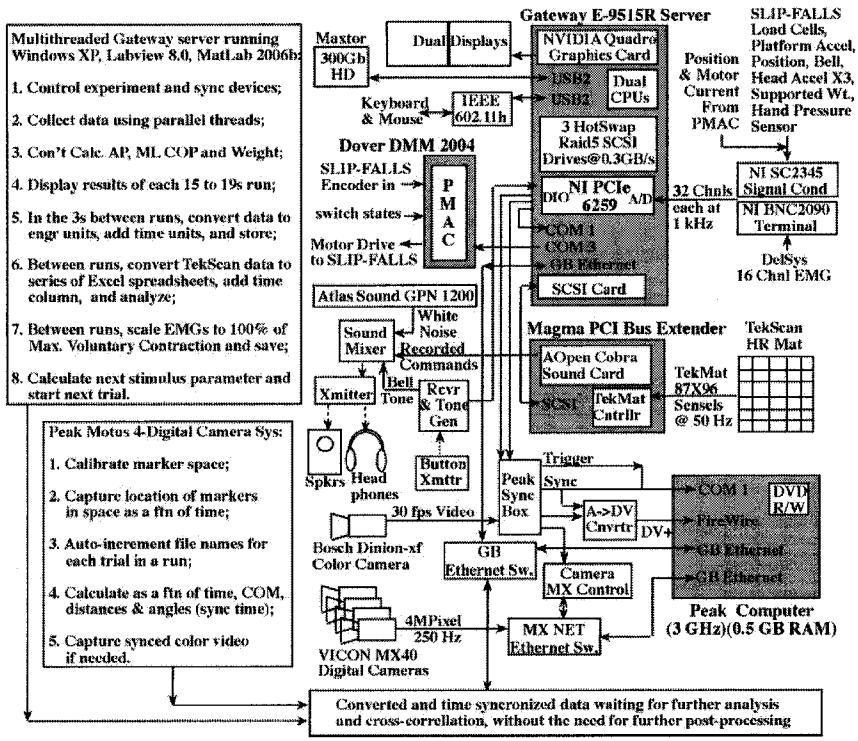

Figure 2: New equipment set up. A dual core, multi-processor Gateway server running Windows XP, LabVIEW 8.0 and MatLab 2006b is the new FALLS computer. The Magma PCI bus extender attached to it via a SCSI connection allows the use of vender cards with the older PCI bus structure. The graphics card in the computer supports up to four simultaneous monitors. Three hot-swappable 200GB drives are configured as a RAID 5 set, to provide for data collection redundancy. The A/D card is expanded to 32 channels, with 16 now coming via cable from a 16 channel Delsys EMG amplifier. The Tekscan HR Mat controller PCI card no longer resides in a separate machine, so that data can now be better time- synced. The motion capture system is upgraded to a 4-camera system, each at 4 MPixel at 250 Hz, along with faster CPU. If desired, an analog video record of the test can be acquired. The output of the new system is such that no post-processing is required before correlative analyses can be carried out.

This addition brought us our first limitation on our server. The latest revision (3.0) to the PCI/PCX standard no longer contains a 5V connection. Some older cards (audio and Tekscan PCI cards) are set up for the old 5V protocol, which required us to develop a work-around. We installed a rack-mounted PCI bus extension system by Magma, which allowed up to 4 PCI devices to share a single PCI slot in the server and be backward-compatible PCI slots. The bus extension worked well with the audio card (used for subject commands) and Tekscan card (used for foot-pressure data acquisition) allowing us to incorporate both in our server configuration.

The small physical size of our server (form factor 2U of a rack enclosure) cuts down the volume of the equipment need for the testing system, which is aided by having low-profile PCI ports. We used low-profile PCI slots for a serial port (RS232) expansion card and SCSI 320 Mb/sec hot swappable RAID 5. The extra serial ports allowed us to control multiple pieces experimental hardware (Dover DMM 2004 and Tekscan HR Mat) simultaneously. Using RAID 5 for disk storage gives great data protection with only minimal loss of space as opposed to mirroring the

hard drive. By striping the data across the hard drives with a parity bit, it enables the user to rebuild a hard drive's data completely if one crashes for high data security.

Server hardware was not designed for any flashy graphics cards, and there is no set high-speed graphic bus to use. However, the server has the new PCIe standard that many high-powered video cards currently use today. For our test monitoring, we chose the workstation class video card by NVIDIA because it gives is the ability to monitor all test parameters simultaneously since it has the ability to run up to four digital monitors. Also on the PCIe bus, we have our National Instruments data acquisition card. It is wired to two external hubs that allow for signal conditioning and data line access. These modules allow for synchronizing to both internal (Tekscan) and external (Vicon-Peak) software for total integration of data collection.

The Vicon-Peak system is a three-dimensional marker based camera system. The digital input and output (DIO) ports of the National Instruments DIO allow for triggering and synchronizing the video capture data to test events. Syncing is needed since there could be a delay before the cameras began recording. Syncing also allows the three-dimensional motion capture data to be aligned with the other data acquired by the server.

We have improved upon the data acquisition parameters of the original setup. Originally all signals were conditioned by separate external Daytronics signal conditioning modules with numeric displays. Now, a National Instruments SCC system is used that enables us to do individual two-stage signal conditioning on each line if needed (e.g., strain gage conditioning, followed by low pass filtering). We have used their SC breadboard modules on some signals to build our own circuitry to remove large DC offset voltages in some of our accelerometer signals. The LabVIEW driver software that comes with the SCC takes care of gain and offset calibration so that data is sent from the SCC already in calibrated engineering units (i.e., mm), rather than in raw numbers. This automated scaling and unit conversion occurring at data collection decreases the need for post-processing, and partially addresses our design criteria 6. With the SCC, we upgraded our data acquisition card from 16 analog inputs to 32, with the SCC taking the lower 16 channels, and EMG inputs the upper 16. The new 16-channel Delsys Bagnoli EMG amplifier has a 50-pin output connector that interfaces directly to a NI BNC breakout box (BNC2090) that handles the upper 16 channels, but that also allows us access to these signals, as well as providing the DIO outputs. With the upgraded EMG system, we can acquire inputs from eight bilateral muscle groups on the body. Changes will be able to be monitored not only in the muscle groups about the ankle as done now, but also the thigh, trunk, and neck muscles.

Our accelerometers (3 on the head and 1 on the platform) now have a peak-to-peak output of ± 20 m/s^2. The signal conditioning provides a gain to allow for 1mV per mm/s^2 output. We maintain the original four load cells of the original force plate. We also still collect the position and motor current (shear force) from the Dover controller. Another change that we have implemented is the using the DIO for our subject acknowledgment signal. The DIO provides much better method of recognizing a subject's response than analog input with peak detectors. More offline processing is alleviated with the advent of global virtual channels in the LabVIEW software.

Discussion

Why did we choose a server over a desktop PC or workstation? First, what actually defines a server? Is it the operating system that it runs, that has "server" in the title? Is it the number of processors? Instead, is it simply any thing that is overly large and bulky or sleek and stylish that cannot be referred to as a desktop or laptop? Even people who are experience computers cringe at the word server due to the lack of support in that environment. From our standpoint, a server is a computer that maximizes the processing power per cubic inch of space it occupies, while not being singled for solitary use, and "serving" several people and purposes at once to offload the burden from desktop machines.

The server's compact size and rack-mountable design make it convenient to house and organize cables out-of-sight. Therefore, there is less clutter in the lab workspace and less confusion of

equipment and function. The low profile PCI standard and PCI bus expansions also allow for the server to maximize the space it occupies without creating airflow problem that could lead to system failure.

We needed a computer that would not be outdated be new software in the near future. The extendable memory and hard drive system will provide increased capacity for years to come. The EM64T allows us to adapt to the new trend toward 64-bit computing. The EM64T permits us to perform tasks that would normally require time on supercomputers, and provides the capacity to upgrade RAM memory to 16 GB from the current 3 GB if needed for intensive analysis and simulations. The hot-swappable hard drive ensures low down time, but allows for almost plug and play expansion for up to six hard drives. This will ensure that we have plenty of capacity for subject data from future tests.

However, the main issue we had with the server was its cost. The price is reasonable given that it replaces two workstation PCs. The rack-mountable setup has allowed us to streamline our electronics in the lab and cut down on the clutter and confusion caused by the use of several PCs for testing. In addition, the new experiment protocol could not run without significant delays when implemented on a 2.4 GHz desktop PC. Therefore, even though our server cost around 3 times the price of a high-end PC, the benefits out weighed cost due to higher productivity of the lab.

Conclusion

The technologies exist to create a single system, which is capable of replacing multiple conventional PCs in current lab setups. The server platform provides the means necessary to combine these technologies into a single unit. By incorporating a server system into our experimental setup, our lab is able to spend more time analyzing usable data, writing, and developing new ideas for research, which allows for a more productive research environment.

Reference

[1] Robinson, C. J., Purucker, M. C., and Faulkner, L. W., 1998, "Design, control, and characterization of a sliding linear investigative platform for analyzing lower limb stability (SLIP-FALLS)," Rehabilitation Engineering, IEEE Transactions on [see also IEEE Trans. on Neural Systems and Rehabilitation], 6(3), pp. 334-350.

Biographical Information

CHRISTOPHER M. STOREY, MS, received his BS degree in computer science from Tulane University in 2003 and his MS in neuroscience from Tulane University in 2004. He is completing his doctorate in biomedical engineering at Louisiana Tech University. He is currently finishing his research on postural control at the Center for Rehabilitation Engineering, Science and Technology at Clarkson University's SLIP-FALLS-STEPm lab.

CHARLES J. ROBINSON, DSc, PE, received his DSc degree in Electrical Engineering from Washington University in 1979. He is the founding Director of Clarkson University's Center for Rehabilitation Engineering, Science, and Technology and holds the Schulman Chair of Electrical and Computer Engineering there. He is a Senior Rehabilitation Research Career Scientist at the Syracuse VA Medical Center. He is a Fellow of the IEEE and of AIMBE.

APPENDIX V

ACCEPTED AUDIOLOGY NOW! 2006

POSTER

High Frequency Hearing Loss Related to Type-2 Diabetes

PP215

C.M. Storey, M.S.[1,2], C.J. Robinson, D.Sc.[1,2,3], A. Hollister, M.D.[1,4], T.D. Magee, M.C.D.[2], D.E. Redman, M.S.[2], V.A. Darblie, M.S.[1], S. Nakappan, M.S.[5], G. Patrick[2]
[1]Center for Biomedical Engineering and Rehabilitation Science, Louisiana Tech Univ., Ruston, LA. [2]Center for Rehabilitation Engineering, Science, and Technologies, Clarkson Univ., Potsdam, NY.
[3]Overton Brooks VA Medical Center, Shreveport, LA. [4]Louisiana State University Health Science Center, Shreveport, LA
[5]Kessler Medical Rehabilitation Research Education Corp.

Problem

Diabetic adults are known to develop large fiber peripheral neuropathy, but few studies have looked at central impairment in diabetic adults. Do mature adults with well-controlled Type-2 diabetes have a cranial nerve (CN) VIII pathology?

Introduction

1. Peripheral Neuropathy of the lower limbs is well documented through the literature in mature adults with type-II diabetes, but few studies have looked at the central nervous effects. CN VIII carries both vestibular and auditory information.
2. Balance studies have shown the effects of diabetic peripheral neuropathy as a source for impaired balance. When all diabetics (with mild peripheral neuropathy of the lower limbs (PN) and neurally intact (NI)) in our study are considered, higher significant differences are seen between diabetic mature adults (DMA; n = 24; H_{alc} = [6%-9%]) and healthy mature adults (HMA; n = 27).
3. Air conduction test provide a simple non-invasive test that allows for the study of a part of the central nervous system.

Methods

- All subjects (ages, 50-75) were screened against past medical histories of cardiovascular disease, neurological disease, drug and alcohol abuse, and falls. All subjects could function independently based on the BERG balance scale (no significant difference between groups). All HMA were neurally intact.
- Air conduction audiology test were performed by certified audiologist at 1, 2, 4, and 8 kHz.
- An ultra-low-vibration Sliding Linear Investigative Platform for Assessing Lower Limb Stability (SLIP-FALLS) was used for threshold detection of perturbations during quiet standing.
- Data was analyzed in SPSS® 14 using Kruskal-Wallis non-parametric test, and ANOVA with Tukey post hoc.

Results - Hearing

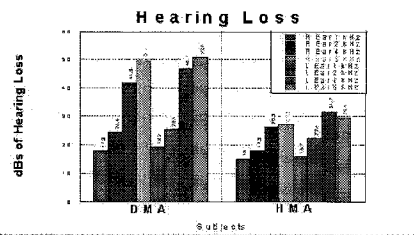

- DMA showed significantly more hearing loss than HMA at 4 and 8 kHz bilaterally ($p < 0.027$ and $p < 0.007$ respectively).
- No significant difference at 1 and 2 k Hz

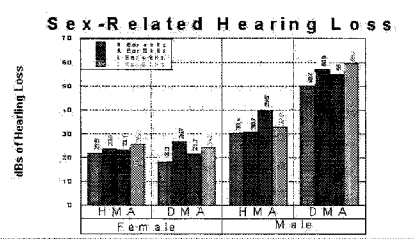

- Male DMA have significantly more hearing loss than other groups at 4 and 8 kHz except on the left ear at 4 kHz versus male HMA.

Results – Balance and Neuropathy

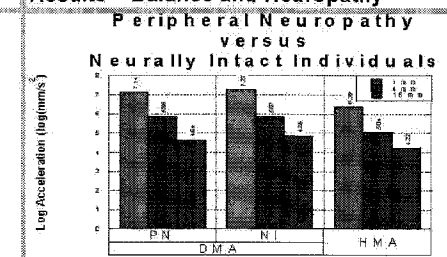

- DMA with PN did not differ that those who were NI in acceleration thresholds
- DMA displayed a significantly decreased ability to detect forward perturbations at 1 and 4 mm than HMA ($p < 0.003$ and $p < 0.002$)

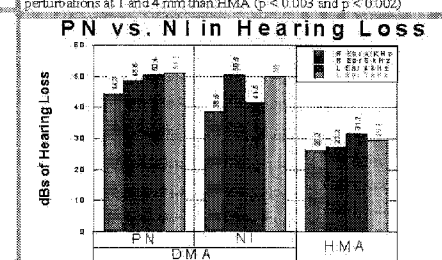

- Hearing Loss in DMA at 4 and 8 kHz is larger than HMA for both PN and NI, but 4 kHz Hearing Loss is less in NI.

Conclusion

1. **DMA have some significant central nervous system impairment as indicated by the air conduction test.**
2. **The sex-related hearing loss in DMA cannot be conclusively confirmed due to the low sample size of female DMA, (n=6).**
3. **The higher significance achieved with hearing and acceleration thresholds when all DMA (PN and NI) not just DMA with PN provides evidence for a peripheral neuropathy of CN VIII or a more central mechanism.**
4. **The lack of difference in acceleration of profiles of both PN and NI, and the lack of significant difference in hearing loss in PN and NI support a vestibular mechanism for pathology and detection of movement.**
5. **Additional audiological studies of DMA might be able to character size signs of undiagnosed diabetes, therefore providing preventative care to patients.**
6. **Future studies should undertake this in combination with other cognitive and evoked potentials to look diabetes effect on other aspects of the central nervous system.**

Acknowledgements

- State of Louisiana Board of Regents Fellowship
- Merit Review grants from VA Rehabilitation R&D Service Grants #E91-355AP, Grant #E2143PC, #E01-2097R and a Sr. Rehab. Research Career Scientist Award to Dr. C.J. Robinson.

APPENDIX W

ACCEPTED NEUROSCIENCE 2005

POSTER

A POSSIBLE DETECTION MECHANISM (TA EMG) FOR A 16 MM UNIAXIAL FORWARD PERTURBATION IN DIABETICS AND ELDERLY ADULTS

C.M. Storey[1], C.J. Robinson[1,2], V.A. Darbhe[1], S. Nakappan[1], K.K. O'Neal[1]
[1]Center for Biomedical Engineering and Rehabilitation Science, Louisiana Tech Univ., Ruston, LA
[2]Overton Brooks VA Medical Center, Shreveport, LA, USA

868.13

Problem

Diabetic mature adults show an increased sway length, which may lead to an increased likelihood of falls. How well does a diabetic individual with mild peripheral neuropathy detect motion?

Introduction

1. Ankle strategies for balance control show activation of Tibialis Anterior and Gastrocnemius Soleus (GS) muscles.
2. We believe that understanding the balance control system requires the use of perturbation probes that are close to the range of sway seen during quiet standing. These moves are around a threshold detection level.
3. We have developed special platform for small moves (mm) that removes noise and the need for harness.
4. Non-diabetic subjects have a lower acceleration threshold for detection of movement than do diabetic subjects.

Methods

- An ultra-low-vibration Sliding Linear Investigative Platform for Assessing Lower Limb Stability (SLIP-FALLS) was used for threshold detection of perturbations during quiet standing.

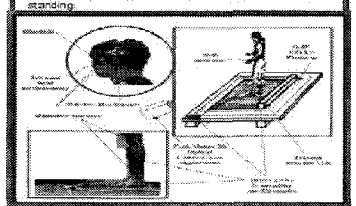

- TA and GS EMGs recorded
  - Delsys Bagnoli EMG Amp Used with Dual Differential Electrodes applied bilaterally to the Tibialis Anterior (TA) and Gastrocnemius Soleus (GS) muscles
  - Sampled at 1000 Hz. RMS value filtered at 50 Hz.
- Two Alternative Forced Choice Protocol was used for sequential test detection of perturbations. A Modified Parameter Estimation for Sequential Testing algorithm was used to lower the number of trials needed to accurately

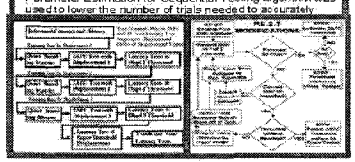

Results

Time- Ensemble-Averaged Tibialis Anterior EMG Activation Resulting from 16mm Perturbations

Interval 1

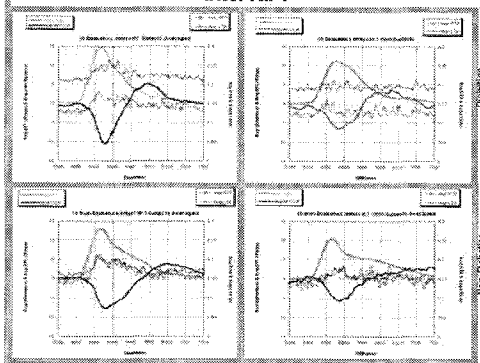

1. For detects, both non-diabetic and diabetic subjects exhibit a similar EMG response.
2. Diabetics require a larger stimulus (acceleration) to elicit a response in detects.
3. No observable response is seen in diabetic subjects for non-detected trials.
4. Non-diabetic subjects display a response, but it is smaller than on detected trials.

Interval 2

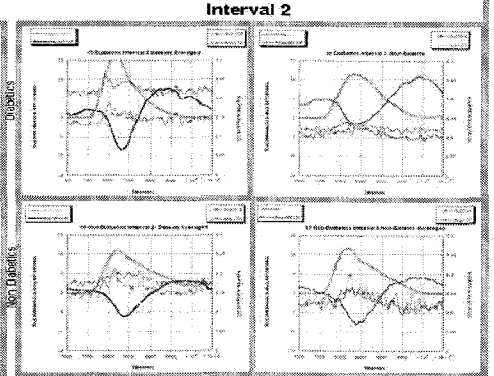

1. The second interval gives a similar EMG response as is seen in first interval.
2. Interval 2 detected trials displayed a higher physical response of APCoP position and velocity changes in diabetic subjects.
3. A activation of TA is larger in non-diabetic than diabetic subjects, even though the acceleration magnitude at threshold is greater in diabetics.

Raster Plots of One Diabetic Subject

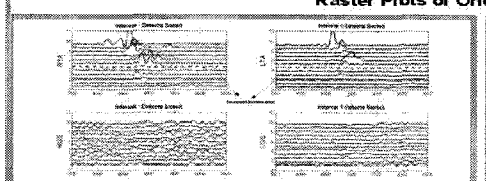

1. Results for one diabetic subject for detected trials in interval one.
   1. Little to no activation for trials below subjects approximated threshold.
   2. No observable activation of GS muscle for detected trials.
   3. Most Trials have high TA activation for detections.
   4. Results are ordered by increasing acceleration, which displays the increased activation of TA with increased input (higher acceleration at top).

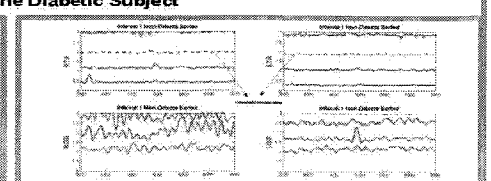

1. Results for one diabetic subject for non-detected trials in interval one.
   1. Rare observable activation of TA for non-detected trials for both perturbations above and below threshold.
   2. No observable GS activation for non-detected trials.
   3. Few non-detected trials above threshold.

TA Activation at 1 & 4 mm

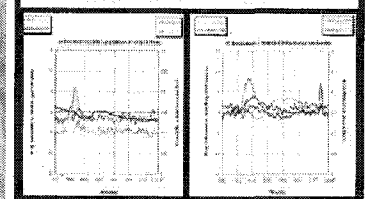

1. Definite (@ 4 mm) and possible (@1 mm) activation in detected trials for non-diabetic subjects. Recall again that thresholds were geometrically higher at 4, then 1 mm.
2. No observable activation in diabetic subjects at 4 or 1 mm for detected trials (Graph not shown).

Conclusions

1. The presence of TA EMGs correlate with detection for moves at 16 mm in diabetic subjects.
2. Mechanisms other than simple presence of TA EMG seem to be used for detection by Non-diabetic subjects since EMG activation seen in non-detect trials.
3. Thus, non-diabetic subjects may require a certain level of TA activation before detection occurs.
4. For diabetic subjects, their increased sway creates a low signal-to-noise ratio which may decrease the chance of TA activation.
5. In diabetic subjects, the loss of a more precise detection system might suggest TA activation is used as a possible detection.
6. The TA activation is not accompanied by any antagonistic GS activation; therefore GS EMG does not seem to be a repositioning reaction to the movement.
7. 1 and 4 mm moves produce proportionally less TA activation even with higher required acceleration, so the level of TA involvement cannot be a detector.
8. Less activation in 1 and 4 mm trials could point to a difference in body reaction to a stimulus with higher frequency than the 16mm perturbation.

Acknowledgements

- State of Louisiana Board of Regents Fellowship
- Merit Review grants from VA Rehabilitation R&D Service Grants #E01-355AF, Grant #E2143FC, #E01-2097R and a Sr. Rehab. Research Career Scientist Award to Dr. C.J. Robinson.
- Ms. Gloria Patrick for screening and recruiting subjects for this study and all the subjects who volunteered to participate in this study.

APPENDIX X

LOUISIANA TECH UNIVERSITY IRB

AND INFORMED CONSENT

HUMAN USE COMMITTEE REVIEW
APPROVAL FORM

TO: Dr. Mary Livingston and Dr. Les Guice

FROM: Barbara Talbot, University Research

SUBJECT: HUMAN USE COMMITTEE REVIEW

DATE: 11/14/05

The following Human Use Research proposal has been submitted for an EXPEDITED EXTENSION REVIEW:

Number: **HUC-073**
PI: **Dr. Charles Robinson**
Title: "Psychophysics of Postural Perturbations in Young and Old"

Please initial this transmittal letter and return it to me when you approve as is, or recommend changes to this proposal.

	Initial	Date
☐ Changes Recommended by Dr. Mary Livingston		11/14/05
☒ Approved by Dr. Mary M. Livingston	MM L	11/14/05
☒ Approved by Dr. Les Guice	LG	11/14/05

Comments:

Inbox Compose Folders Search Fetch Mail Filters Options Help Open Folder Inbox
Log out

Quota status: 602.48MB / 2048.00MB (29.42%)

Inbox: Re: Fw: HUC-073 - Charles J. Robinson (4 of 7945)

Mark as: Move | Copy | This message to Back to Inbox

Delete | Reply | Reply to All | Forward | Redirect | View Thread | Blacklist | Whitelist | Message Source | Save as | Print | Report as Spam

Date: Sat, 12 Nov 2005 08:45:42 -0500 [11/12/05 07:45:42 CST]
From: Charlie Robinson <robinson@clarkson.edu>
To: Terry McConathy <tmm@latech.edu>, Charlie Robinson <robinson@clarkson.edu>
Cc: "Mary M. Livingston" <maryml@latech.edu>, Beth Free <bfree@latech.edu>, Les Guice <guice@latech.edu>
Subject: Re: Fw: HUC-073 - Charles J. Robinson
Headers: Show All Headers

Dear Dr. Terry and Dr. Livingston,

Thank you for your guidance in this manner.

I hereby request an extension of protocol HUC-073 through March 31, 2006.
Accrual on this protocol has stopped, and no more subjects will be entered into it.

All of the basic protocol remains the nearly the same, except that the subject population
should be increased to reflect the number studied. Thus a request is made to change the
proposed accrual number to 40 healthy young adults, 60 healthy mature adults 50 yrs or
older, and 50 diabetic adults over 50. Note that their is a corresponding VA IRB-approved
protocol in which has been updated yearly to reflect all changes.

We wish the protocol to reflect the fact that we have added a TekMat foot pressure sensor
and a Vicon motion capture system to our data collection routine. These were done with no
additional risk to the subject, as the basic perturbation sequence remained exactly the
same throughout our entire study. No adverse effects to our protocol were seen in any of
the 150 individuals tested.

For a progress report, this project has been very successful: Four peer-reviewed papers,
16 or more conf. abstracts, 1 PhD dissertation, 4 MS thesis and 1 project completed, with
another 1 PhD, and 4 thesis that will be forthcoming from Tech students. One of the conf.
papers won a student prize.

-Charlie R.

At 11:03 AM -0600 11/11/05, Terry McConathy wrote:

[Hide Quoted Text]

> Charlie:

researcher was unaware that he needed to also check w/ Tech IRB this unknown corrected see emails MML 1/07/14

Below is Dr. Livingston's assessment.

Please proceed with a request for extension. Also, if you are, as you state, using the
data in blinded studies, you will need to have an extension to cover those studies as
well. We need to keep our documentation accurate and current.

Dr. Livingston is always able to expedite these requests, so I foresee no delay in processing this thesis while the approval is obtained. Dr. Livingston indicates that
this can be accomplished by email.

Thank you.
Terry M. McConathy
Executive Vice President
Dean of the Graduate School
Louisiana Tech University
Box 7923
Ruston, LA 71272
Tel 318-257-2924
Fax 318-257-4487

----- Original Message ----- From: "Mary Margaret Livingston" <maryml@LaTech.edu>
To: "Terry McConathy" <tmm@latech.edu>
Cc: <guice@latech.edu>
Sent: Friday, November 11, 2005 10:51 AM
Subject: Re: HUC-073 - Charles J. Robinson

Terry,
I concur with all you have said.
1) Off site work does need approval. 2) Given the variability in IRBs, Tech has as you
know adopted the general policy of independent approval.
3) The researcher does need to get an extension after a year. It can be done by memo
or email since there has been no change in the study. We have performed expedited approvals on such extensions that involve no changes in the protocol and no unanticipated problems. This could be performed by me, Dr Guice or you as you do when
he is gone, or Dr Guice's delegate. I, like Charlie Robinson, had mistakenly thought
that once data was collected and being analyzed no extension was necessary. At the
OHRP education conference held at Tech last Spring I was informed otherwise by the
OHRP-educator instructors. The folks from OHRP said that the studies have to be re-reviewed even if data is just being analyzed. There is usually no problem with extending beyond a year if things have not changed and are going well. I really appreciate Charlie Robinson's conscientiousness and hope that other researchers will
observe the expiration dates. Thanks for your help, and for keeping me informed.
Mary

Quoting Terry McConathy <tmm@latech.edu>:

Charlie:

It has been our practice that if a Tech student is doing research that requires IRB
approval, even if it is conducted off-site, Tech IRB approval must be obtained.

Terry M. McConathy

Executive Vice President
Dean of the Graduate School
Louisiana Tech University
Box 7923
Ruston, LA 71272
Tel 318-257-2924
Fax 318-257-4487

----- Original Message ----- From: "Charlie Robinson" <robinson@clarkson.edu>
To: "Terry McConathy" <tmm@latech.edu>; "Mary M. Livingston" <marym1@latech.edu>;
"Beth Free" <bfree@latech.edu>; "Les Guice" <guice@latech.edu>; "Vikram Arun Darbhe"
<vad005@LaTech.edu>
Cc: "Charlie Robinson" <robinson@clarkson.edu>
Sent: Friday, November 11, 2005 10:20 AM
Subject: Re: HUC-073 - Charles J. Robinson

At 8:31 AM -0600 11/11/05, Terry McConathy wrote:

Mary Margaret:

Vikram Arun Darbhe, a student working with Dr. Robinson, has submitted a thesis
dated November 2005 and is using the HUC-073 IRB approval issued to Dr. Robinson
and approved on March 20, 2004. The approval states clearly that "This approval is
granted for one year from the date shown above. Projects should be renewed annually." The HUC approval has expired.

Is this HUC 073 approval still valid for this student's thesis? Or do we need a
written extension to cover it?

I would appreciate an answer as soon as possible. This student is trying to
graduate next week.

Thanks,
Terry
Terry M. McConathy
Executive Vice President
Dean of the Graduate School
Louisiana Tech University
Box 7923
Ruston, LA 71272
Tel 318-257-2924
Fax 318-257-4487

Terry,
Thank you for your efforts with respect to Vikram.

The thesis data collected at Tech was all done within the 1 year time frame covered
by the IRB approval from Tech. NO DATA WAS COLLECTED AT TECH after that date,
because of some controller problems. The student is simply analyzing that data as a
part of his thesis (which does not require IRB approval). He DID NOT participate in
carrying out those experiments.

All other data in his thesis was collected at the VA under a VA-approved IRB in my
position as a VA researcher. He included that VA consent in his thesis, and was told

that this was unacceptable. That VA IRB has be continually and annually reviewed,
with required yearly progress reports. If you need a copy of that approval for the
time frame in which the student's data was collected (FY05), I can provide it to
you. I terminated the VA data collection protocol on Sept. 30, 2005, and made a
final progress report. The data is still being analyzed in a blinded fashion, and
will be the subject of additional students' theses. These later theses should not be
subject to having a current IRB approval from Tech, since the data is blinded.

Tech's IRB should recognize comity with the VA IRB.

-Charlie R.

--
****
Charles J. Robinson, D.Sc., P.E. Fellow IEEE, Fellow AIMBE, U.N.E.S.C.O. Academician
Director, Center for Rehabilitation Engineering, Science and Technology (CREST)
Herman L. Shulman Chair Professor, Department of Electrical and Computer Engineering
Office CAMP 227; Clarkson University Box 5730; Potsdam, NY 13699-5730
CREST office: CAMP 225; Phone: 315-268-6528 /6651 Fax: 315-268-4494
Cell Phone 315-244-6241
Offices hours 12:30 to 5:30 PM; Mon-Fri
Email <c.robinson@ieee.org> or <robinson@clarkson.edu>

Senior Rehabilitation Research Career Scientist
DUTY STATION: VA Potsdam Satellite Rehabilitation R&D Center
3rd Floor, Clarkson Hall, Potsdam, NY 13676
Phone: 315-425-vvvv; Fax 315-425-wwww
Offices hours 7 AM to 12 noon; Mon-Fri
HOME AFFILIATION: Syracuse VA Medical Center, Research Service 151
Rm D408; 800 Irvine Ave., Syracuse, NY 13210
Phone 315-425-4400 (X53606)

Adjunct Professor, Orthopaedic Surgery Dept, LSU Health Science Center, Shreveport, LA
Adjunct Professor, Louisiana Tech University, Ruston, LA (Phone: 318-257-4562)
Founding, but Past Editor, IEEE Transactions on Rehabilitation Engineering
****
"Service is the rent we pay for being. It is the very purpose of life
and not something that you do in your spare time."
Marion Wright Edelman
****

This message was sent using IMP, the Internet Messaging Program.

Delete | Reply | Reply to All | Forward | Redirect | View Thread | Blacklist | Whitelist | Message Source | Save as | Print | Report as Spam

Mark as: Move | Copy This message to Back to Inbox

HUMAN USE COMMITTEE REVIEW
APPROVAL FORM

TO: Dr. Mary M. Livingston

FROM: Stephanie Herrmann

SUBJECT: HUMAN USE COMMITTEE REVIEW

DATE: 5/5/2004

The following Human Use Research proposal has been submitted for an EXPEDITED REVIEW:

Number: **HUC-073**
PI: **Charles J. Robinson**
Title: **Psychophysics of Postural Perturbations in Young and Old**

Please initial this transmittal letter and return it to me when you approve as is, or recommend changes to this proposal.

	Initial	Date
☐ Received by University Research		5/5/2004
☐ Changes Recommended by Dr. Mary Livingston		
☒ Approved by Dr. Mary M. Livingston	MML	5/11/04
☐ Approved by Dr. Les Guice	LG	5/18/04

Comments:

I approve pending Dr. Greens approval MML
Green approval attached

FILE COPY

MEMORANDUM

TO: Charles Robinson

FROM: Stephanie Herrmann, University Research

SUBJECT: HUMAN USE COMMITTEE REVIEW

DATE: March 20, 2004

In order to facilitate your project, an **EXPEDITED REVIEW** has been done for your proposed study entitled:

"Psychophysics of Postural Perturbations in Young and Old"
Proposal # HUC-0073

The proposed study procedures were found to provide reasonable and adequate safeguards against possible risks involving human subjects. The information to be collected may be personal in nature or implication. Therefore, diligent care needs to be taken to protect the privacy of the participants and to assure that the data are kept confidential. Further, the subjects must be informed that their participation is voluntary.

Since your reviewed project appears to do no damage to the participants, the Human Use Committee grants approval of the involvement of human subjects as outlined.

This approval is granted for one year from the date shown above. Projects should be renewed annually. Projects involving NIH funds require annual education training to be documented. For more information regarding this, contact the Office of University Research.

You are requested to maintain written records of your procedures, data collected, and subjects involved. These records will need to be available upon request during the conduct of the study and retained by the university for three years after the conclusion of the study.

If you have any questions, please contact Mary Livingston at 257-2292 or Stephanie Herrmann at 257-5075.

Note to Researcher:
Reviewer recommends providing a list of drugs and medications that would qualify and disqualify a candidate on the consent form.

LOUISIANA TECH
UNIVERSITY

OFFICE OF UNIVERSITY RESEARCH

MEMORANDUM

TO: Dr. James Green

FROM: Stephanie Herrmann, University Research

SUBJECT: HUMAN USE COMMITTEE REVIEW

DATE: May 12, 2004

The following Human Use Research Proposal has been submitted for an EXPEDITED REVIEW:

Number: HUC-073
PI: Charles J Robinson
Title: Psychophysics of Postural Perturbations in Young and Old

Due to the physical nature of this study, Dr. Livingston has asked that you review it. After you review this study, please sign this memo and return it to me with either your approval "as is," or your recommendations for changes.

with Comment below

APPROVAL: _____ DATE: 5/13/04

or

CHANGES RECOMMENDED: _____ DATE: 5/13/04

Need a list of what drugs and medications would qualify or disqualify a candidate — at least categories of drugs

The attached information is a copy only. You may discard and only return this approval sheet when complete. You may fax approval and/or changes to 257-5079 or email them to herrmann@gschool.latech.edu. This may also be returned by mail in the enclosed envelope. Call 257-5075 with any questions.

A MEMBER OF THE UNIVERSITY OF LOUISIANA SYSTEM

P.O. BOX 3002 • RUSTON, LA 71272 • TELEPHONE (318) 257-5075 • FAX (318) 257-5079
AN EQUAL OPPORTUNITY UNIVERSITY

LOUISIANA TECH
UNIVERSITY
A MEMBER OF THE UNIVERSITY OF LOUISIANA SYSTEM

HUC-013

MEMORANDUM

TO: Institutional Review Board
University Research Office

FROM: Charles J. Robinson
CyBERS

SUBJECT: Human Use Committee Review (Expedited Review Request)

Date: May 3, 2004

Attached is the Human Subject's Consent Form submitted under the Study Title: Psychophysics of Postural Perturbations in Young and Old. It was originally submitted in February of 2003 and approved; however, the form expired February 2004. Therefore, we are resubmitting the form (without changes) to the Institutional Review Board, and request expedited approval, as we are ready to resume testing.

We will change the start and stop dates on page 3, when notified of the new dates. Thank you for your assistance.

Charles J. Robinson, PI — Date 5/3/04

Dr. Stan Napper, Interim Dean
College of Engineering & Science — Date 5-5-04

CENTER FOR BIOMEDICAL ENGINEERING AND REHABILITATION SCIENCE (CYBERS) • COLLEGE OF ENGINEERING AND SCIENCE
711 SOUTH VIENNA • RUSTON, LOUISIANA 71270 • TELEPHONE (318)257-4562 • FAX (318)255-4175
EMAIL: CYBERS@COES.LATECH.EDU • WEB: WWW.CYBERS.LATECH.EDU
AN EQUAL OPPORTUNITY UNIVERSITY

LOUISIANA TECH UNIVERSITY HUMAN SUBJECT'S CONSENT FORM

STUDY TITLE: **Psychophysics of Postural Perturbations in Young and Old**

DEFINITION OF CONSENT FORM

We are asking you to volunteer for a research study conducted at Louisiana Tech University. It is important that you read and understand the information on this form. This Consent Form gives detailed information about this research study. It is not meant to frighten or alarm you; rather it is an effort to make you better informed in order for you to make a decision as to whether or not you wish to participate. This process is known as "Informed Consent."

PURPOSE OF STUDY/PROJECT AND SELECTION OF SUBJECTS

Slips and falls, and even fear of falling, can represent a mayor medical and functional barrier to living independently. To react to a potential slip or fall, you must be able to detect motion changes that may lead to slips or falls, and be able to fine-tune the control of the muscles used to maintain balance.

You are invited to participate in a research study related to standing balance and postural control. Researchers at Louisiana Tech University hope to learn how much the senses of the limbs (touch sense, joint angle sense, muscle tension sense) contribute to the stability of your posture. With such knowledge, we might later be able to evaluate the potential to fall or slip, and to develop training methods that might reduce the risk of falling or slipping. You were selected as a possible participant in this study because your senses are intact and your responses will be used as reference. You should be 18 years old or older to participate in this study. Before proceeding further, we need to ask you if you have had certain illnesses or neurological problems, since some of these conditions might confuse our study results, and hence, make you not a candidate for this particular research study Your answers will remain confidential.

May we ask you some questions about your medical history?

YES or NO: Initials:_____

We must exclude you from this study if you have a current of past history of severe heart, circulation or breathing problems; diabetes, chronic lower back spasms or pain; deformities of the spine, bones and joints (such as abnormal spinal curvature, arthritic changes or amputation); brain strokes, spinal cord injury or other damage to the nervous system; non-healing skin ulcers; current drug or alcohol dependence; or repeated falls; or if you are taking prescription medication that causes or prevents dizziness. (Any information obtained during this study and identified with you as a subject will remain confidential and disclosed only with your permission.)

Do you have now, or have you had, any of the problems just listed?

YES or NO: Initials:_____

Would you have problems or fears with being blindfolded for 15 to 20 minutes or so at a time?

YES or NO: Initials:_____

If you answered "Yes" to either question, thank you for your time and effort in volunteering to participate, but we cannot use you in this particular study. Please fill out the personal information on the last page before you go. If you answered "No", then you are a likely candidate for our study, which we will now explain to you.

PROCEDURE TO BE USED

If you are an adult in good health and have no physical or neurological problems, you probably do well in sensing changes in balance, and hence will serve in a "control" group. If you decide to participate in this research study we will ask you by phone or in our lab to answer a brief medical questionnaire that helps us

determine in which group you will be placed. In the lab, we will give you a short test called the Mini-Mental test that measures how well you remember things and can follow instructions. The questionnaire and test will require approximately 20 minutes.

When you balance, you might be using your sense of foot pressure and/ or of muscle effort (as signaled by your leg nerves); your vision; or the balance sense organ (called the vestibular system), or any combination. It is important to our study to be able to separate out these effects, so we do the tests outlined below. We will measure how well and how fast you sense small touches to the bottom of your foot and toes; how well and how fast you sense tones of various pitches; and how far your big toes, ankles, knees and hips move (called your range-of-motion) and the strength of the muscles of these joints. We will note any differences in leg length. We will see how well you balance on both legs, on one leg, and with one foot behind the other with your eyes open, and with your eyes closed. You will do this test standing on a tile floor and on a large, thin piece of foam rubber. These tests will take about 40 minutes, but will be given in-between our tests.

While it is important for us to understand via all of these tests how your nervous system is functioning, we also reinforce to you now that you are a volunteer. As such, you can just tell us that you do not want to do one or more of these tests, or to stop a test (or quit altogether) in the middle of a test (or any time) if you do not want to continue. It is your right as a volunteer, and our duty to allow you to do what you feel is best for you. All of these preliminary tests could take upwards of three or four hours to complete.

Testing your ability to detect small movements: All humans sway. It is a natural, every second, occurrence. What we do is to add a small sliding movement (a fraction of an inch) to the plate on which you are standing. The movement might be left/ right/ forward or backward. The main test will have you standing with bare feet on a platform that will be stationary for about 20 seconds before it is moved. You will be told when a possible move may occur and you will be asked to decide and signal al what time the device was moving. In these tests, the platform will move your whole body. You will be wearing a blindfold that will restrict your vision and headphones to reduce outside noise, so that you may only receive motion inputs from your sensory system or balance system. For all tests you will be wearing adhesive muscle activity sensors on your legs. If you complete all these platform tests, we estimate that the completion of this part will take less than 4 hours. We will stop testing if you become dizzy or nauseous. You also can stop the test at any time that you wish, without reprisal.

MEASURES TO INSURE PROTECTION OF YOUR CONFIDENTIALITY AND ANONYMITY

Information and research results will be used to further the field of posture and balance control and to benefit the evaluation and therapy processes related to posture and balance. Therefore the research results will possibly be used for scholarly papers, presentations, and future grant applications. Any information obtained during this study and identified with you as a subject will remain confidential and cannot be disclosed without your written permission. If results of this study are reported in medical journals or at meetings, you will not be identified by name, by recognizable photograph, or by any other means without your specific consent. Your records will be maintained according to this University's requirements. By signing this form you are giving permission for us to make records available to the Louisiana Tech University Institutional Board for Human Research to which information will be released, all of whom must maintain confidentiality.

RISKS

All motions of the platform will be near your natural sway change of position. Because of this, you may not always ~~be able to feel the device move. Also because the movements will be so~~ slight, there is very little chance of your falling. During the times where the platform is moving and while your eyes are closed or blindfolded, and you are wearing the headphones to block out external noises, you may feel a slight loss of balance, dizziness or nausea. A member of the laboratory staff will be standing behind or beside you al all times when you are blindfolded. He or she is located there to correct your position before a potential fall event can occur. Since we

use properly isolated electrical amplifiers, there should be no risk of shock from our measurement of muscle activity. The muscle activity sensors will be held to your skin with a small piece of double-sided tape. The gel that helps conduct your muscle activity in the sensors may have a salt base. You may experience some redness from the tape or the conduction gel. This is common and the redness should disappear within a few hours.

ALTERNATIVES:

You are not required to take part in this study—your participation is entirely voluntary.

NON-PARTICIPATION OR WITHDRAWAL:

Your decision whether or not to participate in this study will not involve any penalty or loss of rights nor will it prejudice your future relationship with this institution. If you decide to participate, you are free to discontinue participation at any time without penalty or loss of benefits to which you are entitled.

BENEFITS/COMPENSATION:

Taking part in this study may not personally help you, but your participation may lead to knowledge that will help others. We will review your own results with you before you leave, and significant overall findings developed as a result of this study will be provided to you at the conclusion of the study. There will be no cost to you for any of the testing done as part of this research study.

CONTACT INFORMATION:

1. If you have questions about your rights as a research participant, you may contact the Chairman of the Institutional Review Board, Dr. Les Guice, at (318) 259-29-26 or Dr. Mary Livingston at 257-4315.
2. If you have questions about this study or problems arising from this study, you should call Dr. Charles Robinson at (318) 424-6080 during the day, and Dr. Robinson at (318) 513-9122 after hours.
3. You will receive a signed copy of this consent form.

AFFIRMATION FROM SUBJECT:

I, _____, attest with my signature that I have read the preceding description of the study, "Postural Control Response to Small Accelerations", and understand its purposes and methods.

I understand that my participation in this research is strictly voluntary and my participation or refusal to participate in this study will not affect my relationship with Louisiana Tech University in any way. Further, I understand that I may withdraw at any time or refuse to answer any questions without penalty.

Upon completion of the study, I understand that the results will be freely available to me upon request.

I understand that the results of my survey will be anonymous and confidential, accessible only to the principal investigators, myself, or a legally appointed representative.

I have not been requested to waive nor do I waive any of my rights related to participating in this study.

_____ _____

Signature of Participant or Guardian Date

_____ _____

Signature of Person Administering the Informed Consent Date

_____ _____

Signature of Witness Date

_____ _____

Signature of the Principal Investigator Date

This form has been approved by the Louisiana Tech University Institutional Review Board on_____ and expires on_____.

REFERENCES

[1] B.-l. Cho, D. Scarpace, and N. B. Alexander, "Tests of Stepping as Indicators of Mobility, Balance, and Fall Risk in Balance-Impaired Older Adults," *Journal of the American Geriatrics Society* vol. 52, pp. 1168-1173, 2004.

[2] Y.-C. Pai, M. W. Rogers, J. Patton, T. D. Cain, and T. A. Hanke, "Static versus dynamic predictions of protective stepping following waist-pull perturbations in young and older adults," *Journal of Biomechanics,* vol. 31, pp. 1111-1118, 1998.

[3] P. E. Pidcoe and M. W. Rogers, "A closed-loop stepper motor waist-pull system for inducing protective stepping in humans," *Journal of Biomechanics,* vol. 31, pp. 377-381, 1998.

[4] B. W. Schulz, J. A. Ashton-Miller, and N. B. Alexander, "Compensatory stepping in response to waist pulls in balance-impaired and unimpaired women," *Gait & Posture,* vol. 22, pp. 198-209, 2005.

[5] M.-L. Mille, M. E. Johnson, K. M. Martinez, and M. W. Rogers, "Age-dependent differences in lateral balance recovery through protective stepping," *Clinical Biomechanics,* vol. 20, pp. 607-616, 2005.

[6] M. W. Rogers, L. D. Hedman, M. E. Johnson, K. M. Martinez, and M.-L. Mille, "Triggering of protective stepping for the control of human balance: age and contextual dependence," *Cognitive Brain Research,* vol. 16, pp. 192-198, 2003.

[7] S. Richerson, S. Morstatt, K. O'Neal, G. Patrick, and C. Robinson, "Effect of lateral perturbations on psychophysical acceleration detection thresholds," *Journal of Neuroengineering and Rehabilitation,* vol. 3, p. 2, 2006.

[8] S. J. Richerson, L. W. Faulkner, C. J. Robinson, M. S. Redfern, and M. C. Purucker, "Acceleration threshold detection during short anterior and posterior perturbations on a translating platform," *Gait & Posture,* vol. 18, pp. 11-19, October 2003.

[9] S. J. Richerson, C. J. Robinson, and T. Ehsan, "Lateral acceleration threshold detection in young adults and healthy elderly," in *[Engineering in Medicine and Biology, 2002. 24th Annual Conference and the Annual Fall Meeting of the Biomedical Engineering Society] EMBS/BMES Conference, 2002. Proceedings of the Second Joint*, 2002, pp. 2461-2462.

[10] C. J. Robinson, L. W. Faulkner, P. J. Sparto, and M. C. Purucker, "Innovative methods to study postural stability and fall initiation," in *Engineering in Medicine and Biology Society, 1998. Proceedings of the 20th Annual International Conference of the IEEE*, 1998, pp. 2264-2269.

[11] C. J. Robinson, M. C. Purucker, and L. W. Faulkner, "Design, control, and characterization of a sliding linear investigative platform for analyzing lower limb stability (SLIP-FALLS)," *Rehabilitation Engineering, IEEE Transactions on [see also IEEE Trans. on Neural Systems and Rehabilitation],* vol. 6, pp. 334-350, 1998.

[12] T. E. Prieto, J. B. Myklebust, R. G. Hoffmann, E. G. Lovett, and B. M. Myklebust, "Measures of postural steadiness: differences between healthy young and elderly adults," *Biomedical Engineering, IEEE Transactions on,* vol. 43, pp. 956-966, 1996.

[13] T. E. Prieto, J. B. Myklebust, and B. M. Myklebust, "Characterization and modeling of postural steadiness in the elderly: a review," *Rehabilitation Engineering, IEEE Transactions on [see also IEEE Trans. on Neural Systems and Rehabilitation],* vol. 1, pp. 26-34, 1993.

[14] R. W. Simmons, C. Richardson, and R. Pozos, "Postural stability of diabetic patients with and without cutaneous sensory deficit in the foot," *Diabetes Research & Clinical Practice,* vol. 36, pp. 153-160, June 1997.

[15] S. Richerson, "Effects of Diabetes and Aging on Posture and Acceleration Thresholds during Lateral Translations," in *Biomedical Engineering*. vol. PhD Ruston, LA: Louisiana Tech University, 2003.

[16] A. Nardone, M. Grasso, and M. Schieppati, "Balance control in peripheral neuropathy: Are patients equally unstable under static and dynamic conditions?," *Gait & Posture,* vol. 23, pp. 364-373, 2006.

[17] C. M. Storey, C. J. Robinson, A. Hollister, T. D. Magee, D. E. Redman, V. A. Darbhe, S. Nakappan, and G. Patrick, "High Frequency Hearing Loss Related to Type-2 Diabetes," in *Audiology Now!* Minneapolis, MN, 2006.

[18] G. Andersson, K. Persson, L. Melin, and H. C. Larsen, "Actual and Perceived Postural Sway During Balance Specific and Non-specific Proprioceptive Stimulation," *Acta Oto-Laryngologica,* vol. 118, pp. 461-465, 1998.

[19] P. Corbeil, M. Simoneau, D. Rancourt, A. Tremblay, and N. Teasdale, "Increased risk for falling associated with obesity: mathematical modeling of postural control," *Neural Systems and Rehabilitation Engineering, IEEE Transactions on [see also IEEE Trans. on Rehabilitation Engineering],* vol. 9, pp. 126-136, 2001.

[20] A. Nardone, M. Grasso, J. Tarantola, S. Corna, and M. Schieppati, "Postural coordination in elderly subjects standing on a periodically moving platform," *Archives of Physical Medicine and Rehabilitation,* vol. 81, pp. 1217-1223, 2000.

[21] A. Nardone, R. Siliotto, M. Grasso, and M. Schieppati, "Influence of aging on leg muscle reflex responses to stance perturbation," *Archives of Physical Medicine and Rehabilitation,* vol. 76, pp. 158-165, 1995.

[22] A. Nardone, J. Tarantola, G. Miscio, F. Pisano, A. Schenone, and M. Schieppati, "Loss of large-diameter spindle afferent fibres is not detrimental to the control of body sway during upright stance: evidence from neuropathy," *Experimental Brain Research,* vol. 135, pp. 155-162, November 2000.

[23] J. H. J. Allum, M. G. Carpenter, and F. Honegger, "Directional aspects of balance corrections in man," *Engineering in Medicine and Biology Magazine, IEEE,* vol. 22, pp. 37-47, 2003.

[24] K. R. Csavina, J. He, and A. Santello, "Postural control of balance under slow platform perturbations," in *[Engineering in Medicine and Biology, 2002. 24th Annual Conference and the Annual Fall Meeting of the Biomedical Engineering Society] EMBS/BMES Conference, 2002. Proceedings of the Second Joint*, 2002, pp. 2459-2460.

[25] K. R. Csavina, J. He, and M. Santello, "Postural response to slow perturbations: a preliminary study of young vs. elderly subjects," in *Engineering in Medicine and Biology Society, 2003. Proceedings of the 25th Annual International Conference of the IEEE*, 2003, pp. 1774-1776.

[26] J. He and C.-X. Tian, "Adaptive postural control for a repeated perturbation," in *Engineering in Medicine and Biology Society, 1996. Bridging Disciplines for Biomedicine. Proceedings of the 18th Annual International Conference of the IEEE*, 1996, pp. 2215-2216.

[27] M. C. Purucker and C. J. Robinson, "Characterization of a sliding linear investigative platform for analyzing lower-limb stability (SLIP-FALLS)," in *Engineering in Medicine and Biology Society, 1996. Bridging Disciplines for Biomedicine. Proceedings of the 18th Annual International Conference of the IEEE*, 1996, pp. 2289-2290.

[28] M. C. Purucker and C. J. Robinson, "Design of a sliding linear investigative platform for analyzing lower-limb stability (SLIP-FALLS)," in *Biomedical Engineering Conference, 1996., Proceedings of the 1996 Fifteenth Southern*, 1996, pp. 89-92.

[29] R. L. James, R. Ely, and D. Paul, "Stabilization of posture by precision touch of the index finger with rigid and flexible filaments," *Experimental Brain Research,* vol. 139, pp. 454-464, 2001.

[30] R. Dickstein, R. J. Peterka, and F. B. Horak, "Effects of light fingertip touch on postural responses in subjects with diabetic neuropathy," *Journal of Neurology, Neurosurgery & Psychiatry,* vol. 74, pp. 620-626, 2003.

[31] R. Dickstein, C. L. Shupert, and F. B. Horak, "Fingertip touch improves postural stability in patients with peripheral neuropathy," *Gait & Posture,* vol. 14, pp. 238-247, 2001.

[32] S. B. Bortolami, P. DiZio, E. Rabin, and J. R. Lackner, "Analysis of human postural responses to recoverable falls," *Experimental Brain Research,* vol. 151, pp. 387-404, 2003.

[33] H. B. Wasling, U. Norrsell, K. Göthner, and H. Olausson, "Tactile directional sensitivity and postural control," *Experimental Brain Research,* vol. 166, pp. 147-156, 2005.

[34] V. Krishnamoorthy, H. Slijper, and M. L. Latash, "Effects of different types of light touch on postural sway," *Experimental Brain Research,* vol. 147, pp. 71-79, November 2002.

[35] L. Borel, F. Harlay, J. Magnan, and M. Lacour, "How changes in vestibular and visual reference frames combine to modify body orientation in space," *Neuroreport,* vol. 12, pp. 3137-3141, October 2001.

[36] D. Simmons, C. F. Thompson, and M. M. Engelgau, "Controlling the diabetes epidemic: how should we screen for undiagnosed diabetes and dysglycaemia?," in *Diabetic Medicine*. vol. 22: Blackwell Publishing Limited, 2005, pp. 207-212.

[37] M. C. Thomas, M. K. Walker, J. R. Emberson, A. G. Thomson, D. A. Lawlor, S. Ebrahim, and P. H. Whincup, "Prevalence of undiagnosed TypeÂ 2 diabetes and impaired fasting glucose in older B ritish men and women," in *Diabetic Medicine*. vol. 22: Blackwell Publishing Limited, 2005, pp. 789-793.

[38] K. V. Allen, B. M. Frier, and M. W. J. Strachan, "The relationship between type 2 diabetes and cognitive dysfunction: longitudinal studies and their methodological limitations," *European Journal of Pharmacology,* vol. 490, pp. 169-175, 2004.

[39] R. Cosway, M. W. J. Strachan, A. Dougall, B. M. Frier, and I. J. Deary, "Cognitive function and information processing in Type-2 diabetes," *Diabetic Medicine,* vol. 18, pp. 803-810, 2001.

[40] R. Stewart and D. Liolitsa, "Type 2 diabetes mellitus, cognitive impairment and dementia," *Diabetic Medicine,* vol. 16, pp. 93-112, 1999.

[41] W. H. Gispen and G.-J. Biessels, "Cognition and synaptic plasticity in diabetes mellitus," *Trends in Neurosciences,* vol. 23, pp. 542-549, 2000.

[42] B. A. Perkins and V. Bril, "Diabetic neuropathy: a review emphasizing diagnostic methods," *Clinical Neurophysiology,* vol. 114, pp. 1167-1175, July 2003.

[43] B. A. Perkins and V. Bril, "Diagnosis and management of diabetic neuropathy," *Current Diabetes Reports,* vol. 2, pp. 495-500, Dec 2002.

[44] V. Bril and B. A. Perkins, "Validation of the Toronto Clinical Scoring System for diabetic polyneuropathy," *Diabetes Care,* vol. 25, pp. 2048-2052, November 2002.

[45] V. Bril and B. A. Perkins, "Comparison of vibration perception thresholds obtained with the Neurothesiometer and the CASE IV and relationship to nerve conduction studies," *Diabetic Medicine,* vol. 19, pp. 661-666, August 2002.

[46] B. A. Perkins, M. Ngo, and V. Bril, "Symmetry of nerve conduction studies in different stages of diabetic polyneuropathy," *Muscle & Nerve,* vol. 25, pp. 212-217, February 2002.

[47] D. Olaleye, B. A. Perkins, and V. Bril, "Evaluation of three screening tests and a risk assessment model for diagnosing peripheral neuropathy in the diabetes clinic," *Diabetes Research & Clinical Practice,* vol. 54, pp. 115-128, November 2001.

[48] B. A. Perkins, D. Olaleye, B. Zinman, and V. Bril, "Simple screening tests for peripheral neuropathy in the diabetes clinic," *Diabetes Care,* vol. 24, pp. 250-256, February 2001.

[49] M. Tan and U. Tan, "Early diagnosis of diabetic neuropathy using double-shock stimulation of peripheral nerves," *Clinical Neurophysiology,* vol. 114, pp. 1419-1422, 2003.

[50] M. E. Kiziltan, G. Benbir, and M. A. Akalin, "Is diabetic dermopathy a sign for severe neuropathy in patients with diabetes mellitus? Nerve conduction studies and symptom analysis," *Clinical Neurophysiology,* vol. 117, pp. 1862-1869, 2006.

[51] A. V. Schwartz, T. A. Hillier, D. E. Sellmeyer, H. E. Resnick, E. Gregg, K. E. Ensrud, P. J. Schreiner, K. L. Margolis, J. A. Cauley, M. C. Nevitt, D. M. Black, and S. R. Cummings, "Older Women With Diabetes Have a Higher Risk of Falls: A prospective study," *Diabetes Care,* vol. 25, pp. 1749-1754, October 2002.

[52] R. E. Hill and P. E. WIlliams, "Perineural cell basement membrane thickening and myelinated nerve fibre loss in diabetic and nondiabetic peripheral nerve," *Journal of the Neurological Sciences,* vol. 217, pp. 157-163, 2004.

[53] D. N. Ishii, "Implication of insulin-like growth factors in the pathogenesis of diabetic neuropathy," *Brain Research Reviews,* vol. 20, pp. 47-67, 1995.

[54] J. D. Stewart, R. McKelvey, L. Durcan, S. Carpenter, and G. Karpati, "Chronic inflammatory demyelinating polyneuropathy (CIDP) in diabetics," *Journal of the Neurological Sciences,* vol. 142, pp. 59-64, 1996.

[55] E. Hoitsma, J. P. H. Reulen, M. de Baets, M. Drent, F. Spaans, and C. G. Faber, "Small fiber neuropathy: a common and important clinical disorder," *Journal of the Neurological Sciences,* vol. Accepted for publication available at online journal, 2004.

[56] L. Eckersley, A. D. Ansselin, and D. R. Tomlinson, "Effects of experimental diabetes on axonal and Schwann cell changes in sciatic nerve isografts," *Molecular Brain Research,* vol. 92, pp. 128-137, 2001.

[57] H. Andersen, S. Nielsen, C. E. Mogensen, and J. Jakobsen, "Muscle Strength in Type 2 Diabetes," *Diabetes,* vol. 53, pp. 1543-1548, June 1, 2004 2004.

[58] F. B. Horak and F. Hlavacka, "Somatosensory Loss Increases Vestibulospinal Sensitivity," *Journal of Neurophysiology,* vol. 86, pp. 575-585, August 1, 2001 2001.

[59] P. A. Wackym and F. H. Linthicum, Jr., "Diabetes mellitus and hearing loss: clinical and histopathologic relationships," *American Journal of Otology,* vol. 7, pp. 176-82, May 1986.

[60] S. W. Duck, J. Prazma, P. S. Bennett, and H. C. Pillsbury, "Interaction between hypertension and diabetes mellitus in the pathogenesis of sensorineural hearing loss," *Laryngoscope,* vol. 107, pp. 1596-1605, December 1997.

[61] S.-F. Weng, Y.-S. Chen, C.-J. Hsu, and F.-Y. Tseng, "Clinical Features of Sudden Sensorineural Hearing Loss in Diabetic Patients," *Laryngoscope,* vol. 115, pp. 1676-1680, 2005.

[62] S.-F. Weng, Y.-S. Chen, T.-C. Liu, C.-J. Hsu, and F.-Y. Tseng, "Prognostic Factors of Sudden Sensorineural Hearing Loss in Diabetic Patients." vol. 27, 2004, pp. 2560-2561.

[63] V. Kakarlapudi, R. Sawyer, and H. Staecker, "The Effect of Diabetes on Sensorineural Hearing Loss," *Otology & Neurotology,* vol. 24, pp. 382-386, 2003.

[64] S. T. Frisina, F. Mapes, S. Kim, D. R. Frisina, and R. D. Frisina, "Characterization of hearing loss in aged type II diabetics," *Hearing Research,* vol. 211, pp. 103-113, 2006.

[65] N. Vaughan, K. James, D. McDermott, S. Griest, and S. Fausti, "A 5-Year Prospective Study of Diabetes and Hearing Loss in a Veteran Population," *Otology & Neurotology,* vol. 27, pp. 37-43, 2006.

[66] P. D. Fowler and N. S. Jones, "REVIEW Diabetes and hearing loss," *Clinical Otolaryngology & Allied Sciences,* vol. 24, pp. 3-8, 1999.

[67] D. H. Romero and G. E. Stelmach, "Changes in postural control with aging and Parkinson's disease," *Engineering in Medicine and Biology Magazine, IEEE,* vol. 22, pp. 27-31, 2003.

[68] D. E. Krebs, C. A. McGibbon, and D. Goldvasser, "Analysis of postural perturbation responses," *Neural Systems and Rehabilitation Engineering, IEEE Transactions on [see also IEEE Trans. on Rehabilitation Engineering],* vol. 9, pp. 76-80, 2001.

[69] M. Schieppati, E. Tacchini, A. Nardone, J. Tarantola, and S. Corna, "Subjective perception of body sway," *Journal of Neurology, Neurosurgery & Psychiatry,* vol. 66, pp. 313-322, March 1999.

[70] A. L. Betker, Z. Moussavi, and T. Szturm, "Center of mass function approximation," in *Engineering in Medicine and Biology Society, 2004. EMBC 2004. Conference Proceedings. 26th Annual International Conference of the,* 2004, pp. 687-690.

[71] A. L. Betker, Z. M. K. Moussavi, and T. Szturm, "Center of mass approximation and prediction as a function of body acceleration," *Biomedical Engineering, IEEE Transactions on,* vol. 53, pp. 686-693, 2006.

[72] B. J. Benda, P. O. Riley, and D. E. Krebs, "Biomechanical relationship between center of gravity and center of pressure during standing," *Rehabilitation Engineering, IEEE Transactions on [see also IEEE Trans. on Neural Systems and Rehabilitation],* vol. 2, pp. 3-10, 1994.

[73] S. Bonnet, P. Couturier, F. Favre-Reguillon, and R. Guillemaud, "Evaluation of postural stability by means of a single inertial sensor," in *Engineering in Medicine and Biology Society, 2004. EMBC 2004. Conference Proceedings. 26th Annual International Conference of the*, 2004, pp. 2275-2278.

[74] E. A. Keshner, R. V. Kenyon, and Y. Dhaher, "Postural research and rehabilitation in an immersive virtual environment," in *Engineering in Medicine and Biology Society, 2004. EMBC 2004. Conference Proceedings. 26th Annual International Conference of the*, 2004, pp. 4862-4865.

[75] V. Krishnamoorthy, M. L. Latash, J. P. Scholz, and V. M. Zatsiorsky, "Muscle synergies during shifts of the center of pressure by standing persons.[erratum appears in Exp Brain Res. 2004 Mar;155(1):134]," *Experimental Brain Research,* vol. 152, pp. 281-292, October 2003.

[76] V. Krishnamoorthy, M. L. Latash, J. P. Scholz, and V. M. Zatsiorsky, "Muscle modes during shifts of the center of pressure by standing persons: effect of instability and additional support," *Experimental Brain Research,* vol. 157, pp. 18-31, July 2004.

[77] D. Lafond, H. Corriveau, and F. Prince, "Postural Control Mechanisms During Quiet Standing in Patients With Diabetic Sensory Neuropathy," *Diabetes Care,* vol. 27, pp. 173-178, January 2004.

[78] P. Loughlin and M. Redfern, "Analysis and modeling of human postural control," *Engineering in Medicine and Biology Magazine, IEEE,* vol. 22, p. 18, 2003.

[79] P. Loughlin, T. Schumann, M. Redfern, J. Furman, L. Chaparro, and A. El-Jaroudi, "Time-frequency analysis of postural sway," in *Signals, Systems and Computers, 1994. 1994 Conference Record of the Twenty-Eighth Asilomar Conference on*, 1994, pp. 378-382.

[80] T. E. Prieto, J. B. Myklebust, and B. M. Myklebust, "Postural steadiness and ankle joint compliance in the elderly," *Engineering in Medicine and Biology Magazine, IEEE,* vol. 11, pp. 25-27, 1992.

[81] J. Jeka, K. Oie, G. Schoner, T. Dijkstra, and E. Henson, "Position and Velocity Coupling of Postural Sway to Somatosensory Drive," *J Neurophysiol,* vol. 79, pp. 1661-1674, April 1998.

[82] I. D. Loram, S. M. Kelly, and M. Lakie, "Human balancing of an inverted pendulum: is sway size controlled by ankle impedance?," *Journal of Physiology,* vol. 532, pp. 879-891, May 2001.

[83] I. D. Loram and M. Lakie, "Direct measurement of human ankle stiffness during quiet standing: the intrinsic mechanical stiffness is insufficient for stability," *Journal of Physiology,* vol. 545, pp. 1041-1053, December 2002.

[84] I. D. Loram and M. Lakie, "Human balancing of an inverted pendulum: position control by small, ballistic-like, throw and catch movements," *Journal of Physiology,* vol. 540, pp. 1111-1124, May 2002.

[85] I. D. Loram, C. N. Maganaris, and M. Lakie, "Paradoxical muscle movement in human standing," *Journal of Physiology,* vol. 556, pp. 683-689, May 2004.

[86] I. D. Loram, C. N. Maganaris, and M. Lakie, "Human postural sway results from frequent, ballistic bias impulses by soleus and gastrocnemius.[see comment]," *Journal of Physiology,* vol. 564, pp. 295-311, April 2005.

[87] I. D. Loram, C. N. Maganaris, and M. Lakie, "Active, non-spring-like muscle movements in human postural sway: how might paradoxical changes in muscle length be produced?[see comment]," *Journal of Physiology,* vol. 564, pp. 281-293, April 2005.

[88] S. J. Richerson, C. J. Robinson, and N. Witriol, "Head Reactions to Platform Movement During Postural Control Tests," in *Proceedings of the RESNA 2001 Annual Conference: The AT Odyssey Continues*, 2001, pp. 236-238.

[89] L. W. Faulkner and C. J. Robinson, "Detecting thresholds and interactions among displacement, acceleration, and velocity, for young adults on a horizontally translated platform," in *Engineering in Medicine and Biology Society, 1998. Proceedings of the 20th Annual International Conference of the IEEE*, 1998, pp. 2382-2385.

[90] B. Kollmeier, R. H. Gilkey, and U. K. Sieben, "Adaptive staircase techniques in psychoacoustics: a comparison of human data and a mathematical model," *Journal of the Acoustical Society of America,* vol. 83, pp. 1852-1862, May 1988.

[91] S. A. Klein, "Measuring, estimating, and understanding the psychometric function: A commentary," *Perception & Psychophysics,* vol. 63, pp. 1421-1455, 2001.

[92] M. M. Taylor and C. D. Creelman, "PEST: Efficient Estimates on Probability Functions," *The Journal of the Acoustical Society of America,* vol. 41, pp. 782-787, 1967.

[93] C. Kaernbach, "A single-interval adjustment-matrix (SIAM) procedure for unbiased adaptive testing," *Journal of the Acoustical Society of America,* vol. 88, pp. 2645-2655, December 1990.

[94] A. Murata and H. Iwase, "Chaotic analysis of body sway," in *Engineering in Medicine and Biology Society, 1998. Proceedings of the 20th Annual International Conference of the IEEE*, 1998, pp. 1557-1560.

[95] P. A. Fransson, A. Hafstrom, M. Karlberg, M. Magnusson, A. Tjader, and R. Johansson, "Postural control adaptation during galvanic vestibular and vibratory proprioceptive stimulation," *Biomedical Engineering, IEEE Transactions on,* vol. 50, pp. 1310-1319, 2003.

[96] A. M. De Nunzio, A. Nardone, and M. Schieppati, "Head stabilization on a continuously oscillating platform: the effect of a proprioceptive disturbance on the balancing strategy," *Experimental Brain Research,* vol. 165, pp. 261-272, August 2005.

[97] E. A. Keshner and R. V. Kenyon, "The influence of an immersive virtual environment on the segmental organization of postural stabilizing responses," *Journal of Vestibular Research,* vol. 10, pp. 207-219, 2000.

[98] E. A. Keshner and R. V. Kenyon, "Using immersive technology for postural research and rehabilitation," *Assistive Technology,* vol. 16, pp. 54-62, 2004.

[99] P. J. Sparto, J. M. Furman, S. L. Whitney, L. F. Hodges, and M. S. Redfern, "Vestibular rehabilitation using a wide field of view virtual environment," in *Engineering in Medicine and Biology Society, 2004. EMBC 2004. Conference Proceedings. 26th Annual International Conference of the*, 2004, pp. 4836-4839.

[100] P. J. Sparto, J. G. Jasko, and P. J. Loughlin, "Detecting postural responses to sinusoidal sensory inputs: a statistical approach," *Neural Systems and Rehabilitation Engineering, IEEE Transactions on [see also IEEE Trans. on Rehabilitation Engineering],* vol. 12, pp. 360-366, 2004.

[101] M. Ferdjallah, G. F. Harris, P. A. Smith, S. Hassani, P. Johnson, and K. Reiners, "Postural stability assessment and orthotics," in *Pediatric Gait, 2000. A new Millennium in Clinical Care and Motion Analysis Technology*, 2000, pp. 69-77.

[102] P. D. Frazier and M. F. Chouikha, "A novel control model for elucidating human postural balance," in *Intelligent Control and Automation, 2004. WCICA 2004. Fifth World Congress on*, 2004, pp. 2369-2375.

[103] R. Johansson, P. A. Fransson, and M. Magnusson, "Identification of adaptation in human postural control using GARCH models," in *Decision and Control, 2001. Proceedings of the 40th IEEE Conference on*, 2001, pp. 7-12.

[104] M. Maltenfort, T. Hamm, and H. Jiping, "A sensory feedback control model of neuromuscular systems," in *[Engineering in Medicine and Biology, 1999. 21st Annual Conf. and the 1999 Annual Fall Meeting of the Biomedical Engineering Soc.] BMES/EMBS Conference, 1999. Proceedings of the First Joint*, 1999, p. 531.

[105] R. Johansson and M. Magnusson, "Identification of human postural dynamics," in *Control and Applications, 1989. Proceedings. ICCON '89. IEEE International Conference on*, 1989, pp. 875-880.

[106] R. Johansson, M. Magnusson, and M. Akesson, "Identification of human postural dynamics," *Biomedical Engineering, IEEE Transactions on,* vol. 35, pp. 858-869, 1988.

[107] A. Banos, M. A. Jimenez, and P. Gonzalez de Santos, "Dynamic simulation of a four-legged gait," in *Systems, Man and Cybernetics, IEEE International Conference on* 1992, pp. 498-503.

[108] J. Estremera and P. Gonzalez de Santos, "Generating continuous free crab gaits for quadruped robots on irregular terrain," *Robotics, IEEE Transactions on,* vol. 21, pp. 1067-1076, 2005.

[109] Z. Fuhai, W. Weiguo, L. Yuedong, and R. Bingyin, "Omni-directional quadruped walking gaits and simulation for a gorilla robot," in *Intelligent Robots and Systems, Proceedings of the 2005 IEEE/RSJ International Conference on*, 2005, pp. 1121-1126.

[110] T. Geng, B. Porr, and F. Worgotter, "Self-stabilized biped walking under control of a novel reflexive network," in *Intelligent Robots and Systems, Proceedings of the 2005 IEEE/RSJ International Conference on*, 2005, pp. 3269-3274.

[111] C. Hwang and K. Sasaki, "Evaluation of robotic fingers based on kinematic analysis," in *Intelligent Robots and Systems, Proceedings of the 2003 IEEE/RSJ International Conference on*, 2003, pp. 3318-3324.

[112] W. Li-quan, C. Dong-liang, S. Lei, M. Qing-xin, and Z. Ling, "The research on bionic crab-liked robot prototype," in *Mechatronics and Automation, 2005 IEEE International Conference*, 2005, pp. 2017-2021.

[113] Y. Matsuoka and P. Afshar, "Neuromuscular strategies for dynamic finger movements: a robotic approach," in *Engineering in Medicine and Biology Society, 26th Annual International Conference of the*, 2004, pp. 4649-4652.

[114] S. Peng, C. P. Lam, and G. R. Cole, "A biologically inspired four legged walking robot," in *Robotics and Automation, Proceedings of the 2003 IEEE International Conference on*, 2003, pp. 2024-2030.

[115] A. Schneider, H. Cruse, and J. Schmitz, "A biologically inspired active compliant joint using local positive velocity feedback (LPVF)," *Systems, Man and Cybernetics, Part B, IEEE Transactions on,* vol. 35, pp. 1120-1130, 2005.

[116] W. Weiguo, L. Yuedong, Z. Fuhai, and R. Bingyin, "Design, simulation and walking experiments for a humanoid and gorilla robot with multiple locomotion modes," in *Intelligent Robots and Systems, Proceedings of the 2005 IEEE/RSJ International Conference on*, 2005, pp. 1157-1162.

[117] J. Yamaguchi and A. Takanishi, "Design of biped walking robots having antagonistic driven joints using nonlinear spring mechanism," in *Intelligent Robots and Systems, Proceedings of the 1997 IEEE/RSJ International Conference on*, 1997, pp. 251-259.

[118] J. Yamaguchi, A. Takanishi, and I. Kato, "Development of a biped walking robot compensating for three-axis moment by trunk motion," in *Intelligent Robots and Systems, Proceedings of the 1993 IEEE/RSJ International Conference on*, Yokohama, Japan, 1993, pp. 561-566.

[119] J. Yang and K. J., "A strategy of optimal fault tolerant gait for the hexapod robot in crab walking," in *Robotics and Automation, Proceedings of the 1998 IEEE International Conference on*, 1998, pp. 1695-1700.

[120] A. Torige, M. Noguchi, and N. Ishizawa, "Centipede type multi-legged walking robot," in *Intelligent Robots and Systems, Proceedings of the 1993 IEEE/RSJ International Conference on*, 1993, pp. 567-571.

[121] M. W. Spong and M. Vidyasagar, in *Robot Dynamics and Control* New York: John Wiley and Sons, 1989, pp. 32-72.

[122] J. Denavit and R. S. Hartenberg, "A kinematic notation for lower-pair mechanisms based on matrices," *ASME Journal of Applied Mechanics,* vol. 22, pp. 215-221, 1955.

[123] J. Agee, A. Hollister, and F. King, "The Longitudinal Axes of Rotation of the Metacarpophalangeal Joint of the Finger," *J Hand Surg,* vol. 11, p. 767, 1986.

[124] S. L. Albright, E. F. Fichter, and B. L. Fichter, "Kinematic Model for Arthropod Legs and Other Manipulators," *Journal of Mechanical Design, Transaction of ASME,* vol. 116, pp. 22-27, 1994.

[125] S. G. Elias, M. A. R. Freeman, and E. I. Gokcay, "A correlative study of the geometry and anatomy of the distal femur," *Clin Orthop Relat Res,* vol. 260, pp. 98-103, 1990.

[126] A. Fick, "Die Gelenke mit sattelformigen Flachen," in *Zeitschrift fur Rationelle Medicin* Heidelberg: Akademische Verlagshandlung von C. F. Winter, 1854, pp. 314-321.

[127] A. Fick, "Lehrbuck der Physik," in *Medicinische Physik* Brunchweig: Verlag Friedrich Vieweg und Sohn, 1866.

[128] R. Fick, "Handbuch der Anatomie und Mechanik der Gelenke unter Berucksichtigung der bewegenden Muskeln," in *Specielle Gelenk und Muskelmechanik.* vol. 2 Jena: Verlag von Gustav Fisher, 1908.

[129] E. F. Fitcher and B. L. Fichter, "A survey of legs of insects and spiders from a kinematic perspective," in *Robotics and Automation, Proceedings of the 1988 IEEE International Conference on*, 1988, pp. 984-986.

[130] M. Freeman, "Knee Flexion: The cruciate ligaments and posterior stability in the flexed knee," in *Total Arthroplasty of the Knee, Proceedings of the Knee Society 1985-1986*, 1986.

[131] A. Hollister, W. L. Buford, L. M. Myers, D. J. Giurintano, and A. Novick, "The Axes of Rotation of the Thumb Carpometacarpal Joint," *Journal of Orthopaedic Research,* vol. 10, pp. 454-460, 1992.

[132] A. Hollister and D. J. Giurintano, "Thumb Movements, Motions, and Moments," *Journal of Hand Therapy,* vol. 8, pp. 106-114, 1995.

[133] A. Hollister, D. J. Giurintano, W. L. Buford, L. M. Myers, and A. Novick, "The Axes of Rotation of the Thumb Interphalangeal and Metacarpophalangeal Joints," *Clinical Orthopaedics and Related Research,* vol. 320, pp. 188-193, 1995.

[134] A. M. Hollister, H. Gellman, and R. L. Waters, "The Relationship of the Interosseus Membrane to the Axis of Rotation of the Forearm," *Clinical Orthopaedics and Related Research,* vol. 298, pp. 272-276, 1994.

[135] A. M. Hollister and D. G. Giruintano, "How Joints Move," in *Clinical Mechanics of the Hand*, P. W. Brand, Hollister, A. M., Ed. Chicago Mosby 1999.

[136] A. M. Hollister, S. Jatana, A. K. Singh, W. W. Sullivan, and A. G. Lupichuk, "The Axes of Rotation of the Knee," *Clinical Orthopaedics and Related Research,* vol. 290, pp. 259-268, 1993.

[137] V. T. Inman, *The joints of the ankle.* Baltimore: Williams & Wilkins, 1976.

[138] R. E. Isman and V. T. Inman, "Anthropometric studies of the human foot and ankle," *Bulletin of Prosthetics Research,* pp. 97-129, 1969.

[139] N. Koti, "Design of a biomimetic manipulator with nonorthogonal Joint Axes," in *Mechanical Engineering.* vol. Masters Ruston, LA: Louisiana Tech University, 2005.

[140] A. F. Krause and V. Dürr, "Tactile efficiency of insect antennae with two hinge joints," *Biological Cybernetics,* vol. 91, pp. 168-181, 2004.

[141] J. T. London, "Kinematics of the Elbow," *The Journal of Bone and Joint Surgery,* vol. 63, pp. 529-535, 1981.

[142] A. G. Lupichuk, "Determining the axis of rotation from 3-D motion data," in *College of Engineering.* vol. Masters Long Beach: California State University, 1995.

[143] J. A. Moore, C. F. Small, J. T. Bryant, R. E. Ellis, D. R. Pichora, and A. M. Hollister, "A Kinematic Technique for Describing Wrist Joint Motion: Analysis of Configuration Space Plots," *Proceedings of the Institution of Mechanical Engineers,* vol. 207, pp. 211-218, 1993.

[144] V. Moyer, E. Fichter, and B. Fichter, "Analyzing dynamics of arthropod walking," in *Medicine and Biology Society, Proceedings of the 1988 Annual International Conference of the IEEE Engineering in*, 1988, pp. 710-711.

[145] A. K. Singh, K. D. Starkweather, A. M. Hollister, S. Jatana, and A. G. Lupichuk, "Kinematics of the ankle: a hinge axis model," *Foot and Ankle,* vol. 13, pp. 439-446, 1992.

[146] W. Weber and E. Weber, in *Mechanik der Menschlichen Gehwerkzeuge* Berlin: Springer Verlag, 1836, pp. 75-97.

[147] D. Hearn and M. P. Baker, in *Computer graphics C version*: Prentice Hall, 1997, pp. 408-423.

[148] D. F. Rogers and J. A. Adams, in *Mathematical Elements for Computer Graphics* New York: McGraw-Hill, 1990, pp. 101-130.

[149] D. F. Rogers and R. A. Earnshaw, *Techniques for computer graphics*. New York: Springer-Verlag, 1987.

[150] C. M. Storey, A. M. Hollister, C. Robinson, N. Witriol, D. O. Anderson, J. C. London, and W. L. Buford, "A System for Measurement and Calibration of Nonorthogonal Joints and Limbs in Humans," in *in Proceedings of the 28th Annual International Conference IEEE EMBS*, New York, NY, USA, 2006.

[151] W. L. Buford, A. M. Hollister, and L. M. Myers, "A Modeling and Simulation System for the Human Hand," *Journal of Clinical Engineering,* vol. 15, pp. 445-451, 1990.

[152] D. J. Giurintano, A. M. Hollister, W. L. Buford, D. E. Thompson, and L. M. Myers, "A virtual five-link model of the thumb," *Medical Engineering & Physics,* vol. 17, pp. 297-303, 1995.

[153] D. E. Thompson and D. J. Giurintano, "A Kinematic Model of the Flexor Tendons of the Hand," *Journal of Biomechanics* vol. 22, pp. 327-334, 1989.

[154] W. L. Buford, Jr. and D. E. Thompson, "A System for Three-Dimensional Interactive Simulation of Hand Biomechanics," *IEEE Transactions on Biomedical Engineering,* vol. 34, pp. 444-453, 1987.

[155] W. L. Buford, Jr. and C. R. Andersen, "Definition of the kinematic plant for the human musculoskeletal system," in *Systems, Man and Cybernetics, 2005 IEEE International Conference on*, 2005, pp. 1246-1251.

[156] E. D. Pohl and H. Lipkin, "Kinematics of complex joint angles in robotics," in *Robotics and Automation, 1990 IEEE International Conference on*, 1990, pp. 86-91.

[157] J. Ziegert and P. Datseris, "Basic considerations for robot calibration," in *Robotics and Automation, Proceedings of the 1988 IEEE International Conference on*, 1988, pp. 932-938.

[158] C. M. Storey and C. J. Robinson, "Using Server Architecture and Multi-Threaded Processors and Software to Time-Lock Multiple Data Streams in Time-Critical Physiological Experiments.," in *ASEE St. Lawrence Section Conference: Interdiscplinary Innovation and Imagination in Engineering Education* Cornell University, Ithaca, NY, 2006.

[159] S. J. Richerson, S. G. Morstatt, R. D. Vanya, A. M. Hollister, and C. J. Robinson, "Factors affecting reaction times to short anterior postural disturbances," *Medical Engineering & Physics,* vol. 26, pp. 581-586, September 2004.

[160] R. D. Hays, C. D. Sherbourne, and R. M. Mazel, "The RAND 36-Item Health Survey 1.0.[see comment]," *Health Economics,* vol. 2, pp. 217-227, October 1993.

[161] M. A. Burnam, K. B. Wells, B. Leake, and J. Landsverk, "Development of a brief screening instrument for detecting depressive disorders," *Medical Care,* vol. 26, pp. 775-789, August 1988.

[162] J. E. Ware, Jr. and C. D. Sherbourne, "The MOS 36-item short-form health survey (SF-36). I. Conceptual framework and item selection," *Medical Care,* vol. 30, pp. 473-483, June 1992.

[163] C. A. McHorney, J. E. Ware, Jr., and A. E. Raczek, "The MOS 36-Item Short-Form Health Survey (SF-36): II. Psychometric and clinical tests of validity in measuring physical and mental health constructs," *Medical Care,* vol. 31, pp. 247-263, March 1993.

[164] C. A. McHorney, J. E. Ware, Jr., J. F. Lu, and C. D. Sherbourne, "The MOS 36-item Short-Form Health Survey (SF-36): III. Tests of data quality, scaling assumptions, and reliability across diverse patient groups," *Medical Care,* vol. 32, pp. 40-66, January 1994.

[165] C. Jenkinson, L. Wright, and A. Coulter, "Criterion validity and reliability of the SF-36 in a population sample," *Quality of Life Research,* vol. 3, pp. 7-12, February 1994.

[166] R. A. Lyons, I. M. Perry, and B. N. C. Littlepage, "Evidence for the Validity of the Short-form 36 Questionnaire (SF-36) in an Elderly Population," *Age & Ageing,* vol. 23, pp. 182-184, May 1994.

[167] M. Suzuki, N. Ohyama, K. Yamada, and M. Kanamori, "The relationship between fear of falling, activities of daily living and quality of life among elderly individuals," *Nursing and Health Sciences,* vol. 4, pp. 155-161, 2002.

[168] R. W. Simmons, C. Richardson, and K. Deutsch, "Limited joint mobility of the ankle in diabetic patients with cutaneous sensory deficit," *Diabetes Research & Clinical Practice,* vol. 37, pp. 137-143, August 1997.

[169] S. Kumar, D. J. Fernando, A. Veves, E. A. Knowles, M. J. Young, and A. J. Boulton, "Semmes-Weinstein monofilaments: a simple, effective and inexpensive screening device for identifying diabetic patients at risk of foot ulceration," *Diabetes Research & Clinical Practice,* vol. 13, pp. 63-67, August 1991.

[170] W. Strobl, F. Reisecker, P. Koltringer, and F. Leblhuber, "A comparative study of the sensory conduction velocity of the sural nerve using surface and needle electrodes," *EEG-EMG Zeitschrift fur Elektroenzephalographie Elektromyographie und Verwandte Gebiete,* vol. 23, pp. 135-139, September 1992.

[171] I. W. Husstedt, K. H. Grotemeyer, and H. P. Schlake, "The effect of the lead electrodes on the conduction velocity of the sural nerve," *EEG-EMG Zeitschrift fur Elektroenzephalographie Elektromyographie und Verwandte Gebiete,* vol. 22, pp. 152-156, September 1991.

[172] T. Ewert, H. Hielscher, K. H. Grotemeyer, and M. Hermanns, "Sural nerve neurography using surface and needle electrodes in polyneuropathies. Comparative study," *EEG-EMG Zeitschrift fur Elektroenzephalographie Elektromyographie und Verwandte Gebiete,* vol. 16, pp. 114-119, June 1985.

[173] B. Neundorfer, D. Kompf, and J. Dedden, "Sural neurography: comparative study in stimulation with surface and needle electrodes," *EEG-EMG Zeitschrift fur Elektroenzephalographie Elektromyographie und Verwandte Gebiete,* vol. 14, pp. 39-42, March 1983.

[174] D. H. McBurney and V. B. Collings, *Introduction to Sensation / Perception*, 2nd edition ed. Englewood Cliffs, NJ: Prentice-Hall Inc, 1984.

[175] C. H. Webb and D. H. McBurney, "Salivary Habituation: Quantitative Similarities to Sensory Adaptation," *The American Journal of Psychology,* vol. 84, pp. 501-512, 1971.

[176] D. L. Kunz, "An object oriented approach to multibody systems analysis," *Computers and Structures,* vol. 69, pp. 209-217, 1998.

[177] M. R. Leek, "Adaptive procedures in psychophysical research," *Perception & Psychophysics,* vol. 63, pp. 1279-1292, 2001.

[178] S. Deshmukh, "Physiological Correlates of Anterior Platform Perturbations," in *Biomedical Engineering*. vol. Masters Ruston, LA: Louisiana Tech University, 2005.

[179] E. A. Keshner, "Modulating active stiffness affects head stabilizing strategies in young and elderly adults during trunk rotations in the vertical plane," *Gait & Posture,* vol. 11, pp. 1-11, February 2000.

[180] M. W. Powell, D. H. Carnegie, and T. J. Burke, "Reversal of diabetic peripheral neuropathy with phototherapy (MIRE) decreases falls and the fear of falling and improves activities of daily living in seniors," *Age & Ageing,* vol. 35, pp. 11-16, 2006.

[181] J. A. Levine, L. M. Lanningham-Foster, S. K. McCrady, A. C. Krizan, L. R. Olson, P. H. Kane, M. D. Jensen, and M. M. Clark, "Interindividual Variation in Posture Allocation: Possible Role in Human Obesity," *Science,* vol. 307, pp. 584-586, January 2005.

[182] J. K. Richardson, "Factors Associated With Falls in Older Patients With Diffuse Polyneuropathy," *Journal of the American Geriatrics Society,* vol. 50, pp. 1767-1773, 2002.

[183] A. Thoroddsen, "Pressure sore prevalence: a national survey," *Journal of Clinical Nursing,* vol. 8, pp. 170-179, 1999.

[184] D. Gould, T. James, A. Tarpey, D. Kelly, D. Pattison, and C. Fox, "Intervention studies to reduce the prevalence and incidence of pressure sores: a literature review," *Journal of Clinical Nursing,* vol. 9, pp. 163-177, 2000.

[185] A. Nardone and M. Schieppati, "Group II spindle fibres and afferent control of stance. Clues from diabetic neuropathy," *Clinical Neurophysiology,* vol. 115, pp. 779-789, 2004.

[186] M. Bove, A. Nardone, and M. Schieppati, "Effects of leg muscle tendon vibration on group Ia and group II reflex responses to stance perturbation in humans," *Journal of Physiology,* vol. 550, pp. 617-630, July 2003.

[187] G. G. Simoneau, J. S. Ulbrecht, J. A. Derr, M. B. Becker, and P. R. Cavanagh, "Postural instability in patients with diabetic sensory neuropathy," *Diabetes Care,* vol. 17, pp. 1411-1421, December 1994.

[188] C. L. Darlington, J. Erasmus, M. Nicholson, J. King, and P. F. Smith, "Comparison of visual--vestibular interaction in insulin-dependent and non-insulin-dependent diabetes mellitus," *Neuroreport,* vol. 11, pp. 487-490, February 2000.

[189] M. Nicholson, J. King, P. F. Smith, and C. L. Darlington, "Vestibulo-ocular, optokinetic and postural function in diabetes mellitus," *Neuroreport,* vol. 13, pp. 153-157, January 2002.

[190] P. J. Loughlin and M. S. Redfern, "Spectral characteristics of visually induced postural sway in healthy elderly and healthy young subjects," *Neural Systems and Rehabilitation Engineering, IEEE Transactions on [see also IEEE Trans. on Rehabilitation Engineering],* vol. 9, pp. 24-30, 2001.

[191] S. Corna, J. Tarantola, A. Nardone, A. Giordano, and M. Schieppati, "Standing on a continuously moving platform: is body inertia counteracted or exploited?," *Experimental Brain Research,* vol. 124, pp. 331-341, 1999.

[192] G. L. Kinzell and L. J. Gutkowski, "Joint models, degrees of freedom, and anatomical measurement," *Journal of Biomechanical Engineering,* vol. 105, pp. 55-62, 1979.

[193] G. L. Kinzell, A. S. Hall, and B. M. Hillberry, "Measurement of total motion between two body segments - 1 Analytical development," *Journal of Biomechanics,* vol. 5, pp. 93-105, 1972.